STUDIES ON THE CYTOSKELETAL PROTEINS

VINCULIN AND TALIN.

Thesis submitted for the degree of

Doctor of Philosophy

at the University of Leicester

by

Sarah J. Bolton B.Sc. (Hons.) (London)

Department of Biochemistry

University of Leicester

June 1995

UMI Number: U085309

UMI U085309

CONTENTS.

CHAPTER 3 - DOWN-REGULATION OF VINCULIN PROTEIN LEVELS USING ANTISENSE TECHNOLOGY.

CHAPTER 4. CHARACTERISATION OF ANTI-HUMAN PLATELET TALIN MONOCLONAL ANTIBODIES.

PREFACE

ABBREVIATIONS.

ATP	adenosine triphosphate
BSA	bovine serum albumin
bp	base pairs
cDNA	complementary DNA
CEF	chick embryo fibroblast
Ci	Curie
CTP	cytidine triphosphate
Da	Daltons
DEPC	diethyl pyrocarbonate
DMSO	dimethly sulfoxide
DMEM	Dulbecco's modified eagle medium
DNA	deoxyribonucleic acid
DNase	deoxyribonuclease
dNTP	deoxyribonucleotide triphosphate
E. coli	*Escherichia coli*
ECM	extracellular matrix
EDTA	diaminoethane-tetraacetic acid
EGTA	ethyleneglycol-bis-(β-aminoethyl ether)N, N, N, N', N'-tetra-acetic acid
ELISA	enzyme linked immunosorbant assay
ERM	ezrin, radixin, moesin
FAK	focal adhesion kinase
FRNK	FAK related non-kinase
FCS	fetal calf serum
FITC	fluorescein isothiocyanate
GTP	guanosine triphosphate
GuITC	guanidium isothiocyanate
HEPES	N-[2-hydroxyethyl]piperazine-N'-[2-ethanesulfonic acid]
HeBS	hepes buffered saline
HRP	horseradish peroxidase
IPA	isopropyl alcohol
IPTG	Isopropyl β-D-thiogalactopyranoside
kb	kilobase
k_d	dissociation constant
LPA	lysophosphatidic acid
MAPK	mitogen activated protein kinase
MES	2-[N-morpholino]-ethanesulfonic acid

mRNA	messenger RNA
MOPS	3-[N-morpholino]propane-sulfonic acid]
MMTV	mouse mammary tumour virus
NCS	newborn calf serum
OD_x	absorbance (optical density) at x nm
oligo	oligonucleotide
PAGE	polyacrylamide gel electrophoresis
PBS	phosphate buffered saline
PCR	polymerase chain reaction
PDGF	platelet-derived growth factor
PEG	polyethylene glycol
PK-C	protein kinase C
PMSF	phenylmethyl sulfonyl fluoride
PVP	polyvinylpyrolidine
RIPA	radio-immune precipitation assay
RNA	ribonucleic acid
RNase	ribonuclease
RSV	Rous sarcoma virus
rUTP	ribouridine triphosphate
SDS	Sodium dodecyl sulphate
SV40	Simian Virus 40
TBS	tris-buffered saline
TEMED	N, N, N', N',-tetramethylethylenediamine
TETD	tetraethylthiuram disulphide
Tris	(hydroxymethyl)aminomethane
Tween 20	polyoxyethylene sorbitan monolaurate
X-gal	5-bromo-4-chloro-3-indolyl-β-D-galactoside

ABSTRACT

Sarah J. Bolton. Studies on the cytoskeletal proteins vinculin and talin.

The role of vinculin in cell adhesion was investigated by isolating NIH3T3 and Balb/c
3T3 cells containing a plasmid vector expressing a vinculin antisense RNA under the
control of the MMTV promoter. Stable cell lines of NIH3T3 cells were cultured with
dexamethasone but none showed any reduction in vinculin protein levels. Two Balb/c
3T3 cell lines, when cultured with dexamethasone displayed a marked reduction in
vinculin levels and displayed an altered cell shape from a spread to a more spindle-
shaped morphology. These phenotypic changes were reversible upon removal of the
dexamethasone. The reduced adhesion corresponded with a reduction in the growth rate
of the clones. The cells were also unable to spread on fibronectin and the ususal
increase in the phosphotyrosine content of two signalling proteins, paxillin and
pp125FAK, normally associated with cell adhesion, was not observed. The results
establish that vinculin is a key component of integrin-mediated cell adhesion. To
explore the structure-functional relationship of talin, six anti-talin monoclonal
antibodies were microinjected into human fibroblasts and the effect upon the actin
cytoskeleton was assessed. Two of the antibodies, TA205 and TD77 resulted in the
disintegration of actin stress fibres, and migration of CEF was also severely impaired
following microinjection of either antibody. The epitopes recognised by TA205 and
TD77 had been mapped to talin residues 102-497 and 2269-2541 respectively.
Microinjection of CEF with a polypeptide containing residues 102-497 demonstrated
that they were mainly associated with the detergent-soluble cytoplasmic portion of the
cell and were also able to disrupt stress fibre and focal adhesion integrity. Residues
2269-2541 were associated with the detergent-insoluble cytoskeletal fraction of the cell
but did not affect stress fibre or focal adhesion integrity. Attempts to identify proteins
that interacted with residues 102-497 of talin were unsuccessful but an actin-binding
site was identified within residues 2269-2541. The results indicate the presence of
domains within the N- and C-terminus of talin that are essential to the involvement of
talin in the formation of focal adhesions.

CHAPTER 1

INTRODUCTION

1.1 General introduction.

The growth of many cells in culture requires the presence of a solid support for the cells to adhere to. This close association with the underlying substrate, usually extra-cellular matrix (ECM) proteins such as fibronectin, is mediated by specialised regions of the ventral plasma membrane referred to as focal adhesions, adhesion plaques, focal contacts or cell-matrix junctions. Cells adhere to the ECM via the extracellular domain of the integrins, a family of transmembrane heterodimeric glycoproteins. The cytoplasmic face of the focal adhesion is characterised by the presence of a complex of proteins including talin, vinculin and α-actinin which anchor the actin filaments to the cytoplasmic tail of the integrins. The focal adhesion observed in cultured cells is therefore regarded as an easily manipulated and accessible system to study the many aspects of cell adhesion.

Cell adhesion is important to many cellular processes.

Cell adhesion is vital for cell division and proliferation (Couchman and Rees, 1979) and is also essential for the migration and differentiation of cells into various tissues and organs during embryogenesis (reviewed in McClay and Ettensohn, 1987; Hynes and Lander, 1992). In adults, cell adhesion is vital to wound healing, ensuring the recruitment of activated platelets to the wound site and their subsequent aggregation which is vital to clot formation (reviewed in Parise, 1989). Also, recruitment of leucocytes to sites of tissue inflammation and the stimulation of T- and B-cells involved in the generation of an immune response are all dependent on cell adhesion (reviewed in Springer, 1990). A dramatic reduction in cell adhesion is a characteristic of cancerous or virally-transformed cells, and this is postulated to play an important role in the metastasis of solid tumours to secondary sites. Transformed epithelial cells within a primary tumour can escape by breaking through the restraining basement membrane and penetrating the underlying blood vessels where they can travel to distant sites and attach to the vessel wall and extravasate into the underlying tissue. These cells are then able to establish themselves by forming

1

contacts within the new environment, and subsequently grow uncontrollably to form the secondary tumour, or metastatic nodule (see Liotta *et al.*, 1986).

The focal adhesion has *in vivo* homologues.

The focal adhesion formed between cultured cells and their substrate has often been considered an artifact of the tissue culture technique as they are often not seen in cells within whole organisms, but it has been demonstrated that protein complexes very similar to the focal adhesion do occur in some cell types *in vivo*. Epithelial cells form cell-cell junctions (zonula adherens) which are structurally very similar to focal adhesions, and they can also form cell-matrix junctions with the under lying extra-cellular matrix (Geiger *et al.*, 1985). Focal adhesion proteins such as talin, vinculin and the focal adhesion kinase, pp125FAK, have also been identified in platelets where they are thought to play an important role in platelet aggregation (Lipfert *et al.*, 1992; Bertagnolli *et al.*, 1993; Vostal and Shulman, 1993).

Myotendinous junctions in skeletal muscle have also been shown to share some of the same proteins and characteristics with focal adhesions (Shear and Bloch, 1985; Tidball *et al.*, 1986; Turner *et al.*, 1991; Bockholt *et al.*, 1992; Baker *et al.*, 1994), as do the dense plaques found in smooth muscle (Small, 1985). Similarly, in the nematode *C.elegans*, the dense body that links the microfilaments to the sarcolemma has been shown to contain both vinculin (Barstead and Waterston, 1989) and α-actinin (Francis and Waterston, 1985). The formation of a bridge between the microfilament cytoskeleton and the cell membrane which is involved in generation of tension and contractile forces across the junction is a common theme of both cell-cell and cell-matrix junctions.

2

1.2 Characteristics of cultured cells.

Much of the initial work examining cells in culture was carried out on fibroblasts isolated from chick heart explants (Abercrombie *et al.*, 1970a, b). These cells, grown on glass coverslips, were highly motile and moved by continually extending a thin projection of the cytoplasm, termed the leading edge or leading lamella, in the direction of movement. The fibroblasts were not adherent to the underlying glass substrate across the whole area of the cells ventral surface, but via discreet electron dense areas where the cytoplasm came to within 30nm of the substrate (Abercrombie *et al.*, 1971). These areas of close contact, which were termed plaques, also appeared to have bundles of microfilaments inserted into them and it was proposed these plaques were involved in the locomotion of the cell. More recently, experiments by Schmidt *et al.*, (1993) demonstrated the preferential recruitment of adhesive proteins into transient adhesions within the leading lamellae, followed by the subsequent migration of these proteins to the rear of the cell as the actin cytoskeleton exerts a rearward force upon the plaque to pull the cell forward. Further studies by Abercrombie and Dunn, (1975) also demonstrated the presence of these plaques in non-motile contact-inhibited cells.

Cell motility and proliferation are related to cell adhesion.

These plaques identified in motile fibroblasts were studied in more detail using interference reflection microscopy (IRM) and the motile cells were observed to contain small transient adhesions or close contacts, and the microfilaments were seen to be less well organised and took the form of a fan-shaped meshwork within the leading edge of the cell. Eventually these cells were seen to become less motile which corresponded with an increase in the number and size of stable adhesions. This transition from a motile cell to a stationary one also corresponded with an entry of the cells from G_1 phase, through S phase and into the cell cycle resulting in cell division (Couchman and Rees, 1979; Couchman *et al.*, 1982), and the authors proposed that the stable anchorage of the cell to

3

the substrate involved a re-organisation of actin filaments and was a prerequisite for entry into the division cycle. They also noted that increased expression of the extracellular matrix protein fibronectin by the cells corresponded with reduced motility, suggesting that fibronectin was intimately involved in the stable adhesion of the cell, and therefore cell proliferation. This phenomenon of anchorage-dependent growth was studied in more detail by Dike and Farmer, (1988). They found that Balb/c 3T3 fibroblast cells cultured in suspension were arrested in G_0 phase of the cell cycle. If the cells were then allowed to adhere to a substrate, there was a dramatic increase in the expression of growth-associated genes which was independent of the presence of serum growth factors confirming that cell adhesion was crucial to the growth cycle of cells. Interestingly, virally-transformed cells adhere via small transient adhesions known as podosomes (Tarone *et al.*, 1985), and the cells, rather than showing a reduced growth rate, are seen to proliferate in an uncontrolled manner.

1.3 Components of the cell-matrix junction.

The composition and regulation of the cell-matrix junction in cultured cells has been summarised in several reviews (Burridge *et al.*, 1988; Luna and Hitt, 1992). Biochemical studies carried out on the purified proteins involved in cell-matrix junctions revealed a wide spectrum of interactions between the various proteins, and Figure 1.1 demonstrates just three of the possible ways in which some or all of the proteins could interact to form a link between integrins and the actin cytoskeleton. ECM proteins such as fibronectin interact with the extra-cellular domain of the membrane-spanning integrin receptors, which can then bind via the cytoplasmic tail of the integrin β subunit to the cytoplasmic components of the focal adhesion. The most widely accepted combination involves integrins binding to talin (Horwitz *et al.*, 1986), which interacts with vinculin (Gilmore *et al.*, 1992, 1993), which in turn binds to the actin cross-linking protein α-actinin (McGregor *et al.*, 1994). However, the integrins can also interact with actin via α-actinin

Figure 1.1.Schematic representation of a focal adhesion.
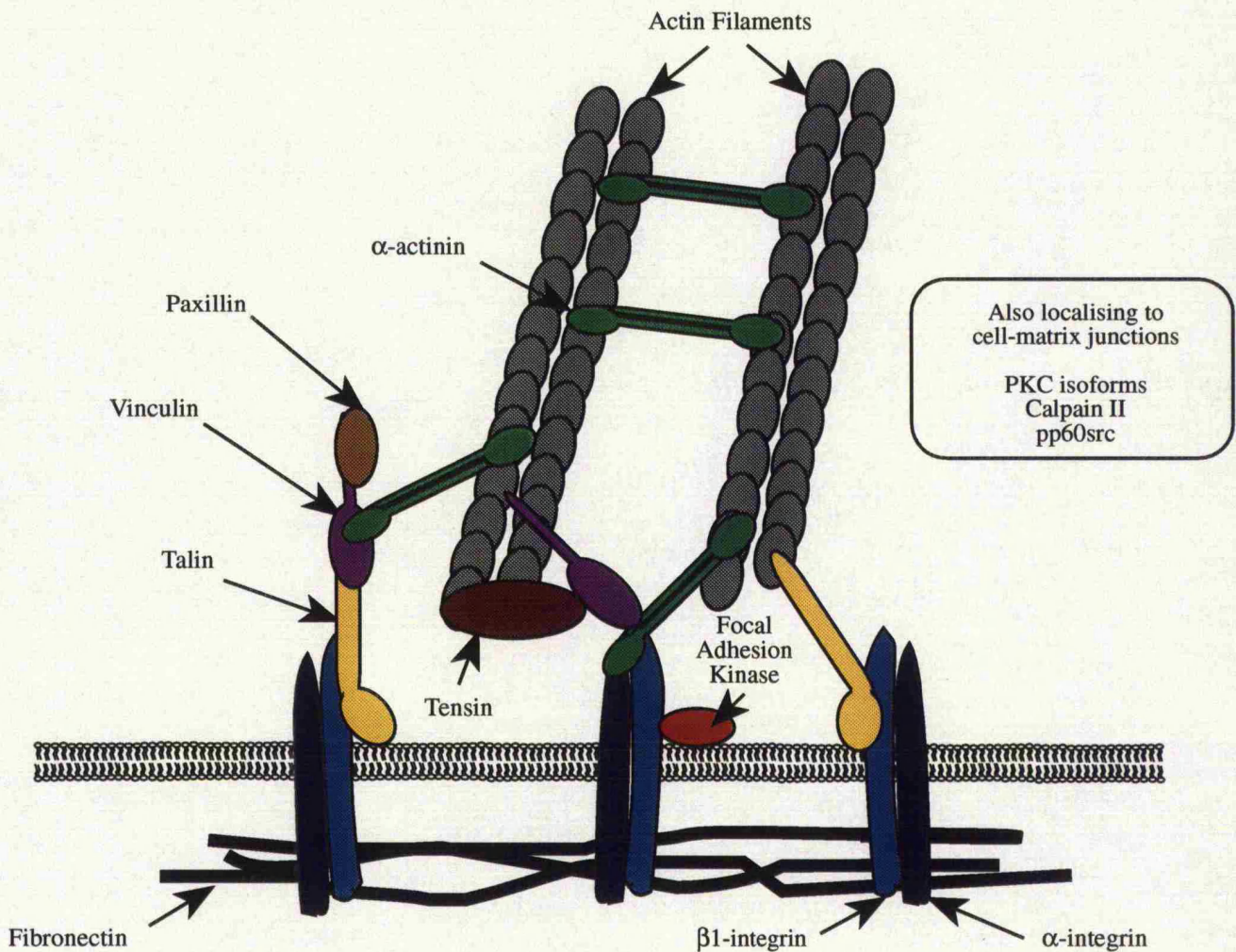
The model shown in the figure has been proposed on the basis of *in vitro* binding experiments carried out on purified components of the focal adhesion and shows three possible linkages from the ECM to the actin cytoskeleton. ECM proteins such as fibronectin can bind to the extracellular domain of the membrane-spanning integrins. The cytoplasmic tail of the β1 integrin can interact with talin, which in turn can bind to vinculin. Vinculin is capable of binding the actin-crosslinking protein α-actinin, which completes one link from the membrane to the actin cytoskeleton. As shown in the diagram, this is not the only combination of proteins that, in theory, can mediate the actin-membrane interaction. Talin and α-actinin can interact directly with both the integrins and actin, and vinculin is also known to bind to the actin binding proteins α-actinin and tensin. Paxillin and pp125FAK are two proteins thought to be involved in regulation of the assembly of the focal adhesion, as well as the enzymes protein kinase-C, Calpain II and the tyrosine kinase activity of the src protein.

(Otey *et al.*, 1993), or talin (Muguruma *et al.*, 1990) as shown in Figure 1.1. The fact that a number of possible linkages between integrins and F-actin can be formed on the basis of the *in vitro* data raises the possibility of redundancy for several proteins and this is discussed later in this chapter. Several focal adhesion proteins such as pp125FAK, paxillin and protein kinase-C (PK-C) have been implicated in the regulation of adhesion and in signal transduction via integrins and this is discussed later in this chapter.

1.4 The extracellular matrix proteins.

The proteins found within the extracellular matrix are large adhesive glycoproteins that can be secreted by fibroblasts. There are many different types of ECM protein including fibronectin, vitronectin, laminin, thrombospondin, von Willebrand factor and several different types of collagen, and a common theme to the structure of all ECM proteins is their modular composition (see Yamada, 1991). This enables a wide spectrum of adhesive interactions to both other ECM proteins, and to cells, to be mediated by a single ECM protein. Conversely, a single integrin receptor present on the cell surface can interact with several different types of ECM protein. Fibronectin is the most widely studied ECM protein and this short discussion will now focus solely on fibronectin. It was initially identified as a Large External Transformation-Sensitive (LETS) glycoprotein that was absent from virally-transformed fibroblast cells which also displayed a concurrent loss of organised actin cytoskeleton (Hynes, 1973). Addition of fibronectin to transformed cells resulted in reversion of the characteristic rounded morphology of these cells to a flatter, more adherent fibroblastic-like phenotype. The fibronectin was seen to be re-organised into a fibrillar matrix extending across the cell surface (Yamada *et al.*, 1976). Fibronectin is important for both the migration of cells (see Hynes and Lander, 1992), and in the formation of stable adhesions required by cells undergoing mitosis (Couchman and Rees, 1979; Woods *et al.*, 1986).

Structure and function of fibronectin.

Fibronectin is a large dimeric glycoprotein comprised of two 250kDa subunits linked by disulphide bonds at the C-terminus. It is seen as a long filamentous molecule via the electron microscope, that can be separated into several proteolytic fragments, each containing specific binding sites as illustrated in Figure 1.2 (Rouslahti, 1988; Potts and Campbell, 1994). Fibronectin consists of three types of repeated motifs, known as fibronectin repeats types 1, 2 and 3. There are two binding sites each for heparin and fibrin, suggesting that fibronectin can cross-link with these two ECM proteins. This is reflected in the ability of fibronectin to interact with fibrin to form a meshlike clot important in wound healing. Fibronectin also has single binding sites for the ECM proteins collagen and gelatin.

Two cell binding domains have also been identified. The central cell-binding domain is composed of type 3 repeats, and the Arg-Gly-Asp-Ser (RGDS) sequence within the tenth type 3 repeat is important to the cell-binding activity observed *in vitro* (Piersbacher and Ruoslahti, 1984). Cultured cells are able to adhere to a substrate composed solely of the RGD peptide although there is a 100 fold decrease in activity compared to the entire cell binding domain. Treatment of cell monolayers with the RGD peptide results in a detachment of cells from the dish, and peptides containing substitutions in the RGD motif were ineffective. This RGD tripeptide motif is common to several other ECM proteins (see Humphries, 1990; Yamada, 1991). Interaction of cells with the RGD sequence is reliant on 2 synergistic sequences found in the 8th and 9th type 3 repeats (Aoti *et al.*, 1991; Nagai *et al.*, 1991). These two domains might also possibly function as independent cell binding domains, but this has not been proven to date.

Two adhesive sequences, CS1 and CS5, were found in the second cell binding domain known as the IIICS region (Humphries *et al.*, 1986, 1987), and either of these peptide

6

Figure 1.2. Schematic representation of the extracellular matrix protein, fibronectin
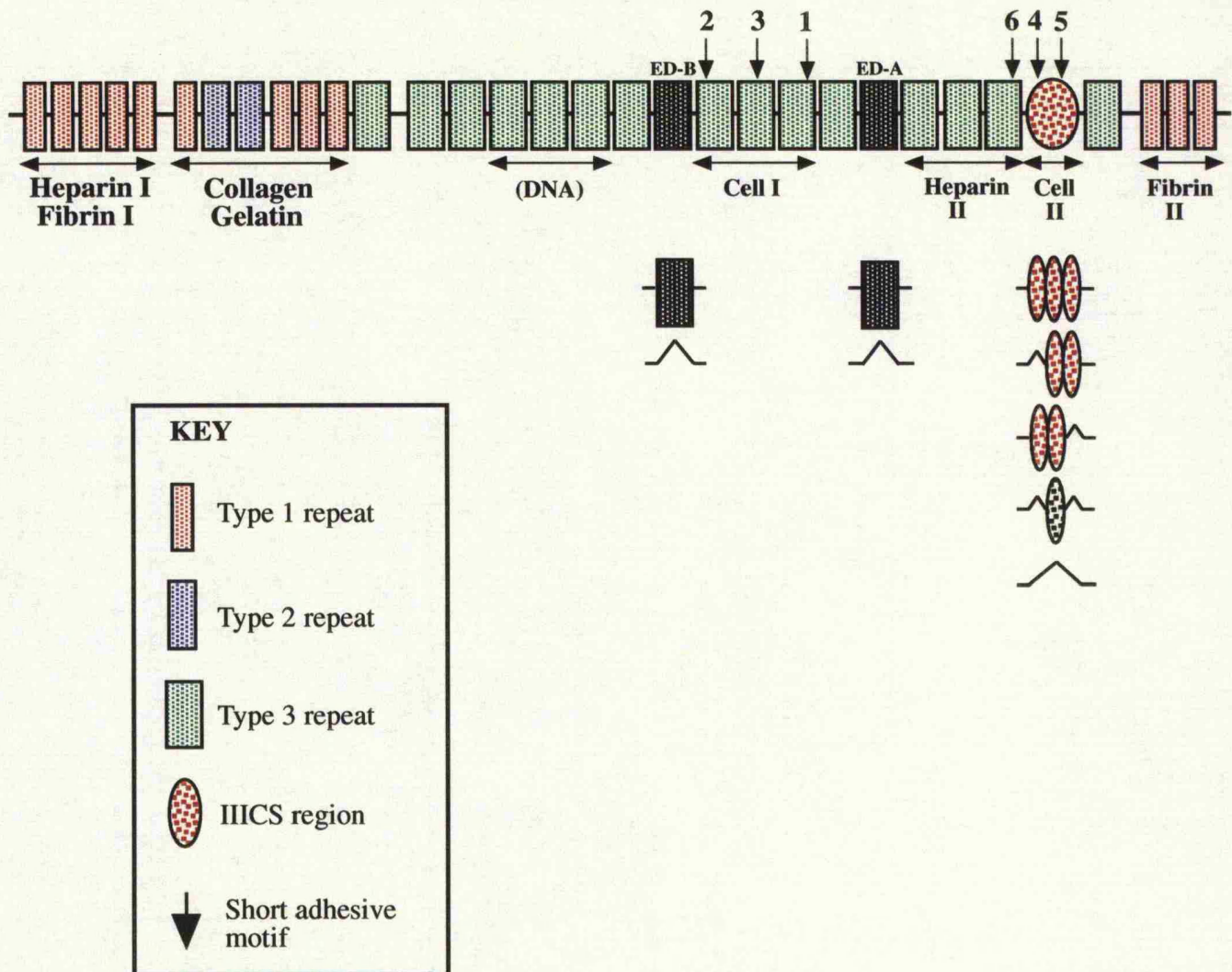
Fibronectin has a modular composition common to all extracellular matrix proteins, and is composed to type 1, 2 and 3 repeats, that combine to form domains that can interact with extracellular matrix proteins as indicated underneath the relevant segment, or to the integrin receptors expressed on the cell surface. Dimerisation can occur via disulphide bridges formed at the C-terminus.There are two cell binding domains - the central cell binding domain (CCBD) and the IIICS domain. Within the CCBD is the RGDS motif (represented by arrow 1), that can interact with integrins, but also requires sequences (arrows 2 and 3) in the flanking type 3 repeats for full activity. Similarly, within the IIICS region is the CS1 domain, containing the LDV tripeptide (arrow 4), and the CS5 region containing an RGD-like motif (arrow 5). Arrow 6 represents at least 2 peptides that can promote adhesion and interact with heparin. The IIICS region is also able to undergo alternative splicing, generating upto 4 variants. Also, two type 3 repeats - ED-A and ED-B, are subject to alternative splicing.

Based on Ruoshlahti, 1988 and Yamada, 1991.

sequences can be omitted in certain fibronectin isoforms by alternative splicing. The CS1 domain contains the Leu-Asp-Val (LDV) tripeptide, and contributes up to 40% of cell-binding activity observed with the full CS1 25mer peptide, implying that there are other helper sequences within this region. The second site, known as the CS5 site, includes the REDV sequence and mediates a much lower affinity interaction.

1.5 The integrin family of cell surface receptors.

The integrin family of proteins consists of transmembrane, heterodimeric receptors that mediate the interaction between two cells, or between cells and the underlying ECM. The first integrin subunit was cloned in 1986 by Tamkun *et al.*, (1986), and to date a further 21 have been identified - 14 α subunits and 8 β subunits (see Humphries, 1990; Hynes, 1987, 1992). Each integrin receptor is composed of one α chain and one β chain, that associate non-covalently to form a functional receptor which spans the cell membrane. The individual subunits can associate in a wide variety of combinations, resulting in an extensive repertoire of both receptors and ligands, which is shown in Table 1.1. It is apparent from the table, that most integrins are extremely versatile as they can recognise more than one ligand, and conversely, each ligand can be recognised by more than one integrin.

Structure and function of the integrin receptor.

There is an abundance of literature about the structural features and functions of integrins, and I shall attempt to summarise only the most relevant points in this next section. Integrins have a large extracellular domain for attachment to ECM proteins or other cell surface receptors, and a smaller cytoplasmic domain for association with proteins at the cytoplasmic face of the membrane. The schematic diagram shown in Figure 1.3 illustrates the domain structure of the two integrin subunits (panel A), and the proposed form of an integrin dimer found in the membrane (panel B). The a subunits vary in size from 120-

7

Table 1.1. Differing combinations of integrin subunits.

β subunit	α subunit	Old Name	Ligand/receptor	Binding motif
β_1	α_1	VLA-1	CO, LM	
	α_2	VLA-2	CO, LM	DGEA
	α_3	VLA-3	FN, LM, CO	RGD
	α_4	VLA-4	FN, VCAM-1	EILDV
	α_5	VLA-5	FN	RGD
	α_6		LM	
	α_7		LM	
	α_8		?	
	α_V		VN, FN	RGD
β_2	α_L	LFA-1	ICAM-1, 2	
	α_M	Mac-1	C3bi,FB,FX,ICAM-1	
	α_X	p150,95	FB, C3bi	GPRP
β_3	α_{IIb}	GPIIb-IIIa	FB,FN,vWB,VN,TS	RGD,KQAGDV
	α_V		VN,FB,vWB,TS, FN,OP,CO	RGD
β_4	α_6		LM?	
β_5	α_V		VN	RGD
β_6	α_V		FN	RGD
β_7	α_4		FN, VCAM-1	EILDV
	α_{IEL}		?	
β_8	α_V		?	

KEY.
C3bi, inactive form of complement protein C3b; CO, collagen; FX, Factor X; FB, fibrinogen; FN, fibronectin; ICAM-1, 2, Inter cellular adhesion molecule 1 and 2; LM, laminin; OP, osteopontin; TS, thrombospondin; VCAM-1, vascular cell adhesion molecule 1; VN, vitronectin; vWB, von Willebrand factor

Figure 1.3. Schematic representation of integrin structure.
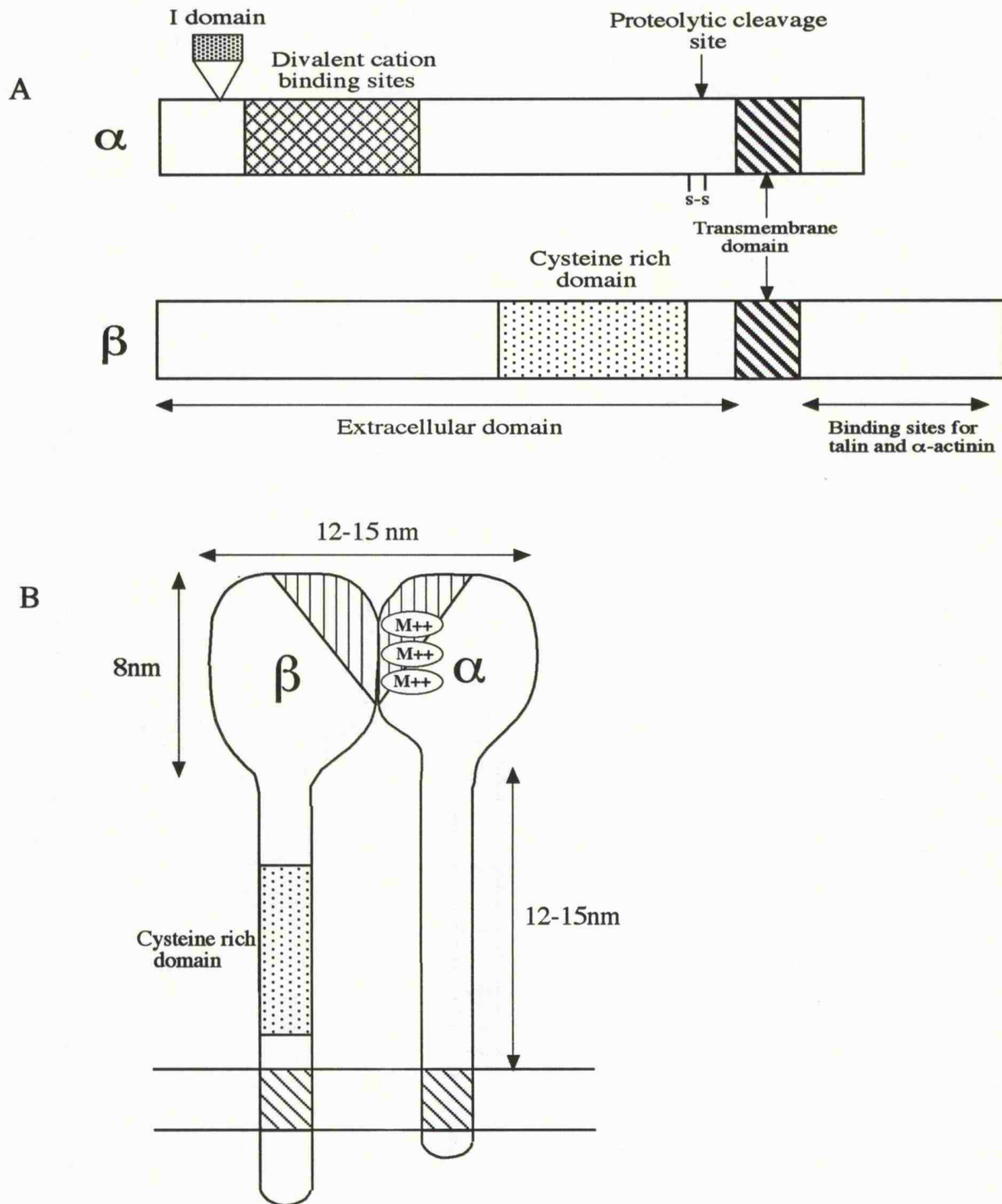
Panel A shows the domain structure of the two integrin subunits. The α subunit does not appear to interact with any cytoplasmic components. The I domain found in the extracellular portion of the molecule is possibly involved in determining ligand specificity. The β subunit is able to interact with two cytoplasmic components of adhesion plaques - talin and α-actinin, that form the link to the actin cytoskeleton.

Panel B represents the possible structure of the functional receptor found in the membrane. The ligand binding site is formed from the extracellular domains of both subunits, and incorporates a cation-binding site, that is important for ligand affinity and specificity.

From Hynes, 1992.

180kDa, whilst the β subunits are somewhat smaller, ranging from 90-110kDa. Both subunits contain a large extracellular domain which form the ligand-binding site following subunit dimerisation. Experiments carried out by Bodary et al., (1991) revealed that removal of either the cytoplasmic or the transmembrane domains did not affect the ability of the mutant integrins to dimerise and Solowska et al., (1989) demonstrated that deletion of the cytoplasmic tail of the integrin reduces its ability to localise to focal adhesions.

The ligand-binding site within the extracellular domain of the α chain is known to be in close proximity to the cation binding sites (D'Souza et al., 1990), and a 7-fold repeated motif within this region is thought to be involved in binding these divalent cations. Presence of such cations have been shown to affect the specificity of an integrin for a given ligand (Elices et al., 1991; Kirchofer et al., 1991). A segment of around 180 amino acids may be inserted into the α chain in the region containing the cation-binding site, and this so-called I domain has been demonstrated to be involved in the selective recognition of either ICAM-1 or ICAM-3 by the LFA-1 integrin (Landis et al., 1994). Truncation of the cytoplasmic face of the α subunit has been shown to interfere with the recruitment of integrins to focal contacts (Ylanne et al., 1993), and different α subunits can alter the distribution patterns of certain integrins (Tawil et al., 1993).

Residues 100-200 within the extracellular domain of the β subunit, are directly involved in ligand binding (Smith and Cheresh, 1988, 1990), and removal or alteration of residue 119 is able to abolish ligand-binding (Loftus et al., 1990). The 47 amino acid cytoplasmic tail of the β subunit is responsible for interactions within the cell and removal of amino acids from the extreme carboxyl terminus of the tail (Hayashi et al., 1990) or expression of the β3B subunit which contains a modified cytoplasmic domain generated by alternative splicing (LaFlamme et al., 1994) results in integrins that are able form heterodimers, but cannot support adhesion or localise to focal contacts. This C-terminal tail of the β1 integrin

8

has been shown to support interactions with cytoplasmic focal adhesion proteins talin (Horwitz *et al.*, 1986), and has two binding sites for α-actinin (Otey *et al.*, 1990a, 1993).

As a consequence of mediating cell-cell and cell-matrix interactions, integrins are also known to play a role in a variety of cellular functions such as cell spreading (Tawil *et al.*, 1993; Ylanne *et al.*, 1993), and cell migration (Regen and Horwitz, 1992; LaFlamme *et al.*, 1994). Cell function can be affected by several factors that influence integrins such as the presence of cations as discussed previously. For example, adhesion and migration of human umbilical vein endothelial cells (HUVECs) on vitronectin via αvβ3 requires an external calcium source, whereas migration on collagen via α2β1 does not (Leavesley *et al.*, 1993). Integrins can also mediate interactions with different ECM proteins depending upon the cell type that they are expressed in. For example the VLA2 integrin receptor is able to bind collagen when expressed in certain cell types, but it can bind both collagen and laminin when expressed in other cell types (Elices and Hemler, 1989). *In vivo* integrin-mediated cell-cell interactions are important in the response of various cell types to inflammation or injury, and are crucial to the recruitment of leucocytes to these areas of inflammation (see Springer, 1990).

Integrins are known to be substrates for virus-encoded kinases (Hirst *et al.*, 1986), and phosphorylation of integrins is known to affect cell adhesion, integrin expression (Plantefaber and Hynes, 1989), and integrin distribution (Johansson *et al.*, 1994). Interestingly, integrins isolated from RSV-transformed CEF were also shown to exhibit a decreased affinity for talin and fibronectin *in vitro* (Tapley *et al.*, 1989). Adhesion of fibroblasts to ECM proteins such as fibronectin via integrins, or cross-linking of integrin receptors using antibodies is known to cause an increase in tyrosine phosphorylation of a specific subset of proteins that are involved in signal transduction pathways and this aspect of integrin function is discussed in more detail later in this chapter.

9

1.6 Talin.

The cytoskeletal protein talin is encoded by 8.2kb of RNA message that generates a protein of 2541 amino acids (Rees *et al.*, 1990) and the gene for human talin has recently been mapped to chromosome 9p (Gilmore *et al.*, in press). Talin has been shown to localise to the focal adhesions, membrane ruffles and the leading lamellae of cultured fibroblast cells (Burridge and Connell, 1983a, b; DePasquale and Izzard, 1991; Hock *et al.*, 1989). Talin is also a major component of platelets (O'Halloran *et al.*, 1985), and is also found in the myotendinous junction of skeletal muscle cells (Tidball *et al.*, 1986). Talin was first isolated from human platelets, and by SDS-PAGE, has an apparent molecular mass of 235kDa (Collier and Wang, 1982), whereas talin isolated from chicken gizzard smooth muscle has an apparent molecular mass of 215-225kDa (Burridge and Connell, 1983a; Molony *et al.*, 1986), although there is no apparent difference between the two talin molecules.

Talin Structure.

A schematic representation of talin is shown in Figure 1.4, and attempts to summarise the structural information obtained to date for mouse and/or chick talin. The full length protein (2541 amino acids) can be cleaved between residues 433 and 434 by the calcium-dependent protease, Calpain II, to generate a 47kDa head and a 190kDa tail fragment (Beckerle *et al.*, 1987). Electron microscope (EM) studies by Molony *et al.*, (1987) revealed talin to be a monomeric protein, which is composed of a globular head and a long flexible tail, and further studies by McLachlan *et al.*, (1994) demonstrated that the rod-like tail consisted of an alanin-rich repeated motif sequence of around 32 amino acids. Talin is known to bind to actin and it appears that talin, viewed by the EM, takes the form of an anti-parallel dimer when interacting with actin *in vitro* (Goldmann *et al.*, 1994). Analysis of the mouse sequence by Rees *et al.*, (1990) showed that the first 600 residues contain

Figure 1.4. Schematic representation of talin domain structure, and the regions of homology with other actin-binding proteins.
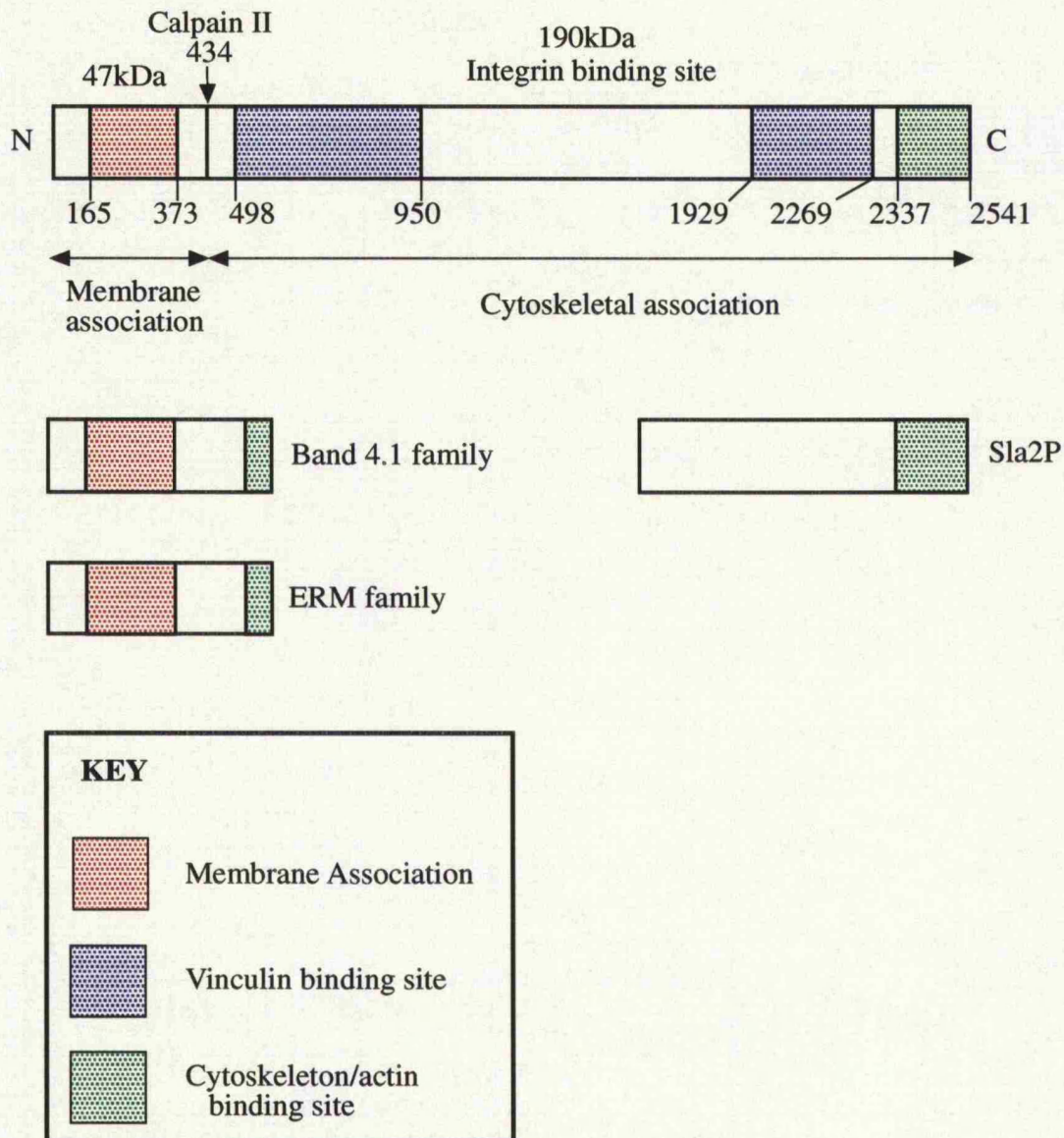
Talin can be cleaved between residues 433 and 434 by Calpain II to generate a 47kDa and a 190kDa fragment. Talin also displays homology with the band 4.1/ERM family of proteins and the relative positions of the regions responsible for either membrane or cytoskeletal interactions, that are a recurring theme in this family of proteins, are illustrated. The 47kDa fragment is known to be responsible for localisation of talin to cell-matrix junctions, and there is possibly a putative membrane interaction site in this region, though this has not been identified. The 190kDa fragment contains binding sites for 3 other cytoskeletal components of the adhesion plaque. The three vinculin binding sites have been defined as illustrated, but the site capable of interacting with integrins has not yet been characterised. Talin also has limited homology with the yeast actin-binding protein Sla2 as shown at the C-terminus, and the actin-binding capacity of talin would appear to reside in this region of the protein.

28% charged residues, and the last 1,900 residues are enriched in alanine residues (18%). Greater then 30% of the last 60 residues are highly charged.

Talin is excluded from cell-cell junctions (Geiger *et al.*, 1985), and the N-terminus of the protein has been proposed to be responsible for the exclusive incorporation of talin into cell-matrix junctions as opposed to cell-cell junctions. Nuckolls *et al.*, (1990) fluorescently tagged both the 47kDa and 190kDa fragments of chick talin and microinjected them into fibroblasts and epithelial cells. The 47kDa fragment localised to only the focal adhesions in either fibroblasts or epithelial cells i.e. displayed a similar distribution to intact talin. The 190kDa fragment was also found in focal adhesions in both fibroblasts and epithelial cells, but it was also clearly seen to localise to the cell-cell junctions formed between the epithelial cells. These experiments imply that both the 47kDa fragment and 190kDa fragment contain sites that can target talin to focal adhesions, but the 47kDa also contains an additional region that is responsible for restricting intact talin exclusively to cell-matrix junctions. There is also considerable evidence that the N-terminal fragment of talin is responsible for a direct interaction between talin and the plasma membrane and this is discussed later in this section.

The 190kDa fragment has been shown to support interactions with integrins (Horwitz *et al.*, 1986), vinculin (Burridge and Mangeat, 1984; Gilmore *et al.*, 1993) and actin (Muguruma *et al.*, 1990, 1992; Kaufmann *et al.*, 1991). Horwitz *et al.*, (1986) pre-equilibrated gel filtration columns with either intact talin or the 190kDa fragment, and integrins were passed through the column. The elution profile of the integrins was altered indicating that the two proteins were interacting. Inclusion of the fibronectin RGDS tetrapeptide did not affect the elution profile of the integrins from the talin column, indicating that integrins have separate binding sites for fibronectin and talin. Similar experiments demonstrated that talin could also interact with vinculin using a different

11

binding site to that which binds integrins. Surprisingly, neither Western blot overlay-type assays nor sedimentation experiments were able to confirm this interaction. More recently, Simon and Burridge, (1991) used a solid phase *in vitro* binding assay to show a direct interaction between the 47 amino acid cytoplasmic tail of β1 integrin and both intact talin and the 190kDa fragment, but not the 47kDa fragment of talin.

Talin was first shown to bind vinculin by Burridge and Mangeat, (1984). This interaction was further analysed by Gilmore *et al.*, (1993) using both *in vitro* binding assays, and expression of truncated talin cDNAs in fibroblast cells. These experiments defined two separate regions of talin that were capable of binding to residues 1-258 in the head region of vinculin. The first region lies between talin residues 498 and 950 and appears to contain two binding sites. The third site lies between residues 1304-2269, although subsequent experiments have further defined this site to residues 1929-2069 (Gilmore and Critchley, unpublished observations). However, the experiments described in Chapter 5 illustrate that residues 2269-2541 are capable of binding to vinculin in a blot overlay-type assay, suggesting that there is possibly a fourth binding site. Expression of various talin cDNAs in both Cos and NIH3T3 cells revealed that ability to bind to vinculin, corresponded with an ability to localise to focal adhesions (Gilmore *et al.*, 1993). Experiments by Johnson and Craig, (1994) demonstrated that the association between talin and the vinculin head can be modulated by an intra-molecular interaction between the head and tail portions of vinculin.

The interaction of talin with actin has been demonstrated by several different groups. Muguruma *et al.*, (1990) demonstrated that both intact talin and the 190kDa fragment could co-sediment with F-actin. Whole talin was able to interact directly with G-actin using a gel filtration technique, and was also seen to increase the polymerisation rate of G-actin into filaments. Results obtained by Kaufmann *et al.*, (1992), and Niggli *et*

al., (1994) confirmed this interaction, and demonstrated that talin promotes actin polymerisation via a nucleating activity. Talin was also able to increase the ability of α-actinin to induce actin gelation by forming talin oligomers and crosslinking the actin filaments although it is not able to interact directly with the α-actinin (Muguruma *et al.*, 1992). Chapter 5 of this thesis describes experiments that have defined an actin-binding site within the C-terminus of talin between residues 2269-2541.

Homology of talin to the band 4.1 family of proteins and a yeast actin-binding protein.

Band 4.1 is one of a number of proteins that mediate the interaction between the erythrocyte cytoskeleton and the membrane (reviewed in Luna and Hitt, 1992; Hitt and Luna, 1994). Band 4.1 is able to bind to the integral membrane proteins glycophorin C (Anderson and Lovrien, 1984), and band 3 (Pasternack *et al.*, 1985) via separate binding sites at the N-terminus, and to cytoskeletal proteins via the C-terminus (Discher *et al.*, 1993). Studies by Shiffer and Goodman, (1984) demonstrated that band 4.1 could associate with the purified membrane components of erythrocytes *in vitro*, and recent studies by Marfatia *et al.*, (1994) have demonstrated a direct association of the N-terminus of band 4.1 with the peripheral membrane phospholipid p55 and glycophorin C. Sequence analysis has revealed a number of other proteins which display varying degrees of sequence identity with the N-terminus membrane-interacting domain of band 4.1 (see Figure 1.4, reviewed in Algrain *et al.*, 1993a; Arpin *et al.*, 1994) including ezrin (Gould *et al.*, 1989), radixin (Funayama *et al.*, 1991), moesin (Lankes and Furthmayr, 1991), two protein tyrosine phosphatases (Yang and Tonkes, 1991; Gu *et al.*, 1991) and the recently identified product of the NF2 tumour suppressor gene, known as MERLIN or schwannomin (Rouleau *et al.*, 1993; Trofatter *et al.*, 1993). Ezrin, radixin and moesin have now been classified as a separate subfamily known as the E(ezrin)R(radixin)M(moesin) family as they display greater than 75% amino acid identity.

In particular, ezrin has been shown to contain a membrane interaction site at the N-terminus of the protein (Algrain *et al.*, 1993b), and an actin-binding site at the C-terminus (Turunen *et al.*, 1994), and both of these properties are considered to be a common feature of proteins included in this band 4.1/ERM superfamily.

Talin has been included in this band 4.1/ERM superfamily as the N-terminal residues from 165-373 display 23% sequence identity with ezrin (residues 49-261), and 20% identity with band 4.1 (residues 47-245). There is plenty of evidence that talin can interact with lipids or lipid analogues and insert into lipid bilayers under a variety of *in vitro* conditions (Heise *et al.*, 1991; Goldmann *et al.*, 1992; Dietrich *et al.*, 1993), and this activity has been shown to be particular to the 47kDa N-terminal fragment of talin (Niggli *et al.*, 1994). Also, talin has been shown to redistribute to the membrane in an integrin-independent fashion in thrombin-stimulated platelets taken from patients with Glanzmann's thrombasthenia which lack the GPIIb-IIIa integrins (Bertagnolli *et al.*, 1993). Chapter 5 of this thesis describes the localisation patterns obtained following microinjection of two N-terminal fragments of talin into fibroblasts, which closely resemble the distribution pattern seen in cultured cells of the N-terminal ezrin polypeptide containing the putative membrane-interaction site (Algrain *et al.*, 1993b). Similarly, there is evidence for the presence of an actin-binding site at the C-terminus of talin as this region displays limited sequence identity with the recently-identified yeast actin-binding protein Sla2 (Holtzman *et al.*, 1992). Figure 1.5.shows the alignment of the two C-terminal protein sequences and it is interesting to note that the actin-binding site in ezrin did not reveal any sequence similarities to either talin or Sla2. To confirm this hypothesis, the presence of an actin-binding site within residues 2269-2541 of talin has been confirmed by the experiments detailed in Chapter 5.

Figure 1.5. Comparison of the C-terminal amino acid sequence of murine talin with the yeast actin binding protein Sla2.

```
Mu. Talin  ..LNFEEQIL  EAAKSIAAAT  SALVKAASAA  QRELVAQGKV  GAIPANALD.  2385
                 :      :|   |   |   |    ||||||    | |:
      Sla2  LRVDVPKPLL  SLALMIIDAV  VALVKAAIQC  QNEI..ATTT  SIPLNQFYLK  810


Mu. Talin  DGQXSQGLIS  AARMVAAATN  NLCEAANAAV  QGHA....SQ  EKLISSAKQV  2431
             |: ||||  ||: || |||   |:  |   :        |    | |   | |
      Sla2  NSRXTEGLIS  AAKAVAGATN  VLITTASKLI  TSEDNENTSP  EQFIVASKEV  861


Mu. Talin  AASTAQLLVA  CKVKADQDSE  AMKRLQAAGN  AVKRA....S  DNLVKAAQKA  2477
           |||| ||: |    :||   |   |  :|       | |         . .
      Sla2  AASTIQLVAA  SRVKTSIHSK  AQDKLEHCSK  DVTDACRSLG  NHVMGMIEDD  911


Mu. Talin  AAFEDQENET  VVVKEKMVGG  IAQIIAAQEE  MLRKERELEE  ARKKLAQIRQ  2527
                |                    :   | |   :|: | |    |||:|  ||
      Sla2  HSTSQQQQPL  DFT..SEHTL  KTAEMEQQVE  TLKLEQSLSN  ARKRLGEIRR  959


Mu. Talin  QQYKFLPSEL  RDEH 2541
                |      :
      Sla2  HAYYNQDDD       968
```

Comparison of the extreme N-terminal amino acid sequence of murine talin and the yeast actin-binding protein, Sla2. Identical residues ares indicated by a solid line and conservative changes are indicated by a colon.

Modified from Holtzman *et al.*, 1993.

Functions of talin.

Talin is one of a number of proteins involved in mediating cytoskeleton-membrane interactions both in cultured cells and *in vivo*, e.g. myotendinous junctions and platelets. The experiments described above on the band 4.1/ERM superfamily of proteins strongly suggest that talin may be also involved in directly linking the actin cytoskeleton and the cell membrane. It is known that talin can bind to actin and promote the polymerisation of the actin filaments in the focal adhesion precursor, but as yet no membrane interaction site has been identified. DePasquale and Izzard, (1991) observed that vinculin was not present in focal adhesion precursors, but was recruited into the maturing adhesion after talin, implying that talin may help to initiate assembly of the focal adhesion by recruiting both actin and vinculin. Further experiments that support the theory that talin is involved in the assembly of focal adhesions come from experiments carried out by Nuckolls *et al.*, (1992). They found that microinjection of an anti-talin polyclonal antibody into migrating CEF cells was sufficient to inhibit any subsequent cell migration i.e. the cell was unable to assemble new focal adhesions. Also, injection of the same antibody into freshly-plated CEF cells was able to impair the subsequent spreading of the cell, whereas injections into well-spread cells did not perturb the focal adhesion or stress fibre integrity indicating that talin was involved in the formation but not maintenence of focal adhesions.

Regulation of talin function.

Several studies regarding the regulation of talin function have been carried out in platelets in which talin is a major cytoplasmic protein. Talin is a known substrate for Calpain II, cleaving it into a 47kDa and a 190kDa fragment (Collier and Wang, 1982). Following activation of platelets by e.g thrombin, there is an increase in Calpain II activity and a rapid re-organisation of the actin cytoskeleton. This is accompanied by alteration in cell shape resulting in highly adhesive platelet cells that are required for clot formation. Talin is subsequently redistributed from the cytoplasm to the cytoplasmic face of the membrane

15

following platelet activation though exactly how generation of the two talin fragments by Calpain II aids this re-organisation is unclear (Beckerle *et al.*, 1989). Interestingly, Calpain II is also found within focal adhesions suggesting that cleavage of talin may play a similar role in the re-organisation of the actin cytoskeleton in cultured cells (Beckerle *et al.*, 1987). However, experiments by Bertagnolli *et al.*, (1993) demonstrated that the redistribution of talin in thrombin-activated platelets can occur independently of the GPIIb-IIIa platelet integrin, and does not involve cleavage of talin by the Calpain II protease. There was, however, a concurrent four fold increase in tyrosine phosphorylation suggesting that this is an alternative mechanism by which platelets control talin distribution and function. The involvement of tyrosine phosphorylation of talin function in platelets was also studied by Guinebault *et al.*, (1993), who demonstrated that treatment of human platelets with tyrosine kinase inhibitors was able to significantly inhibit platelet activation and aggregation. Also, the 47kDa fragment of talin has been shown to be a substrate for protein kinase P and protein kinase C in leucocytes prepared from patients suffering from acute myelogenous leukaemia although the physiological relevance of this phosphorylation event is still unclear (Simons and Elias, 1993).

There is also substantial evidence that phosphorylation can affect talin function in cultured cells. Talin is known to be a phosphoprotein (Burridge and Connell, 1983a) and is a substrate for tyrosine kinases encoded by viral oncogenes (Pasquale *et al.*, 1986). Tyrosine phosphorylation of talin in virally-transformed cells (DeClue and Martin, 1987), or serine phosphorylation by PK-C in phorbol ester-treated fibroblast cells (Turner *et al.*, 1989), corresponds to a reduction in cell adhesion and disorganisaton of both actin cytoskeleton and focal adhesion integrity. Turner *et al.*, (1989) also demonstrated that talin was not proteolytically cleaved during the events that resulted in a reduction in cell adhesion. In skeletal muscle, platelet-derived growth factor (PDGF) is also known to induce a rapid, but transient dissociation of actin stress fibres and vinculin from the

16

membrane, but the distribution of both talin and the β1 integrin subunit are unaffected and both displayed increased levels of phosphotyrosine (Tidball and Spencer, 1993). The observation that talin and integrins are retained at the membrane following phosphorylation, whilst vinculin was released may well suggest that phosphorylation of talin only affects the talin-vinculin interaction. Presumably, the perturbation of the vinculin-talin interaction results in disintegration of the focal adhesion and associated actin stress fibres. Agents such as phorbol esters and PDGF can lead to a rise in intracellular calcium concentrations, but there is no evidence that this activates Calpain II leading to talin cleavage in either of the experiments discussed above.

The experiments outlined above indicate that the cell can control talin function via at least two mechanisms. Tyrosine/serine/threonine phosphorylation and possibly cleavage of talin by Calpain II appears to promote cell adhesion and cytoskeletal reorganisation in platelets. Conversely, phosphorylation is implicated in the breakdown of membrane-cytoskeleton interactions in both cultured cells and skeletal muscle.The reasons behind this difference in response to Calpain II and phosphorylation *in vitro* compared to *in vivo* is unclear.

Talin as a putative tumour suppressor protein.

Talin has been implicated as a possible tumour suppressor protein, and there are two separate pieces of evidence for this theory. First, talin is known to share limited sequence identity with the the band 4.1/ERM family of proteins, which includes the newly-identified product of the NF2 tumour suppresor gene product (see above and Algrain *et al.*, 1993a; Arpin *et al.*, 1994). Secondly, Wistar Furth (WF) rats, which were initially studied due to the high incidence of tumours, were also observed to display abnormal differentiation of the megakaryocytes into platelets, suggesting a defect in the normal membrane-cytoskeleton function (Jackson *et al.*, 1992). A unique point mutation was

17

identified in the talin gene and was proposed to be responsible for the defective platelet formation (Jackson *et al.*, 1993), although the relationship between this and the high incidence of tumours is unclear. Both these examples would suggest that talin, and possibly other members of the band 4.1 superfamily might be regarded as possible tumour suppressors.

1.7 Vinculin.

Vinculin is a 1066 amino acid, 130kDa protein (apparent molecular mass of 117kDa) that was originally identified as a contaminant during the isolation of the actin-binding protein α-actinin (Geiger and Singer, 1979). Vinculin has been shown to localise to focal adhesions at the tips of actin stress fibres as demonstrated by immunofluorescence, IRM and microinjection of the intact protein (Geiger, 1979; Burridge and Feramsico, 1980). Studies by Geiger, (1981) indicated that in well-spread cells only 10% of vinculin protein was found in focal adhesions with the remaining 90% forming a cytosolic pool. Vinculin is also found in the myotendinous junction of skeletal muscle (Shear and Bloch, 1985), dense plaques in smooth muscle (Small, 1985), and dense bodies in the muscle wall of nematodes (Barstead and Waterston, 1989) where it forms part of a complex to anchor actin fibres to the membrane. Vinculin has also been found in the actin-associated cytoskeleton of neutrophils (Yuruker and Niggli, 1992), and platelets (Vostal and Shulman, 1993) where it is thought to aid in the reorganisation of the actin cytoskeleton following cell activation.

Vinculin stucture.

The full length cDNA sequence for chick (Price *et al.*, 1987; Coutu and Craig, 1988; Price *et al.*, 1989) and human vinculin (Weller *et al.*, 1990) have been published, but only a small portion (residues 345-1402) of the mouse cDNA has been isolated (Ben-Ze'ev *et al.*, 1990). Both the chick and human cDNAs consist of 3198 base pairs of coding

sequence, resulting in a protein of 1066 amino acids, and there are high levels of identity (>80%) at both the nucleic acid and the protein level between the different species. The vinculin gene is found on chromosome 10q11.2qter (Weller *et al.*, 1990) and is comprised of 22 exons. Exon 19 can be alternatively spliced to generate the larger isoform known as metavinculin. A serum-response element was also located within the promoter of the vinculin gene (Moiseyeva *et al.*, 1993).

The vinculin protein has been well studied and is now known to interact with at least four other cytoskeletal components of focal adhesions. Individual functions have been assigned to discreet regions of the protein, as well as the identification of key amino acids within the protein that represent proteolytic cleavage sites and possible phosphorylation sites, and this information is summarised in Figure 1.6. The V8 protease is responsible for cleaving the protein into a 95kDa globular head and a 32kDa tail region. Recently, Johnson and Craig, (1994) demonstrated that the head and talin of vinculin could interact with each other and that this self-association modulated the talin binding activity located in the 95kDa head region of the molecule. They demonstrated that residues 884-1066 of the vinculin tail were able to protect the head from cleavage with the V8 protease. Similarly, residues 1013-1043, expressed as a GST-fusion protein, were able to co-precipitate with the 95kDa globular head of vinculin and this interaction competes with talin for a binding site in the head region. This intramolecular interaction between the head and tail region of vinculin has subsquently been shown to affect the association of intact vinculin with both α-actinin (Kroemker *et al.*, 1994) and F-actin (Johnson and Craig, 1995).

Burridge and Mangeat, (1984) were the first to show a direct interacton between vinculin and talin, using both sucrose density gradients and blot overlay-type assays. Quantitative analysis of the data indicated a high affinity interaction, with an apparent K_d of $10^{-8}M$ with the possibility of a second, lower affinity binding site within talin. This interaction

Figure 1.6. Schematic representation of vinculin domain structure.
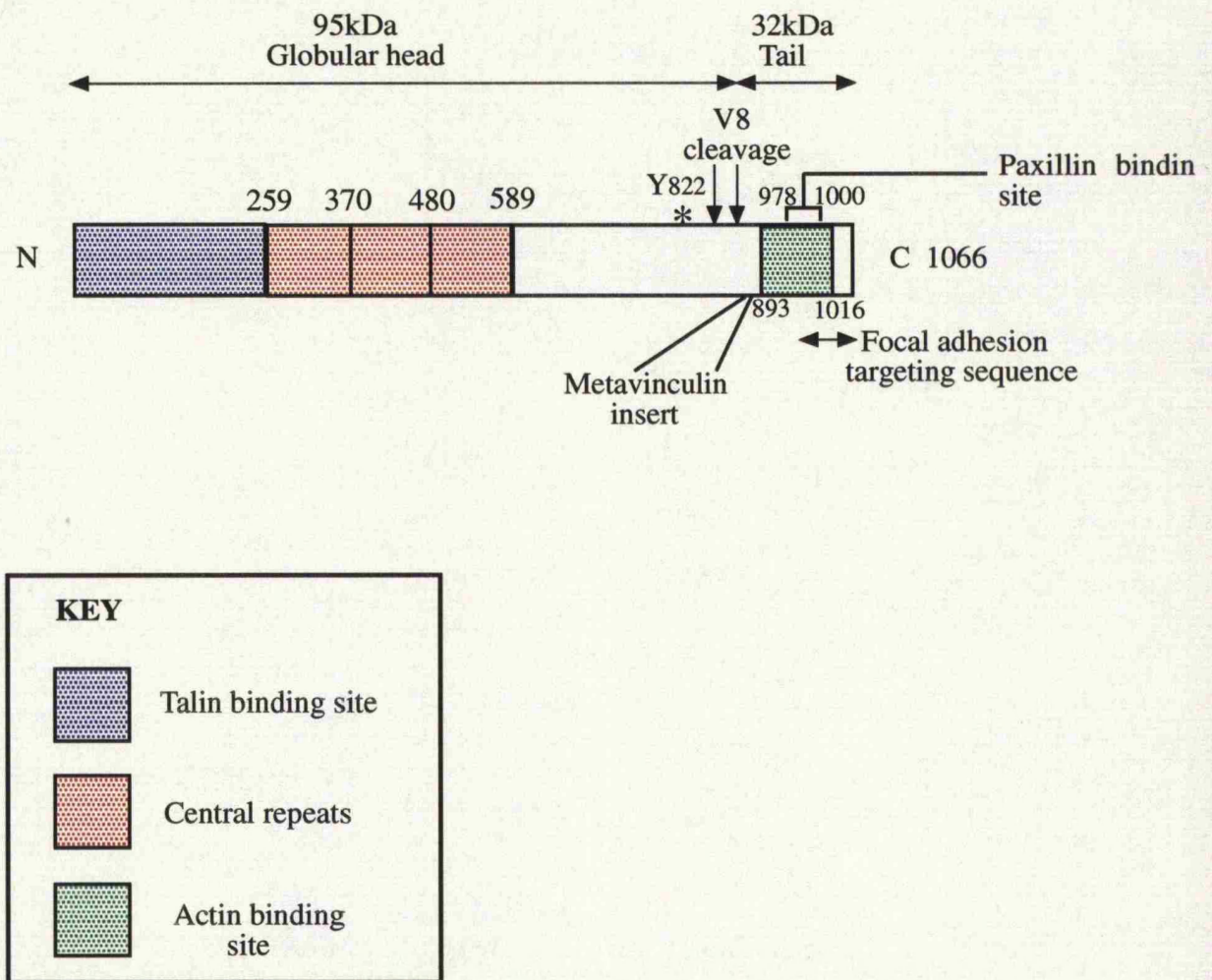
The diagram shows the relative positions of the different domains so far identified within the vinculin protein. The talin binding activity is restricted to the N-terminal 258 residues, and residues 167-207 are known to be crucial to binding, although they are also dependent on surrounding residues. Also within this region is a separate focal adhesion targeting sequence although this has not been clearly defined. At the C-terminal, residues 893-1016 appear to support an actin binding site, whilst residues 978-1000 can interact with paxillin. There is also a separate focal adhesion targeting sequence at this C-terminus, from residues 1000-1028. The function of the three identical central repeats is still unclear. There are two V8 cleavage sites at residues 851 and 858, which are flanked on either side by proline residues. There is also a putative phosphorylation site within this region at tyrosine residue 822.

was confirmed by Jones *et al.*, (1989) and Gilmore *et al.*, (1992), who defined the talin binding activity to residues 1-258 in the globular vinculin head. Deletion of vinculin residues 167-207 eliminated the ability of vinculin to bind talin *in vitro* and to localise to cell-matrix junctions. However, residues 167-207 were not able to support an interaction with talin alone and residues within 1-166 were required for this interaction *in vitro*. Also, expression of the same truncated vinculin cDNAs in mammalian cells indicated that the ability to bind to talin *in vitro* is mediated by a separate region of the protein than that which is responsible for targeting vinculin to focal adhesions. It is worth noting that the coding region for residues 167-207 is contained entirely on exon 5, implying that a vinculin variant lacking talin binding activity could be generated by alternative splicing.

Vinculin has been shown to interact directly with actin (Jockusch and Isenberg, 1981; Isenberg *et al.*, 1982, Wilkins and Lin, 1982), although much of this controversial data has since been attributed to contaminants in the vinculin preparation made fom chicken gizzard (Wilkins and Lin, 1986, Wilkins *et al.*, 1986). Both Evans *et al.*, (1984), and Wilkins and Lin, (1986), demonstrated that highly purified vinculin could not interact with actin. However, experiments carried out by Westmeyer *et al.*, (1990) showed that an anti-vinculin monoclonal antibody could inhibit the binding of vinculin to actin *in vitro*, but this antibody had no effect on actin stress fibre integrity when microinjected into fibroblast cells. Once again, the experiments were carried out using vinculin purified from chicken gizzard, but the authors concluded that the extent of actin binding observed was very unlikely to be attributable to contaminants which were not even visible on a Coomassie-stained polyacrylamide gel. Further experiments by Menkel *et al.*, (1994) used an actin co-sedimentation assay performed with vinculin deletion mutants expressed as fusion proteins to demonstrate that the actin-binding site lay between residues 893-1016 in the tail region of the vinculin protein. Microinjection of this polypeptide into fibroblast and epithelial cells was also seen to decorate stress fibres, and other actin-containing

structures. The experiments were performed with vinculin constructs expressed as maltose binding protein-fusion proteins which eliminated the possibility that any actin-binding activity was due to the presence of the contaminants previously found in the chicken gizzard preparations of vinculin. Co-sedimentation experiments by Johnson and Craig, (1995) using both intact vinculin and the purified head and tail domains demonstrated that the actin binding site in vinculin is cryptic and is therefore masked by the recently demonstrated intramolecular association of the vinculin head with its tail. This significant finding would appear to partly resolve the previous controversy surrounding the interaction between vinculin and actin *in vitro*. The authors also propose that the association of vinculin, via it's head region, with talin in the newly-forming focal adhesion serves to unfold the intact protein thus exposing the actin binding site present in the tail of vinculin leading to the recruitment of actin filaments to the focal adhesion.

The C-terminus of vinculin has also been demonstrate to support an interaction with paxillin, a recently identified focal adhesion protein (Turner *et al.*, 1990), and also contains a separate focal adhesion targeting sequence (Wood *et al.*, 1994). Using GST fusion proteins, a range of vinculin deletion mutants were expressed and their ability to bind [125]-I paxillin was assessed. The minimum region of vinculin able to bind to paxillin was found to lie within residues 978-1000. Expression of the vinculin-GST polypepetides in both Cos and NIH3T3 cells were carried out and demonstrated that residues 1000-1028 were also capable of targeting vinculin to focal adhesions.

Vinculin has also been demonstrated to mediate an interaction with the actin crosslinking protein, α-actinin. Experiments using a variety of *in vitro* binding techniques by both Belkin *et al.*, (1987), and Wacchstock *et al.*, (1987) confirmed the interaction between vinculin and α-actinin. More recently, Kroemker *et al.*, (1994) employed a blot overlay-type assay to demonstrate that residues 1-107 in the N-terminal head region of the vinculin

protein are responsible for the vinculin/α-actinin interaction. Conversely, McGregor *et al.*, (1994), also using a blot overlay-type assay, demonstrated that the vinculin binding site in α-actinin lay between residues 713-749. The experiments described above demonstrate that vinculin is capable of binding to four different focal adhesion proteins - talin, actin, paxillin and α-actinin, as well as to itself.

Function of the vinculin protein.

Vinculin is found *in vivo* in both smooth muscle (Small, 1985) and skeletal muscle (Shear and Bloch, 1985), where the actin stress fibres attach to the cell membrane. A mutant of the nematode *Caenorhabditis elegans*, was found to express a defective vinculin protein, and was therefore unable to progress beyond the larval stages of development during which muscle twitching is observed (Barstead and Waterston, 1991). This would imply that *in vivo*, vinculin is essential for the anchorage of actin to the muscle wall and is required for the generation of contractile forces by muscle cells. A similar role is proposed for vinculin in the focal adhesion of cultured cells where actin-membrane interactions are involved in cell adhesion and the generation of contractile forces required for cell motility.

In cultured fibroblasts, vinculin is found primarily in focal adhesions where it is known to interact with other cytoskeletal proteins that mediate the link between the cell membrane to the actin cytoskeleton. Evidence that vinculin is essential to focal adhesion function and can promote cell adhesion comes from several experiments. Firstly, a mutant F9 mouse embryonal carcinoma cell line that was unable to form either cell-cell or cell-matrix junctions, and was consequently very poorly adherent, was shown to be lacking the vinculin protein. Subsequent transfection of these mutant cells with a full length vinculin cDNA was able to restore the normal adhesive phenotype of the cells and promoted actin stress fibre formation (Samuels *et al.*, 1993). Also, treatment of F9 mouse embryonal cells with retinoic acid stimulates them to differentiate from tightly-packed aggregates into

an endodermal-like cell sheet (Strickland and Mahdavi, 1978). This differentiation resulted in cells that were well spread and adherent, and also corresponded with an increase in vinculin levels and the appearance of vinculin-rich adhesive complexes, followed by the formation of actin stress fibres (Lehtonen *et al.*, 1983).

Experiments by Rodriguez Fernandez *et al.*, (1992a, 1993) demonstrated that the over-expression of vinculin results in a more adherent cell that is less motile, whilst a reduction in vinculin levels increases the motility of a less-well adherent cell. Similarly, fibroblasts transformed with the SV-40 virus are highly-motile and less adhesive, and a normal adherent fibroblastic phenotype could be restored by expression of a full length vinculin cDNA (Rodriguez Fernandez *et al.*, 1992b). The results provide convincing evidence for a direct correlation between the adhesive and migratory properties of a cell, and the levels of the vinculin protein. This is in agreement with the earlier observations of Couchman and Rees, (1979), who showed that well-adherent fibroblasts were less motile compared to motile cells which formed predominantly transient adhesions with the underlying ECM, and this shift to a more adherent phenotype corresponded with an entry into the cell cycle. This relationship between cell adhesion and growth rate is not observed in transformed cells which are less adherent but growth very rapidly in an uncontrolled manner. The contribution of vinculin to this aspect of cell adhesion and cell growth is examined in more detail in Chapter 3.

Regulation of vinculin function.

The cell must be able to exert some form of control over its adhesive properties if it is to function appropriately. Cells transformed with viruses such as the RSV, are seen to be rounded up and poorly adherent with few stress fibres or focal adhesions. Vinculin is known to be a substrate for the RSV tyrosine kinase, pp60$^{v\text{-}src}$, and an increase in the levels of phosphoserine, phosphothreonine and phosphotyrosine on vinculin residues is

observed in RSV-transformed chick fibroblasts compared to untransformed cells (Sefton *et al.*, 1981). Experiments by Kellie *et al.*, (1986a,b) examined the correlation between vinculin phosphorylation and loss of adhesion. Their experiments clearly indicated the presence of an active pp60^{v-src} within focal adhesions of RSV-CEF cells, but the subsequent phosphorylation of vinculin was not entirely sufficient to result in the characteristic rounded phenotype of RSV-transformed cells. Also, addition of fibronectin to RSV-transformed cells resulted in restoration of a flattened phenotype, but with no alteration in the phosphotyrosine content of vinculin compared to untreated RSV-CEF cells. These results seem to suggest that vinculin phosphorylation is not solely responsible for the changes in cell morphology seen in virally-transformed cells.

This loss of cell adhesion can be mimicked by the addition of either phorbol esters (Rifkin *et al.*, 1979) or growth factors such as PDGF (Herman and Pledger, 1985; Herman *et al.*, 1986) to cultured cells, indicating that phosphorylation of vinculin, through a PK-C-dependent mechanism can lead to its removal from focal adhesions. Experiments by Werth and Pastan, (1984) demonstrated that treatment of both Swiss 3T3 cells and chick embryo fibroblasts with the phorbol ester PMA lead to an increase in vinculin phosphorylation on serine, threonine and tyrosine residues, but a correlation between treatment of cells with phorbol ester and alteration of cell morphology was only seen in Swiss 3T3 cells. This is somewhat surprising as Rifkin *et al.*, (1979) demonstrated the treatment of CEF with the phorbol ester TPA had a dramatic effect on cell morphology. Similarly, experiments by Turner *et al.*, (1989) demonstrated that treatment of rat fibroblast cells with phorbol esters disrupted stress fibre and focal adhesion integrity, but rather surprisingly, they did not find an increase in vinculin phosphorylation. There is however, recent evidence that phosphorylation of vinculin does have a role to play in the cytoskeletal re-organisation of platelets. Following thrombin stimulation there is an increase in the levels of tyrosine phosphorylation of vinculin and a corresponding

redistribution of vinculin to sites of membrane-actin interactions (Vostal and Shulman, 1993).

Experiments by Ben-Ze'ev *et al.*, (1990) showed that vinculin gene expression could be rapidly and transiently increased by the addition of serum or growth factors to Balb/c 3T3 cells (presumably via the serum response element in the vinculin promoter), and that this response could be mimicked by phorbol esters, i.e. occured in a PK-C dependent manner. However, there is also evidence to the contrary, as Bellas *et al.*, (1991), demonstated that direct activation of the cells with phorbol esters did not induce the vinculin gene expression, nor was it adversely affected by the down-regulation of PK-C by prolonged exposure of the cells to phorbol esters. These results suggest that there are alternative mechanisms to control vinculin expression, that do not involve PK-C pathways.

It is difficult to draw a clear conclusion from the experiments outlined above as much of the data appears to be contradictory. Stimulation of PK-C would appear to be linked to alterations in both vinculin phosphorylation and expression, and loss of adhesive properties, but whether the two occur independently or are directly related remains unclear. Similarly, the direct correlation between vinculin phosphorylation and loss of adhesion has been neither conclusively nor consistently proven.

1.8. The actin cytoskeleton and associated proteins.

The actin cytoskeleton is composed of long filaments of F-actin, that associate into bundles to form stress fibres which are anchored to the cell membrane via the focal adhesion. The actin fibres generate tension across the cell membrane that is required for certain cellular functions such as muscle contraction and cell motility. The actin stress fibres are able to interact with a variety of proteins found in focal adhesions such as α-actinin (Hemmings *et al.*, 1992; Kuhlman *et al.*, 1992), vinculin (Jockusch and Isenberg,

25

1981; Isenberg *et al.*, 1982; Wilkins and Lin, 1982; Menkel *et al.*, 1994; Johnson and Craig, 1995), talin (Muguruma *et al.*, 1990, 1992; Chapter 5 of this thesis) and tensin (see Lo and Chen, 1993), all of which serve to anchor the fibres to the membrane. More recently, actin stress fibre assembly has been implicated in adhesion-mediated signal transduction mechanisms and this is discussed in more detail later in this chapter.

α-Actinin.

α-Actinin, an actin crosslinking and bundling protein, is also concentrated at regions where actin stress fibres are associated with the cell membrane such as focal adhesions in cultured cells (Lazarides and Burridge, 1975). α-Actinin is composed of two identical monomers, each with a molecular weight of approximately 97-103 kDa, and is composed of three domains - an N-terminal actin-binding domain, a central spectrin-like repeats region and a C-terminal EF hand calcium-binding region (reviewed in Blanchard *et al.*, 1989). A variety of distinct isoforms of α-actinin have been isolated and sequenced from chick tissues, including a skeletal (Arimura *et al.*, 1988) and a smooth muscle isoform (Baron *et al.*, 1987), and a non-muscle isoform from brain (Waites *et al.*, 1992). The α-actinin muscle isoforms are the products of separate genes (Baron *et al.*, 1987), and both can undergo alternative splicing giving rise to a non-muscle type isoform (Waites *et al.*, 1992; Parr *et al.*, 1992). The only known difference between the isoforms appears to be that the non-muscle isoforms are sensitive to calcium with respect to actin-binding (Burridge and Feramisco, 1981). The splice variants presumably fulfill different cellular function. For example, it would clearly be inappropriate to include a calcium-sensitive isoform in the Z-lines of skeletal muscle cells where α-actinin serves to anchor the actin filaments to cell membrane.

The α-actinin monomer is susceptible to proteolytic cleavage by thermolysin which generates a 27kDa fragment that contains the actin-binding domain, and a 53kDa fragment

which contains the four spectrin-like repeats and the EF hands. At least one actin-binding site within α-actinin has been defined and lies between residues 120-134 at the N-terminus (Hemmings *et al.*, 1992; Kuhlman *et al.*, 1992), and the formation of an anti-parallel dimer creates an actin-binding domain at either end of the molecule, enabling α-actinin to crosslink actin filaments. This N-terminal region is also known to support the interaction with zyxin (Crawford *et al.*, 1992). The central rod-like region has been shown to interact with integrins (Otey *et al.*, 1990a, 1993), and is known to be important in formation of the α-actinin dimer. The vinculin-binding site has recently been mapped to within residues 713-749 at the C-terminus of the protein close to the EF hands (McGregor *et al.*, 1994).The non-muscle isoform of α-actinin has been shown to be important to the organisation and integrity of both actin stress fibres and focal adhesions in cultured cells. Microinjection of either the 27kDa or the 53kDa fragment of α-actinin into fibroblast cells, results in a dissociation of the actin cytoskeleton and focal adhesions (Pavalko and Burridge, 1991). α-Actinin is therefore seen to be involved not only in formation of actin bundles, but helps to maintain the link from the membrane-spanning integrin receptors to the actin cytoskeleton.

Tensin.

Tensin is a 215kDa protein that was originally identified as a contaminant of vinculin preparations (Wilkins *et al.*, 1986). The tensin protein can interact with a variety of proteins via separate domains and is known to cap the barbed ends of actin filaments (for review see Lo and Chen, 1994). Antibodies raised against phosphotyrosine proteins in RSV-transformed CEF cells revealed one of the antigens to be a protein of 215kDa, that localised to focal adhesions (Glenney and Zokas, 1989). Experiments by Bockholt *et al.*, (1992) demonstrated that the 215kDa phosphotyrosine protein was indeed tensin, and was also found at myotendinous and neuromuscular junctions, suggesting that it functions in complexes that anchor the actin stress fibres to cell membranes. Further experiments have

27

implicated the phosphorylation of tensin to be involved in signal transduction mechanisms stimulated by cell adhesion (Bockholt and Burridge, 1993), and this is discussed later in this chapter.

1.9. Paxillin and pp125FAK.

Paxillin, a 68 kDa protein, and pp125FAK, a 125kDa protein were first identified as phosphotyrosine proteins associated with the cytoskeleton of RSV-transformed CEF cells (Glenney and Zokas, 1989). Paxillin can be isolated and purified from chicken gizzard and it has been shown to localise to focal adhesions in cultured cells (Turner *et al.*, 1990), the dense plaques in smooth muscle, and both the myotendinous and neuromuscular junctions of skeletal muscle (Turner *et al.*, 1991). pp125FAK has also shown to be associated with focal adhesions in cultured cells (Schaller *et al.*, 1992) and the myotendinous junction of *Xenopus* skeletal muscle (Baker *et al.*, 1994), although it was not observed within the neuromuscular junction. Both paxillin and pp125FAK are expressed during embryogenesis where they exhibit increased levels of tyrosine phosphorylation compared to adult tissue (Turner, 1991; Turner *et al.*, 1993).

Structure and possible functions of paxillin.

Paxillin has recently been sequenced and the binding sites responsible for interactions with both vinculin and pp125FAK have been identified (Turner and Miller, 1994). A summary of the different domains identified in paxillin are illustrated schematically in Figure 1.7. Following the initial isolation of paxillin, Turner *et al.*, (1990) demonstrated that it was able to interact *in vitro* with the 32 kDa vinculin tail, and further experiments by Wood *et al.*, (1994) defined the paxillin-binding site to within residues 978-1000 at the C-terminus of vinculin. Paxillin residues 51-308, expressed as a GST-fusion protein, was able to bind to vinculin, metavinculin, pp125FAK and the truncated C-terminal portion of pp125FAK, but not talin, present in chicken gizzard lysate (Turner *et al.*, 1990).

Figure 1.7. Schematic diagram of the domain structure of paxillin.
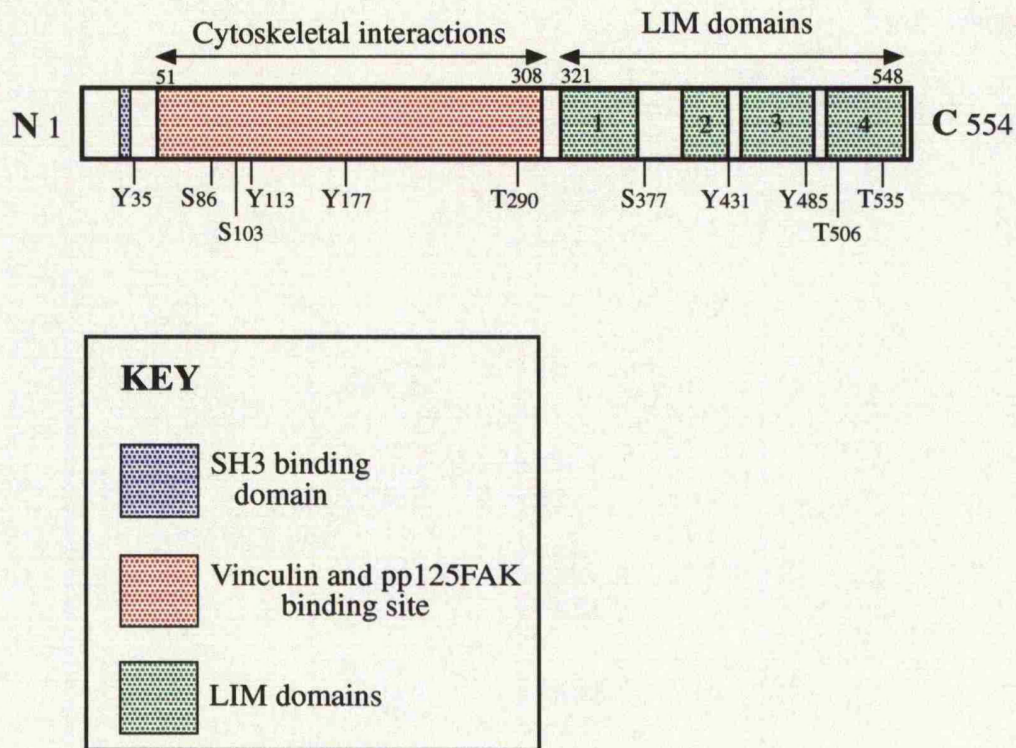
Residues 51-308 of paxillin are able to interact with both vinculin and pp125FAK *in vitro*. There are 5 tyrosine residues that contain flanking residues common to SH2 binding domain motifs as indicated. There are also 3 serine (residues 86, 103 and 377) and 3 threonine (residues 290, 506, 535) residues that are potential PK-C phosphorylation sites. Residues 43-52 represent a putative SH3 binding domain at the N-terminus. The C-terminus half of the protein contains four cysteine-rich regions, the third (residues 439-489) of which is a LIM domain. The other 3 regions (residues 321-371, 400-430, 498-548) are all LIM-like domains.

Within the C-terminus of the paxillin protein, there are four cysteine-rich regions known as LIM domains which show homology to similar domains found in both zyxin and the cysteine-rich protein cCRP (Sadler *et al.*, 1992). Indeed, an interaction *in vitro* has been demonstrated between zyxin and cCRP implying that LIM domains play a role in protein-protein interactions, but no such interaction between the zyxin and paxillin has yet been demonstrated. LIM domains are also found in proteins involved in cell lineage and development, and thought to function as transcription factors (Freyd *et al.*, 1990), but as yet neither zyxin, paxillin nor the cysteine-rich protein have been shown to localise to the nucleus.

Analysis of the paxillin sequence (Turner and Miller, 1994) revealed the presence of five short binding motifs that can interact with SH2 and SH3 domains (for review see Pawson and Schlessinger, 1993) following tyrosine phosphorylation of paxillin which suggests that paxillin can mediate protein-protein interactions with phosphoproteins involved in signalling cascades. Similar interactions with proteins involved in signal transduction cascades can be mediated by the SH3-binding domain that lies between residues 43-52 of the paxillin protein. Serine residues at positions 86, 103, and 377, and threonine residues at 290, 506 and 535 are potential sites for phosphorylation by PK-C (Turner and Miller, 1994).

Paxillin is thought to play a dual role in the focal adhesion as it would appear to be able to function as both a structural protein and a regulatory protein. Paxillin has been implicated in the regulation of the dynamics of the focal adhesion as it is readily phosphorylated during events associated with cell adhesion, and it also contains SH2- and SH3-binding domains, for interaction with other proteins involved in phosphorylation and signal

transduction pathways. This aspect of paxillin function is discussed in more detail later in this chapter.

Structure and possible functions of pp125FAK.

Sequence analysis of the chick pp125FAK cDNA and predicted amino acid sequence that constitutes the 125kDa protein, showed that it contained certain motifs common to all protein tyrosine kinases (PTK). However, the percent identity to other PTKs was only 31-41%, indicating that this particular enzyme constituted an additional family of PTKs. Antibodies against the 125kDa protein were used for immunofluorescent analysis of CEF, and illustrated that pp125FAK localises to focal adhesions (Schaller et al., 1992). A human pp125FAK (hFAK) has also been isolated which shows 95% similarity at the amino acid level to the chick protein (Andre and Becker-Andre, 1993). Northern blot analysis indicated that hFAK is expressed in nearly all organs and tissues, and an additional brain isoform lacking the first 157 amino acid residues has also been identified. The information known about pp125FAK to date is summarised in two reviews by Schaller and Parsons (1993, 1994) and includes brief details of some unpublished results regarding structural features of the molecule. A schematic representation of the structural features of pp125FAK is shown in Figure 1.8.

Experiments by Hildebrand et al., (1993) assessed the ability of a range of pp125FAK-GST fusion protein deletion mutants to undergo phosphorylation in an in vitro kinase assay, and also to target to focal adhesions in CEF cells. All mutants that contained the kinase domain (amino acid residues 390-650) were positive with respect to kinase activity, and were expressed at equal levels in the transfected cells. Mutation of residue 454 in the kinase domain, resulted in a dramatic reduction in the phosphorylation of this mutant, despite good expression levels, implicating this a key residue for kinase activity. It was observed that deletion of residues 131-144 resulted in a genuine decrease in protein

30

Figure 1.8. Domain structure of chicken pp125FAK.
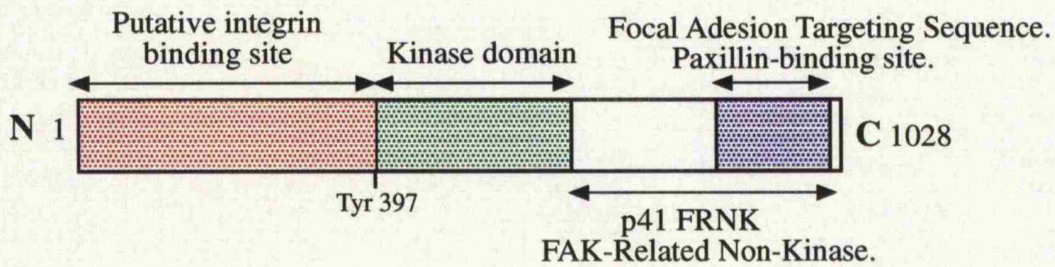
The cDNA encoding the 1028 amino acid chick pp125FAK contains a kinase domain spanning residues 391-651. Residue 454 within the kinase domain is responsible for ATP-binding, and is crucial to the kinase activity of this domain. Tyrosine 397 has been identified as the site of autophosphorylation. The 159 residues forming the focal adhesion targeting (FAT) sequence is illustrated and the short FRNK protein which comprises only this cytoplasmic, focal adhesion associated portion of pp125FAK is also shown. This C-terminal portion of pp125FAK is also capable of binding to paxillin.

expression, though whether this was due to a reduction in the rate of synthesis, or an increased rate of degredation was unclear. It is now known that residue tyrosine 397 is the major site of tyrosine phosphorylation on pp125FAK including autophosphorylation (Schaller et al., 1994). Mutation of this residue, which lies at the junction between the N-terminal and the catalytic domain of pp125FAK, significantly reduced the levels of phosphorylation of the protein, and also inhibited the formation of a stable association with the SH2 domain of the pp60src protein. It would appear that pp125FAK can interact directly with the cytoplasmic domain of integrins and this is proposed to result in the activation of the molecule enhancing its kinase activity (see Schaller and Parsons, 1994).

The C-terminus of pp125FAK, illustrated in Figure 1.8, is also expressed as an independent 41kDa which is known as FRNK, for FAK-Related Non-Kinase. Both the full length protein and FRNK are known to localise to focal adhesions (Schaller et al, 1993), and both have been shown to interact with paxillin (Turner and Miller, 1994). Epitope-tagged mutants were transiently expressed in CEF cells and deletion of residues 853-1012 was able to inhibit the localisation of this mutant to otherwise intact adhesions, and this stretch of residues is known as the FAT region, for Focal Adhesion Targeting. These results demonstrate that pp125FAK contains both a tyrosine kinase domain and a separate, independent region that targets the protein to focal adhesions. The presence of the kinase domain is not required for targeting by the FAT sequence, and conversely, the FAT sequence does not affect the kinase activity of the protein.

pp125FAK is found at focal adhesions, smooth muscle dense plaques and myotendinous junctions, which directly implicate it in the linkage of actin stress fibres to the membrane. However, because it does not appear to interact directly with other focal adhesion proteins except paxillin and possibly integrins, it seems likely that this protein fulfills a regulatory function as a PTK, rather than a structural one, and it is therefore considered as a primary

candidate as a key protein involved in controlling focal adhesion assembly. Many studies have demonstrated that pp125FAK (and paxillin) is tyrosine phosphorylated following the stimulation of cells to assemble new focal adhesions and stress fibres, and this involvement of pp125FAK in the various signalling pathways associated with focal adhesion formation is discussed in the next section.

1.10. Control of focal adhesion dynamics.

The control of the dissociation and assembly of the focal adhesion needs to be finely controlled as the adhesive status of the cell is important for appropriate cell function as discussed earlier. Many groups have studied the phenotype of cells that are deficient in one of the focal adhesion proteins in an attempt to identify which proteins are crucial to the integrity of the focal adhesion and therefore can directly affect cell adhesion. A reduction in the amount of vinculin in Balb/c 3T3 cells resulted in adhesion-defective cells (Rodriguez Fernandez *et al.*, 1993), and transformed cells which display an adhesion-deficient phenotype can be restored to a normal fibroblastic cell morphology by overexpression of proteins such as vinculin (Rodriguez Fernandez *et al.*, 1992b) or the fibronectin receptor $\alpha_5\beta_1$ (Giancotti and Ruoslahti, 1990). Similarly, an F9 mouse embryonal cell line that was adhesion-defective and lacked vinculin protein, could be restored to a normal phenotype by expression of the full length vinculin cDNA (Samuels *et al.*, 1993). Inactivation of either talin (Nuckolls *et al.*, 1990, 1992) or α-actinin (Pavalko and Burridge, 1991) by microinjection of either antibodies, or the proteolytic fragments of the proteins results in a rapid loss of actin stress fibres and a disassembly of the focal adhesion. These experiments provide substantial evidence that interference with the levels of just one of the proteins involved in the focal adhesion is sufficient to disrupt the focal adhesion resulting in a loss of cell adhesion.

32

Initial studies on events that controlled focal adhesion integrity concentrated on transformed cells, as they not only displayed a loss of adhesion, but the oncogenes responsible for transformation had cellular homologues involved in regulation of normal cell growth. Brands *et al.*, (1990) demonstrated that infection of CEF cells with a temperature sensitive mutant of RSV resulted in a dissociation of both stress fibres and focal adhesions when the cells were cultured at the permissive temperature of the virus. The focal adhesion proteins talin (Pasquale *et al.*, 1986; DeClue and Martin, 1987), vinculin (Sefton *et al.*, 1981), and the transmembrane integrin receptors (Hirst *et al.*, 1986) are all substrates for pp60^{v-src}, the transforming component of RSV. Experiments by Werth and Pastan, (1984), Kellie *et al.*, (1986a,b), DeClue and Martin, (1987) and Horvath *et al.*, (1990) attempted to prove that the phosphorylation of the cytoplasmic components of the focal adhesion was responsible for the loss of the adhesive phenotype. The results remained inconclusive, indicating that phosphorylation of the proteins was not in itself entirely sufficient to induce the phenotypic changes. There also appeared little difference between the levels of phosphorylation in normal and RSV-transformed cells (Maher *et al.*, 1985), which suggests that phosphorylation is also involved in the maintenance of normal focal adhesions.

More recently, the focus of this aspect of cell adhesion has switched to the assembly of focal adhesions, where there is consistent and conclusive evidence that tyrosine phosphorylation plays an important role in this process. Paxillin, pp125FAK and tensin were all specifically tyrosine phosphorylated following integrin-mediated cell adhesion of fibroblasts onto a substrate of either fibronectin or the RGD tripeptide (Burridge *et al.*, 1992; Guan and Shalloway, 1992; Hanks *et al.*, 1992; Bockholt and Burridge, 1993). Similarly, clustering of the integrins with integrin-specific antibodies results in an increase in protein tyrosine phosphorylation (Kornberg *et al.*, 1991, 1992; Sanchez-Mateos *et al.*, 1993). Treatment of cells with specific tyrosine kinase inhibitors resulted in a reduction in

the levels of adhesion-induced tyrosine phosphorylation, and inhibited the formation of focal adhesions and polymerisation of new actin stress fibres. Interestingly, blocking actin polymerisation by treating the cells with cytochalasin D also elicited the same effect as the tyrosine inhibitors (Bockholt and Burridge, 1993). These results imply that tyrosine phosphorylation of pp125FAK, paxillin and tensin is important to cell spreading which requires the formation of new focal adhesions, and polymerisation of new actin stress fibres.

The function of pp125FAK has also been studied *in vivo* using platelets isolated from patients with Glanzmann's thrombasthenia which are deficient in the fibronectin receptor, integrin GPIIb-IIIa. Lipfert *et al.*, (1992) demonstrated that stimulation of these integrin-deficient platelets with either thrombin or collagen, unlike normal platelets, did not result in an increase in tyrosine phosphorylation of pp125FAK. The phosphorylation was also dependent on platelet aggregation, and was inhibited by treatment of the cells with cytochalasin D. Similar observations were made using the β2 integrin-deficient neutrophils isolated from patients suffering from Leucocyte Adhesion Deficiency (LAD) (Berton *et al.*, 1994), providing convincing *in vivo* evidence that phosphorylation and activation of pp125FAK is involved in integrin-mediated cell adhesion and associated cellular functions.

Initial studies by Ridley and Hall, (1992) demonstrated that the serum lipid lysophosphatidic acid (LPA) could trigger the formation of focal adhesions and actin stress fibres in serum-starved Swiss 3T3 cells, and that this stimulation was mediated by rhoA, a small GTP-binding protein. Similar treatment of cells with LPA (Barry and Critchley, 1994; Ridley and Hall, 1994; Seufflein and Rozengurt, 1994) or growth factors (Zachary *et al.*, 1993; Rankin and Rozengurt, 1994) causes phosphorylation of pp125FAK and paxillin. Treatment of cells with tyrosine kinase inhibitors or blocking

actin polymerisation with cytochalasin D, prevented the formation of the focal adhesions and actin stress fibres (Zachary *et al.*, 1993; Seufflein and Rozengurt, 1994). Similarly, inhibition of protein tyrosine phosphatases can promote tyrosine phosphorylation and mimic the effects of LPA (Barry and Critchley, 1994; Chrzanowska-Wodnicka and Burridge, 1994). These results indicate that phosphorylation of these two proteins is also required for non-adhesion induced formation of focal adhesions and stress fibres.

PK-C∂ was shown to co-localise with newly-forming adhesions in cultured cells (Jaken *et al.*, 1989; Barry and Critchley, 1994), and activation of PK-C by treatment of cells with phorbol esters can promote cell adhesion (Danilov and Juliano, 1989; Woods and Couchman, 1992; Vouri and Rouslahti, 1993). This treatment results in an increase in the tyrosine phosphorylation of both paxillin (Zachary *et al.*, 1993), and pp125FAK (Vouri and Ruoslahti, 1993), and similar experiments have also been carried out *in vivo* on platelets (Huang *et al.*, (1993). The experiments carried out by Vouri and Rouslahti, (1993) indicated that a novel tyrosine kinase is activated prior to PK-C activation and subsequent cell spreading, and recent experiments by Li *et al.*, (1994) have strongly indicated that tyrosine phosphorylation of PK-C∂ can enhance its subsequent kinase activity. However, experiments by Rifkin *et al.*, (1979), Werth and Pastan, (1984) and Turner *et al.*, (1989), demonstrated that treatment of cells with phorbol esters perturbs cell adhesion and Housey *et al.*, (1988) demonstrated that overproduction of PK-C in rat fibroblasts produced a transformed phenotype. Similarly, Ridley and Hall (1994) demonstrated that stimulation of PK-C by phorbol esters alone was not sufficient to promote stress fibre and focal adhesion formation in starved Swiss 3T3 cells. The involvement of PK-C in the modulation of cell adhesion is somewhat confusing as it appears to be able to both promote stress fibre and focal adhesion formation and disrupt cell adhesion.

1.11 Signal transduction via the focal adhesion.

The focal adhesion is a unique region where the cell membrane comes into closest contact with the underlying substrate and it is therefore not surprising that the focal adhesion is thought to operate as an area of communication between the cell and its external environment. This is perhaps most easily observed in cultured cells which will not proliferate unless they are strongly attached to the underlying substrate such as fibronectin (Couchman et al., 1982). The pathways that transmit this signal from the exterior of the cell to the nucleus are now beginning to be dissected into their different steps. There is some recent evidence for a direct contribution of various focal adhesion components to the mitogen activated protein (MAP) kinase pathway that triggers gene transcription via a cascade of lipid second messengers in response to various mitogens e.g. PDGF. Integrin-mediated cell adhesion results in the direct activation of MAP kinase and its subsequent re-location to the nucleus (Chen et al., 1994). In a similar manner to the phosphorylation and activation of pp125FAK, the activation of MAP kinase was also inhibited by treatment of the cells with cytochalasin D. Also, vinculin and α-actinin have been shown to bind to the lipid second messengers phosphatidylinositol 4,5-bisphosphate (PIP2), (Fukami et al., 1994). Also, α-actinin (Shibasaki et al., 1994) and pp125FAK (Chen and Guan, 1994) have been identified as substrates for the p85 subunit of phosphatidylinositol 3-kinase (PI3-kinase), which is involved in the production of lipid-based second messangers utilised by the MAP kinase pathway. Recent studies by Kumagai et al., (1993) and Nobes et al., (1995) have also suggested that PI3-kinase is involved the rho-mediated response of cells to either LPA or growth factors. The direct involvement of focal adhesion components in both integrin-mediated and growth factor or LPA-stimulated signal transduction has been discussed in the previous section and has also been the subject of a wide number of reviews (Damsky and Werb, 1992; Schwartz, 1992; Juliano and Haskill, 1993; Juliano, 1994; Kiley and Jaken, 1994; Lo and Chen, 1994; Moolenaar, 1994; Panaretto, 1994; Williams et al., 1994).

Interaction between the cell and its substrate is known to trigger certain signalling pathways resulting in specific gene transcription. For example, Werb *et al.*, (1989) demonstrated that engagement of the fibronectin receptor (integrins) of fibroblasts lead to the induction of expression of two metalloproteinase genes. Within 2 hours, there was a significant increase in the levels of both collagenase and stromelysin mRNA. Another example of the modulation of cell function in response to its substrate is seen in mouse mammary epithelial cells which are able to increase the production and secretion of milk proteins in response to certain lactogenic hormones when cultured on reconstituted basement membrane. There is also a corresponding structural change in the cell enabling it to resemble a secretory cell (Li *et al.*, 1987). Further experiments by Schmidhauser *et al.*, (1990, 1992), demonstrated that the ECM and lactogenic hormones act synergistically to increase β-casein gene expression, and they were able to identify a short 169 base pair region of the promoter that was responsible for the matrix and hormone dependency. Also, these cells, when cultured on a preferred substrate, were able to express and secrete their own basement proteins that promote milk secretion (Streuli and Bissell, 1990). These results demonstrate unequivocably that the underlying substrate is able to affect cell function, and suggests the existence of matrix response elements within the promoter regions of certain genes.

An attempt has been made to summarise the multiple and complex events that are involved in focal adhesion formation and this is shown in Figure 1.9. It is apparent that phosphorylation plays a key role in these events, both via tyrosine kinases such as pp125FAK, or serine/threonine kinase such as PK-C. The role of phosphorylation in focal adhesion disocciation is unclear as much of the data obtained on virally-transformed cells is somewhat contradictory, but tyrosine phosphorylation of pp125FAK, paxillin and tensin appear to be primary responses involved in the focal adhesion formation. The role

Figure 1.9. Signalling pathways involved in the reformation of actin stress fibres and focal adhesions.
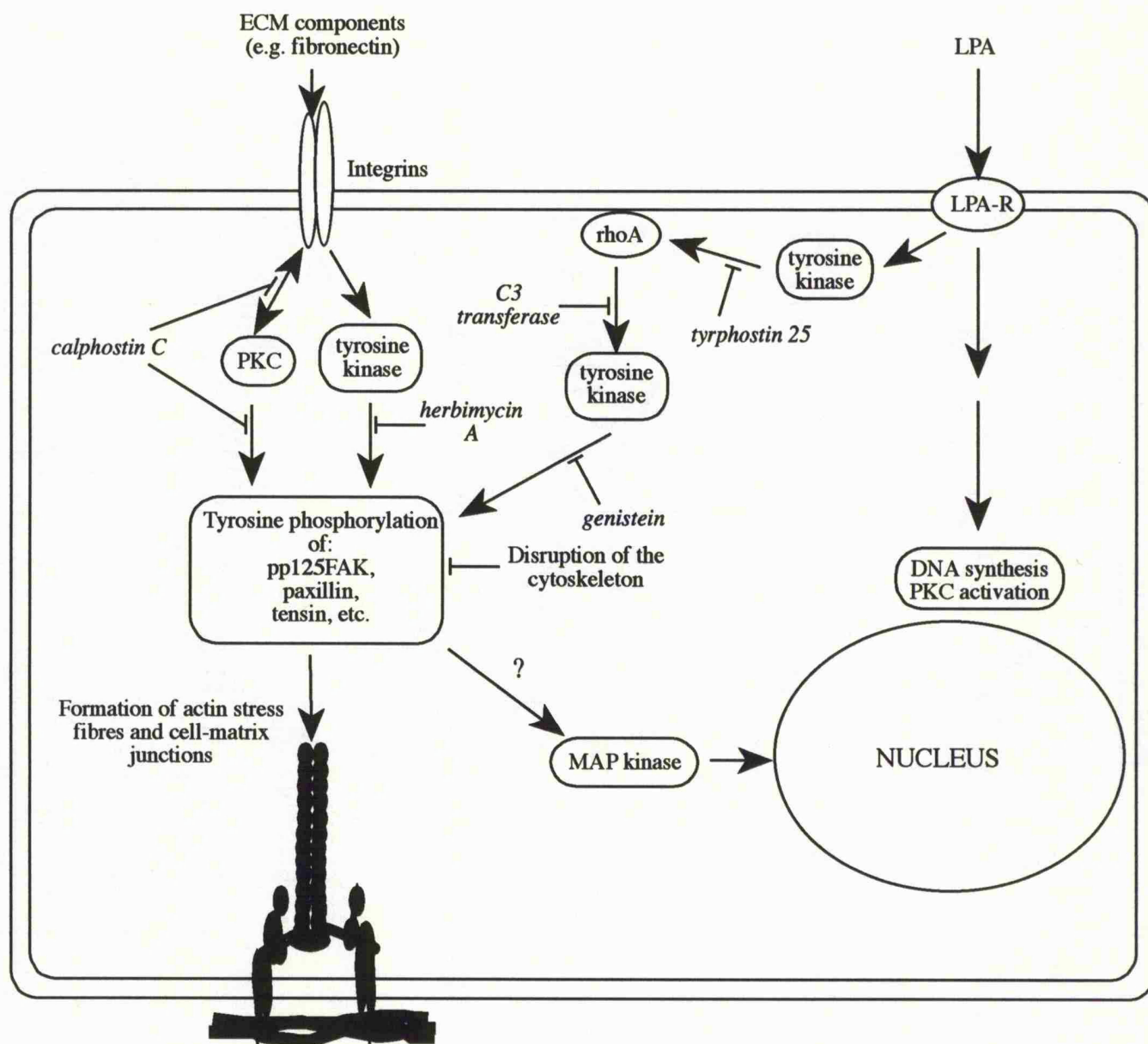
Cultured cells can be stimulated to reform actin stress fibres and focal adhesions by either LPA, a serum component or integrin-mediated adhesion. The triggering of various cascades by these two stimuli can also result in gene expression via the MAP kinase pathway. Arrows show the progression of the signalling pathways and inhibitors are shown in italics.

of PK-C in either focal adhesion disruption or formation is also unclear, again with contradictory data being presented, but is is obvious that it must play some role in the control of adhesion. It has also become clear from the many experiments performed that the ability to reorganise the actin cytoskeleton is also a critical component in both integrin- and receptor-mediated stimulation, although precisely how this works is again unclear. The data discussed above provides a brief insight into how the cell may regulate gene transcription and cell proliferation in response to its external environment via the phosphorylation cascades triggered by integrins or external mitogens such as serum. It also provides a possible explanation and mechanism as to how cells are anchorage-dependent for growth.

1.12 Antisense technology as a tool to study protein function.

In order to further probe the involvement of individual focal adhesion proteins in cell adhesion and signal transduction, antisense techology has been identified as a useful method by which to reduce levels of specific proteins to study the effect this has on the cell. This approach to probing protein function has been utilised by many different groups to target a very wide range of proteins as summarised in Table 1.2. The use of antisense technologies to down-regulate protein expression, exploits the ability of two complementary stretches of nucleotides to hybridise and form a duplex. If one of the nucleic acid partners involved in the duplex formation is messenger RNA, the mRNA can generally no longer be translated by the ribosomal complex into protein. The incoming nucleic acid that hybridises to messenger RNA can be either RNA or DNA. The antisense RNA is most often transcribed using the endogenous transcription machinery, from a plasmid that has been transfected into growing cultures and has become integrated into the cells genome. The alternative mechanism to plasmid transfection, is to treat cells with a short DNA oligonucleotides, or, as they will be referred to, oligos. There are some reports where the experiments have included microinjection of the antisense nucleic acids

Table 1.2 Summary of previous antisense experiments.

TARGET PROTEIN	TYPE OF ANTISENSE	mRNA TARGET	OTHER INFORMATION	REFERENCE
Integrin	Expressed RNA	coding region	4% clones affected	Hayashi *et al*, 1991
Integrin	Oligo	coding region	guessmer oligos used	Lallier *et al*, 1993
ICAM-1	Oligo	coding & AUG codon	Lipid delivery	Chiang *et al*, 1991
Vinculin	Expressed RNA	coding region	20% clones affected, Balb/c3T3	Fernandez *et al*, 1993
ERM family	Oligos	span AUG codon		Takeuchi *et al*, 1994
α-actinin	Expressed RNA	coding region	non-homologous cDNA	Schulze *et al*, 1989
Fibronectin	Expressed RNA	coding region	80% clones affected	Steel and Harris, 1989
H-ras	Expressed RNA	coding region, 1st exon	No reduction in NIH3T3 cells	Salmons *et al*, 1986
H-ras	Oligos	coding region, codon 12	HeLa cells, lipid delivery	Monia *et al*, 1992
c-fos	Expressed RNA	span AUG codon	MMTV promoter, NIH3T3 cells	Nishikura&Murray, 1987
c-fos	Expressed RNA	coding region	MMTV promoter, Swiss 3T3 cells	Holt *et al*, 1986
c-myc	Expressed RNA	coding region	MMTV promoter, NIH3T3 cells	Sklar *et al*, 1991
c-myb	Oligos	coding region, codon 2-7		Melani *et al*, 1991
RSV	Expressed RNA	coding region, env gene	12:1 antisense:sense ratio needed	Chang and Stolzfus, 1985
RSV	Expressed RNA	5'UT, coding, 3'UT	All 3 constructs equally efficient	Chang and Stolzfus, 1987
EGF-R	Expressed RNA	5'UT, coding, 3'UT	All 3 constructs equally efficient	Moroni *et al*, 1992
Troponin C	Oligos	coding region	Treated cells every 3-4 hours	Thinkaran & Bag, 1991
β-globin	Injected RNA	various in coding region	Only 5' constructs effective	Melton, 1985
Thymidine kinase	Expressed RNA	?coding region	duplexes found in nucleus	Kim and Wold, 1985

into the cells (Izant and Weintraub, 1984; Melton, 1985; Schulze *et al.*, 1989; Girard *et al.*, 1991; Moroni *et al.*, 1992), and Figure 1.10 summarises the 3 main ways the antisense sequences are introduced into cells.

Most oligos are now modified by attachement of a phosphorothioate moeity to the phosphate backbone of the oligo (see Figure 1.11) which is thought to help prevent degradation of the oligo within the cell culture medium, and aid uptake by the cell, although other modifications have also been used (reviewed in Colman, 1990; Murray, 1992; Akhtar and Juliano, 1992). The range of concentrations of oligos used to treat cells varies enormously. Some groups report that addition of oligos in the region of nM concentrations each day is sufficient to reduce protein levels (Chiang *et al.*, 1991; Monia *et al.*, 1992; Lallier and Bronner Fraser, 1993), whilst other groups use a higher concentration, in the order of μM, and administer treatment every 3-4 hours (Thinkaran and Bag, 1991; Takeuchi *et al.*, 1994). Experiments by Monia *et al.*, (1992) tested oligos ranging from 5-25 bases in length, to specifically target a point mutation in codon 12 of the H-ras RNA. The most effective oligo was 17 bases long, and the effectiveness of the oligo to target the specific point mutation was also dependent on the concentrations used. However, Lallier and Bronner-Fraser, (1993) used a selection of "guess-mer" oligos based on non-identical sequence to successfully down-regulate integrin expression. Oligos are now being used with some success as therapeutic agents to inhibit protein synthesis *in vivo* (Osen-Sand *et al.*, 1993; Simons *et al.*, 1992), and several attempts have been made to inhibit expression of HIV, with regard to using them also as therapeutic agents for treatment of AIDS patients (Rhodes and James, 1990; Joshi *et al.*, 1991)

Many groups are now also using lipid-based transfection reagents such as Lipofectamine™ (Life Technologies) or DOTAP (Boehringer Mannheim), to enhance the uptake of the oligo by the cell (Felgner *et al.*, 1987; Chiang *et al.*, 1991; Monia *et al.*,

Figure 1.10. Delivery of antisense nucleotides into cells.
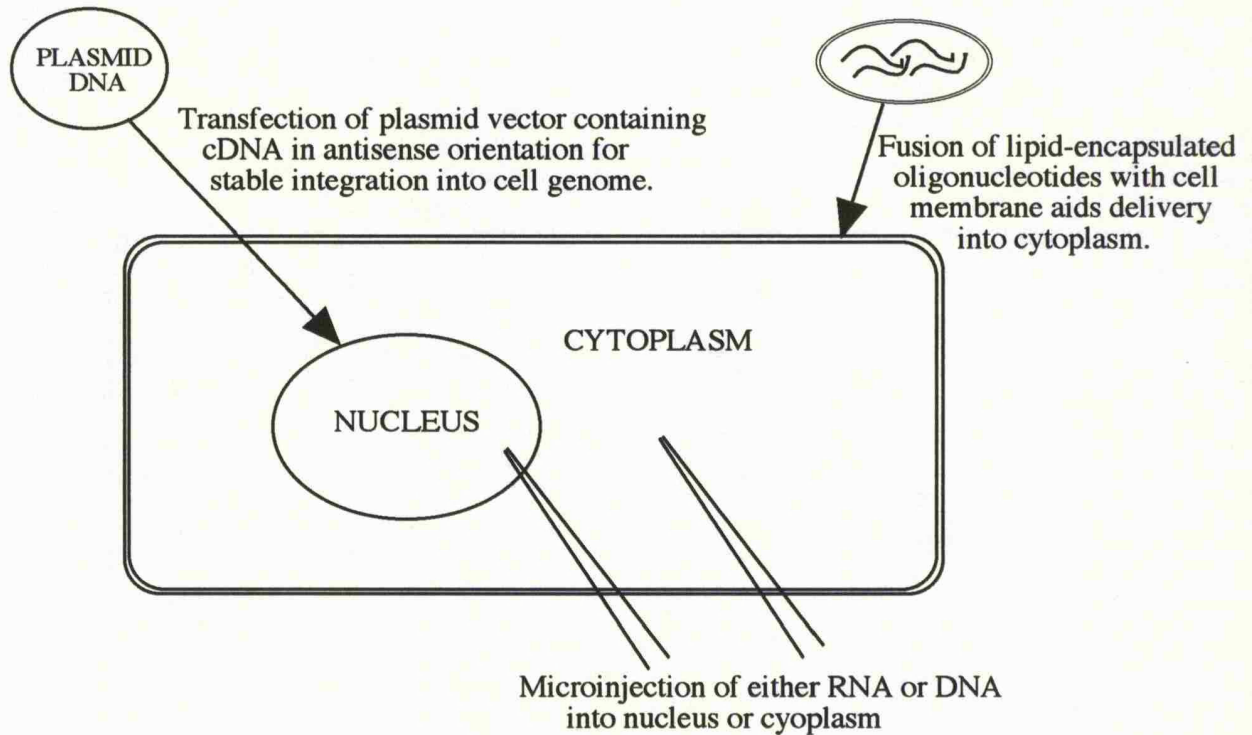
Antisense nucleotides can be introduced into a cell using various systems. Most commonly, to generate antisense RNA, the corresponding cDNA of interest is cloned into a plasmid vector in the opposite orientation, transfected into cells where it incorporates into the cells genome. Expression of the plasmid uses the cells own transcription machinery within the nucleus and produces a strand of antisense RNA that can hybridise to the target RNA. DNA oligos are often encapsulated in a lipid coating to form a liposome, that can fuse with the lipid cell membrane to enhance uptake by the cell. Both RNA and DNA can be microinjected into the cell. Injection into the nucleus may inhibit transcription, or may block exit of the mature RNA from the nucleus. Injection into the cytoplasm blocks message translation into protein.

Figure 1.11. Structure of modified antisense oligonucleotides.
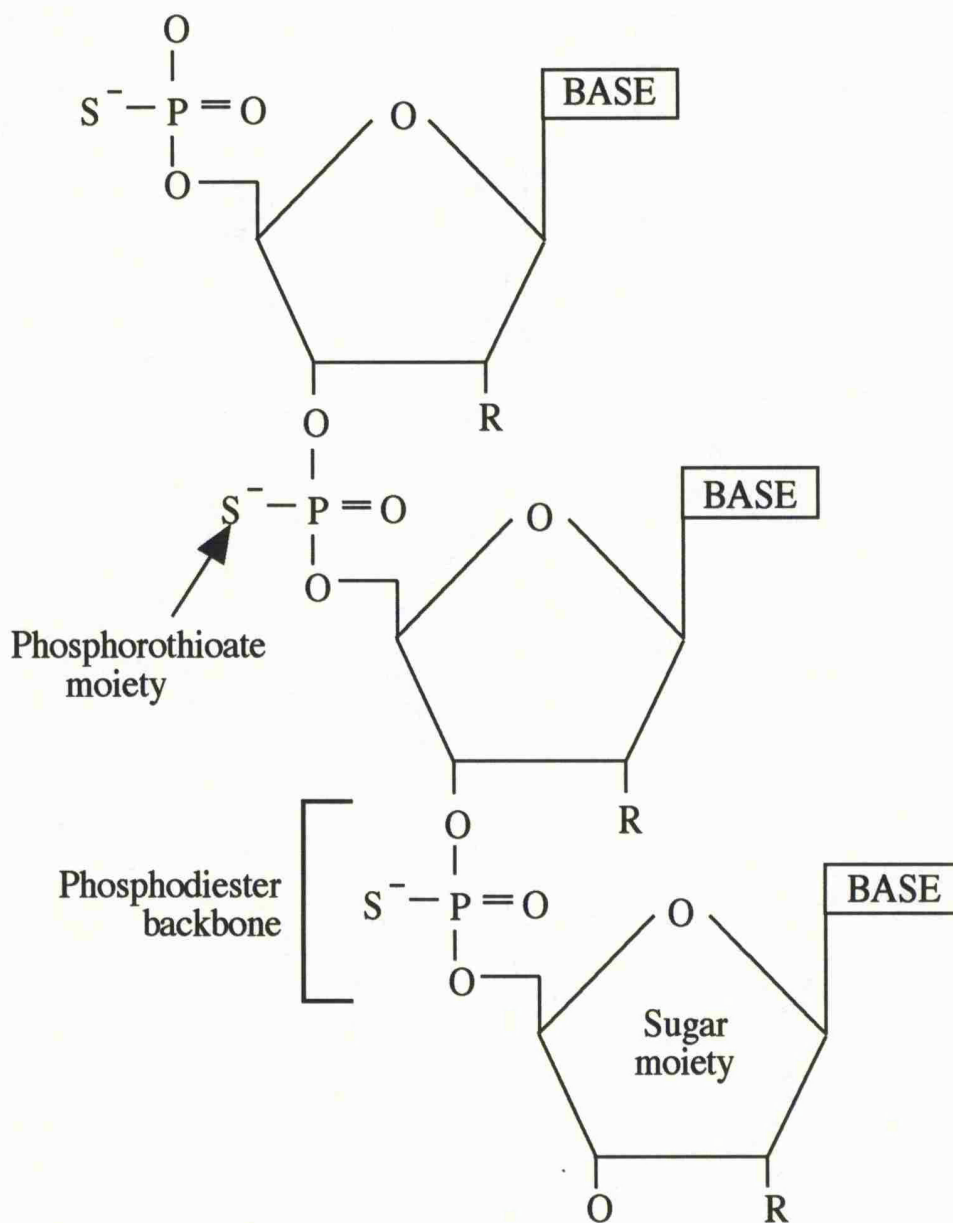
The base (adenine, cytosine, thymine or guanine) hybridises via hydrogen bonds to target RNA. The phosphorothioate moiety replaces an oxygen atom in the phosphodiester linkage, but alternatively a methylphosphonate (CH_3) or a phosphoramidate (NR_2) group may also be added. Replacement of the R group, normally hydrogen, with an OCH_3 group creates a 2' O-Methyl oligonucleotide, that is RNase H resistant.

1992; manufacturers notes). It is believed that encapsulation of the oligo in a lipid envelope can increase its uptake by up to 100 fold (Chiang *et al.*, 1991), and the half-life of the oligos is considerably increased from 5 minutes up to 60 minutes, presumably by aiding entry into the cell via membrane fusion, and also protection against degradative enzymes (see Akhtar and Juliano, 1992). They may also be effective for use with oligos that target proteins with slow turnover rates, as the release of the oligo from the lipid capsule is quite slow, occuring over several days (Akhtar *et al.*, 1991).

The exact mechanisms by which the antisense sequences bring about a reduction in protein levels is still unclear, although certain experiments have attempted to directly address this issue (for reviews, see Colman, 1990; Helene, 1991; Akhtar and Juliano, 1992; Murray, 1992). The most reasonable explanation is formation of an RNA:RNA or RNA:DNA duplex physically impedes translation, or that formation of the RND:DNA duplex makes the RNA a target for nucleases, such as RNase H. It is of course possible that both mechanisms work together to impede translation. The main mechnisms currently being proposed are summarised in Figure 1.12.

A few groups have attempted to study the direct involvement of RNase H in eliciting a reduction in the levels of translatable RNA message. Boziau *et al.*, (1992), exploited the ability of the reverse transcriptase enzyme (RT) to generate a cDNA template from RNA. Oligonucleotides that hybridised to a region of the RNA upstream of the reverse transcriptase primer, were sufficient to arrest cDNA production resulting in truncated cDNAs. When this was repeated with RT enzymes lacking the RNase H activity, nuclease-resistant oligonucleotides or inhibitors of RNase H activity, full length cDNA transcripts were produced. Similar experiments by Chiang *et al.*, (1991) found that modified oligonucleotides which do not support RNase H cleavage, were inefficient at decreasing protein levels, but only when targeted to the 3' untranslated region of the

Figure 1.12. Mechanisms by which antisense RNA or DNA reduce protein levels.
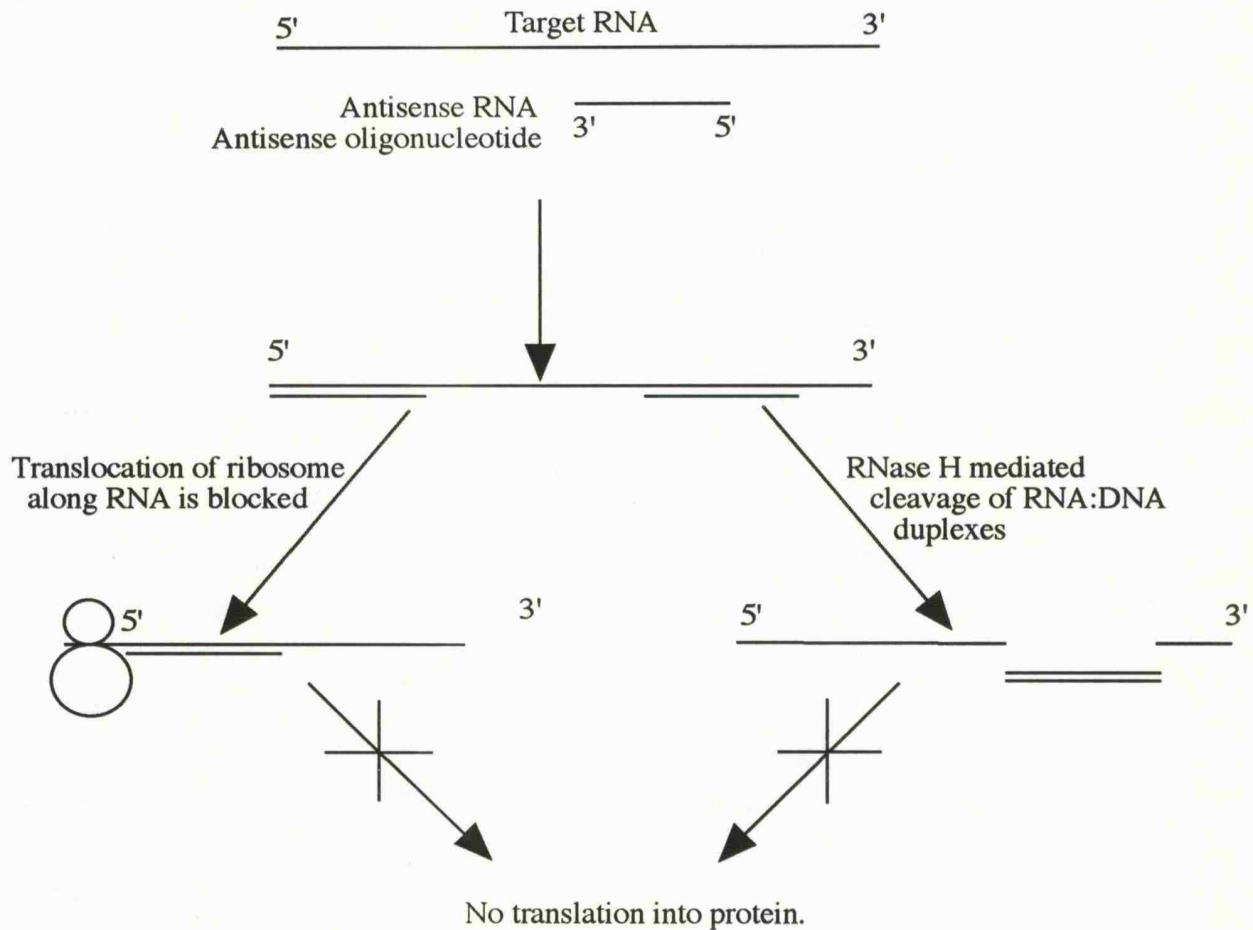
The diagram represents the two main mechanisms thought to be responsible for the reduction in protein levels brought about by antisense sequences. Formation of the duplex is thought to physically prevent translation, but, if formed in the nucleus, it may impede the passage of the RNA into the cytoplasm. RNase H appears to be responsible for reducing the amount of full length message by cleaving the RNA partner in the duplex. Neither of the mechanisms would appear to affect transcription.

RNA, which suggests that RNase H is not the only mechanism by which down regulation occurs. These experiments demonstrate that degradation of the RNA:DNA duplex by the RNase H enzyme, and therefore generation of an incomplete RNA template for translation, is just one of the mechanisms responsible for down regulation of protein levels.

Several experiments have provided evidence that formation of the duplex physically blocks the binding and/or translocation of the translation machinery. Melton, (1985) microinjected *Xenopus* oocytes with β-globin mRNA (sense) which subsequently synthesised large quantities of β-globin protein. Production of the protein could be abolished by a prior injection of an antisense β-globin RNA that covered the 5' portion of the sense transcript, and RNA analysis demonstrated the formation of RNA:RNA duplexes within the oocytes. Kim and Wold, (1985) attempted to down-regulate production of the thymidine kinase protein via transfection of plasmid DNA into mouse L cells. They demonstrated the formation of RNA:RNA duplexes that were present in the nucleus, leading them to speculate that the transcripts then fail to enter the cytoplasm with the normal efficiency, leading to a reduction in translatable message, and therefore protein. These two results demonstrate that one of the mechanisms responsible for the down-regulation of protein levels via antisense RNA, involves interference of the translation process.

Experiments by Chiang *et al.*, (1991) targeted two regions of the ICAM-1 RNA with oligonucleotides. The oligo targeted to the 5' AUG translation start site effected a reduction in protein levels, but did not reduce the levels of mRNA, and appeared to be working in an RHase-H independent manner. The oligo targeted to the 3' untranslated region of the RNA reduced both the levels of mRNA and protein in an RHase H-dependent manner. These experiments provide clear evidence that inhibition by antisense

works via two separate mechanisms, and oligos targeted to the AUG codon exert their effect by impeding translation, whilst oligos targeted to other regions such as the 3' untranslated mRNA work via RNase H mechanisms.

Target sites within the RNA were often considered crucial to the success of antisense experiments and, based on the information obtained by Chiang *et al.*, (1991), it is perhaps unsurprising that virtually all regions of the mRNA have been shown to be successful in bringing about a reduction of protein levels. However, the AUG codon is still regarded as the most acceptable target as it has yet to prove unsuccessful. Moroni *et al.*, (1992) reduced the levels of the epidermal growth factor receptor following transfection of KB human carcinoma cells, using vectors containing cDNAs targeted to both 3' and 5' regions and full length RNA. Each of the constructs were able to reduce protein levels to less than 50% with equal efficiency. Similarly, Chang and Stoltzfus, (1985, 1987) demonstrated that targeting the 3' untranslated regions of the RSV *env* gene was as effective as 5' coding sequence in reducing protein synthesis. Their experiments also demonstrated that both intron-containing and intronless sequences were equally effective, suggesting that antisense inhibition does not affect RNA splicing.

Many groups have used cultured fibroblasts for their antisense experiments, with NIH3T3 cells being the most widely used cell line (Salmons *et al.*, 1986; Nishikura and Murray, 1987; Sklar *et al.*, 1991; Perlaky *et al.*, 1992), although both Swiss 3T3 cells (Holt *et al.*, 1986) and Balb/c 3T3 cells (Rodriguez Fernandez *et al.*, 1993) have also been used. Similarly, use of inducible promoters such as the mouse mammary tumour virus promoter (MMTV), is also quite common (Holt *et al.*, 1986; Nishikura and Murray, 1987; Selinfreud *et al.*, 1990; Sklar *et al.*, 1991), as this enables expression of the antisense RNA to be controlled by the addition of the glucocorticoid dexamethasone into the culture

medium (Ringold *et al.*, 1979). This is of course important if reduction of the target protein were to adversely affect the isolation and growth of the cloned cells.

There have also been several examples where downregulation of specific proteins has not been achieved. Salmons *et al.*, (1986) attempted to reduce the levels of the *H-ras* protein in NIH3T3 cells. This experiment was unsuccessful, despite a 10-20 fold excess of antisense to sense RNA, and the authors report that only a small fraction of the antisense transcript was present as a duplex in the cytoplasm. There does not appear to be any other obvious reason for this failure as other transcription factors such as *c-fos* (Holt *et al.*, 1986), and *c-myc* (Sklar *et al.*, 1991) have been successfully down regulated in NIH3T3 cells. Many transcription factors have been the subject of antisense experiments, most of which work very successfully. The half lives of these transcription factors is usually quite short, approximately 2-3 hours, suggesting that this may be a contributory factor to the success of the experiment (Nishikura and Murray, 1987). However, the reluctance of scientists to report failed antisense attempts makes it difficult to find any recurring theme within the target RNAs or proteins that may be responsible for a lack of success. In some cases the reports do detail the success rate of the transfections i.e. the number of clones that result in down-regulation, and this is very variable. For example, Green *et al.*, (1991) reported that all 7 clones isolated were significantly affected, and both Sklar *et al.*, (1991) and Steel and Harris, (1989) reported that up to 80% of clones isolated showed significant down-regulation of the target protein. Other experiments were not so successful as Moroni *et al.*, (1992) and Rodriguez Fernandez *et al.*, (1993) found only 20% of clones were significantly affected, whilst Hayashi *et al.*, (1991) found only 2 out of 50 clones were down-regulated. The reason for this is presumably due to the position of integration, and possibly the number of copies of the plasmid integrated into the genome.

To conclude, the use of antisense technology to down-regulate proteins is becoming more wide spread, as more papers detail successful specific reduction of the target protein. The mechanisms underlying protein down-regulation are becoming a little better understood, but still remain unclear, particularly following the observation that different targets elicit different mechanisms. Also the choice of target region does not appear to be as critical as once previously thought, making design of antisense experiements easier. Use of oligos is also expanding as the technology to improve the life-span and uptake of oligos increases, and they are now becoming a very popular choice for antisense experiments.

AIMS OF THE VINCULIN AND TALIN PROJECTS.

The main goal of the two projects described in the forthcoming chapters was to investigate the contribution of vinculin and talin to actin stress fibre and focal adhesion integrity, and to assess the effect a lack of either protein had on cell function. An antisense approach was chosen to create fibroblast cell lines that specifically lacked the vinculin protein. A plasmid vector containing a vinculin cDNA cloned in the opposite orientation with respect to the MMTV glucocorticoid-inducible promoter was constructed for transfection into mouse fibroblast cells for the generation of stable cell lines expressing the antisense vinculin RNA. The clones could then be easily screened using the light microscope for any alterations in cellular morphology following the addition of dexamethasone in the culture medium. The effect the lack of vinculin protein has on cell adhesion and related functions such as cell proliferation, cell spreading and signal transduction via the focal adhesion can be examined in these stable cell lines.

The structure-function relationship of the talin molecule was to be investigated using microinjection technology. A panel of anti-talin monoclonal antibodies was available, which, following characterisation and epitope mapping, could prove useful tools to probe the functions of the discreet domains of the molecule recognised by each antibody. The talin protein can be essentially inactivated by microinjecting either the antibody itself, or the polypeptide recognised by the antibody, into fibroblast cells. Immunofluorescent analysis of the injected cells would reveal whether talin was essential to the maintenance of actin stress fibre and focal adhesion integrity. Similarly, the requirement of talin for the formation of new focal adhesions could be investigated by injecting the antibodies into migrating fibroblasts and examining the effect this had on subsequent mobility of the injected cells. Following identification of possible functional domains of talin using this approach *in vivo*, it is then important to determine, using *in vitro* assays, exactly what proteins, if any, these domains are interacting with.

CHAPTER 2

MATERIALS AND METHODS

2.1 REAGENTS, ANTIBODIES AND cDNA CLONES.

2.1.1 General reagents.

Unless otherwise stated all chemical reagents were of analytical grade, and most were obtained from BDH Laboratory Supplies (Lutterworth, Leicestershire, UK), Fisons (Loughborough, Leicestershire., UK) or Sigma Chemical Company Ltd, (Poole, Dorset, UK). Reagents for bacterial cell culture were obtained from Oxoid (Unipath, Basingstoke, Hampshire, UK) and media for mamalian/chick cell culture were obtained from Life Technologies (Paisley, Renfrewshire, Scotland). All serum was purchased from Advanced Protein Products (Brierley Hill, West Midlands, UK). Reagents for manipulation of DNA were purchased from either Pharmacia Biotech (Milton Keynes, Buckinghamshire, UK.) or New England BioLabs (c/o CP Labs, Bishops Stortford, Hertfordshire, UK). Sequenase™ enzyme was purchased from United States Biochemicals Corporation (USB Corporation, Cleveland, Ohio, USA). All radioisotopes were purchased from Amersham International plc (Amersham, Buckinghamshire, UK). Synthetic oligonucleotides were made using the facilities available in the Biochemistry Department, Leicester University. The tetraethylthiuram disulfide (TETD) reagent for the preparation of phosphorothioate-modified oligonucleotides was obtained from Applied Biosciences (Foster City, CA, USA).

2.1.2 Antibodies.

The six monoclonal antibodies raised against human platelet talin were supplied by Dr. J. M. Wilkinson (Wellcome Trust, London. U. K). The monoclonal anti-human vinculin antibody, V284, was a generous gift from Dr. J. M. Wilkinson. The affinity purified polyclonal anti-glutathione-S-transferase (GST) was a generous gift from Dr. E. Moiseyeva (Biochemistry Dept., Leicester University). The monoclonal antibodies against phosphotyrosine (clone PT-66) and α-tubulin (clone DM1a) were both purchased from

Sigma. The Texas Red-labelled and horseradish peroxidase (HRP)-labelled anti-IgG secondary antibodies were all purchased from Amersham.

2.1.3 cDNA clones.

The 1.06kb mouse vinculin cDNA used in this study has been described previously (Ben-Ze'ev *et al.*, 1989), and was a generous gift of Dr. Avri Ben-Ze'ev (Weizmann Institute of Science, Rehovot, Israel). Sequence comparisons revealed that the cDNA displays >90% identity to nucleotides 345-1402 of both human (Weller *et al.*, 1990) and chicken vinculin (Price *et al.*, 1989), which encodes for amino acids 116-468. The cDNA, in the pBluescript plasmid (Stratagene Ltd, Cambridge, UK), was subsequently subcloned into the pMAMneo-Blue expression plasmid (Clontech Labs. Inc., Palo Alto, CA). The chick talin cDNAs used for expression of GST-fusion proteins have been described by Gilmore *et al.*, (1993), with the exception of C1 (amino acid residues 1554-2060), C2 (1554-2029), C3 (1554-1929) and C4 (1554-1829) which were generated by polymerase chain reaction (PCR) using existing pGEX/talin vectors as templates. All fusion protein constructs were made by Drs. V. Ohanion and A. P. Gilmore.

2.2 BACTERIAL CELL CULTURE.

2.2.1 Media recipes.

Working stocks of *E. coli* (strain JM101) were maintained on M9 minimal media plates (see below) and cultures of non-transformed JM101 were grown in 2TY media (see below) without ampicillin. Once JM101 bacteria had been transformed with plasmid DNA they were maintained on ampicillin-containing agar plates and all liquid cultures were grown in ampicillin-containing 2TY media as detailed below. Reserve stocks of all *E.coli* cultures were preserved in 20% glycerol/80% 2TY at -70°C. Following autoclaving of the different media, where appropriate, ampicillin was added to a final concentration of 100µg/ml.

M9 Minimal Media plates were composed of the following ingrediants:

6g Na_2HPO_4, 3g KH_2PO_4, 0.5g NaCl, 1g NH_4Cl, 15g Bacto-Agar, 900ml deionised water. Once autoclaved and cooled to approximately 50°C, the following was added: 1ml 1M $MgSO_4$, 10ml 10mM $CaCl_2$, 10ml 20% glucose, 1ml 10mg/ml thiamine, deionised water to 1 litre.

2TY media was made up as follows: 16g tryptone, 10g yeast extract, 5g NaCl, deionised water to 1 litre.

General agar plates were made up as follows:

10g tryptone, 5g yeast extract, 10g NaCl, 1g glucose, 15g Bacto-agar, de-ionised water to 1 litre.

2.2.2 Transformation *E. coli* strain JM101 with plasmid DNA.

A single colony of JM101 cells were grown overnight in 2TY without ampicillin. The following morning the culture was back-diluted 1:100 in fresh 2TY medium and grown for 2 hours. The bacterial cells were pelleted and resuspended in an equal volume of ice-cold 50mM $CaCl_2$, re-pelleted and resuspended in 1:20th volume 50mM $CaCl_2$. The cells were divided into 5 equal aliquots, the DNA added, and incubated on ice for 30 minutes. Following a heat-shock step at 37°C for 2 minutes, the cells were then incubated on ice for 30 minutes. 9 volumes of 2TY medium was added and the cells grown at 37°C for 90 minutes and then spread onto specially prepared agar plates. The plates had been spread with 40μl of a 20mg/ml solution of X-gal (5-bromo-4-chloro-3-indolyl-β-D-galactoside) made up in dimethylformamide, and 4μl of 200mg/ml IPTG (isopropyl β-D-thiogalactopyranoside) made up in sterile water. The plates were left to dry for 4-5 hours prior to spreading of the transformed JM101 cells, and were incubated overnight at 37°C to allow the bacterial colonies to grow.

2.3 NUCLEIC ACID METHODS.

2.3.1 General molecular techniques.

General methods including digestion of cDNAs and plasmid vectors with restriction endonucleases, agarose/ethidium bromide gel electrophoresis, treatment of DNA with phosphatases and ligation of DNA fragments was carried out essentially as described by Sambrook *et al.,* (1989). Radiolabeling of DNA was carried out using the QuickPrime kit (Amersham) using the random prime method of Feinberg and Vogelstein, (1984) according to manufacturers instructions. Purification of DNA fragments from agarose gels was carried out using the GeneClean kit (BIO 101, La Jolla, USA) according to the manufacturers instructions. DNA sequencing (by the chain termination method as described by Sanger *et al.*, 1977) was carried out using the Sequenase™ enzyme (version 2.0) and reagents (USB) according to manufacturers instructions. All RNA work was carried out using baked glassware and diethyl pyrocarbonate-treated(DEPC)-water essentially as detailed in Sambrook *et al.*, (1989).

2.3.2 Preparation of plasmid DNA from *E.coli* cultures.

2TY medium containing 100µg/ml ampicillin was inoculated with *E.coli* transformed with appropriate plasmid DNA and grown overnight at 37°C. Cells were pelleted by centrifugation at 5,800g for 10 minutes at 4°C. Pellets were resuspended in ice-cold GTE buffer (50mM glucose, 25mM Tris-HCl, pH8.0, 10mM EDTA pH8.0), and 2.5 volumes 1% sodium dodecyl sulphate (SDS):0.2M NaOH added, followed by 2 volumes 3M potassium acetate and incubated on ice for 10-20 minutes with occasional mixing. Bacterial protein debris was pelleted by centrifugation at 5,800g, the supernatant removed and 20-30mg DNase-free RNase added and incubated at 37°C for 30 minutes. Following extraction with a 1:1 mixture of phenol:chloroform, the DNA was precipitated with 0.6 volumes isopropyl alcohol (IPA). The DNA was pelleted by centrifugation at 12,000g, resuspended in sterile water, and incubated with an equal volume of ice-cold 5M LiCl for

10-20 minutes at 4°C. The RNA was then pelleted by centrifugation at 12,000g, 10

minutes, 4°C and the DNA present in the supernatant precipitated by incubation with 2.5

volumes 13% polyethylene glycol (PEG) 6000 and 0.5 volumes 5M NaCl, at 4°C for 20-

30 minutes. DNA was pelleted by centrifugation and resuspended in water. A further 1:1

phenol:chloroform extraction was performed, followed by precipitation of the DNA with

1/10 volume potassium acetate and 2 volumes absolute ethanol, at 4°C, for 10-20

minutes. The DNA was pelleted by centrifugation and washed once in 70% ethanol, left to

air dry and resuspended in water. The concentration of the DNA was determined by an

OD_{260} reading.

2.3.3 Amplification of cDNA by polymerase chain reaction.

Amplification of cDNA sequences by PCR was carried out essentially as described by

Sambrook *et al.,* (1989). The oligonucleotide primers were 20 nucleotides long, with 8

adenine nucleotides, followed by the six base restriction endonuclease sites at the 5' end.

Oligonucleotides were precipitated with 2 volumes potassium acetate and 4 volumes

ethanol, pelleted and resuspended in 0.25 volumes of distilled water. Reactions were

carried out using 5-10ng of plasmid DNA as a template, over 25-30 cycles in an

automated DNA thermal cycler (Perkin-Elmer-Cetus, Norwalk, USA). Reactions were

carried out in a 1x PCR buffer (50mM KCl, 10mM Tris.HCl pH8.0, 1.5mM $MgCl_2$)

containing 200μM of each dNTP (Ultrapure, Pharmacia), 25pmol of each oligonucleotide

primer and Taq polymerase. Following amplification, a small aliqout was removed for

analysis by agarose/ethidium bromide gel electrophoresis, and the remainder ethanol

precipitated. The pellet was resuspended in water and half was digested with the

appropriate restriction endonuclease and gel purified using the GeneClean kit. The

purified fragment was then subcloned into the appropriately prepared vector.

2.3.4 Preparation of total RNA from cultured cells.

The method used to extract RNA from cells was essentially as described by Chomczynski and Sacchi, (1987). Sub-confluent monolayers of cultured cells were rinsed twice in phosphate buffered saline (PBS; 138mM NaCl, 2.7mM KCl, 9.6mM Na_2HPO_4, 1.76mM KH_2PO_4, pH7.4) and lysed by addition of 2mls solution D/9cm dish (4M guanidium isothiocyanate, 25mM sodium citrate pH7.0, 0.5% sarcosyl, 0.1M 2-mercaptoethanol), and the DNA sheared by passing the lysate repeatedly through a 23 gauge needle. The RNA was extracted by sequential addition of 0.1 volume sodium acetate pH4.0, 1 volume phenol, 0.2 volumes chloroform/isoamylalcohol (24:1), and the solution mixed vigorously by vortexing. The solution was then cooled on ice for 15-20 minutes, and the RNA contained in the upper aqueous phase separated from the DNA/protein by centrifugation at 10,000g, 4°C. The RNA was precipitated by addition of an equal volume of IPA followed by centrifugation as before. The RNA pellet was then resuspended in 0.5ml solution D and reprecipitated with an equal volume of IPA. Following centrifugation as before, the RNA pellet was washed in 70% ethanol and resuspended in 0.1ml DEPC-water. The concentration was determined by taking an OD_{260} reading, and 30µg aliquots stored at -70°C.

2.3.5 Northern blotting.

30µg of total RNA was separated by electrophoresis in a 1% agarose gel, dissolved in 2.2M formaldehyde and 1xMOPS buffer, run in 1xMOPS buffer (MOPS buffer, 0.02M MOPS, 5mM sodium acetate, 0.1mM EDTA). The RNA was denatured by addition of 0.5 volume MOPS buffer, 0.75 volume formaldehyde and 2.5 volumes de-ionised formamide, and heated to 65°C for 10-15 minutes prior to loading. The RNA was transferred to Hybond-N nylon membrane (Amersham) by capillary action in 20xSSC (3M NaCl, 0.3M Na citrate) for 18-24 hours as described by Sambrook *et al.*, (1989). The filter was dried and the RNA fixed by UV crosslinking. The filter was then pre-

51

equilibrated in hybridisation solution (3xSSC (0.45M NaCl, 0.045M Na citrate), 2X Denhardts solution (0.4% Ficoll 400, 0.4% polyvinylpyrolidone (PVP), 0.4% bovine serum albumin (BSA)), 0.1% SDS, 6% PEG 6000, 0.2mg/ml calf thymus DNA) at 65°C for 1-5 hours. The ^{32}P-labelled probe was added directly to the hybridisation chamber and incubated for a further 12-18 hours. The filters were washed in 1xSSC/0.1% SDS (DNA probe) or 0.05xSSC/0.1% SDS (RNA riboprobe) until background counts were low (as determined by a γ counter). The filters were then exposed to autoradiographic film (Kodax X-OMAT AR) at -70°C for 1-7 days.

2.3.6 Preparation of radio-labelled RNA riboprobe.

Incorporation of ^{32}P-labelled rUTP into *in vitro* transcribed RNA was carried out using a modification of the method of Melton *et al.*, (1984). Template plasmid DNA (pMV1:AS, see Figure 3.3) was linearized using the *EcoR* V restriction enzyme and extracted with an equal volume of 1:1 phenol:chloroform mixture. The aqueous phase was removed and ethanol precipitated. Following resuspension in DEPC-treated water, a small aliquot of the DNA was analysed by agarose gel electrophoresis to determine the extent of linearisation. The *in vitro* transcription reaction was carried out in 1x transcription buffer (200mM Tris.HCl pH7.5, 30mM MgCl$_2$, 10mM spermidine, 50mM NaCl) containing 10mM dithiothreitol (DTT), 1unit RNAguard (Pharmacia), 2.5mM each rA/C/GTP, 50μCi ^{32}P-rUTP, 60 units T3 RNA polymerase (Pharmacia) using 1μg linearised plasmid DNA as the template. Following incubation at 37°C for 60 minutes, the template DNA was digested using RNase-free DNase I (Pharmacia) at 37°C for a further 15 minutes. The RNA was extracted with a 1:1 mixture of phenol:chloroform and ethanol precipitated twice and resuspended in DEPC-water. A small aliquot was analysed by agarose gel electrophoresis along with an aliquot removed from the reaction mixture prior to addition of the T3 polymerase. The gel was dried onto filter paper and exposed to autoradiographic

film (Kodak) to determine incorporation of the ^{32}P-rUTP into the transcribed RNA. The remainder of the RNA was added directly to the hybridisation chamber.

2.4 MAMMALIAN AND AVIAN CELL CULTURE METHODS.

2.4.1 General culture of mammalian and avian cell lines.

The following cell lines were cultured:

NIH3T3	Mouse embryo fibroblasts isolated from NIH Swiss mouse embryo ATCC No. CRL 1658
Balb/c 3T3	Mouse embryo fibroblasts isolated from Balb/c 3T3 mouse embryo, clone A31. ATCC No. CCL 163
MRC5	Human embryo lung fibroblasts. ATCC No. CCL 171
CEF	Primary chick embryo fibroblast cultures prepared as follows.

The head, limbs and gut of 9-10 day old chick embryos were removed and the remaining tissue finely minced. Following digestion with 0.25% trypsin at initially 4°C and then at 37°C, each for 20 minutes, the tissue fragments were pelleted and the supernatant filtered through sterile gauze to remove any large fragments. The resultant cells were pelleted, washed and plated out. The medium was changed after 2-3 hours to remove any contaminating myoblasts

All cell lines were cultured in Dulbeccos Modified Eagle medium (DMEM) supplemented with 100 units/ml penicillin, 100 µg/ml streptomycin and 250 ng/ml fungizone™ (Life Technologies). Medium used for both 3T3 cell lines were supplemented with 10% newborn calf serum (NCS). MRC5 cell culture medium was supplemented with 15% fetal calf serum (FCS), and CEF culture medium was supplemented with 10% tryptose phosphate broth, 5% NCS and 1% chick serum. Medium for all cell lines except MRC5 cells contained 1000 mg/litre D-glucose and 110 mg/litre sodium pyruvate. DMEM used

53

for MRC5 culture contained 4500 mg/litre D-glucose without sodium pyruvate. Subconfluent cells were passaged twice weekly using a 1:5 trypsin/versene mixture. Cultures of both CEF and MRC5 cells were discarded after 10-15 passages. All cells were maintained at a temperature of 37°C and 5% CO_2. Light microscope phase contrast pictures of growing cell cultures were taken on a Nikon light microscope, fitted with an Olympus camera, using Ilford HP5 film, ASA 400.

2.4.2 Isolation of stable 3T3 cell lines expressing a mouse vinculin antisense RNA.

Either Balb/c 3T3 or NIH3T3 cells were seeded at a concentration of 5×10^5 cells/9cm dish 24 hours prior to transfection. Typically 20μg of plasmid DNA was diluted in 2mls of 1xHepes buffered saline (HeBS) (140mM NaCl, 0.75mM Na_2HPO_4, 2.5mM HEPES), containing 125mM freshly-prepared $CaCl_2$, and air bubbled briefly through this mixture. Following a 30 minute incubation at room temperature, the DNA/$CaCl_2$ mixture was added directly to the culture medium of duplicated dishes and the cells returned to the incubator for 6-8 hours. The medium was removed from the dish and the cells rinsed in serum-containing growth medium. The cells were then treated with 2ml of 20% glycerol/PBS for 2 minutes. Fresh medium containing 7mM sodium butyrate was then added to the cells and the dishes returned to the incubator for 48 hours. The cells were then trypsinised and split into five 9cm dishes containing fresh medium with 0.5mg/ml G418 (Life Technologies) for selection of cells containing the plasmid. The G418-containing growth medium was replaced every 3-4 days until isolated colonies of resistant cells were seen. Each of these clones was isolated from the parent dish by tower cloning. The dishes were rinsed twice in PBS, and a small metal cylinder, dipped in vaseline was placed over the colony of cells. 2-3 drops of trypsin were pipetted into the cylinder, and once all the cells had detached, 2-3 drops of medium were added to the cylinder and the cells removed to a 3cm dish containing fresh medium plus G418. Clones were expanded

up to 9cm dishes and one dish of each clone was trypsinized and the cells resuspended in a mixture of 65% FCS, 25% DMEM and 10% dimethyl sulfoxide (DMSO) for long term storage in liquid nitrogen. Clones were cultured in the presence and absence of $1\mu M$ dexamethasone (Sigma, dissolved in absolute ethanol, stock concentration $100\mu M$) for 4-5 days, with fresh dexamethasone being added directly to the culture medium every day during the treatment.

2.4.3 Cell spreading assay.

Cells were grown in the presence and absence of $1\mu M$ dexamethasone for 4-5 days. Prior to the spreading assay, tissue culture plastic was coated with fibronectin (Sigma), collagen type IV (Sigma, $10\mu g/cm^2$) and laminin (isolated from the basement membrane of Engelbreth Holm-Swarm (EHS) mouse sarcoma by Mr. Bipin Patel, $4\mu g/cm^2$). Collagen and laminin were dried onto the tissue culture plastic. Fibronectin was diluted to $50\mu g/ml$ in PBS, added to the wells and removed after 1-2 hours, which were then washed briefly with PBS before use. Cells were rinsed in PBS, trypsinised and resuspended in serum-free DMEM. Cells were added to the coated wells and returned to the incubator for 60 minutes and phase contrast photographs were taken of the spread cells for subsequent analysis.

2.4.4 Derivatisation of fibronectin onto glass coverslips.

Cells for immunofluorescence analysis of the spreading assay (see above) were plated onto glass coverslips upon which the fibronectin had been covalently derivatised using the following method. Coverslips were immersed in 20% (v/v) H_2SO_4 overnight at room temperature and then washed twice in distilled water and once in 0.1M NaOH. After blotting dry on tissue paper, the coverslips were covered in 3-aminopropyltriethysilane (Sigma) and rocked for 4 minutes at room temperature. After extensive washing with distilled water, they were washed once in PBS and overlaid with gluteraldehyde (0.25%

in PBS) for 45 minutes at room temperature. Coverslips were rinsed three times in PBS and coated with fibronectin as described above.

2.4.5. Growth of fibroblast cells in agar.

For these experiments the NCS was filtered to remove any protein aggregates that may act as growth surface. Cells were trypsinised and diluted to 1×10^6 cells/ml and 0.1ml of cell suspension was added to 2.9 mls of DMEM/10% NCS/0.3% bacto-agar (Oxoid) and quickly mixed by pipetting up and down and overlaid onto a freshly-made base of 0.5% bacto-agar/10% NCS/DMEM in a 6cm dish. Where appropriate, $1\mu M$ dexamethasone was added to both the agar and the medium. After 24 hours, the agar was then overlaid with 1-2mls of 10% NCS/DMEM, and dexamethasone was added to the medium each day, and the cells fed with 0.3% agar/DMEM weekly. The dishes were incubated at $37°C$ for 2-3 weeks until obvious colonies were seen and phase contrast photographs taken.

2.4.6 Treatment of 3T3 cells with antisense oligonucleotides.

Cells were seeded at a density of 2×10^4/6cm dish one day prior to use. Phosphorothioate oligonucleotides were precipited with 2 volumes potassium acetate (filter sterilised) and 4 volumes ethanol, pelleted and resuspended in filter-sterilised water. The concentration was determined by taking an OD_{260} reading and then diluted as described in the text. Oligonucleotides was diluted with an equal concentration of DOTAP transfection reagent (Boehringer Mannheim UK, Lewes, East Sussex, UK) in 1x HeBS to a volume of $100\mu l$, incubated for 10-15 minutes at room temperature and added directly to the culture medium. Cells were treated each day for 4 days.

2.4.7 Preparation of total cell proteins from cultured cells.

Cells were grown to approximately 90% confluence, placed on ice and washed twice in PBS. $150\mu l$ radioimmune precipitation assay (RIPA) buffer (0.01M Tris-HCl, pH 7.0,

0.15M NaCl, 2mM EDTA, 50μM sodium orthovanadate, 0.1% SDS, 1% Nonidet P40, 1% sodium deoxycholate) containing freshly made 5mM phenylmethyl sulfonyl fluoride (PMSF) added to each dish, and the monolayers lysed by scraping them into the buffer using rubber policemen. The cell debris was then pelleted by centrifugation and the concentration of total protein was determined using the Coomassie protein assay kit (Pierce and Warriner, Chester, UK), according to manufacturers instructions. Lysates were stored at -20°C as 50μg aliquots.

2.4.8 Microinjection of cultured cells.

Microinjection was carried out essentially as described by Graessmann *et al.*, (1980). Cells for microinjection were seeded at least 2 days prior to injection onto glass coverslips that had been scored with a cross using a glass etcher. Needles for microinjection were pulled from borosilicate glass capillaries (inner diameter 1mm, Clarke Bio-Medical, Reading, Berkshire, UK) using a microelectrode puller (Campden Instruments Ltd, Sileby, Leicestershire, UK). Each needle was checked under a Leitz Diavert light microscope (Leica UK Ltd, Milton Keynes, Buckinghamshire, UK) prior to use. Needles were back-filled using GELoader tips (BDH) with 1-2μl of sample, and the needle then attached to the microinjector unit (Narashige c/o Leica UK Ltd.). The needles were manipulated over the cells using a Leitz micromanipulator rig and the sample (under positive pressure) injected into the cell. Using this method, all cells were injected with approximately the same amount of sample (1-5 x 10⁻¹⁰ml) relative to their size. An estimated 1:10th of the cell volume is injected/cell (Kreis and Birchmeier, 1982), and approximately 50 cells could be injected within 5 minutes. Both antibodies and fusion proteins were injected from a stock solution at a concentration of 2mg/ml.

2.4.9 Motility assay.

Cultures of CEF cells were grown to confluence on glass coverslips. A portion of the monolayer was removed from the coverslip using a Gilson pipette tip and the coverslip was washed briefly in PBS to remove the dead cells and fresh medium added. Cells along the margin of the wound were injected with antibody, and the cells returned to the incubator for a further 12 hours. Coverslips were fixed in formaldehyde prior to permeabilisation in Triton-X-100 as described below.

2.5 IMMUNOLOGICAL METHODS.

2.5.1 Immunofluorescence staining of cultured cells.

All cells requiring analysis by immunofluorescence were grown on glass coverslips. Cells were either fixed in 3.8% formaldehyde/PBS for 20 minutes and then permeabilised in 0.2% Triton-X-100/PBS for 2 minutes at room temperature, or they were extracted in MES buffer (50mM MES, 3mM EGTA, 5mM $MgCl_2$, 0.5% Triton-X-100, pH6.0) for either 2 minutes (MRC5 and 3T3 cell lines) or 20 seconds (CEF cells) at 4°C, and then fixed in 3.8% formaldehyde for 20 minutes at room temperature. Cells were rinsed briefly in PBS between fixation and permeabilisation or extraction. Primary and Texas Red-labelled secondary antibody incubations were carried out at 37°C for 30 minutes with extensive washing between antibodies. Monoclonal primary antibodies were diluted 1:500, polyclonal primary antibodies were diluted 1:100 and secondary antibodies were diluted 1:50 in PBS containing 0.1% BSA and 0.02% sodium azide. Staining for actin was carried out using fluorescein isothiocynate (FITC)-labelled phalloidin (Sigma), diluted 1:100 in PBS, for 20 minutes at room temperature. All coverslips were mounted in 90% glycerol/PBS and the edges of the slips were sealed in nail varnish. All coverslips were viewed on a Zeiss Axiophot microscope and pictures were taken using Ilford HP5 film uprated to 1600 ASA.

2.5.2 Western Blotting.

Transfer of proteins from SDS-polyacrylamide gels (see below) to nitrocellulose membranes was carried out according to the method of Towbin et al., (1979). The polyacrylamide gel and blotting paper were soaked in transfer buffer (12.5mM Tris, 200mM glycine, 10% methanol, 90% water) for 5-10 minutes, and the Hybond-C extra nitrocellulose membrane (Amersham) was rinsed in distilled water and then soaked in transfer buffer for 5-10 minutes. Following electrophoretic transfer for 45-60 minutes at 200mAmps, the membrane was soaked in Ponceau S stain (0.5% w/v in 5% w/v trichloroacetic acid) to determine the success of transfer. Excess stain was washed away in 1x Tris-buffered saline (TBS, 0.025M Tris-Cl, pH7.5, 0.15M NaCl) with 0.1% Tween 20 (TBS-T) and the non-specific sites on the membrane were blocked in 5% BSA/TBS-T for 60 minutes at room temperature. The filters were rinsed and the primary antibody incubations were carried out for 60 minutes at room temperature followed by extensive washing. Monoclonal primary antibodies were diluted 1:10,000 and polyclonal primary antibodies diluted 1:500. The horseradish peroxidase (HRP)-conjugated secondary antibodies were diluted 1:5000 prior to incubation with the filters for 60 minutes at room temperature. The filter was developed using the enhanced chemi-luminescence (ECL) kit (Amersham) with an average exposure time to autoradiographic film (Fuji RX) for 30 seconds. All washes and antibody dilutions were made in 1xTBS/T with 1% BSA.

2.6 PROTEIN METHODS.

2.6.1 Separation of proteins via SDS-polyacrylamide gel electrophoresis (SDS-PAGE).

The LKB midget electrophoretic unit was used as a support to cast the acrylamide gels which were prepared as detailed in Table 2.1. The resolving gels, either 8, 10 or 12%, and the stacking gels were prepared using a stock 30% acrylamide solution and

polymerisation was initiated by addition of freshly prepared ammonium persulphate (APS) and TEMED. Samples were boiled into sample buffer (50mM Tris, pH8.0, 10% glycerol, 2% SDS, 0.1% bromophenol blue, 10% 2-mercaptoethanol) for 2-5 minutes prior to loading on the gel. Gels were run in 2.5mM Tris, 19.2mM glycine and 0.01% SDS, pH8.3. Proteins were visualised by staining with 1% Coomassie Brilliant Blue (Sigma) made up in 10% acetic acid, 10% methanol, 80% H_2O. Excess stain was removed by extensive washing in the stain solution detailed above without Coomassie Brilliant Blue stain.

Table 2.1. SDS-polyacrylamide gels.

	RUNNING GEL			STACKING GEL
	8%	10%	12%	
30% Acrylamide	2.33ml	2.92	3.5	0.665
1M Tris pH8.8	3.36	3.36	3.36	0.625 * pH6.8
H_2O	2.98	2.40	1.82	3.68
10% SDS	0.09	0.09	0.09	0.05
10% APS	0.2	0.2	0.2	0.1
TEMED	0.01	0.01	0.01	0.008

2.6.2 Expression and purification of glutathione-S-transferase (GST) fusion proteins from *E.coli* cultures.

Single colonies of *E.coli* transformed with the appropriate plasmid DNA were used to inoculate 10ml cultures of 2TY medium containing 100μg/ml ampicillin, and grown overnight at 37°C. Cultures were then diluted 1:20 into 200mls fresh ampicillin-containing 2TY medium, and grown for a further 1-2 hours until the OD_{600} was between 0.4-0.5. Cultures were then treated with 0.1mM IPTG to induce expression of the fusion protein, and grown for a further 2 hours. At this stage, small aliquots of the culture could be pelleted and lysed directly into sample buffer and resolved by SDS-PAGE to check for fusion protein expression if required. Cells were pelleted by centrifugation at 5,800g rpm, 4°C, and resuspended in 1:100 vols. 0.1% Triton-X-100 in PBS containing 5mM PMSF. Following sonication, the bacterial cell debris was pelleted by centrifugation at 12,000g,

at 4°C, and the supernatant removed. 400µl of glutathione-linked agarose beads (made up as a 50% slurry in PBS) was added to the supernatant and incubated with gentle agitation for 10-15 minutes at room temperature. The beads were then washed 3 times in a large volume of PBS and pelleted by brief centrifugation. The GST-fusion proteins were eluted from the glutathione-agarose beads by incubation with an equal volume 5mM glutathione in 50mM Tris, pH8.0, with gentle agitiation for 5-10 minutes. The elution was repeated a second time. Fusion proteins required for microinjection were eluted into 0.5x PBS. The concentration of fusion proteins was determined by Coomassie protein assay kit (Pierce and Warriner) as described by the manufacturers, and the purity of the proteins checked by SDS-PAGE.

2.6.3 Fusion protein/blot-overlay assay.

50µg of CEF total cell protein was resolved by SDS-PAGE (12% gel) and transferred to nitrocellulose as described above. The filter was cut into separate strips corresponding to individual lanes, and blocked in 5% BSA in TBS-T, at 4°C for 1-2 hours. Fusion proteins were diluted in 1% BSA/TBS-T to a concentration of 400µg/ml, and incubated with the filter strips overnight at 4°C. Following extensive washing bound fusion protein was detected using a polyclonal anti-GST antibody and an HRP-linked anti-rabbit antibody as described above.

2.6.4 Actin cosedimentation assay.

20µg of G-actin (Sigma) was mixed with an equal concentration of fusion protein in pelleting buffer (1mM Tris-HCl pH8.0, 0.02mM ATP, 50mM KCl, 0.4mM MgCl$_2$, 0.02mM DTT, 0.1mM NaN$_3$, 0.02mM CaCl$_2$, 0.05% Triton-X-100). Actin polymerisation was initiated by addition of NaCl to a final concentration of 100mM, and the samples were gently mixed and incubated at room temperature for 60 minutes. Samples without actin were prepared as a control. Polymerised actin was pelleted by

61

centrifugation at 100,000g for 15 minutes at 4°C using a Beckman TL-100 Ultrafuge. The supernatant was separated from the pellet, which was resuspended in the same volume of PBS as the supernatant. Equal volumes of both supernatant and pellet were resolved by SDS-PAGE (12% gel) and the proteins visualised by Coomassie blue staining.

CHAPTER 3

DOWN-REGULATION OF VINCULIN PROTEIN LEVELS
USING ANTISENSE TECHNOLOGY

3.1 Introduction.

Antisense technology has been widely used to investigate the functions of various proteins (see Chapter 1 for full review), and several adhesion-related proteins have been sussessfully down-regulated including integrins (Hayashi *et al.*, 1991; Lallier and Bronner-Fraser, 1993), ICAM-1 (Chiang *et al.*, 1991), fibronectin (Steel and Harris, 1989) and the ERM family of proteins (Takeuchi *et al.*, 1994). To investigate the function of the cytoskeletal protein vinculin, we have attempted to down-regulate the vinculin protein levels in both NIH3T3 and Balb/c 3T3 mouse fibroblast cells, using a 1.06kb mouse cDNA (Ben-Ze'ev *et al.*, 1990), which codes for amino acids 116-468 of mouse vinculin. Isolated clones shown to be vinculin-deficient were then further examined to see if a loss of vinculin affected various aspects of cell function.

RESULTS

3.2 Construction of a plasmid vector for the stable expression of an antisense vinculin RNA in mouse fibroblasts.

The 1.06 kb mouse vinculin cDNA (Ben-Ze'ev *et al.*, 1990), in the pBluescript vector was used as a template for PCR amplification of the cDNA, incorporating an *Xba 1* restriction endonuclease site at both the 5' end and the 3' end. The resultant PCR product was cut with the restriction endonuclease *Xba 1*, and analysed using agarose/ethidium bromide gel electrophoresis. The appropriate band was then excised and the DNA fragment gel purified using the Geneclean kit. The pMAMneoBlue vector was linearised with *Xba 1* and the 5' phosphate groups removed with calf intestinal alkaline phosphatase. The plasmid vector and the PCR product were mixed at a ratio of 1:10 with DNA ligase overnight, and then used to transform competent *E.coli* strain JM101 cells.

Following selection on X-gal/IPTG plates, plasmid DNA was isolated from white colonies, and the orientation of the insert determined by restriction endonuclease digestion

63

(Figure 3.1). Digestion of the plasmid with the *Xba 1* restriction endonuclease resulted in liberation of the 1.06 kb mouse cDNA from the 8.8kb plasmid vector (Fig.3.1, Lanes 1 and 3). There are two *Xho 1* sites in the plasmid (see Figure 3.2), one is 32 bases 5' to the *Xba 1* site in the pMAMneoBlue vector, the other is 20 bases from the 3' end of the mouse vinculin cDNA. Digestion of the plasmid with the insert cloned in the sense orientation resulted in liberation of a 1.06 kb fragment, that essentially spans the cloned insert (Fig.3.1, Lane 4). Digestion of plasmid containing the insert in the antisense orientation generated a 9.8 kb fragment (Fig.3.1, Lane 2), and a small, not visible 0.06kb fragment.The plasmid containing the cloned insert in the antisense orientation was designated pMV1:AS, and is shown diagramatically in Figure 3.2. The orientation of the insert was confirmed by dideoxy sequencing using primers based on pMAMneoBlue plasmid sequence either side of the *Xba 1* cloning site, and the Sequenase™ enzyme kit (Figure 3.3).

3.3 Transfection of NIH3T3 cells with pMV1:AS and initial screen of isolated clones for antisense RNA expression by Northern blotting.

NIH3T3 cells were transfected with 20µg of pMV1:AS as described in Materials and Methods. Following selection with G418, 27 cloned cell lines were isolated and expanded. Initially, the amount of vinculin protein in each clone cultured in the presence of 1µM dexamethasone for 4 days was examined by Western blotting of total cell protein, but none of the clones showed any reduction in vinculin protein levels (data not shown). Total RNA was then prepared from each of the clones cultured in the presence of dexamethasone and analysed by Northern blotting. The filters were probed with the ^{32}P-labelled 1.06kb mouse cDNA for detection of both sense and antisense RNA transcripts. Vinculin mRNA was detected in all clones as a diffuse band of approximately 6-7kb, but clones NAS:20 and NAS:22 also contained a lower molecular weight RNA species of approximately 2.5-3kb (data not shown). The Northern blot was repeated with RNA

Figure 3.1. Restriction enzyme digest of plasmids pMV1:AS and pMV1:SE.
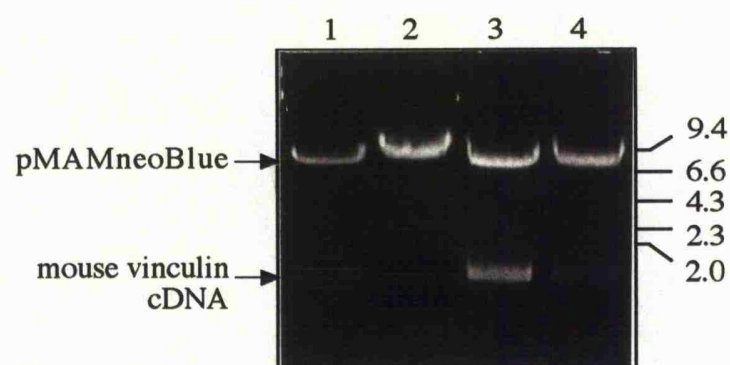
The 1.06 kb mouse vinculin was cloned into the *Xba* 1 site of 8.8kb plasmid pMAMneoBlue in both the antisense (pMV1:AS, lanes 1 and 2), and the sense orientation (pMV1:SE, lanes 3 and 4). Digestion of either plasmid with *Xba* 1 released the 1.06kb cloned insert (lanes 1 and 3). Digestion with *Xho* 1 generated a 9.8 kb and a 0.06 kb (not visible) fragment from pMV1:AS (lane 2), and an 8.8 and a 1.06kb fragment from pMV1:SE (lane 4). DNA size markers (kb) are shown to the right of the figure.

Figure 3.2. Schematic representation of plasmid pMV1:AS.
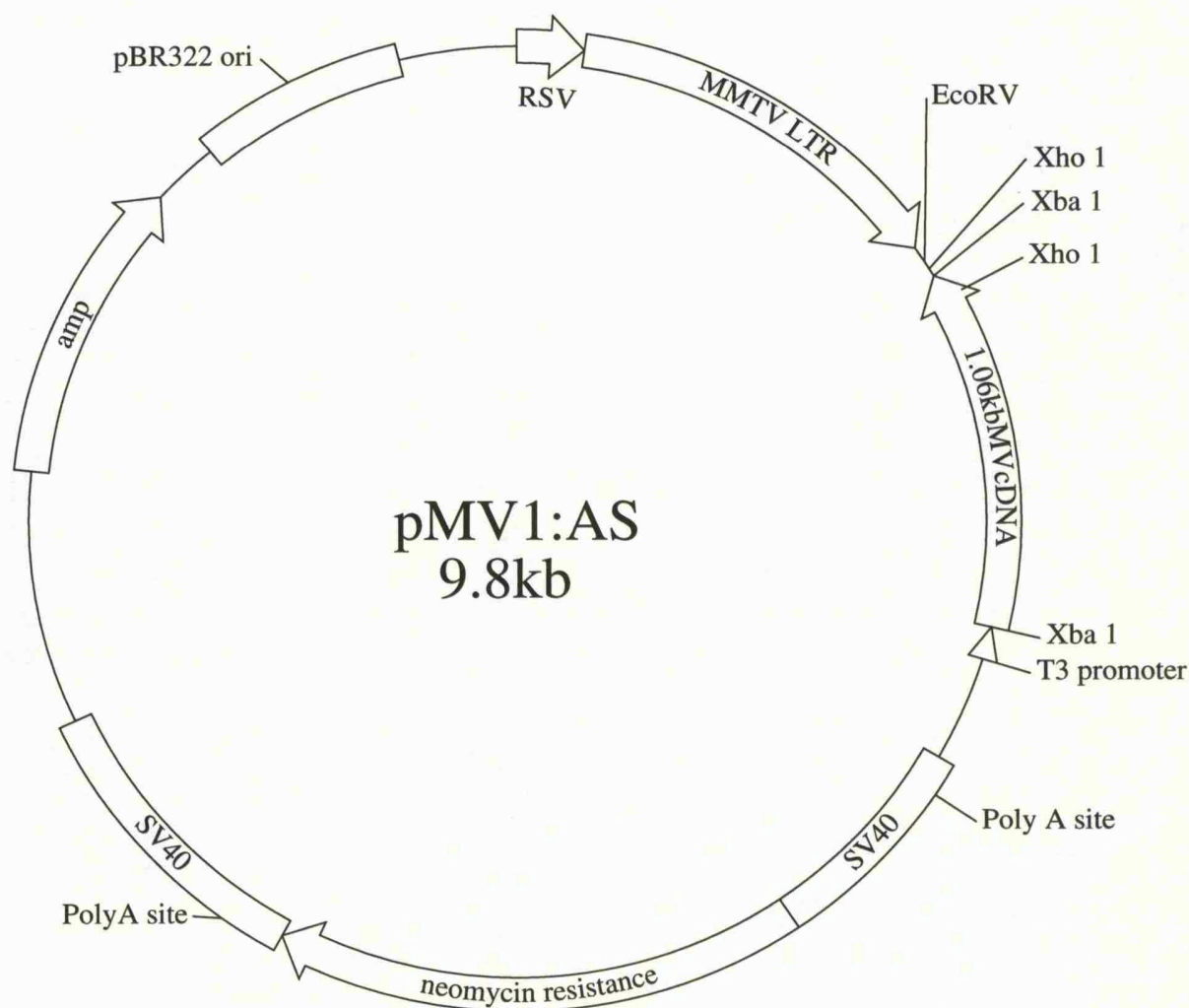
The 1.06kb mouse vinculin (MV) cDNA was generated by PCR and cloned into the *Xba*1 site of the pMAMneoBlue plasmid. The orientation of the insert was determined by restriction mapping using the *Xho*1 site, and confirmed by dideoxy chain termination sequencing. RNA was transcribed *in vitro* from the T3 promoter from *EcoR* V-linearised plasmid. SV40 sequences provide the polyA adenylation sites for correct processing of cloned insert and the promoter for neomycin resistance gene.

Figure 3.3 Confirmation of the orientation of the mouse vinculin cDNA insert in plasmid pMV1:AS.

Sense Orientation.

M13 primer ▶ ◀ *Xba* 1 ▶ ◀ 1.06kb mouse vinculin cDNA ▶

```
GATCC  TCTAGA  CCTTTCTGGA...//...ACAAGTGGCG  TCTAGA  GTCGA
CTAGG  AGATCT  GGAAAGACCT...//...TGTTCACCGC  AGATCT  CAGCT
```

◀ T3 primer

Antisense Orientation.

M13 primer ▶ ◀ *Xba* 1 ▶ ◀ 1.06kb mouse vinculin cDNA ▶

```
GATCC  TCTAGA  CGCCACTTGT...//...TCCAGAAAGG  TCTAGA  GTCGA
CTAGG  AGATCT  GCGGTGAACA...//...AGGTCTTTCC  AGATCT  CAGCT
```

◀ T3 primer
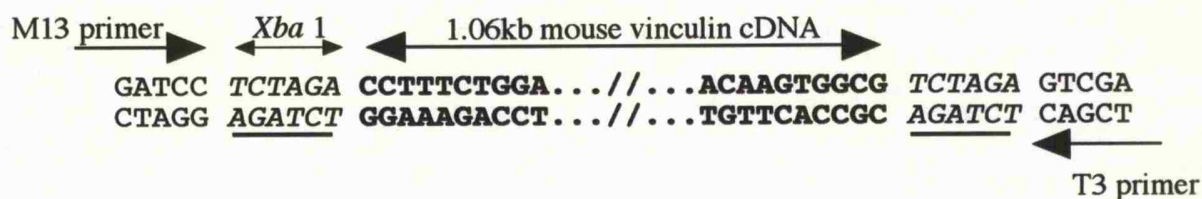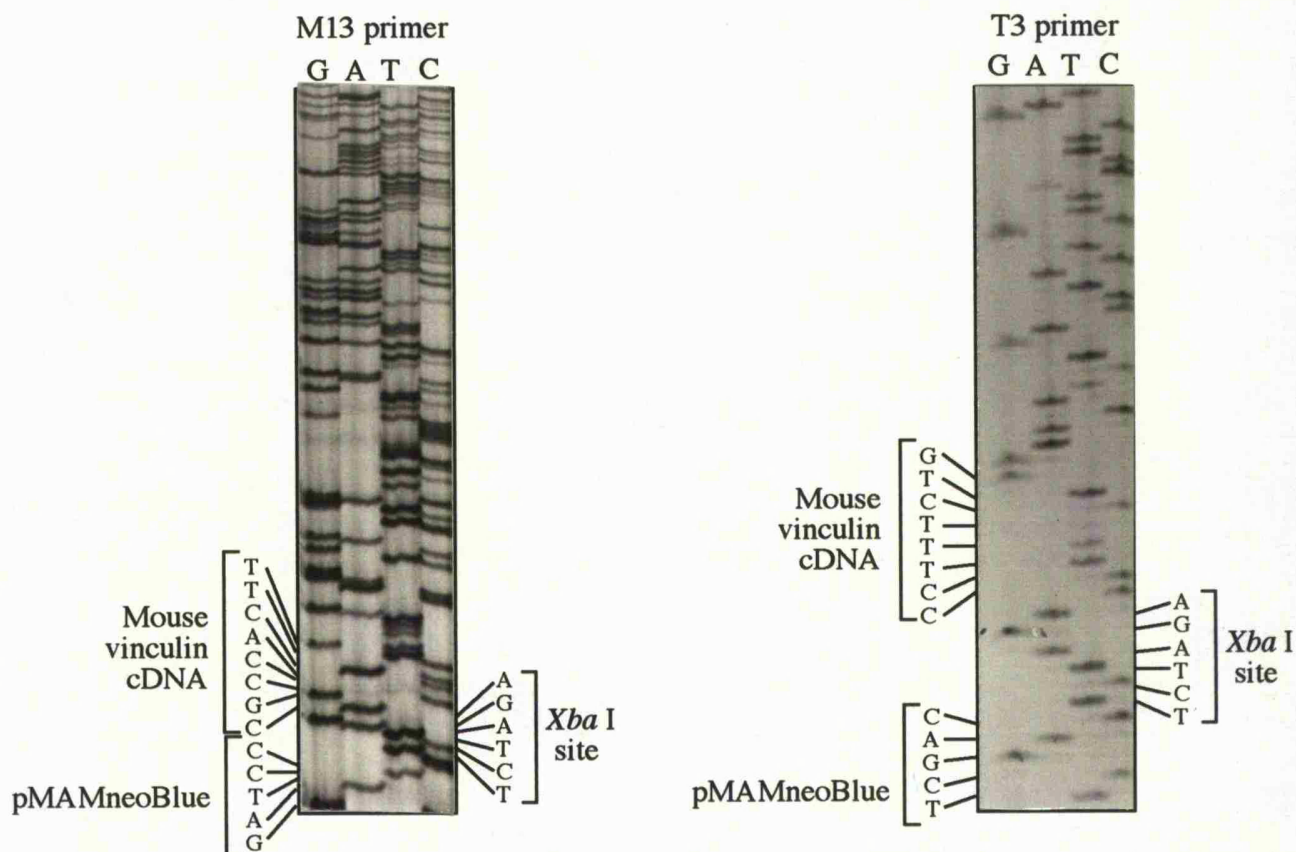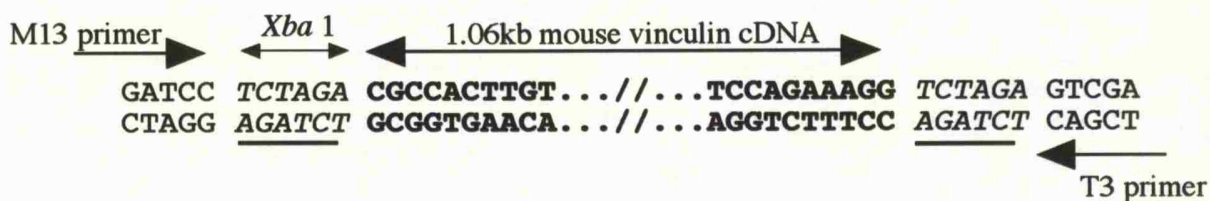
The sequence of the 1.06kb mouse vinculin cDNA (bold type) is shown cloned into the pMAMneoBlue plasmid (plain type) in both the sense and the antisense orientation. The single cloning site, *Xba* 1 is underlined. Below, the sequence of plasmid pMV1:AS from both the M13 primer and the T3 primer using the di-deoxy sequencing method (as described in Materials and Methods) is shown and confirms that the mouse vinculin cDNA is present in the antisense orientation with respect to the MMTV promoter which is 5' to the M13 primer.

isolated from cultures of NAS:20 and NAS:22 grown in the presence (+) and absence (-) of dexamethasone (Figure 3.4A). The putative 2.5-3kb antisense RNA was detected in both of the clones regardless of addition of the dexamethasone to the culture medium and appeared to be expressed in vast excess compared to endogenous vinculin RNA. The levels of endogenous vinculin mRNA did not appear to change in either clone or in NIH3T3 cells grown in either the presence and absence of dexamethasone.

The Northern blot was repeated and probed with a ^{32}P-labelled single stranded vinculin RNA riboprobe for the specific detection of the antisense vinculin RNA. As predicted, the riboprobe only hybridised to the putative antisense vinculin RNA and not to the vinculin message (Fig.3.4B). This confirms that the highly expressed 2.5-3kb RNA detected with the double-stranded cDNA probe is indeed the antisense vinculin RNA expressed from the transfected pMV1:AS plasmid. As none of the other clones were seen to express the antisense vinculin RNA, the subsquent experiments focused on examining the vinculin protein levels in only clones NAS:20 and NAS:22.

3.4 Morphology of clones NAS:20 and NAS:22.

Control untransfected NIH3T3 cells and the two clones NAS:20 and NAS:22 were grown in the absence (Figure 3.5; A, C, E) and presence (Figure 3.5; B, D, F) of 1μM dexamethasone and screened for any change in morphology using the light microscope. After 4 days of culture in the presence of dexamethasone, neither the control NIH3T3 cells (Fig.3.5A, B) nor the clones NAS:20 (Fig.3.5C, D) and NAS:22 (Fig.3.5E, F) displayed any alteration in morphology from the normal well spread phenotype of fibroblasts.

Figure 3.4. Northern blot of NIH3T3 cells and clones NAS:20 and NAS:22.
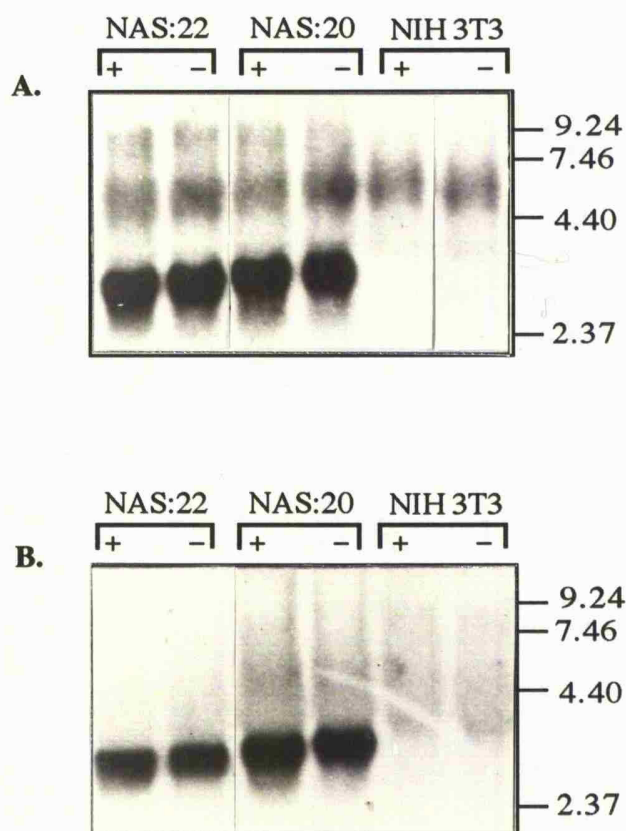
Total RNA was prepared from cultures of NIH 3T3 cells and clones NAS:20 and NAS:22 grown in the presence (+) and absence (-) of 1μM dexamethasone. 30μg of total RNA was separated by agarose/formaldehyde gel electrophoresis and transfered to nylon membranes. (A) The blot was probed with a ^{32}P-labelled 1.06kb mouse vinculin cDNA for detection of both sense and antisense RNA transcripts. The 6-7kb vinculin message is seen in all tracks. Clones NAS:20 and NAS:22 contain another RNA transcript at 2.5-3kb.
(B) The blot was probed with a ^{32}P-labelled 1.06kb sense riboprobe for detection of antisense vinculin RNA transcripts only. The 2.5-3 kb band seen in clones NAS:20 and NAS:22 is the only RNA species detected by the riboprobe.
Size markers (kb) are shown to the right of the figures.

Figure 3.5. Morphology of NIH3T3 cells and clones NAS:20 and NAS:22 cultured in the presence and absence of dexamethasone.
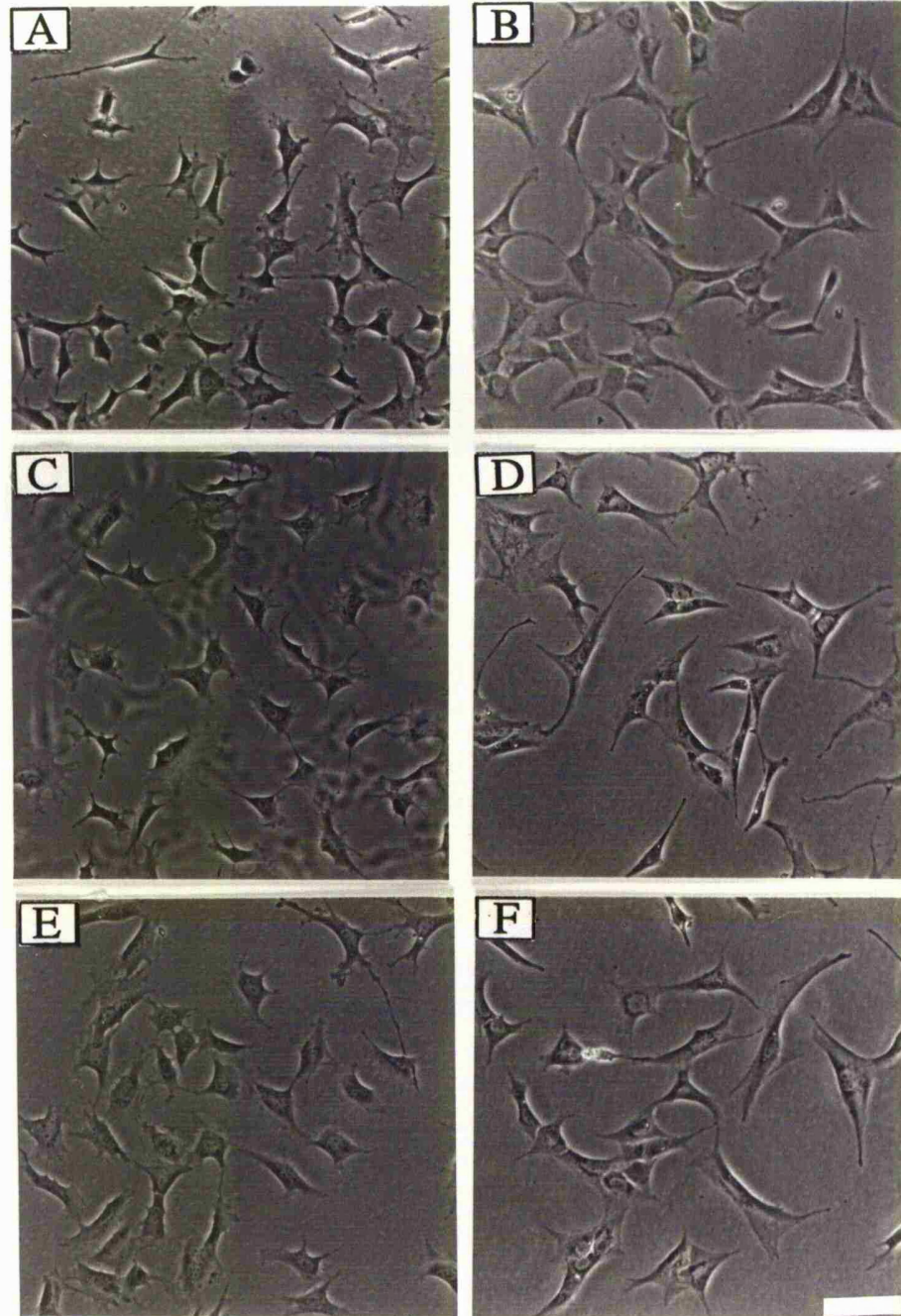
NIH3T3 cells (A, B), and clones NAS:20 (C, D), and NAS:22 (E, F), were cultured in the presence (B, D, F) and absence (A, C, E) of 1μM dexamethasone for 4 days. The cells were viewed under phase conditions and photographed. Bar 25μm.

3.5 Analysis of vinculin expression in clones NAS:20 and NAS:22 by immunofluorescence and Western blotting.

NAS:20, NAS:22 and untransfected control NIH3T3 cells were grown in the presence and absence of dexamethasone for 4 days and the vinculin distribution and protein levels analysed by immunofluorescence and Western blotting, using an anti-vinculin monoclonal antibody V284. Immunofluorescent staining of the control NIH3T3 cells revealed that vinculin localised to focal adhesions seen at the tips of the actin stress fibres and did not show any difference when cultured in the absence (Figure 3.6B) or presence (Figure 3.6D) of dexamethasone. The actin cytoskeleton was visualised by staining with FITC-labelled phalloidin, and was seen to be unaffected by the presence of the dexamethasone (Fig.3.6C) when compared to untreated cells (Fig.3.6A). Only data obtained from clone NAS:20 (Fig.3.6E, F) or NAS:22 (Fig.3.6G, H) cultured in the presence of dexamethasone is shown here, as the distribution of both vinculin (Fig.3.6F, H), and actin (Fig.3.6E, G) remained unchanged compared to either control NIH3T3 cells or non-induced cloned cells.

Whole cell protein lysates prepared from of each of the clones were analysed for vinculin protein levels by Western blotting using the anti-vinculin monoclonal antibody, V284. Figure 3.7. shows the results obtained for clones NAS:20 and NAS:22 prepared in the absence (-) and presence (+) of dexamethasone compared to untransfected NIH3T3 cells. The amount of vinculin seen in control untransfected NIH 3T3 cells is unaffected by addition of the dexamethasone to the culture medium, and there does not appear to be any variation in the vinculin levels in either clone NAS:20 or NAS:22 when cultured in the presence or absence of the dexamethasone.

Figure 3.6. Immunofluorescent staining of NIH3T3 cells and clones NAS:20 and NAS:22. (see opposite)

NIH3T3 cells (A-D), and clones NAS:20 (E, F), and NAS:22 (G, H), were cultured in the presence (C, D, E-H) and absence (A, B) of 1μM dexamethasone for 4 days. Cells were processed for immunofluorescence as described in Materials and Methods and stained for actin with FITC-phalloidin (A, C, E, G), and vinculin with monoclonal antibody, V284 (B, D, F, H). Data obtained from clones NAS:20 and NAS:22 grown in the absence of dexamethasone was identical to either clone grown in the presence of dexamethasone and is not shown. Bar 5μm
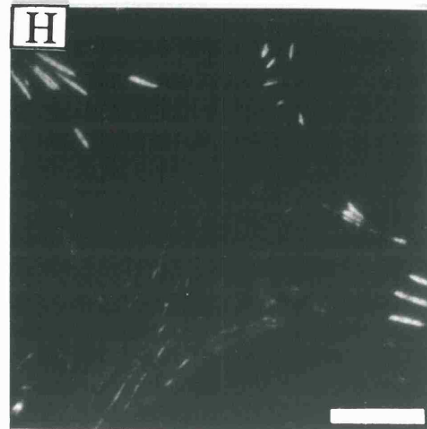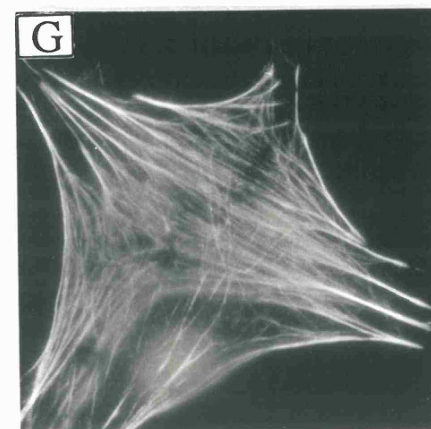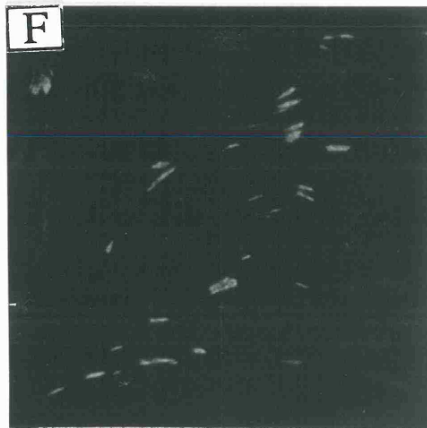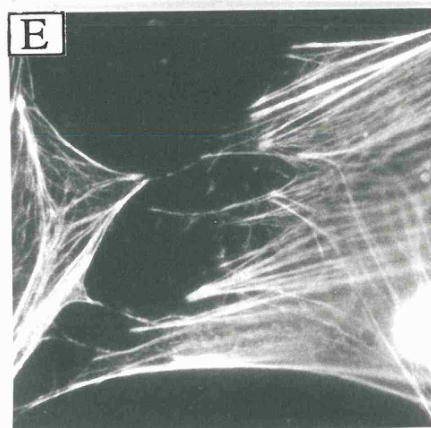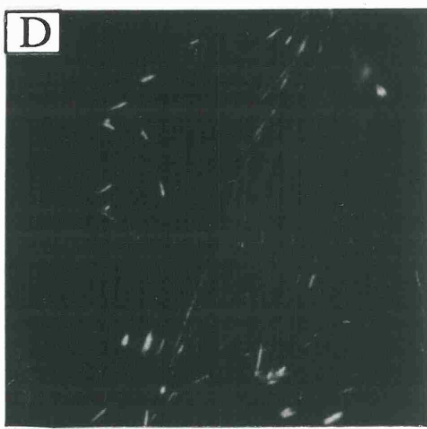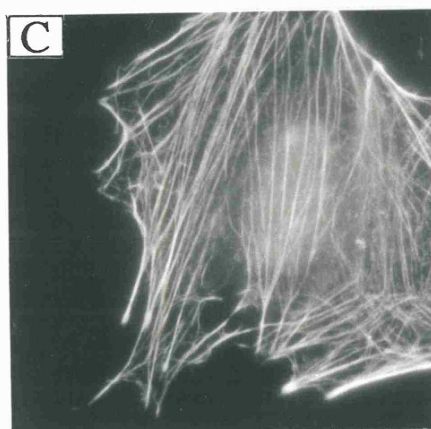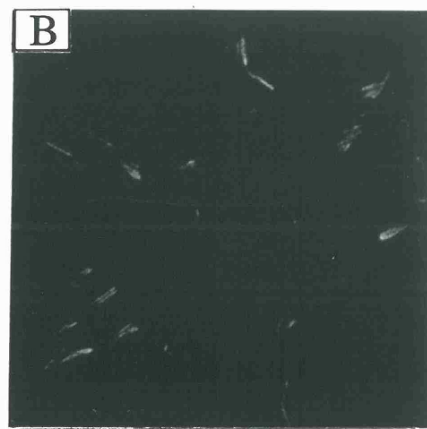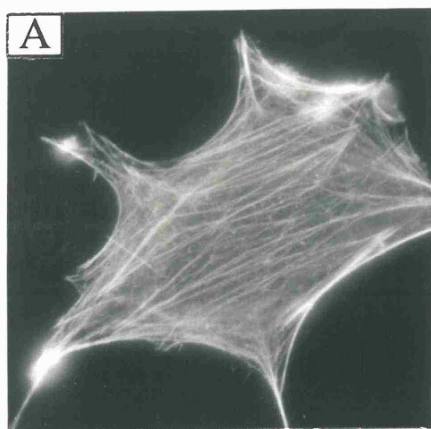
Figure 3.7. Western blot of analysis of vinculin levels in NIH3T3 cells and clones NAS:20 and NAS:22.
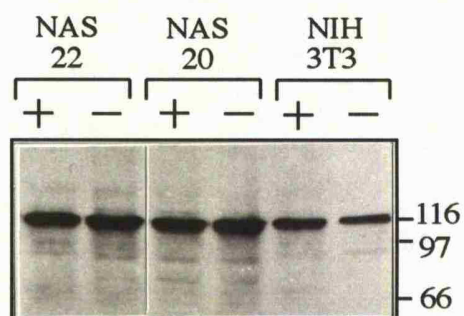
NIH3T3 cells and clones NAS:20 and NAS:22 were cultured in the absence (-) and presence (+) of 1µM dexamethasone for 4 days. Whole cell lysates were prepared and 50µg of total cell protein was resolved by SDS-PAGE and electroblotted to nitrocellulose. The blot was probed for vinculin with monoclonal antibody, V284. Molecular weight markers (kDa) are shown to the right of the figure.

3.6 Transfection of Balb/c 3T3 cells with pMV1:AS and initial screen of clones for an alteration in morphology.

Balb/c 3T3 cells were transfected with pMV1:AS as described in Materials and Methods, and following selection with G418, 30 separate clones were isolated. Initially, the clones were cultured in the presence of dexamethasone for 4-5 days and screened for any alterations in the phenotype using the light microscope. The morphology of the Balb/c 3T3 control cells was similar whether grown in the presence or absence of dexamethasone (Figure 3.8AB), although the cells did seem to grow in small groups rather than separately when dexamethasone was included in the medium. Two of the clones, BAS:8 and BAS:10 displayed a normal fibroblastic morphology when cultured without dexamethasone (Fig.3.8C, E respectively). Inclusion of dexamethasone in the culture medium for either clone BAS:8 (Fig.3.8D) or BAS:10 (Fig.3.8F) resulted in a change from well-spread fibroblastic-looking cells to spindle-shaped cells that appears to be adherent only at either end.

3.7 Analysis of vinculin expression in Balb/c 3T3 clones BAS:8 and BAS:10 by immunofluorescence and Western blotting.

Clones BAS:8 and BAS:10 and untransfected Balb/c 3T3 cells were cultured in the presence and absence of dexamethasone and the vinculin distribution and protein levels were analysed by immunofluoresence and Western blotting. Balb/c 3T3 cells grown in the absence of dexamethasone display a well-spread phenotype with numerous vinculin-containing focal adhesions (Figure 3.9B), which co-localised with the tips of actin stress fibres (Fig.3.9A). When the Balb/c 3T3 cells were then cultured in the presence of dexamethasone there was essentially no change to the vinculin (Fig.3.9D) or actin (Fig.3.9C) staining profile. Untreated cells of clone BAS:8 displayed an identical phenotype to Balb/c 3T3 in terms of both actin organisation (Fig.3.9E) and vinculin (Fig.3.9F) distribution. However, when clone BAS:8 was grown in the presence of

Figure 3.8. Morphology of Balb/c 3T3 cells and clones BAS:8 and BAS:10 cultured in the presence of dexamethasone.
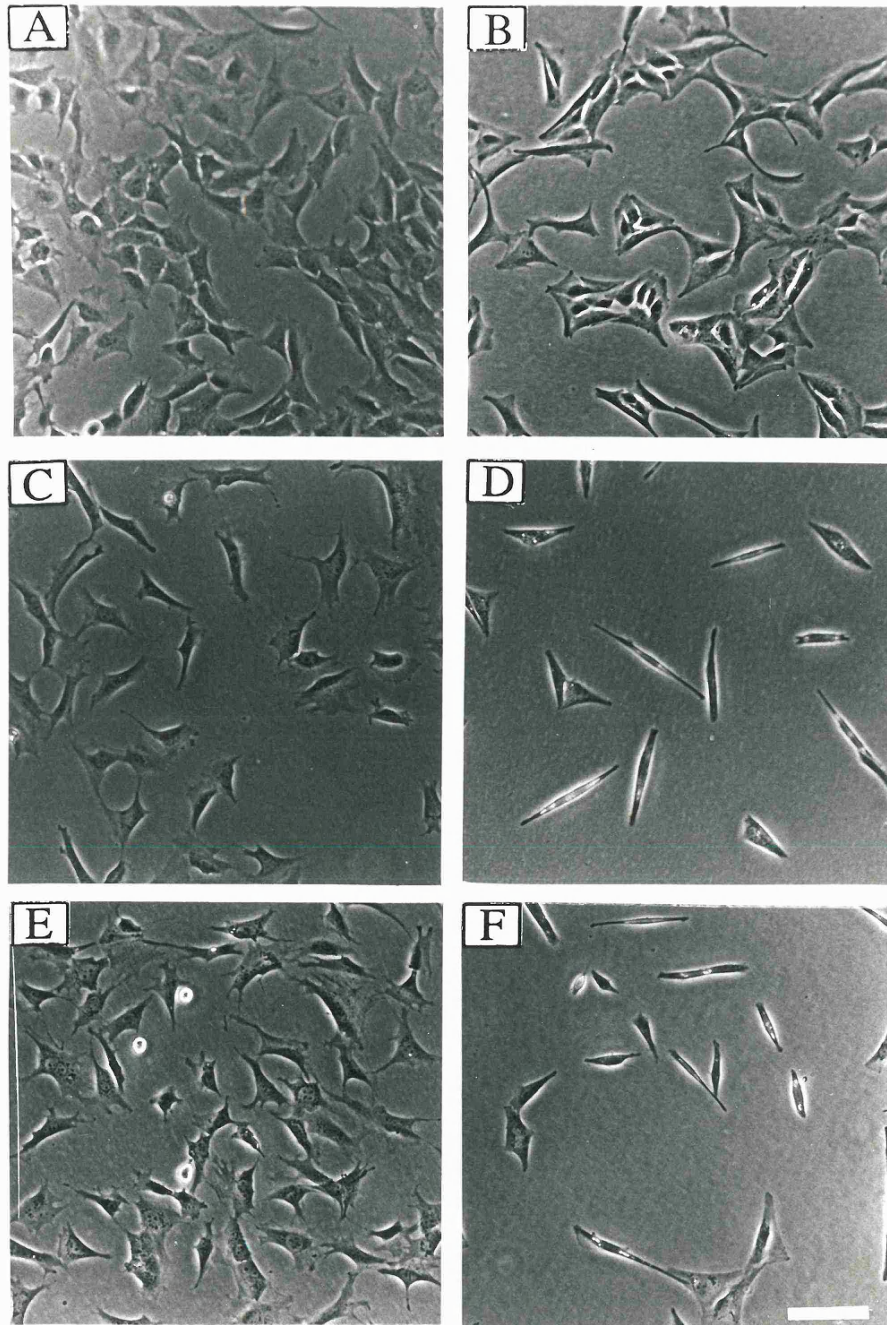
Balb/c 3T3 cells (A, B), and clones BAS:8 (C, D), and BAS:10 (E, F) were cultured in the presence (B, D, F), and absence (A, C, E) of 1μM dexamethasone for 4 days. The cells were analysed under phase conditions and photographed. Bar 25μm.

Figure 3.9. Immunofluorescent staining of Balb/c 3T3 cells and clone BAS:8 (see opposite).

Balb/c 3T3 cells (A-D), and clone BAS:8 (E-H), were cultured in the absence (A, B, E, F), and presence (C, D, G, H) of 1μM dexamethasone for 4 days. The cells were processed for immunofluorescence as described in Materials and Methods and stained for actin with FITC-phalloidin (A, C, E, G). Vinculin (B, D, F, H) was detected using monoclonal antibody V284. Data obtained from clone BAS:10 (not shown) was identical to that of clone BAS:8. Bar 5μm
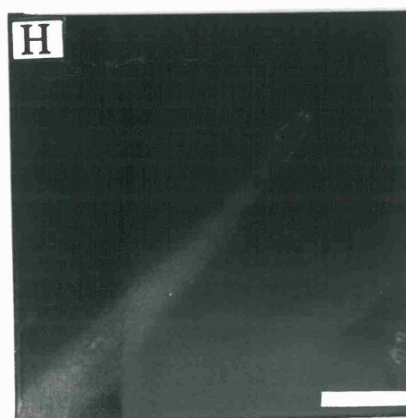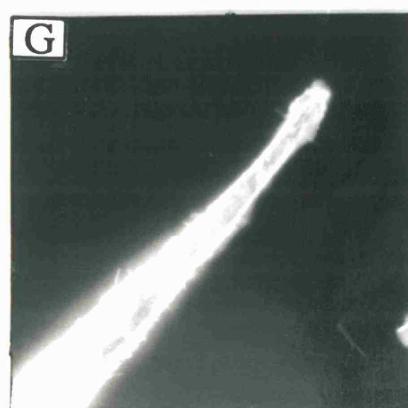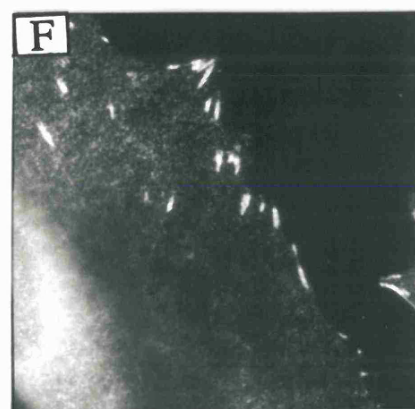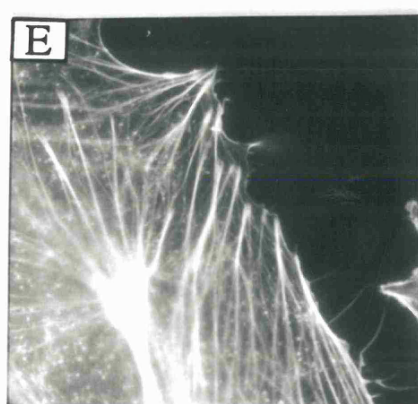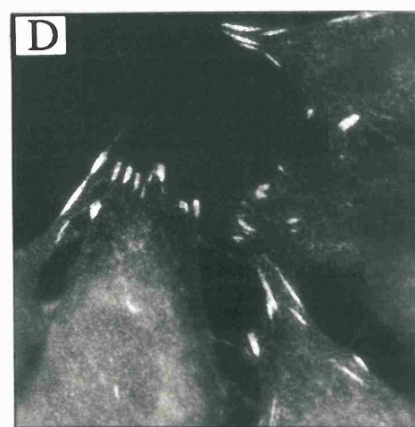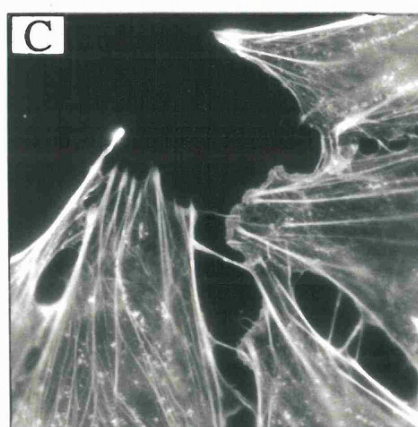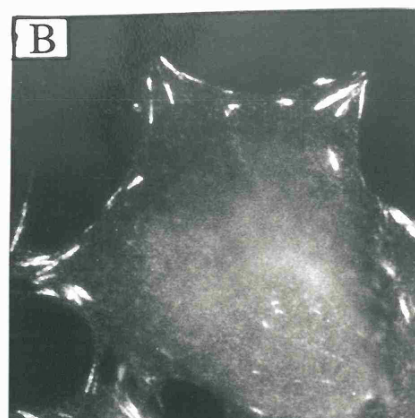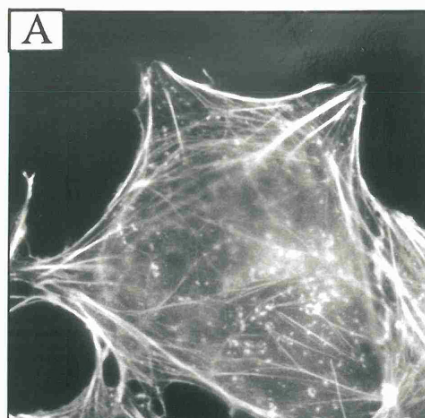
dexamethasone, the actin stain was seen as diffuse fluorescence throughout the cell and there were no actin stress fibres running across the body of the cell (Fig.3.9G). These morphologically-altered cells also displayed drastically reduced numbers of focal adhesions. Although the staining of the cells with the V284 anti-vinculin monoclonal antibody was very faint, the focal adhesions were seen to be much smaller in size and mainly confined to the extreme tips of the cells (Fig.3.9 H). Data from clone BAS:10 (not shown), was identical to that obtained with clone BAS:8

Total cell protein was prepared from both clones cultured with and without dexamethasone and total cell protein was resolved by SDS-PAGE and analysed by Western blotting using the anti-vinculin monoclonal antibody V284. As shown in Figure 3.10A, clones BAS:8 and BAS:10 have reduced levels of vinculin only when cultured in the presence (+) but not the absence (-) of dexamethasone. Balb/c 3T3 cells cultured either with or without dexamethasone contained approximately equal levels of vinculin protein. The blot was then re-probed with a monoclonal antibody raised against α-tubulin (Sigma) indicating that the blot was carried out on equal amounts of whole cell lysate (Fig.3.10B).

3.8 Quantitation of vinculin protein levels in clones BAS:8 and BAS:10.

The levels of vinculin protein as detected by Western blotting, were quantitated by scanning the digitised image of the individual bands seen on the exposed film using the UV-Products gel documentation system. Initially, a standard curve was constructed using Western blots of decreasing amounts of cell lysate from 50μg total protein to 10μg which were probed with V284, the anti-vinculin monoclonal antibody. The bands corresponding to vinculin seen on the exposed film were then scanned and analysed using the gel documentation system, and the amount of vinculin in 50μg of control Balb/c cell lysate was taken as 100%, and a standard curve was plotted. The vinculin bands on the film from the exposed Western blots from each of the clones was then similarly analysed, and

Figure 3.10. Analysis of the vinculin levels in Balb/c 3T3 cells and clones BAS:8 and BAS:10 by Western blotting.
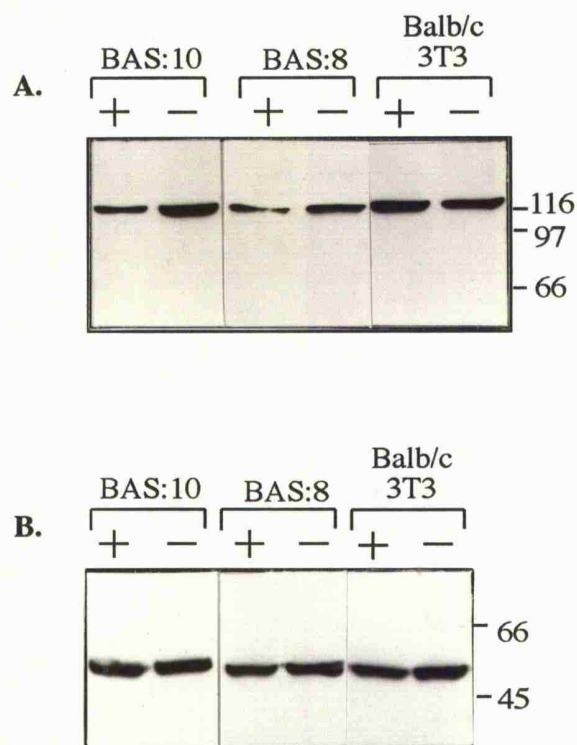
Balb/c 3T3 cells and clones BAS:8 and BAS:10 cultured in the absence (-) and presence (+) of 1µM dexamethasone for 4 days. Cell lysates were prepared and 50µg of total cell protein was resolved by SDS-PAGE and electroblotted to nitrocellulose. The blot was probed for either vinculin with monoclonal antibody V284, (Panel A), or α-tubulin with an α-tubulin monoclonal antibody (Panel B). Molecular weight markers (kDa) are shown to the right of the figure.

the amount of vinculin in each band relative to the untransfected control cells was calculated from the standard curve. Both clone BAS:8 and BAS:10, when cultured without dexamethasone and control Balb/c 3T3 cultured either with or without the dexamethasone, contained approximately equal amounts of vinculin, similar to the amounts seen in 50μg control lysate used to construct the standard curve i.e. 100%. The vinculin levels in clones BAS:8 and BAS:10 grown with dexamethasone, was estimated to be reduced to 29% and 37% respectively compared to control Balb/c 3T3 cells. A summary of the quantitation data and corresponding alteration in cell morphology is given in Table 3.1.

3.9 Reversion of phenotype and subsequent increase in vinculin levels following removal of dexamethasone from clones BAS:8 and BAS:10.

Cultures of Balb/c 3T3 and clones BAS:8 and BAS:10 were grown in the presence of dexamethasone for 4 days and the characteristic spindle-shaped phenotype was observed. The medium on these cells was then replaced with fresh 10% NCS-containing medium without dexamethasone. Within 24 hours, clones BAS:8 and BAS:10 were seen to have a normal well-spread phenotype (Figure 3.11B and C respectively). There was little change seen in the appearance of the control Balb/c 3T3 cells (Fig.3.11A), which were essentially unaffected by addition of the dexamethasone to the cultures. This return to a normal fibroblastic phenotype following removal of the dexamethasone corresponded with an increase in vinculin protein as determined by Western blotting (Fig.3.11D). The vinculin levels, previously seen to be reduced in both BAS:8 and BAS:10 (see Fig.3.10), were restored to the levels of either untreated clones or control Balb/c 3T3 cells.

Table 3.1. Quantitation of the decrease in the vinculin levels in Balb/c 3T3 clones BAS:8 and BAS:10 and corresponding alteration in morphology.

CLONE	PHENOTYPE	% OF 3T3
Balb/c 3T3	Flat	100
BAS:8	Spindle	29 ± 8.5
BAS:10	Spindle	37.5 ± 6.4

Balb/c 3T3 cells and clones BAS:8 and BAS:10 were cultured in the presence of 1μM dexamethasone for 4 days. The levels of vinculin in the cells was analysed by Western blotting using enhanced chemi-luminescence, and the digitised image of the exposed film was scanned, analysed and the amount of protein in each vinculin protein band determined as described in Materials and Methods. The value is the mean +/- S.D. of three blots. The levels of vinculin in clones BAS:8 and BAS:10 cultured without the dexamethasone were similar to Balb/c 3T3 cells i.e.100%. The changes in morphology were assessed by light microscopy and are described in the text.

Figure 3.11. Reversion of phenotype and corresponding increase in vinculin levels in clones BAS:8 and BAS:10 following removal of dexamethasone-containing medium.
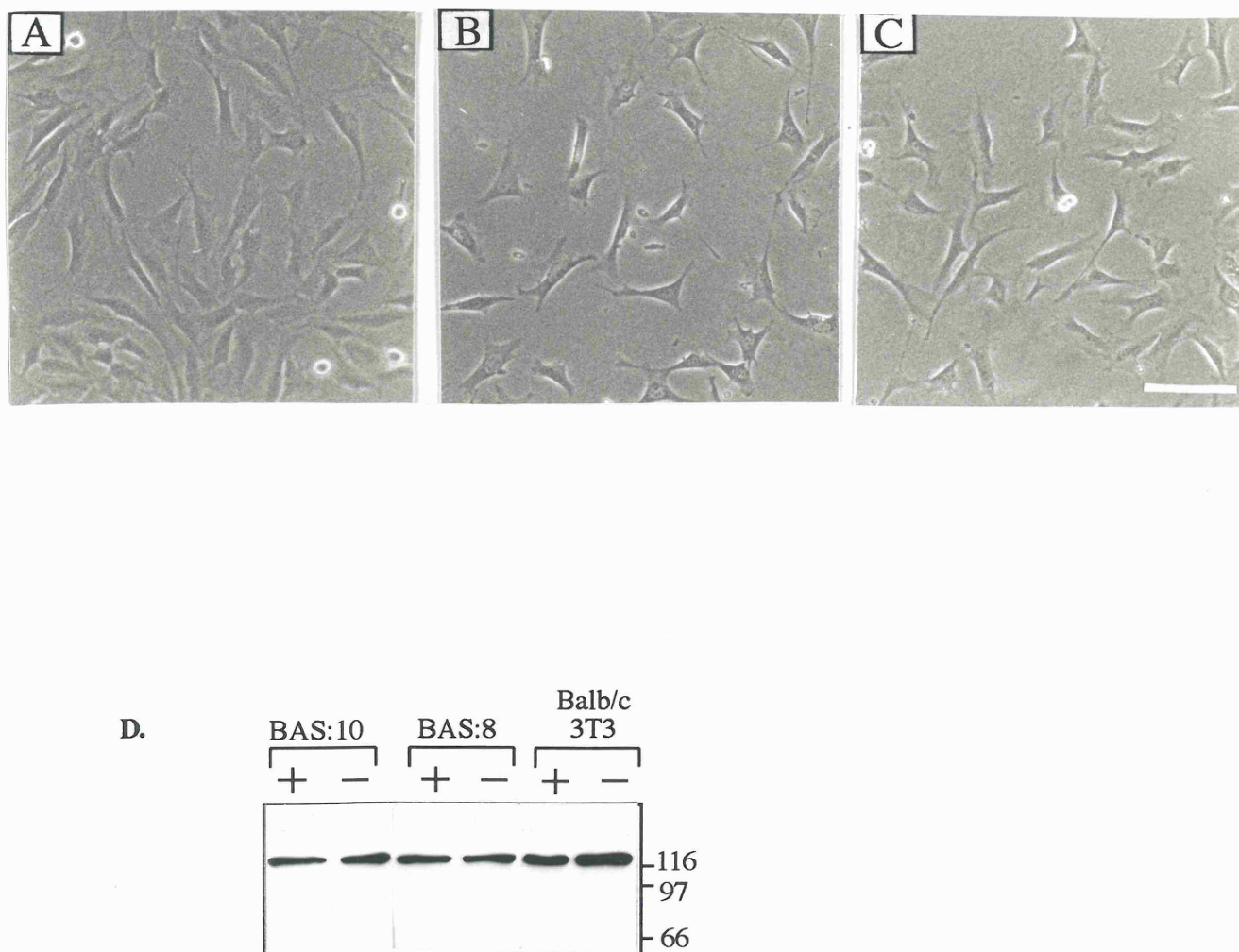
A-C. Balb/c 3T3 cells and clones BAS:8 and BAS:10 were cultured with 1μM dexamethasone for 4 days and an alteration in phenotype was observed only in clones BAS:8 and BAS:10. The medium was replaced with fresh dexamethasone-free medium for 24 hours and clones BAS:8 (B) and BAS:10 (C) are seen to be restored to a normal well-spread fibroblastic phenotype similar to Balb/c 3T3 cells (A). Bar 25μm

D. Balb/c 3T3 cells and clones BAS:8 and BAS:10 were cultured both with (+) and without (-) dexamethasone for 4 days and the dexamethasone-containing medium was then replaced with fresh growth medium. Cell lysates were prepared and 50μg total cell protein was resolved by SDS-PAGE and electroblotted to nitrocellulose. The blot was probed for vinculin using monoclonal antibody, V284. Molecular weight markers (kDa) are shown to the right of the figure.

3.10 Time course of the changes in vinculin protein levels and cell morphology in Balb/c clone BAS:8 cultured with 1µM dexamethasone.

In order to study the time course of both the reduction of vinculin protein levels and the subsequent return to normal levels following removal of the dexamethasone, dishes of clone BAS:8 were set up in the presence of 1µM dexamethasone. After an initial incubation period of 24 hours, the cultures were photographed under phase conditions and then whole cell lysates were prepared from each dish, every 12 hours for the next 60 hours (total time span 84 hours). Figure 3.12A-F charts the appearance of the altered cell morphology with time. The first changes were seen at about 60-72 hours (Fig.3.12D, E), with virtually all the cells displaying the spindle-shaped morphology by 84 hours (Fig.3.12F). The corresponding Western blot of this experiment is shown in Figure 3.12G, and cells cultured with the dexamethasone for 60-72 hours begin to show a reduction in the levels of vinculin protein. The blot was exposed to film and the bands scanned and the amounts of vinculin quantitated as described above. The levels of vinculin protein are reduced to 68% of control Balb/c 3T3 cells after 60 hours and 20% after 72 hours, with a maximum reduction down to 10% of Balb/c 3T3 control cells after 84 hours. The relatively low amounts of vinculin in cells taken from the first two time points is most likely due to the low numbers of cells in the dishes requiring that all or most of the sample is needed for the blot. The quantitative data following the reduction in vinculin protein levels is shown in Table 3.2.

To study the subsequent reversion of vinculin levels following removal of the dexamethasone, the medium on cells displaying the alteration in morphology was replaced with fresh 10% NCS/DMEM and phase contrast photographs taken after 2, 4, 8 and 12 hours. Cell lysates were also prepared from these dishes and equal amounts of total cellular protein were analysed by Western blotting using the anti-vinculin monoconal antibody V284. After 2 hours (Figure 3.13A) many of the cells were already displaying a

Figure 3.12. Time course of appearance of spindle-shaped phenotype and corresponding reduction in vinculin protein levels in clones BAS:8 and BAS:10.
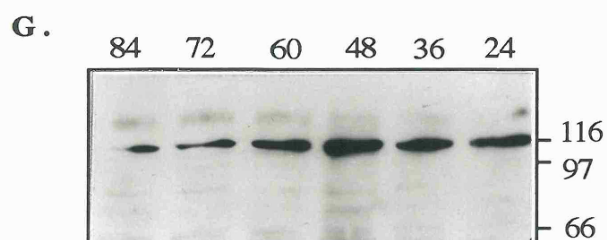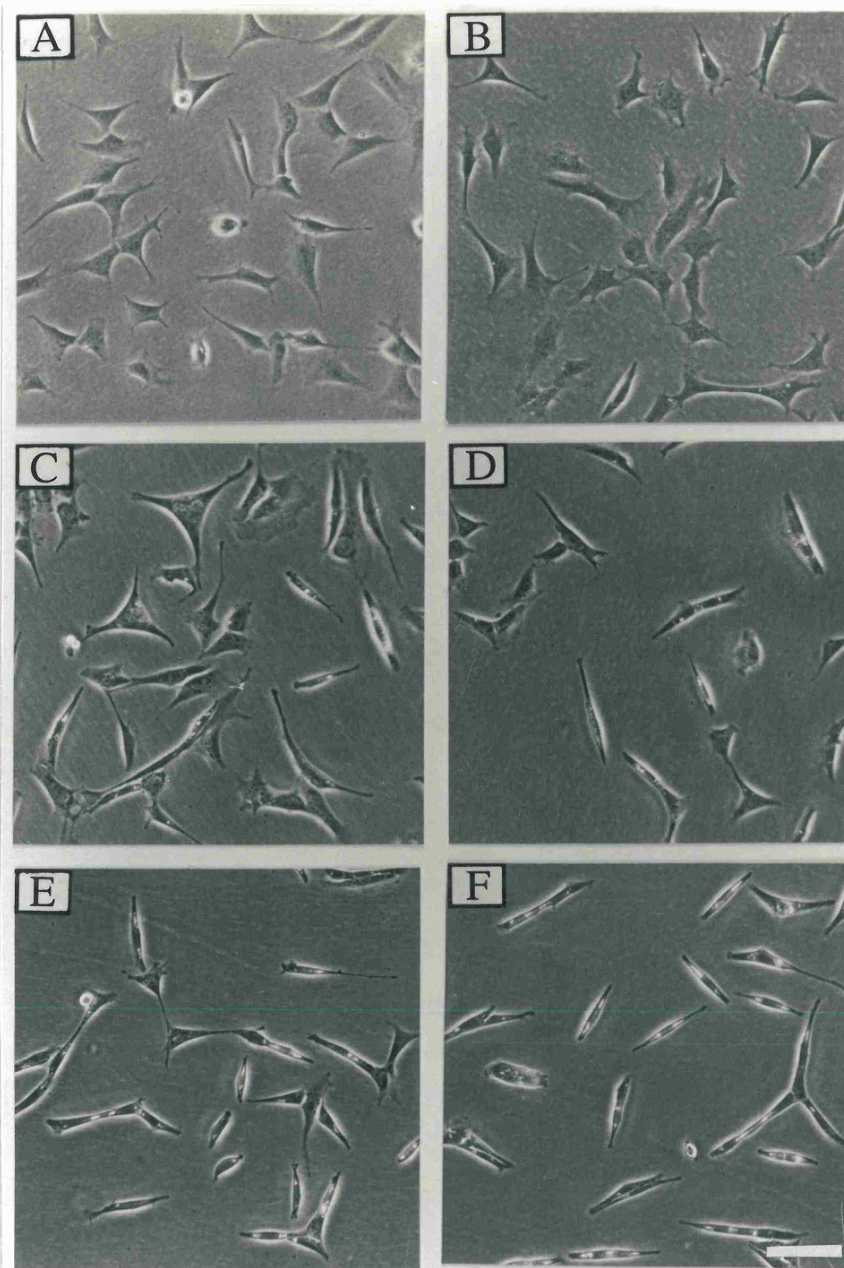
A-F. Clone BAS:8 was cultured in the presence of 1μM dexamethasone for 84 hours. After an initial 24 hour period, the cells were viewed under phase conditions and photographed every 12 hours. A. 24 hours; B. 36 hours; C. 48 hours; D. 60 hours; E. 72 hours; F. 84 hours. Bar 25μm

G. Cell lysates were prepared from each dish photographed and 50μg of total cell protein was resolved by SDS-PAGE and electroblotted to nitrocellulose. The blot was probed for vinculin with monoclonal antibody V284. Time (hours), is shown above each lane and molecular weight markers (kDa), are shown to the right of the figure.

Table 3.2. Quantitation of the reduction in the levels of vinculin protein in clone BAS:8 over a time course of 84 hours.

Hours with dex.	% of control
24-48	60-100*
60	68
72	20
84	10

Clone BAS:8 was cultured with 1µM dexamethasone for upto 84 hours, and cell lysates was prepared at different time points. Total cellular protein was resolved by SDS-PAGE and electroblotted to nitrocellulose. The blot was probed for vinculin with monoclonal antibody V284. The decrease in vinculin protein levels was analysed and quantitated as described previously.

* the data for 24, 36 and 48 hours are shown together as the levels of vinculin in the first two time points were quite low possibly due to the reduced numbers of cells in these early time points. By 48 hours the levels of vinculin were judged to be equivalent to 100%.

Figure 3.13. Time course of reversion to a normal fibroblastic-type phenotype and corresponding increase in vinculin levels in clone BAS:8 following removal of dexamethasone-containing medium.
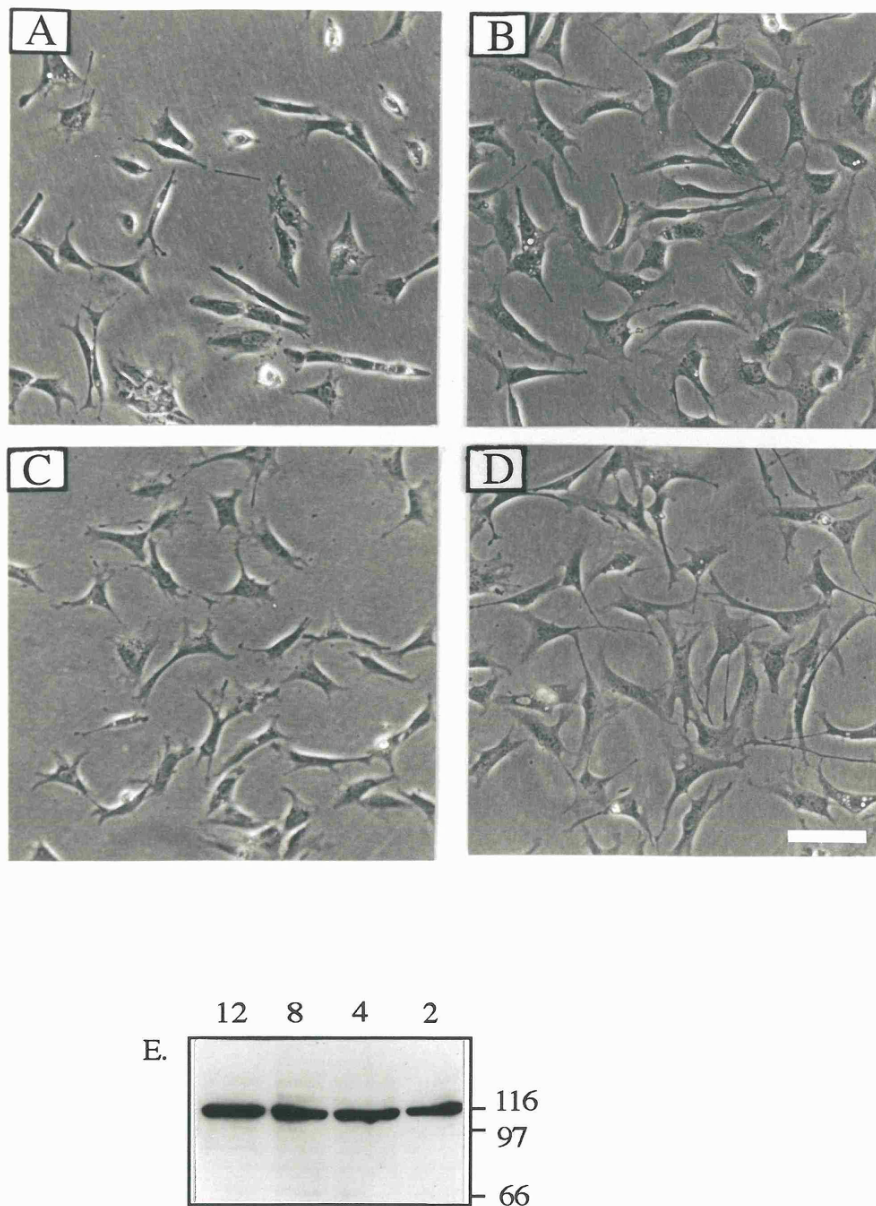
A-D. Cultures of clone BAS:8 were cultured in 1μM dexamethasone for 4 days until the cells displayed the spindle-shaped phenotype. The cells then had their medium replaced with dexamethasone-free medium and were viewed under phase conditions and photographed after 2 (A), 4 (B), 8 (C), and 12 (D) hours. Bar 25μm

E. Cell lysates were prepared from each dish photographed and 50μg of whole cell protein was resolved by SDS-PAGE and electroblotted to nitrocellulose. The blot was probed for vinculin with monoclonal antibody V284. Time (hours) is shown above each lane and molecular weight markers (kDa) are shown to the right of the figure.

flat morphology, and all cells are seen to be fully spread by 12 hours (Fig.3.13D). The corresponding Western blot shown in Fig. 3.13E indicates that the amounts of vinculin protein increase rapidly to levels found in control cells by 12 hours. The film exposed to the blot was scanned as described previously and the amounts of vinculin quantitated (Table 3.3), and indicates that by 2 hours although many of the cells appear to be spread, there is still a 43% reduction in vinculin protein. The levels of vinculin are seen to rise to 100% by 12 hours when virtually all cells appear spread.

3.11 Growth characteristics of clones BAS:8 and BAS:10 cultured in the presence and absence of dexamethasone.

Clones BAS:8 and BAS:10 were seen to grow slower in the presence of dexamethasone when compared to either their untreated counterparts or control Balb/c 3T3 cells. Cultures of both clones and control Balb/c 3T3 cells were grown with (+) and without (-) dexamethasone for upto 4 days. Each day, dishes were trypsinised in duplicate, and the number of cells determined using a Neubauer haemocytometer. The growth curve, expressed in terms of the number of cells/dish, (Figure 3.14), shows that the addition of dexamethasone has little effect on the growth of control Balb/c 3T3 cells. Both clones BAS:8 and BAS:10 when cultured without the dexamethasone grow at a rate comparable to the control Balb/c 3T3 cells. However, when the dexamethasone is added to either clone there is a dramatic reduction in the rate of growth of these cells. Cell growth is slightly reduced after 48 hours, and does not appear to significantly increase after 72 hours of culture with dexamethasone. Interestingly, if the cells are left for any longer periods of time with the dexamethasone, they round up and die.

The ability of the cells to grow in an anchorage-independent environment was assessed by growing the cells in soft agar. SV40-transformed 3T3 cells were used as a positive control and over 75% of cells were seen to grow into large colonies of cells within 2-3 weeks

Table 3.3. Quantitation of the increase in the levels of vinculin in clone BAS:8 following removal of dexamethasone-containing medium.

Hours after removal of dex.	% of control
2	43
4	60
8	76
12	100

Clone BAS:8 was cultured with 1μM dexamethasone for 84 hours until the spindle-shaped phenotype was observed. The medium was then removed and fresh growth medium without dexamethasone was added to the cells, and whole cell lysates prepared after 2, 4, 8 and 12 hours. Total cell protein was analysed by Western blotting using the anti-vinculin monoclonal antibody V284 and the vinculin protein levels were analysed and quantitated as described previously.

Figure 3.14. Growth curve of Balb/c 3T3 cells and clones BAS:8 and BAS:10 in the presence and absence of 1µM dexamethasone.
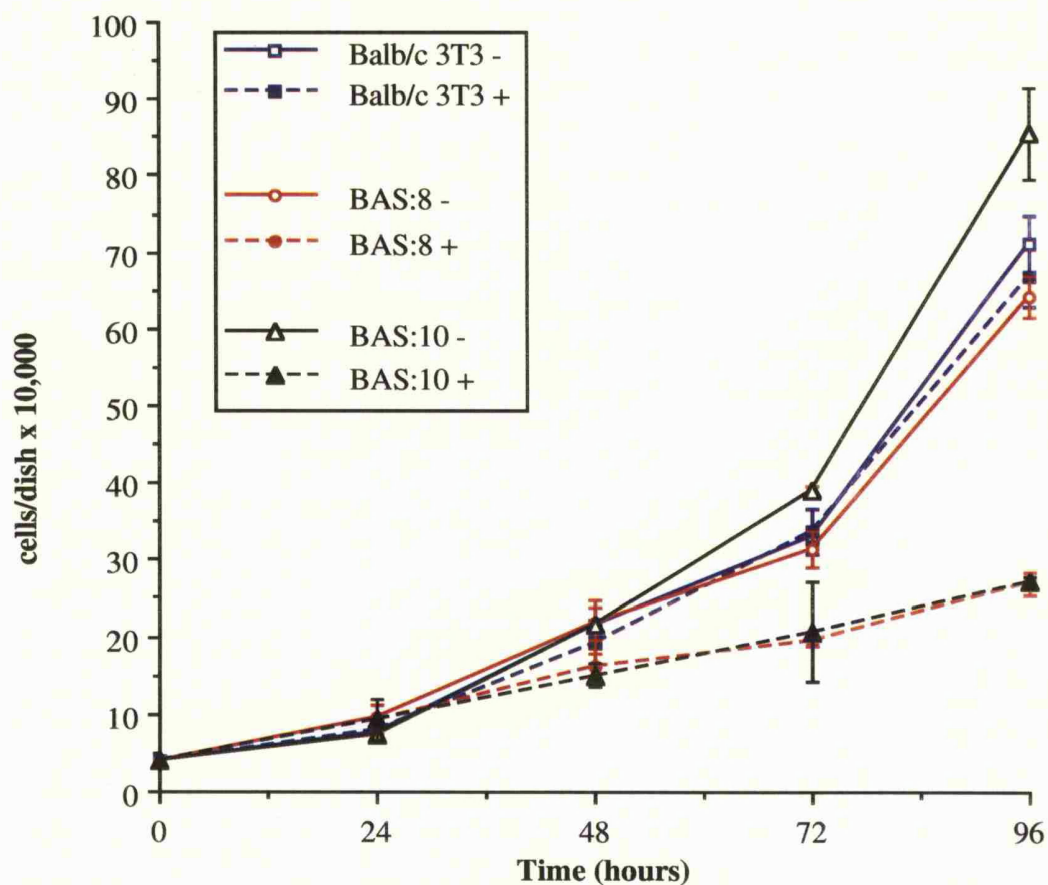
Balb/c 3T3 cells and clones BAS:8 and BAS:10 were grown in the presence (+) and absence (-) of 1µM dexamethasone in 6cm dishes. Every 24 hours, dishes were trypsinised in duplicate and the number of cells/dish was calculated. Values are expressed as a mean, +/- no. cells.

(Table 3.4). Prior to seeding either clone or control Balb/c 3T3 cells in soft agar, they were grown in dexamethasone for 4 days to allow the vinculin levels to decrease and dexamethasone was added to the agar cultures each day. Neither Balb/c 3T3 cells, nor clones BAS:8 and BAS:10 were able to grow in the soft agar either with or without dexamethasone in the agar. No colonies were observed in these dishes and as a consequence only single cells were seen in the agar.

3.12 Vinculin-deficient cells fail to spread when plated onto fibronectin.

Balb/c 3T3 cells and clones BAS:8 and BAS:10 were grown in the presence and absence of dexamethasone for 4 days, trypsinised and plated onto fibronectin, collagen or laminin. Following a 60 minute incubation at 37°C to allow the cells to spread, the dishes were then photographed under phase conditions on the light microscope. Of the three ECM substrates used, the cells adhered best to fibronectin and the majority of Balb/c 3T3 cells (Figure 3.15A), BAS:8 (Fig.3.15C) and BAS:10 (data not shown) cells cultured without dexamethasone were seen as well spread (S) on the fibronectin substrate. Balb/c 3T3 cells cultured in the presence of dexamethasone (Fig.3.15B) were still able to spread, but when either BAS:8 (Fig.3.15D) or BAS:10 (data not shown) were previously cultured with dexamethasone and re-plated onto fibronectin, only a few cells were able to spread and the remainder of the cells were classified as only partially spread (PS), or rounded (R).

Table 3.5 summarises the data obtained for Balb/c 3T3 cells and clone BAS:8 plated on all 3 substrates. The data were collected from the photographs taken after the 60 minute incubation, and cells were classified as well spread, partially spread or rounded up as shown in Figure 3.15. The percent of cells seen as spread following plating on fibronectin (Table 3.5A) was not significantly different between Balb/c 3T3 cells cultured with (73%) or without dexamethasone (60%) and clone BAS:8 cultured in dexamethasone-free medium (63%). When BAS:8 cells had been previously cultured in dexamethasone, there

Table 3.4. Growth of normal and SV40-transformed Balb/c 3T3 and clones BAS:8 and BAS:10 in soft agar.

Cell Line	No. Colonies (n=)
SV-40/3T3	75 (107)
Balb/c 3T3 - DEX.	0 (85)
Balb/c 3T3 + DEX.	0 (85)
BAS:8 - DEX.	0 (64)
BAS:8 + DEX.	0 (56)
BAS:10 - DEX.	0 (67)
BAS:10 + DEX.	0 (96)

Balb/c 3T3 cells and clones BAS:8 and BAS:10 were grown in the presence and absence of dexamethasone for 4 days. The cells were trypsinised and resuspended in equal concentrations into soft agar, and where appropriate, $1\mu M$ dexamethasone was added to the agar. SV40-transformed 3T3 cells were included as a positive control cell line. The cells were fed each week with fresh agar and grown for 3 weeks until large colonies were visible in the SV40-transformed 3T3 cells. The dishes were examined under the light microscope and the number colonies was counted. The data was obtained from duplicate dishes in two separate experiments.

Figure 3.15. Spreading of Balb/c 3T3 cells and clones BAS:8 on fibronectin.
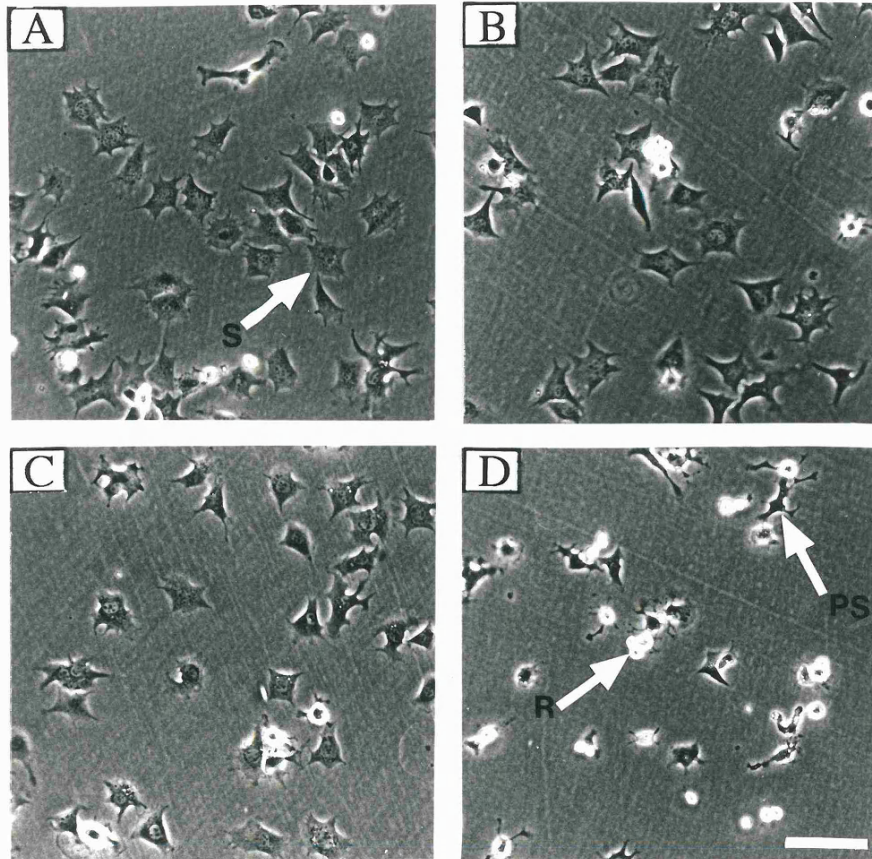
Balb/c 3T3 cells (A, B), and clone BAS:8 (C, D) were cultured in the presence (B, D), and absence (A, C) of 1μM dexamethasone for 4 days. The cells were trypsinised and replated onto fibronectin-coated tissue plastic and incubated for 60 minutes. The spreading cells were viewed under phase conditions and photographed. Bar 25μm.

Table 3.5. Comparison of the abilty of Balb/c 3T3 and clone BAS:8 cells to spread on fibronectin, laminin and collagen.

A. Fibronectin.

Phenotype	Balb/c 3T3 - DEX.	Balb/c 3T3 + DEX.	BAS:8 - DEX.	BAS:8 + DEX.
Spread	73 ± 5	60 ± 1	63 ± 5	17 ± 3
Partially spread	9 ± 2	13 ± 2	13 ± 4	20 ± 4
Rounded	18 ± 3	27 ± 2	24 ± 2	63 ± 5

B. Laminin.

Phenotype	Balb/c 3T3 - DEX.	Balb/c 3T3 + DEX.	BAS:8 - DEX.	BAS:8 + DEX.
Spread	70.5 ± 8.5	46 ± 13	48 ± 6	21.5 ± 2.5
Partially spread	11.5 ± 1.5	18 ± 0	25 ± 6	23.5 ± 1.5
Rounded	18 ± 7	36 ± 23	27 ± 0	55 ± 4

C. Collagen.

Phenotype	Balb/c 3T3 - DEX.	Balb/c 3T3 + DEX.	BAS:8 - DEX.	BAS:8 + DEX.
Spread	53 ± 4	30.5 ± 1.5	47.5 ± 6.5	4.5 ± 1.5
Partially spread	14.5 ± 0.5	16.5 ± 2.5	17 ± 1	19 ± 1
Rounded	32.5 ± 4.5	53 ± 4	35.5 ± 5.5	69.5 ± 0.5

Balb/c 3T3 cells and clone BAS:8 cells were cultured in the presence and absence of 1μM dexamethasone for 4 days. Cells were trypsinised and allowed to re-spread on tissue culture plastic coated with either fibronectin, laminin or collagen as described in materials and Methods. After a 60 minute incubation period, the cells were photographed and the number of cells classified as either spread, partially spread or rounded was determined from the photographs. Data is expressed as a percentage of total cells counted and was obtained from 3 separate experiments. Values are the mean +/- % and typically, between 300-500 cells were counted for each cell line.

was a significant decrease in the numbers of spread cells from 63% to 17%, and the numbers of rounded cells had increased from 24% to 63%. In both cases the numbers of partially spread cells increased only slightly.

The observation that vinculin-deficient cells were unable to spread on fibronectin as efficiently as their normal non-induced counterparts was also seen when the cells were plated on either laminin (Table 3.5B) or collagen (Table 3.5C), although neither substrate supported cell spreading as well, or as consistently when compared to fibronectin. Collagen was seen as the least attractive substrate for both Balb/c 3T3 cells and BAS:8 cells, with reduced numbers of spread cells and a corresponding increase in the numbers of rounded cells compared to those spread on either fibronectin of laminin. The levels of partially spread cells did not increase significantly under any circumstance.

3.13 Vinculin-deficient cells do not display elevated levels of phosphotyrosine when plated onto fibronectin.

The spreading assay described above was repeated using fibronectin-derivatised glass coverslips and the cells stained for actin and either vinculin (Figure 3.16), or phosphotyrosine (Figure 3.17). Balb/c 3T3 cells (Figs.3.16/17A, B) and both clones BAS:8 (Figs.3.16/17E, F) and BAS:10 (data not shown) cultured in the absence of dexamethasone contain both vinculin-rich (Fig.3.16B, F) and phosphotyrosine-rich focal adhesions (Fig.3.17B, F), located at the ends of actin stress fibres (Figs.3.16/17A, E). Similarly, Balb/c 3T3 cells cultured in the presence of dexamethasone (Fig.3.16/17C, D) were also spread with both vinculin (Fig.3.16D) and phosphotyrosine (Fig.3.17D) present in focal adhesions with a well organised actin cytoskeleton (Fig.3.16/17C). When clone BAS:8 was grown with dexamethasone and immunostained for vinculin and phosphotyrosine, most cells were not able to spread and consequently displayed a disorganised actin cytoskeleton which was seen as diffuse staining throughout the cell

Figure 3.16. Immunofluorescent staining of Balb/c 3T3 cells and clone BAS:8 following spreading on fibronectin (see opposite).

Balb/c 3T3 cells (A-D) and clone BAS:8 cells (E-H) were cultured in the presence (C, D, G, H), and absence (A, B, E, F) of 1μM dexamethasone for 4 days. The cells were trypsinised and replated onto fibronectin-coated tissue culture plastic and the cells allowed to spread at 37°C for 60 minutes. The cells were then processed for immunofluorescence as described in Materials and Methods and stained for actin with FITC-phalloidin (A, C, E, G). Vinculin was visualised using monoclonal antibody, V284 (B, D, F, H). Bar 5μm.
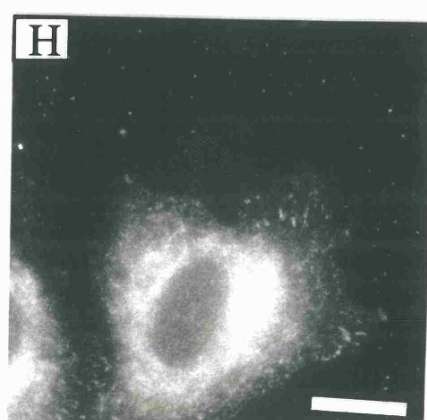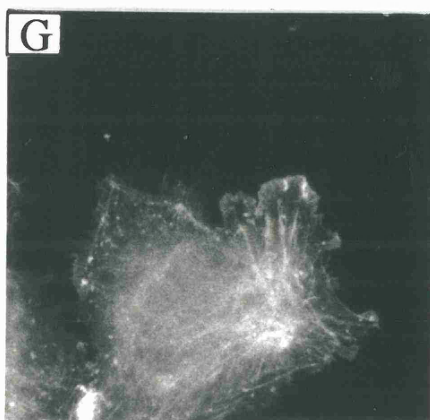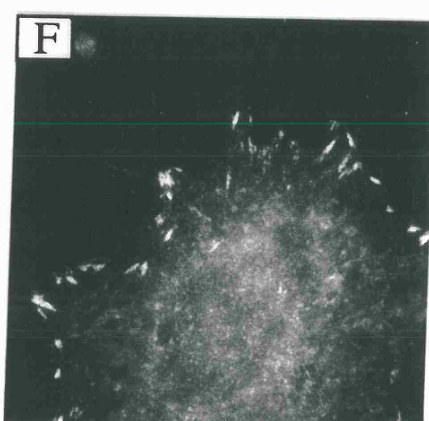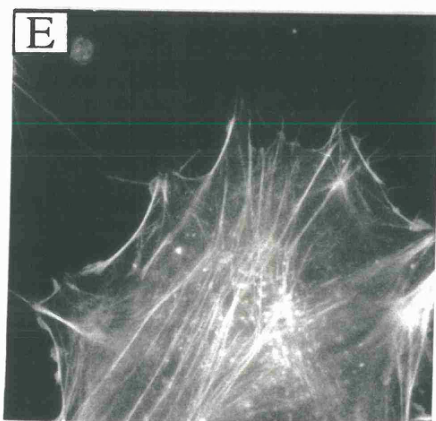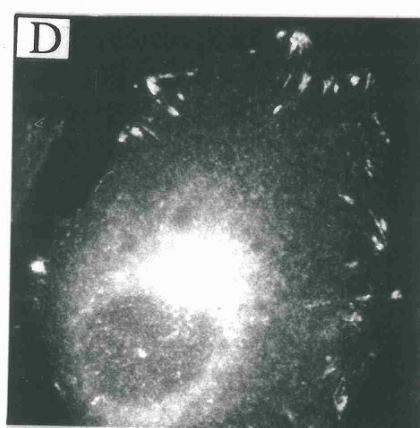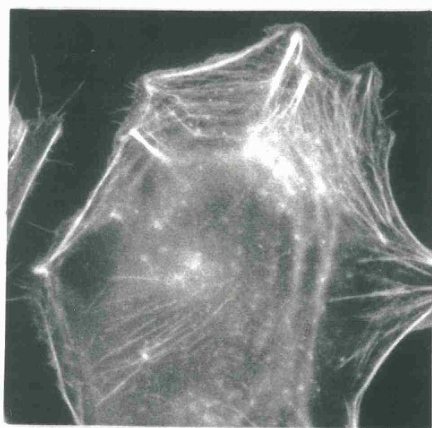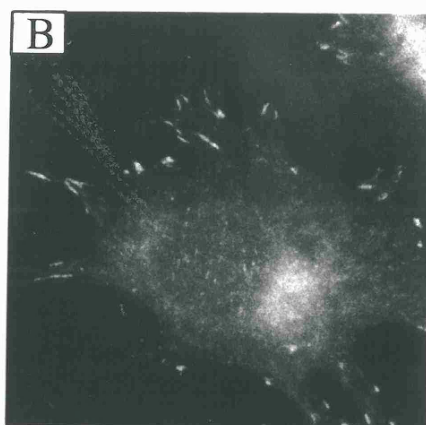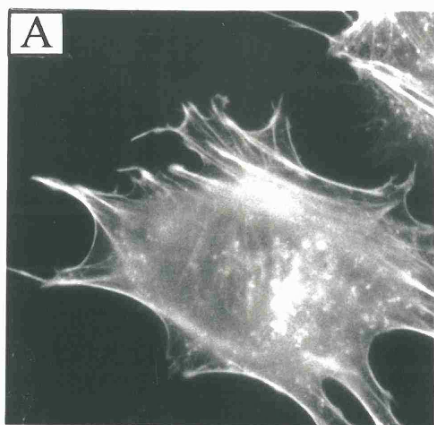
Figure 3.17. Immunofluorescent staining of Balb/c 3T3 cells and clone BAS:8 following spreading on fibronectin (see opposite).

Balb/c 3T3 cells (A-D) and clone BAS:8 cells (E-H) were cultured in the presence (C, D, G, H), and absence (A, B, E, F) of 1 µM dexamethasone for 4 days. The cells were trypsinised and replated onto fibronectin-coated tissue culture plastic and incubated at 37°C for 60 minutes. The cells were then processed for immunofluorescence as described in Materials and Methods and stained for actin with FITC-phalloidin (A, C, E, G). Phosphotyrosine-containing proteins were visualised using an anti-phosphotyrosine monoclonal antibody (clone PT-66, Sigma) (B, D, F, H). Bar 5 µm.
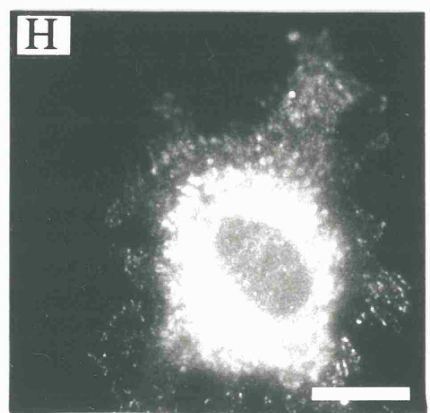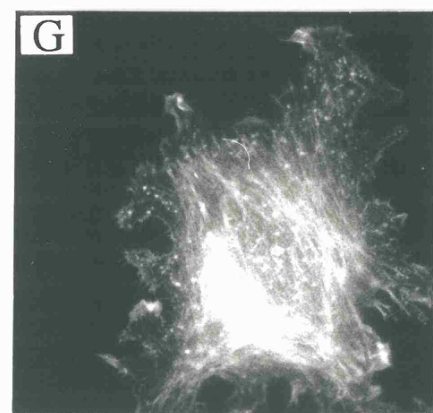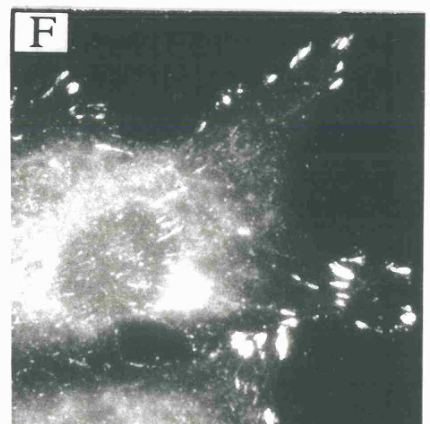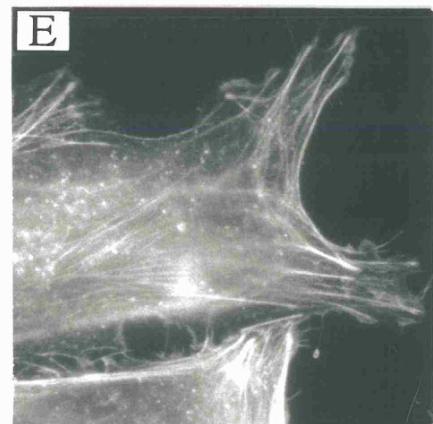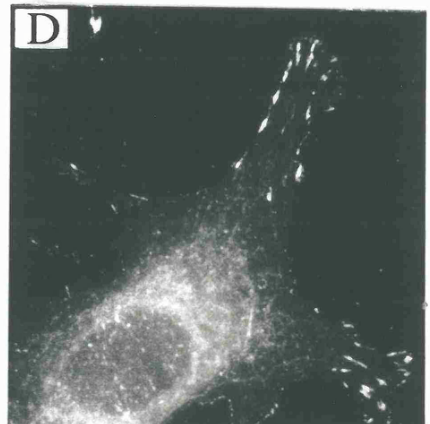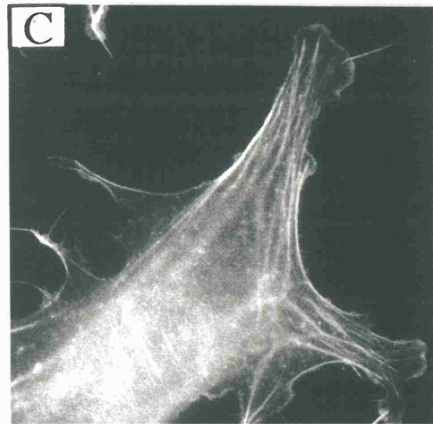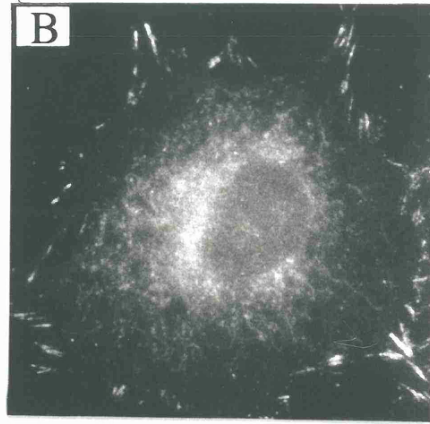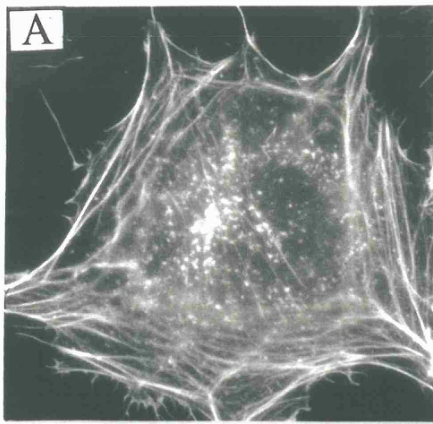
(Fig.3.16/17G). There was little or no staining for either vinculin (Fig.3.16H) or phosphotyrosine (Fig.3.17H) in the rounded cells.

The spreading assay was repeated again using Balb/c 3T3 cells and clone BAS:8 only, but the cells were serum-starved in suspension prior to plating on fibronectin to reduce the levels of phosphotyrosine. Half the cells were plated onto fibronectin and returned to the incubator for 60 minutes, whilst the rest were kept in suspension. Total cell protein was prepared from both the cells in suspension (S), and the fibronectin-plated cells (P), and the levels of phosphotyrosine examined by Western blotting (Figure 3.18A). All cells that were kept in suspension, regardless of previous culture condition, had low levels of phosphotyrosine-containing proteins as expected. When Balb/c 3T3 cells, previously cultured both with (+) and without (-) the dexamethasone, were plated onto fibronectin, there was a dramatic increase in the levels of phosphotyrosine in both pp125FAK and paxillin compared to the cells kept in suspension. When clone BAS:8 was cultured without dexamethasone and plated onto fibronectin, the same increases in amounts of phosphotyrosine were seen. However, when BAS:8 cells that had been previously cultured with dexamethasone, and therefore vinculin-deficient, were plated onto fibronectin, there was no increase in the levels of phosphotyrosine in either pp125FAK or paxillin. The blot was then stripped and probed for α-tubulin (Fig.3.18B) demonstrating that the blot was performed on similar amounts of total cell protein, although normalisation of protein loading was not perfect in this experiment.

3.14 Treatment of Balb/c 3T3 cells with antisense vinculin oligonucleotides.

There is no mouse vinculin cDNA sequence available that spans the region of the ATG translation start site, therefore the antisense vinculin oligos were designed using the human vinculin sequence for which the entire coding sequence is known.

Figure 3.18. Western blot analysis of the levels of phosphotyrosine-containing proteins in Balb/c 3T3 cells and clone BAS:8 cells following adhesion to fibronectin.
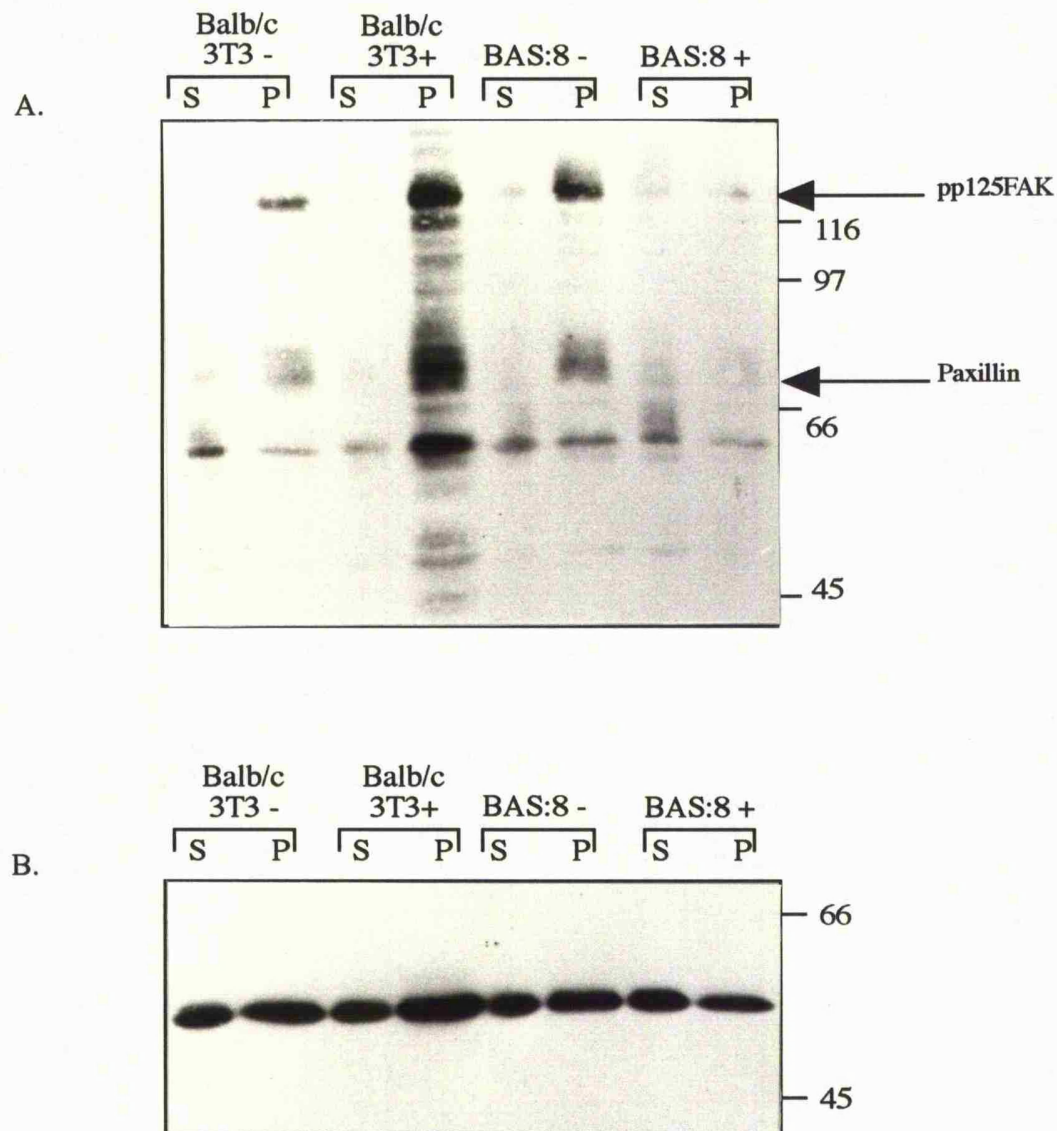
Balb/c 3T3 cells and clone BAS:8 cells were cultured in the presence (+) and absence (-) of 1μM dexamethasone for 4 days. Cells were then trypsinised and kept in suspension in serum-free medium for 30 minutes. Cells either remained in suspension (S), or were re-plated (P) onto fibronectin-coated dishes for 60 minutes. Total cell protein was prepared from both suspension and re-plated cultures and 30μg of total cell protein resolved by SDS-PAGE and electoblotted to nitrocellulose.
A. Blot probed for phosphotyrosine.
B. Blot probed for α-tubulin.
Molecular weight markers (kDa) are shown to the right of the figure.

Phosphorothioate-modified oligos were synthesised that were complementary to the sense strand (an antisense oligo) and the antisense strand (a sense oligo) of human vinculin cDNA. A control oligo was also synthesised that showed limited sequence identity with the human vinculin sequence. The sequences of the three oligos are shown in Figure 3.19. Initially, Balb/c 3T3 cells were seeded at 5×10^3 cells/1cm well and after 24 hours, treated with a range of oligo concentrations from 0.005µM to 5µM (0.03-30µg/ml), mixed with 0.5x, 1x or 2x the concentration of DOTAP reagent to determine the optimum concentrations of the two reagents. The DOTAP lipid transfection reagent was used as a vehicle to increase the efficiency of entry of the oligos into the cells, and the manufacturers recommended 1µl DOTAP (1mg/ml) for each µg of oligo used. Cells treated with more than 0.5µM of oligo or greater than 1x (3µg/ml) DOTAP reagent were seen to round up and die within 2-3 days (data not shown), therefore, all further experiments were carried out using 0.5µM (3µg/ml) oligo, with an equal concentration of DOTAP. The cells were treated each day for 4 days and initially screened under the light microscope for any changes in cell morphology. The vinculin protein distribution and levels were then examined by immunofluorescence and Western blotting.

Figure 3.20 shows treated cells photographed under phase conditions. Cells treated with the sense (Fig.3.20B) or the contol oligo (Fig.3.20C) were unaffected by the treatment and displayed a normal well-spread flat phenotype. Balb/c 3T3 cells treated with the antisense oligo (Fig.3.20A), were also seen as flat and well-spread, indicating that the oligo did not cause any change in gross cellular morphology.

The experiment was then repeated on cells cultured on glass coverslips and the vinculin distribution analysed by immunofluorescence. Cells treated with either the sense oligo (Figure 3.21C, D), or the control oligo (Fig.3.21E, F) displayed no effect on the size and distribution of the focal adhesions as visualised using an anti-vinculin monoclonal

Figure 3.19. Sequence of antisense vinculin oligonucleotides used to treat Balb/c 3T3 cells.

Human vinculin cDNA   5' <u>A T G</u> C C A G T G T T T C A T A C G 3'
                      3' T A C G G T C A C A A A G T A T G C 5'
                      1 18

Antisense oligo   T A C G G T C A C A A A G T A T G C
                       100% identity with residues 1-18
                       80% identity with residues 4623-4637 (15 residues)

Sense oligo   A T G C C A G T G T T T C A T A C G
                       100% identity with residues 1-18
                       85% identity with residues 5017-5030 (13 residues)

Control oligo   G T A A A A C G A C G G C C A G T
                       90% identity with residues 4945-4954 (10 residues)

The human vinculin cDNA sequence was used to design the antisense oligonucleotides (Weller *et al.*, 1990), and the ATG sequence that is transcribed into the AUG translation start codon is underlined. The percent identity between the oligo and the human sequence is shown. The antisense and the sense oligo are identical to residues 1-18 but also show limited identity to other sequences within the cDNA and this is indicated. The control oligo has a high percent identity to human vinculin, but only over a very short stretch of residues.

Figure 3.20. Morphology of antisense oligo-treated Balb/c 3T3 cells.
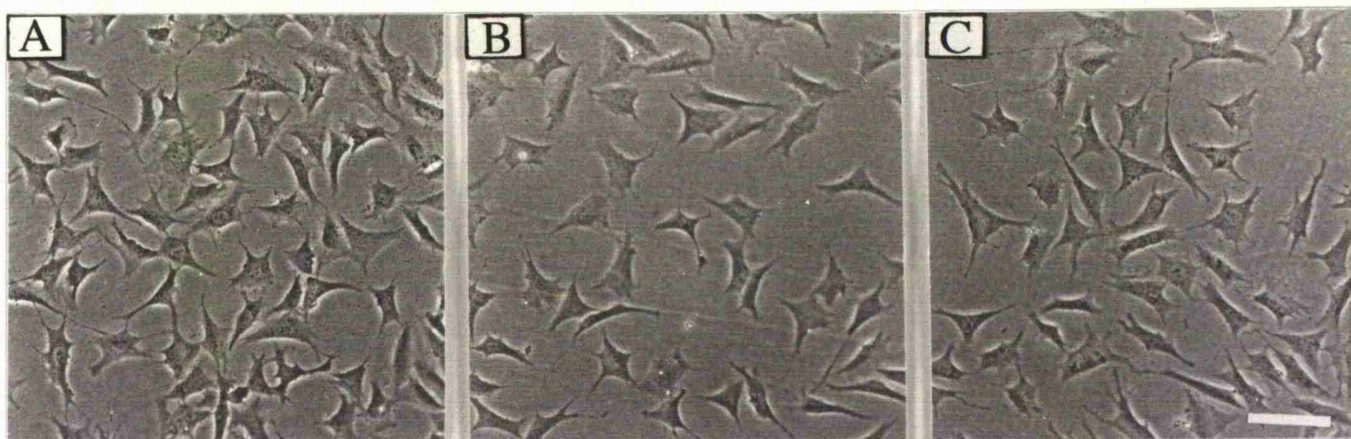
Balb/c 3T3 cells were treated with either an antisense (A), a sense (B) or a control oligo (C), each day for 4 days as described in Materials and Methods. Cells were analysed under phase conditions for any deviation in morphology and photographed. Bar 25μm.

Figure 3.21. Immunofluorescent staining of antisense oligo-treated Balb/c 3T3 cells.
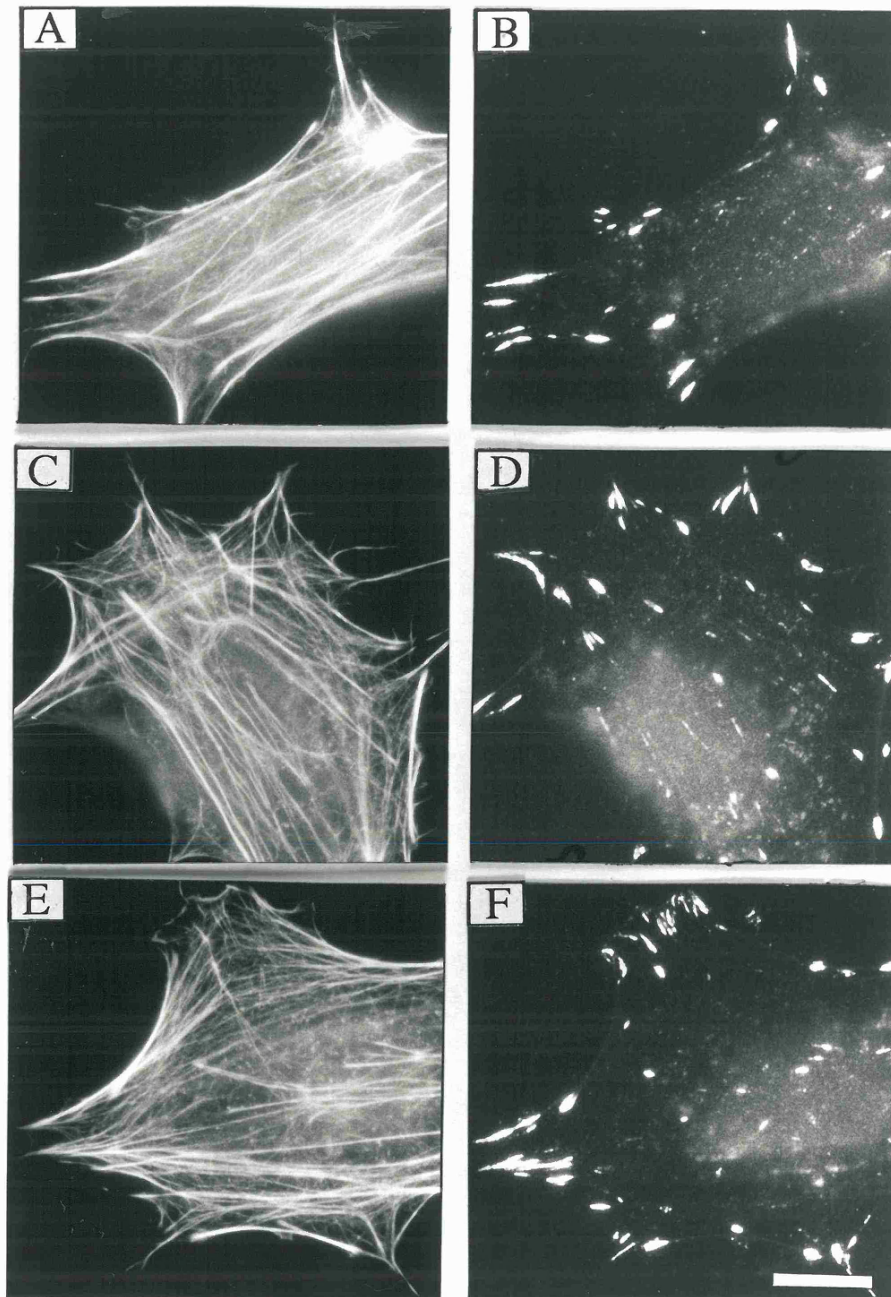
Balb/c 3T3 cells were treated with either an antisense (A, B), a sense (C, D), or a control oligo (E, F), each day for 4 days as described in Materials and Methods. Cultures of treated cell were processed for immunofluorescence and stained for either actin with FITC-phalloidin (A, C, E), or for vinculin with monoclonal antibody V284 (B, D, F). Bar 5μm.

antibody (Fig.3.21D, F). The actin stress fibre organisation was similarly unaffected by treatment with either the sense (Fig.3.21C) or control (Fig.3.21E) oligos. Cells treated with the antisense oligo were also seen to exhibit a normal staining pattern for both vinculin (Fig.3.21B) and actin (Fig.3.21A), similar to either of the control treatments. The amounts of total vinculin protein was then analysed by Western blotting using the vinculin monoclonal antibody V284. The blots were performed on equal amounts (50μg) of total cellular protein prepared from cells treated with each of the oligonucleotides (Figure 3.22), and there did not appear to be a reduction in the levels of vinculin from cells treated with either of the two control oligos, or the antisense oligo.

3.15 Discussion.

The initial goal of this project was to assess the feasibility of an antisense approach to establish the function of components of focal adhesions, using vinculin as the initial target protein. The cDNA available was a 1.06 kb cDNA that coded for amino acid residues 116-468 of mouse vinculin. The fact that antisense RNA produced from this cDNA did not hybridise to sequences surrounding the AUG translation start codon was not viewed as a problem, as many other groups have reported efficient reduction in protein levels using RNAs that spanned regions of the coding sequence other than the translation start site (see Chapter 1 for review). A plasmid vector possessing the MMTV glucocorticoid-inducible promoter was chosen and the mouse vinculin cDNA was cloned in the antisense orientation with respect to the MMTV promoter. Ringold *et al.*, (1975) demonstrated that addition of a synthetic glucocorticoid, such as dexamethasone, to cell culture medium resulted in a specific increase in MMTV RNA. Use of this plasmid, which also contained a gene for neomycin resistance, ensured that stable cell lines could be cloned, and that the expression of the antisense RNA from the transfected plasmid could be controlled. This eliminated the possibility that any antisense-expressing clones with reduced levels of vinculin, and therefore possibly adhesion deficient, would be lost during the selection and

76

Figure 3.22. Western blot analysis of the vinculin protein levels of antisense oligo-treated Balb/c 3T3 cells.
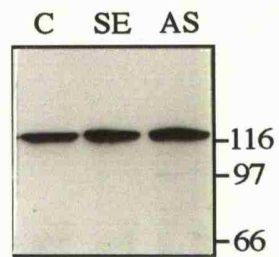
Balb/c 3T3 cells were treated with either an antisense (AS), a sense (SE) or a control (C) oligo each day for 4 days as described in Materials and Methods. Whole cell lysates were prepared from the treated cells and 50µg of total cell protein was resolved by SDS-PAGE and electroblotted to nitrocellulose. The blot was probed for vinculin with monoclonal antibody V284. Molecular weight markers (kDa) are shown to the right of the figure.

cloning procedure. The expression of an inducible antisense RNA also allowed an unequivocable demonstration that any alteration in phenotype was due to expression of the antisense vinculin RNA from the transfected plasmid, and could not be attributed to clonal variation following the isolation of the stable cell lines.

Expression of an antisense vinculin RNA in NIH3T3 cells did not reduce the levels of vinculin protein.

NIH3T3 cells, transfected with pMV1:AS, when cultured in the presence of 1μM dexamethasone over a period of 4 days did not show any observable alteration in the morphology of these cells, nor was there a reduction in the levels of vinculin protein as determined by Western blotting. As there was no apparent reduction in the levels of the vinculin protein, it was necessary to establish that the antisense RNA was being expressed from the transfected plasmid vector in these cells.

Northern blotting with an antisense-specific riboprobe showed that only clones NAS:20 and NAS:22 expressed an appropriate antisense RNA of 2.5-3kb in size, although it's expression appeared to be constitutive i.e. was not under the control of the dexamethasone-inducible promoter. Expression of the cloned insert from the multiple cloning site included, approximately, an extra 1600 bases due to the presence of flanking sequence either side of the multiple cloning site responsible for correct polyadenylation and processing of the RNA transcript resulting in an RNA species of approximately 2.5kb. The antisense RNA was expressed in considerable excess compared to the endogenous vinculin message which did not appear to be reduced when compared to control NIH3T3 cells. Sklar *et al.*, (1991) attempted to down-regulate the *c-myc* protein in NIH3T3 cells using an expressed antisense RNA also under the control of the MMTV promoter. Subsequent analysis of G418-resistant stable cell lines revealed that 10-15% of isolated clones exhibited an altered morphology regardless of the inclusion of

dexamethasone in the culture medium. The authors attributed this to a combination of the presence of serum glucocorticoids and constitutive expression of antisense *c-myc* transcripts due to positional effects on the MMTV promoter. This may also be the explanation for the constitutive expression of the antisense RNA observed in clones NAS:20 and NAS:22. The lack of expression in the other 25 cloned cell lines may due to integration of the plasmid into a transcriptionally silent area of the genome, although this is unlikely as the gene for neomycin resistance was active. This lack of apparent expression of the specific antisense RNA despite the cloned cells being neomycin-resistant is not uncommon and many groups carrying out antisense experiments have also reported similar observations as discussed in Chapter 1. It is unlikely that the NIH3T3 cells used for this study were unresponsive to the dexamethasone as Dr. L. Hemmings from our laboratory had successfully controlled the expression of an α-actinin cDNA using the pMAMneoBlue plasmid in NIH3T3 cells taken from the same stock. It was concluded however that, despite a vast excess of antisense RNA, there was no down-regulation in either vinculin message or protein when NIH3T3 cells were used.

Downregulation of vinculin protein levels in Balb/c 3T3 cells following expression of a mouse vinculin antisense RNA.

Rodriguez Fernandez *et al.*, (1993) successfully reduced the levels of vinculin protein following expression of the same mouse vinculin antisense RNA used in this study, except they used Balb/c 3T3 cells, not NIH3T3 cells. The pMV1:AS plasmid was therefore transfected into Balb/c 3T3 cells and G418-resistant colonies isolated. Two of the cloned cell lines, when cultured in the presence of 1μM dexamethasone for 4-5 days, displayed an altered morphology from a flat well-spread cell to a spindle-shaped cell. Subsequently immunostaining for actin and vinculin indicated that there was a change in the distribution of both proteins. Actin filaments were seen only at the periphery of the cell, with no stress fibres running across the body of the cell. Similarly, the intensity of

vinculin staining was dramatically reduced and only seen in small focal adhesions located at either end of the cell. Western blotting confirmed that the amount of vinculin in these morphologically-altered cells was also drastically depleted to 20-30% of the levels found in non-induced clones or control Balb/c 3T3 cells. The reduction in vinculin protein levels can be directly attributed to expression of the antisense RNA because it was absolutely dependent upon the addition of dexamethasone to the culture medium of the cloned cells. This reduction in vinculin levels following addition of dexamethasone to the cells, is also co-incident with the appearance of the spindle-shaped cells, at approximately 60-72 hours after the addition of the dexamethasone to the culture medium.

The two vinculin-deficient clones were able to revert to a normal, well-spread adherent morphology following replacement of the dexamethasone-containing medium with fresh serum-containing medium lacking dexamethasone, and this corresponded with an increase in the levels of vinculin protein. The vinculin gene is known to be stimulated by serum via a serum response element present in the promoter of the gene (Moiseyeva *et al.*, 1993), resulting in a rapid increase in vinculin message within 0.5-1 hour, and vinculin protein in 2-4 hours (Ben-Ze'ev *et al.*, 1990). The kinetics of the reversion of the morphology of clone BAS:8 demonstrated a significant increase in vinculin protein levels, from 10% to 43%, within 2 hours of removal of the dexamethasone rising to a maximum (100%) within 12 hours, which correlates well with data obtained Ben-Ze'ev *et al.*, (1990). It is interesting to note that although the vinculin levels have increased to only 43% of control after 2 hours, many of the cells are spread, indicating that any alteration in morphology would only be obvious in cells whose vinculin protein levels were reduced to below this level.

Lack of vinculin protein adversely affects cell growth.

It was observed that vinculin-deficient clones BAS:8 and BAS:10. when cultured in the presence of dexamethasone grew much slower compared to either their uninduced counterparts, or control Balb/c 3T3 cells cultured both with and without dexamethasone. The drop in the rate of cell proliferation co-incided with the appearance of the spindle-shaped morphology and the reduction in the levels of vinculin protein. This would agree with the theory that normal cultured fibroblast cells are anchorage-dependent for growth. This theory is further supported by the observation that these vinculin-deficient cells were unable to grow in soft agar i.e. did not show anchorage-independent growth.

Rodriguez Fernandez *et al.*, (1993) isolated a number of Balb/c 3T3 cloned cell lines constitutively expressing the same vinculin antisense RNA used in this study. The cloned cells were found to contain reduced levels of vinculin protein and consequently also displayed a similar lack of adhesion, although many cells were seen to be rounded rather than spindle-shaped. Further analysis of these cloned cells revealed an increase in motility and they were seen to close an artificial wound created in a confluent monolayer more rapidly when compared to untransfected Balb/c 3T3 cells. The authors also demonstrated that the cloned cell lines were able to grow in soft agar with a greater efficiency compared to transformed cells. The results outlined in this thesis and the data obtained by Rodriguez Fernandez *et al.*, (1993), both agree that a lack of vinculin results in a cell which cannot adhere properly. Indeed, both sets of data demonstrate that the levels of vinculin need to be reduced to less than 43% of control cells in order to affect cell morphology and result in a more rounded, less adherent phenotype. The increase in the motility of the clones isolated by Rodriguez Fernandez *et al.*, (1993), also seems a logical characteristic of adhesion-defective cells as Couchman *et al.*, (1982) demonstrated that a motile cell has fewer, more labile adhesions compared to a stationary dividing cell. It would have been informative to assess the motility of the BAS:8 and BAS:10 clones, but unfortunately,

these cells, unlike those of Rodriguez Fernandez *et al.*, (1993) could not grow to form a confluent monolayer when cultured in the presence of dexamethasone. The observation that the vinculin-deficient Balb/c 3T3 clones obtained by Rodriguez Fernandez *et al.*, (1993) behaved more like virally-transformed cells and were able to grow in soft agar does not agree with the results obtained in this study. It would seem more reasonable that adhesion-deficient cells, which have a reduced growth rate, would not be able to grow in an anchorage-independent environment of soft agar, as demonstrated in this report. The vector employed by Rodriguez Fernandez *et al.*, (1993) for their antisense studies resulted in constitutive expression of the vinculin antisense RNA and it is therefore possible that any differences in cell characteristics observed arose through clonal variation during isolation of the clones. In order to address this problem, Rodriguez Fernandez *et al.*, (1993) screened over 120 separate clones transfected with only the vector, for similar alterations in phenotype, and none of the clones showed any variation. The lack of adhesion and the corresponding loss of vinculin protein in both sets of data is most obviously due to expression of the vinculin antisense RNA and the data is consistent with previous experiments. If however, the ability to grow in soft agar arose through clonal variation and was not directly due to the expression of an antisense vinculin RNA, then the screen for an alteration in phenotype of the vector-only transfected clones is uninformative, and a similar screen for growth in agar should have been performed. However, both sets of data agree that a reduction in the amount of vinculin results in a loss of cell adhesion.

Vinculin-deficient cells are unable to spread on fibronectin and do not show elevated levels of phosphotyrosine upon adhesion.

When vinculin-deficient cells are plated onto fibronectin they are unable to spread, but appear to be rounded and only loosely associated with the underlying substrate. Immunofluorescence of these rounded cells revealed there was no significant re-

organisation of the actin cytoskeleton or assembly of focal adhesions which is normally associated with cell spreading. This observation therefore implies that vinculin is a key component of the focal adhesion and is essential for the formation of focal adhesions.

Burridge *et al.*, (1992), have previously demonstrated that adhesion of cells, previously kept in suspension, to ECM proteins resulted in the formation of new focal adhesions and stress fibres with a concurrent increase in tyrosine phosphorylation of both pp125FAK and paxillin. However, when vinculin-deficient BAS:8 cells previously cultured in the presence of dexamethasone were plated onto fibronectin they were unable to elicit this increase in phosphotyrosine-containing proteins. Similarly, when the experiment was repeated and the cells analysed by immunofluorescence, there was little observable staining for either vinculin or phosphotyrosine and the cells remained rounded. This demonstrates that a cell which cannot make a functional focal adhesion is unable to initiate the signalling mechanisms thought to be associated with integrin-mediated cell adhesion and the formation of the focal adhesions and actin stress fibres. Several groups have presented strong evidence that blocking actin polymerisation with cytochalasin D also inhibits tyrosine phosphorylation. This would therefore suggest that both formation of focal adhesions and reorganisation of the actin cytoskeleton is crucial to the recruitment and phosphorylation of specific proteins and the subsequent stimulation of signalling cascades and not *vice versa.*

The experiments described in this chapter have illustrated that vinculin-deficient cells grow much slower than control cells, nor can they grown in the absence of a solid substrate. Neither can these cells trigger the normal signalling mechanisms associated with integrin-mediated cell adhesion that ultimately result in cell proliferation. Recent work has highlighted the ability of integrin-mediated adhesion to activate MAP kinase and the subsequent signalling pathways that ultimately result in gene expression (Chen *et al.*,

(1994). The results outlined in this thesis regarding the lack of growth by the vinculin deficient clones is entirely consistent with this observation and indicates that a loss of adhesion results in reduced cell growth through a deficiency in the usual signalling mechanisms.

Balb/c 3T3 versus NIH3T3 fibroblasts as suitable cell lines for antisense experiments.

The fact that down-regulation of vinculin protein levels was acheived in Balb/c 3T3 cells and not NIH3T3 cells, despite using the same vector for generation of the antisense RNA, raises some interesting questions as to the suitability of NIH3T3 as a candidate cell line for antisense experiments. The same vector was used for both studies eliminating the possibility that the RNA expressed by the vector targeted an inappropriate site on the vinculin mRNA. As expression of the antisense RNA in NIH3T3 cells was confirmed, the lack of reduction in vinculin protein levels has to indicate a difference in the cell lines themselves. Both cell lines are isolated from mouse embryos, but from different strains of mouse - NIH3T3 cells are isolated from the Swiss 3T3 mouse and Balb/c 3T3 from the Balb/c 3T3 mouse, strain A31, and the significance of this difference in mouse strain is unclear. Several papers have been published documenting the susceptibility of Balb/c 3T3 cells to a lack of, or a reduction in serum levels. Both Tamm *et al.,* (1992) and Kulkarni and McCulloch, (1994) have demonstrated that removal of serum from the culture medium of Balb/c 3T3 cells results in a rapid dissociation of actin stress fibres and focal adhesions, leading to cell death within a short period of time, although this could be avoided by the addition of either serum, or various serum growth factors within 2 hours of serum withdrawal. In contrast, NIH3T3 cells are not affected by withdrawal of serum for this length of time, indeed, they seemed quite content to go without serum for 8-10 hours. This difference in susceptibility to serum-deprivation between the mouse fibroblast cell lines may be responsible for the lack of success using NIH3T3 cells, but exactly how

or why is unclear. Interestingly, experiments targeting e.g. transcription factors, have been successful in NIH3T3 cells (see Table 1.2), possibly because transcription factors have a much shorter half life (minutes) compared to adhesion-related proteins (hours). The ability to down regulate vinculin in Balb/c 3T3 cells and not NIH3T3 cells could therefore possibly be explained if the relative turnover of the vinculin protein in Balb/c 3T3 cells was more rapid than in NIH3T3 cells.

Attempts to downregulate vinculin in Balb/c 3T3 cells using antisense oligonucleotides.

Balb/c 3T3 cells were treated with phosphorothioate-modified DNA oligonucleotides that were complementary to the first 18 nucleotides of the mouse vinculin mRNA beginning from the AUG translation start codon. This is generally regarded as the most logical target region of the RNA message for antisense experiments, as nobody has yet reported being unsuccessful when this region has been covered. These experiments were carried out using oligos designed according to the human vinculin sequence as there was no mouse sequence data available for the region surrounding the AUG translation start codon, and there is 90% sequence identity at the nucleic acid level between mouse and human vinculin. Balb/c 3T3 cells and not human fibroblast cells were chosen for the experiments as this cell line was shown to be suitable for antisense experiments using an expressed RNA (see this thesis and Table 1.3). Many researchers are now using commercially available lipid transfection reagents to increase the uptake of the oligos by the cell, and this is regarded as the most suitable treatment method for proteins with a long half-life as release from the lipid carrier can often occur over several days (see Chapter 1). The DOTAP reagent from Boehringer Mannheim was chosen because this reagent, unlike its competitors, can be used in the presence of serum, which was a very important consideration as Balb/c 3T3 cells are sensitive to loss of serum for any length of time (Tamm *et al.*, 1992; Kulkarni and McCulloch, 1994).

Treatment of the cells with the either oligo at concentrations above $0.5\mu M$ or DOTAP at more than $1\mu g$ DOTAP/μg of oligo appeared to have a toxic effect on the cells resulting in cell death. This was considered a limiting factor when treating the cells because it would have masked any specific vinculin-deficient alteration in morphology from being obviously seen. Treatment with the oligo/DOTAP mixture was carried out every day for 4 days but with no success, as neither a phenotype nor a reduction in vinculin levels was observed. It is unlikely that the region of the RNA message targeted was at fault, therefore the inability of the oligo treatment to deplete vinculin levels is most likely explained by an insufficient oligo:vinculin mRNA ratio within the cell. Experiments using an expressed RNA in Balb/c 3T3 cells, as described earlier, produced a reduction of vinculin protein levels within 3-4 days, so it is unlikely that the cells required a more prolonged period of exposure to the antisense oligo. However, this does rely on the assumption that the cells are being treated with sufficient oligo, and in this case the cells were being given the higest dose of oligo possible. Increasing either the amount of the oligo or the DOTAP reagent, or the period over which it was administered was not a realistic alternative as both had an adverse affect on the morphology of the cells. It is possible that the protocol utilised by Takeuchi *et al.*, (1994) to down regulate the ERM proteins might have been more succesfull. They maintained that due to the low turnover rate of the ERM proteins, the levels of oligo in the culture medium must remain high for several days. In their experiments they administered high concentrations of oligo ($20\mu M$) every 3-4 hours for several days with profound alterations in cellular morphology being seen after 48-60 hours.

The oligos were modified by addition of a phosphorothioate group to the sugar backbone and encapsulated in DOTAP reagent prior to addition to the cells, making it unlikely that they were degraded in the culture medium or that uptake by the cell was at fault. I have

therefore concluded that the most probable explanation for the inability of the oligos to reduce vinculin protein levels, is a combination of insufficient oligo concentrations, degradation once inside the cell and the relatively long half-life of the vinculin protein.

3.16 Conclusions.

The aim of the project was to examine the ability of an antisense approach to provide useful answers regarding the function of the vinculin protein. The initial work was carried out in NIH3T3 cells and was unsuccessful, despite high levels of expression of the antisense RNA. A similar approach was used by Rodriguez Fernandez *et al.*, (1993) using Balb/c 3T3 cells and they were successful in down-regulating vinculin protein levels. When this work was repeated in Balb/c 3T3 cells, two stable cell lines were isolated expressing reduced levels of the vinculin protein under the control of the MMTV promoter. Not only did this then provide us with an easily manipulated system to study vinculin function, but it highlighted the possibility of some subtle differences between the two 3T3 fibroblast cell lines used. The main advantage that the glucocorticoid-inducible system used in this study has over experiments carried out using constitutively expressed RNAs, is the ability to control the expression of the cloned insert, and if necessary to turn it's expression off. This is of course a major advantage if, like the clones isolated in this study, the isolated cells exhibited total or even partial adhesion and growth deficiencies. Being able to control the expression of the antisense RNA and thus switching the cells from a normal phenotype to an altered phenotype by inclusion of dexamethasone in the culture medium, also eliminates the possibility of clonal variation accounting for any alteration in phenotype. The use of the dexamethasone-inducible system has proved vital to the observation that the vinculin-deficient cloned cell lines do not grow in an anchorage-independent fashion, allowing us to present strong evidence that a lack of vinculin does not necessarily coincide with the appearance of all the characteristics of a transformed

phenotype. A lack of vinculin protein, and therefore ability to reform focal adhesions when plated onto a variety of ECM substrates, also adversely affects the signalling pathways initated by integrin-mediated cell adhesion. The data obtained from these experiments have provided more evidence that the focal adhesion is involved not only in mediating the interaction between the cell and its substrate, but is also intimately involved in the signal transduction pathways elicited by cell adhesion.

CHAPTER 4

CHARACTERISATION OF ANTI-HUMAN PLATELET
TALIN MONOCLONAL ANTIBODIES

4.1 Introduction.

Identification of proteins that localise to focal adhesions has largely relied on the production of monoclonal antibodies to cytoskeletal fractions purified from chicken smooth muscle. For instance, vinculin was initially seen as a contaminant during the preparation of α-actinin from chicken gizzard (Geiger and Singer, 1979). Geiger, (1979) then purified this 130kDa protein and used it as an immunogen to generate monoclonal antibodies. Immunostaining of chick embryo fibroblasts with the antibody demonstrated that vinculin localised to the areas of close contact between the cell and the substratum known as focal adhesions. Antibodies raised against other proteins including talin (Burridge and Connell, 1983a; Otey et al., 1990b), paxillin and pp125FAK (Glenney and Zokas, 1989), have been used to demonstrate that these proteins also localise to the focal adhesion complex that links the extracellular matrix to the actin cytoskeleton. Monoclonal antibodies have also be used to isolate proteins from total cell protein extracts by immune precipitation. Glenney and Zokas (1990) used an anti-phosphotyrosine monoclonal antibody coupled to Sepharose as as affinity matrix to isolate phosphotyrosine-containing proteins, such as paxillin, pp125FAK and tensin, from CEF lysates. Each of the phosphotyrosine-containing proteins was then used as an immunogen to raise protein-specific antibodies.

Antibodies can serve as useful tools to probe the functions of their target proteins such as vinculin (Westmeyer et al.,1990) and talin (Nuckolls et al., 1992). The involvement of talin in the spreading and migration of fibroblasts was investigated by Nuckolls et al., (1992) using an affinity-purified polyclonal antibody raised against chicken gizzard talin. CEF cells were microinjected with the polyclonal antibody at various time points and it was found that the anti-talin antibody reduced the spreading of newly-plated cells but it did not adversely affect well-spread cells. The ability of the injected cells to migrate into an artificially created wound was also impaired by injection of the antibody. However,

because the experiments were carried out using a polyclonal antibody it was not possible to identify the functional domains within the talin protein responsible for the effects observed. Nevertheless, the results clearly demonstrated that talin is essential for the formation of focal adhesions required during processes such as cell spreading and migration.

In this study, a panel of monoclonal antibodies raised against human platelet talin by Dr. J. Michael Wilkinson (The Wellcome Trust, London), were characterised. The antibodies were raised using a partially purified preparation of human platelet talin, prepared by the method of Collier and Wang (1982), as the immunogen. Initial screening of hybridoma supernatants was carried out using an ELISA assay with the original immunogen as the target antigen. Positive supernatants were re-screened by immunoblotting of SDS extracts of whole human platelets and only those hybridomas giving positive immunoblots were re-cloned, and six antibodies of varying immunoglobulin (Ig) subtype were isolated by this method (see Table 4.1). In this study, the six antibodies - TA205, TD77, TD74, TA9, TA44 and TA269, have been characterised using Western blotting, immunofluorescence and immunoprecipitation, and the epitopes of each monoclonal antibody mapped using a panel of chick talin fusion proteins.

RESULTS

4.2 Detection of talin in whole cell lysates by Western blotting.

The species specificity of the six anti-human platelet talin monoclonal antibodies was initially investigated by Western blotting using total cell protein lysates prepared from human MRC5 cells, mouse Balb/c 3T3 cells and CEF. As shown in Figure 4.1, all antibodies were capable of detecting talin in cell lysates prepared from human MRC5 cells. TA205 and TD77 were the only monoclonal antibodies that recognised talin in CEF, although TA9 does appear to show very weak reactivity against talin in CEF lysates.

89

Figure 4.1. Cross-reactivity of anti-human talin monoclonal antibodies with human, mouse and chick talin.
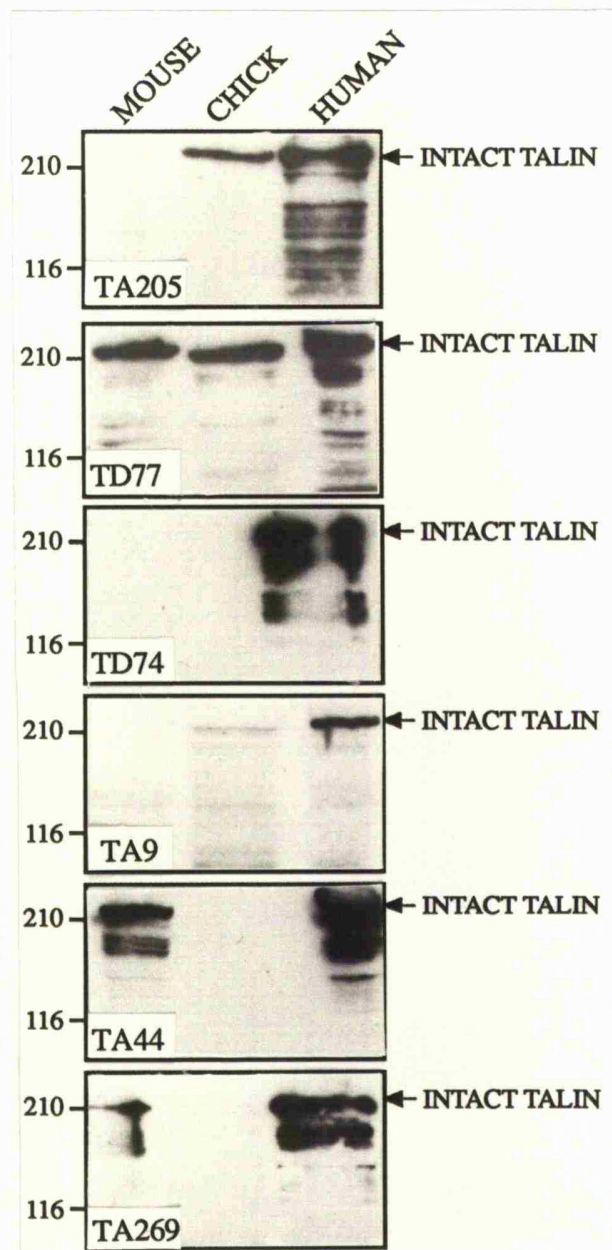
Whole cell lysates were prepared from human MRC5, CEF and mouse 3T3 fibroblast cell lines, and 50μg of total cell protein was resolved by SDS-PAGE and electroblotted to nitrocellulose. The blots were then probed with each of the anti-talin monoclonal antibodies as indicated. The position of intact talin is shown to the right of the figure and the molecular weight markers (kDa) to the left.

Monoclonal antibodies TD77, TA44 and TA269 were the only antibodies that recognised talin in mouse cell lysates.

4.3 Epitope mapping of anti-talin monoclonal antibodies using chick talin GST-fusion proteins.

A series of overlapping chick talin cDNAs, cloned into the pGEX vector (Gilmore *et al.*, 1992), were available within our laboratory and the positions of the expressed GST-fusion proteins in relation to the full length talin molecule is shown diagramatically in Figure 4.2. The chick talin-GST fusion proteins were expressed in *E. coli* and bacterial cell pellets lysed directly into sample buffer and resolved by SDS-PAGE (12%). Each of the fusion proteins can be seen as the most abundant protein present in the bacterial cell lysates (Figure 4.3). The GST-fusion proteins were then transferred to nitrocellulose, and the blots probed with each of the anti-talin monoclonal antibodies (Figure 4.4). TA205 was the only monoclonal antibody that recognised the two most N-terminal fusion proteins that spanned residues 102-497 and 102-656. Monoclonal antibodies TD77, TD74, TA9 and TA44 all recognised the two most C-terminal fusion proteins that spanned residues 1646-2541 and 2269-2541. Monoclonal antibody TA269 did not appear to recognise any of the chick talin GST-fusion proteins.

4.4 Immunofluorescent staining of human, mouse and chick fibroblasts with anti-talin monoclonal antibodies.

Cultures of human MRC5 fibroblasts, mouse Balb/c 3T3 fibroblasts and CEF cells were cultured on glass coverslips and immunostained for talin using each of the six anti-talin monoclonal antibodies. MRC5 human fibroblasts and mouse 3T3 fibroblasts were extracted in MES buffer prior to fixation to remove the soluble cytosolic pool of talin. CEF, which are sensitive to extraction in MES buffer, were fixed and then permeabilised with Triton-X-100 prior to incubation with the antibodies. Figure 4.5 shows the results

90

Figure 4.2. Schematic representation of talin to show the positions of the chick talin GST-fusion proteins relative to the full length molecule.


```
        1       434                                    2541
      N │ 47kDa │            190kDa              │ C

54A5'R1  102___497
    54A  102_____656
54A/23B PCR  498_853
         23B  642_____1328
      23B3'R1  852____1328
   23B 3'PCR  951___1327
              G3  1304_____2023
                   G2  1554_____2124
              C1  1554_1829
              C2  1554_1929
              C3  1554____2029
              C4  1554_____2060
                 GG4A  1646_____2541
                    GG4A-P  2269__2541
```
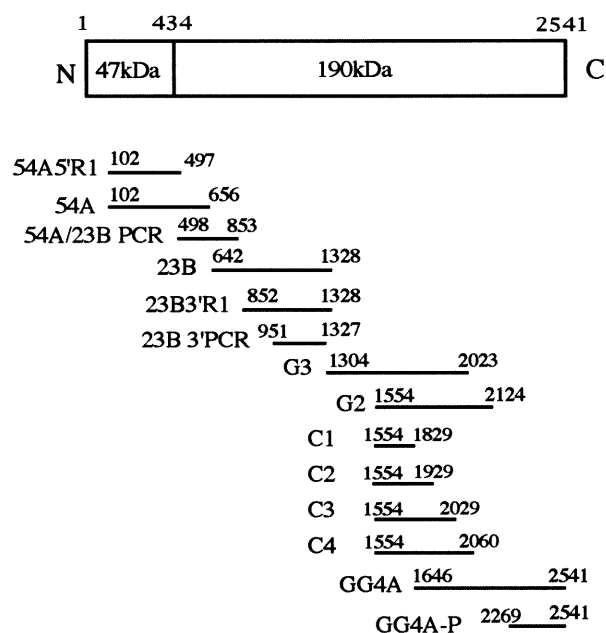
Chick talin cDNAs were cloned into the pGEX vector and the resultant overlapping GST-fusion proteins span virtually the entire length of the talin molecule from amino acid residues 102-2541. The amino acid co-ordinates for each fusion protein and the name of the cDNA used to generate each construct are shown. The talin cDNA/pGEX vectors were constructed by Drs. V. Ohanion and A. Gilmore and have been previously described with the exception of C1-C4 (see Materials and Methods and Gilmore et al., 1993).

Figure 4.3. Expression of chick talin GST-fusion proteins in *E. coli*.
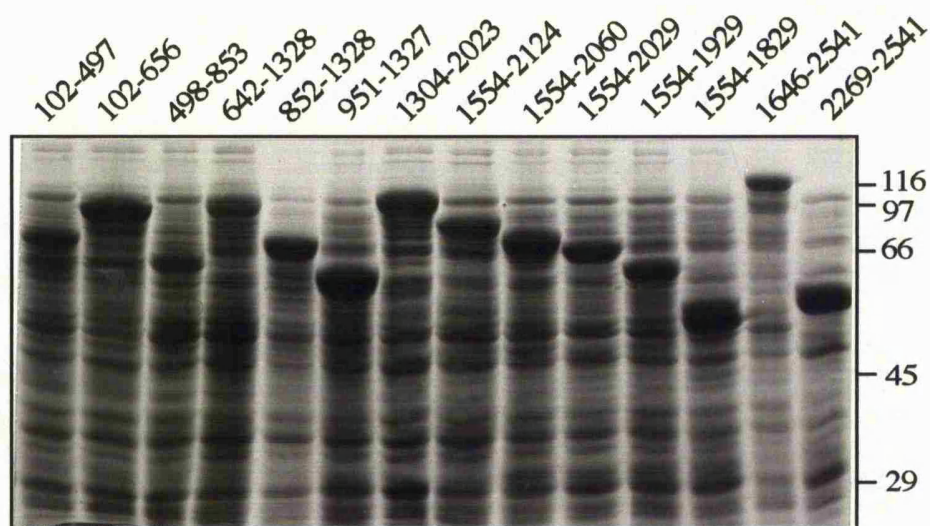
The chick talin cDNAs shown in Figure 4.2 were cloned into the pGEX expression vector. Cultures of *E.coli* expressing the fusion proteins were pelleted and lysed directly into sample buffer and resolved by SDS-PAGE (12% gel). The proteins were visualised using Coomassie Blue stain, and the talin-GST fusion proteins can be seen as the most abundant protein in each track. The amino acid residue co-ordinates of each fusion protein are indicated across the top of the figure and the position of the molecular weight markers (kDa) are indicated to the right of the figure.

Figure 4.4. Epitope mapping of anti-talin monoclonal antibodies.
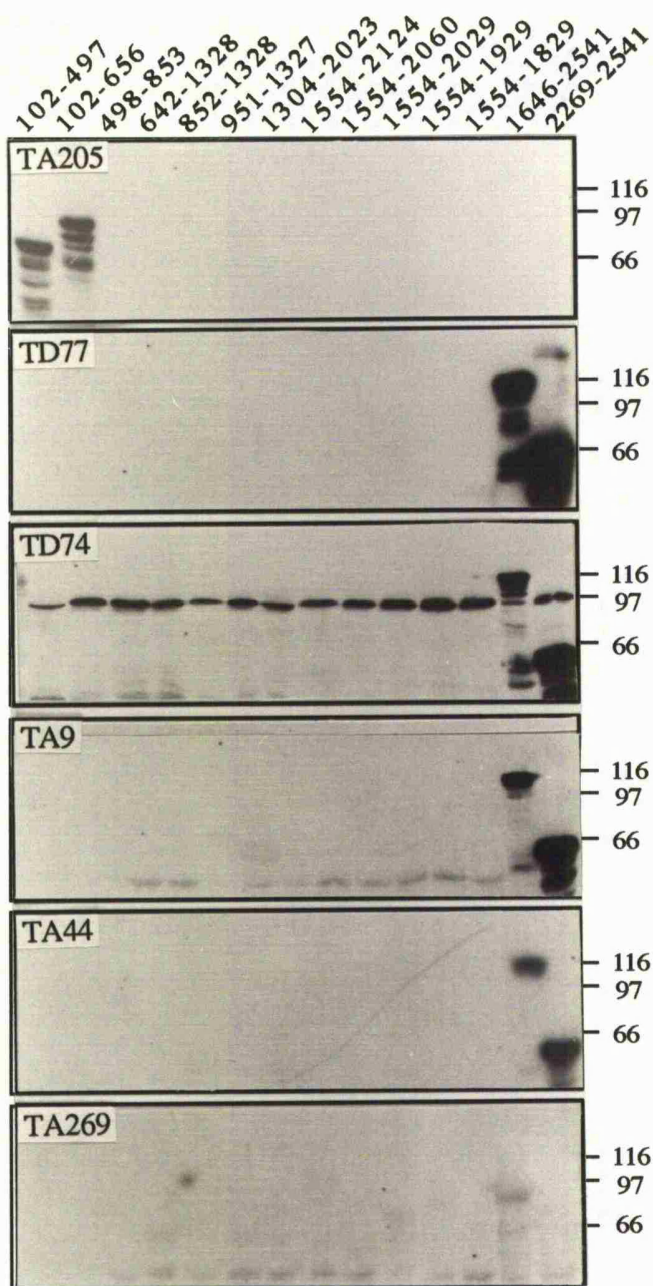
The chick talin-GST fusion proteins were resolved by SDS-PAGE and electroblotted to nitrocellulose. The blots were incubated with each of the anti-talin monoclonal antibodies as indicated. The amino acid co-ordinates are shown along the top of the figure and the molecular weight markers (kDa) to the right of the figure.

obtained using the human MRC5 cells. TA205 (Fig.4.5B) and TD77 (Fig.4.5D) gave strong staining of talin, which was seen to localise to the extreme tips of the actin stress fibres (Fig.4.5A, C respectively). TD74 (Fig.4.5F) gave weaker staining of talin compared to either TD77 or TA205, whilst TA9 (Fig.4.5H), TA44 (Fig.4.5J) and TA269 (Fig.4.5L) did not appear to stain talin. These three latter antibodies were not able to stain talin even when the cells were fixed and extracted with Triton-X-100 (data not shown).

When CEF cells were immunostained, only TA205 (Figure 4.6B), and TD77 (Fig.4.6D), detected talin present in focal adhesions (arrows) at the tips of the actin stress fibres and also along the length of the stress fibres (arrowheads, Fig.4.6A, C). TD77 was the only monoclonal antibody that detected talin present in focal adhesions in mouse Balb/c 3T3 cells (Fig.4.6F). None of the other four antibodies were seen to stain talin in either CEF or mouse fibroblasts under any conditions (data not shown).

4.5 Discussion.

All the data collected on the anti-human platelet talin monoclonal antibodies is summarised in Table 4.1, and includes the immune precipitation data from the experiments carried out by Simon Barry in this laboratory. Monoclonal antibody TA205 was the only antibody that recognised an epitope at the N-terminus of the talin molecule (residues 102-497). Western blotting and immune precipitation of total cell proteins and immunofluorescence demonstrated that TA205 recognised human and chick talin, but not mouse talin. TD77 was the only monoclonal antibody capable of recognising human, chick and mouse talin when used for Western blotting, immune precipitation and immunofluorescence. Epitope mapping revealed that the TD77 antibody recognised amino acids 2269-2541 at the C-terminus of chick talin. Monoclonal antibody TD74 was shown to detect only human talin in Western blotting and immune precipitation of cell lysates, and also only weakly stained talin when used for immunofluorescence of MRC5 cells. Surprisingly, this antibody

91

Figure 4.5. Immunofluorescent staining of MRC5 human lung fibroblasts with anti-talin antibodies (see opposite).

MRC5 fibroblast cells were processed for immunofluorescence as described in Materials and Methods. Cells were stained for actin with FITC-phalloidin (A, C, E, G, I, K), and talin with each of the monoclonal antibodies as indicated (B, D, F, H, J, L). Arrows indicate the presence of talin in the focal adhesions at the tips of the actin stress fibres. Bar 5μm

TA205 (A, B); TD77 (C, D); TD74 (E, F); TA9 (G, H); TA44 (I, J); TA269 (K, L).
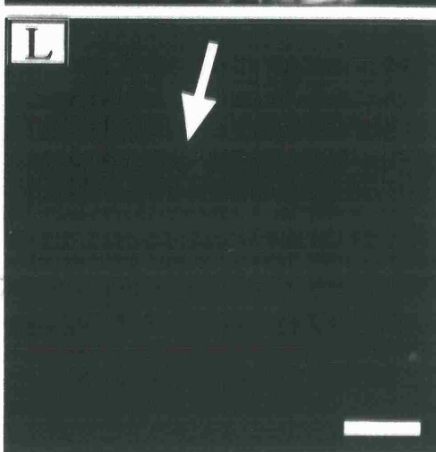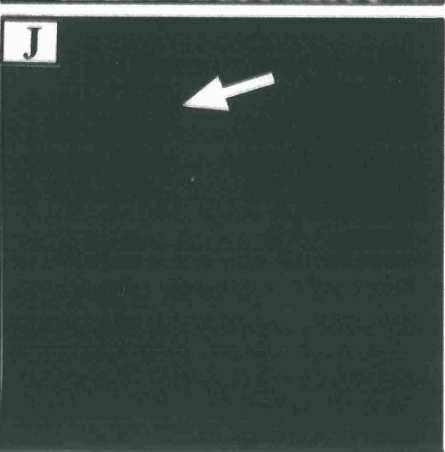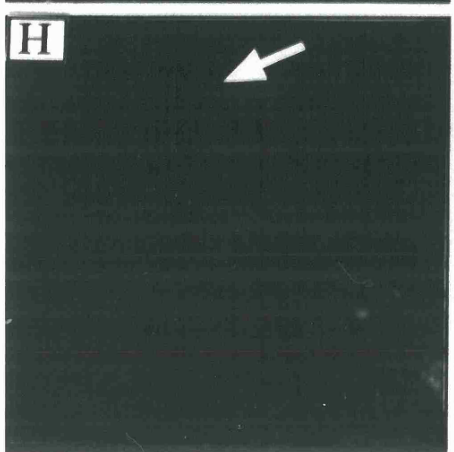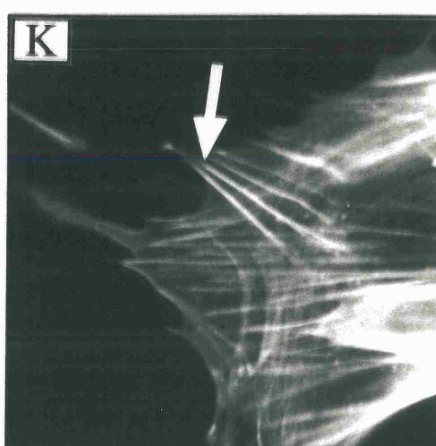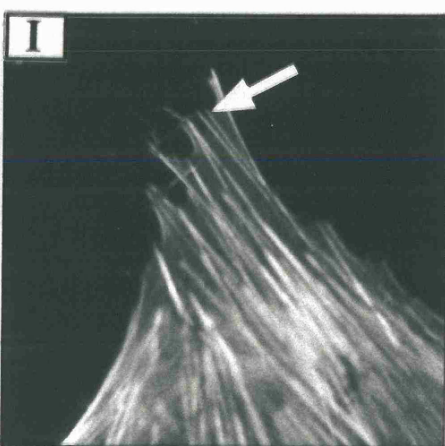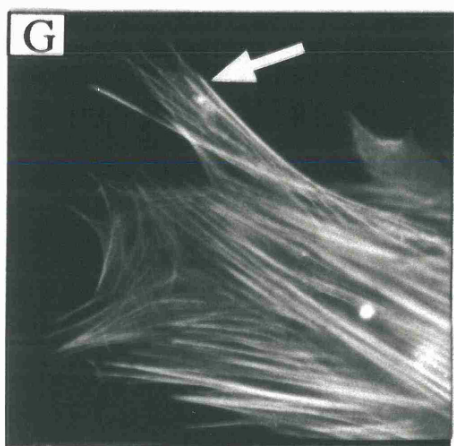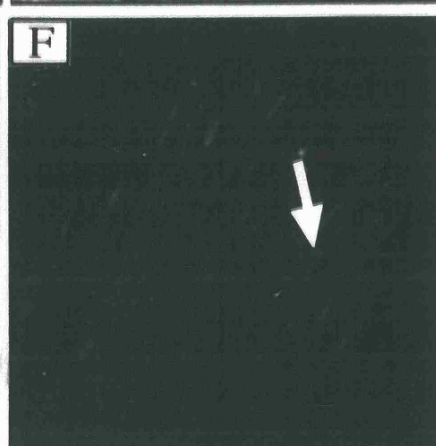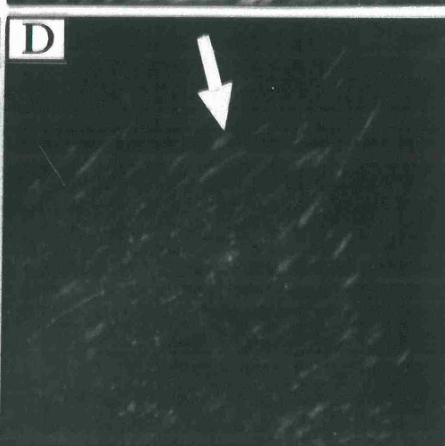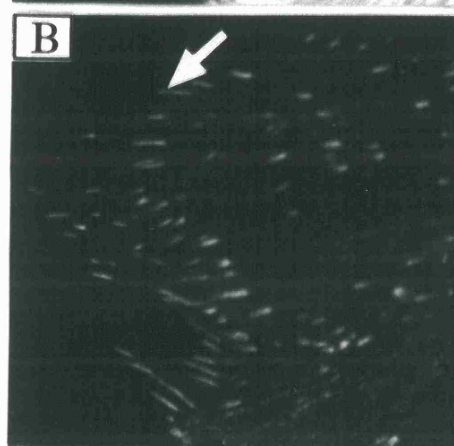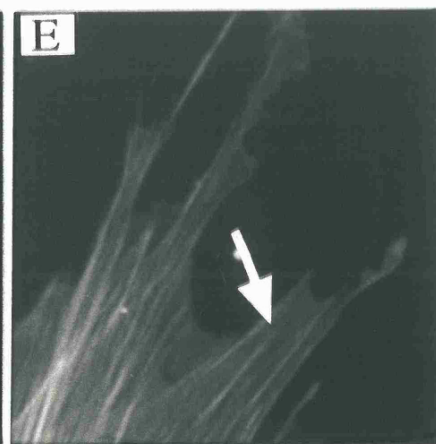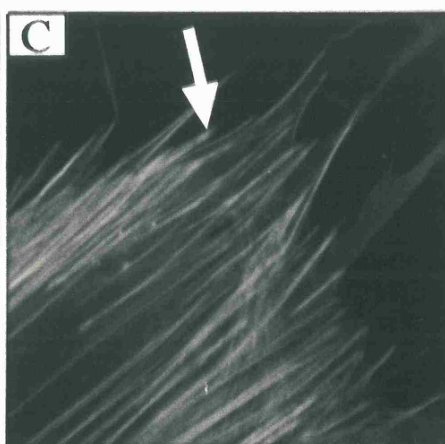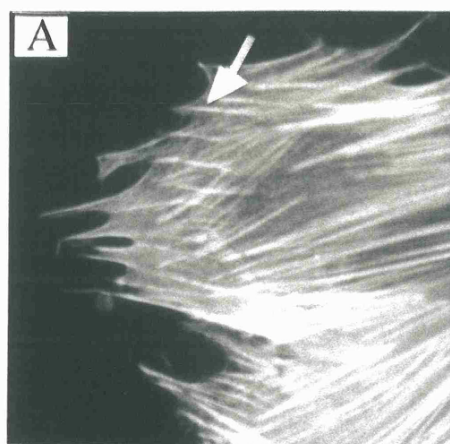
Figure 4.6. Immunofluorescent staining of CEF cells and mouse 3T3 fibroblasts with anti-talin monoclonal antibodies TA205 and TD77.
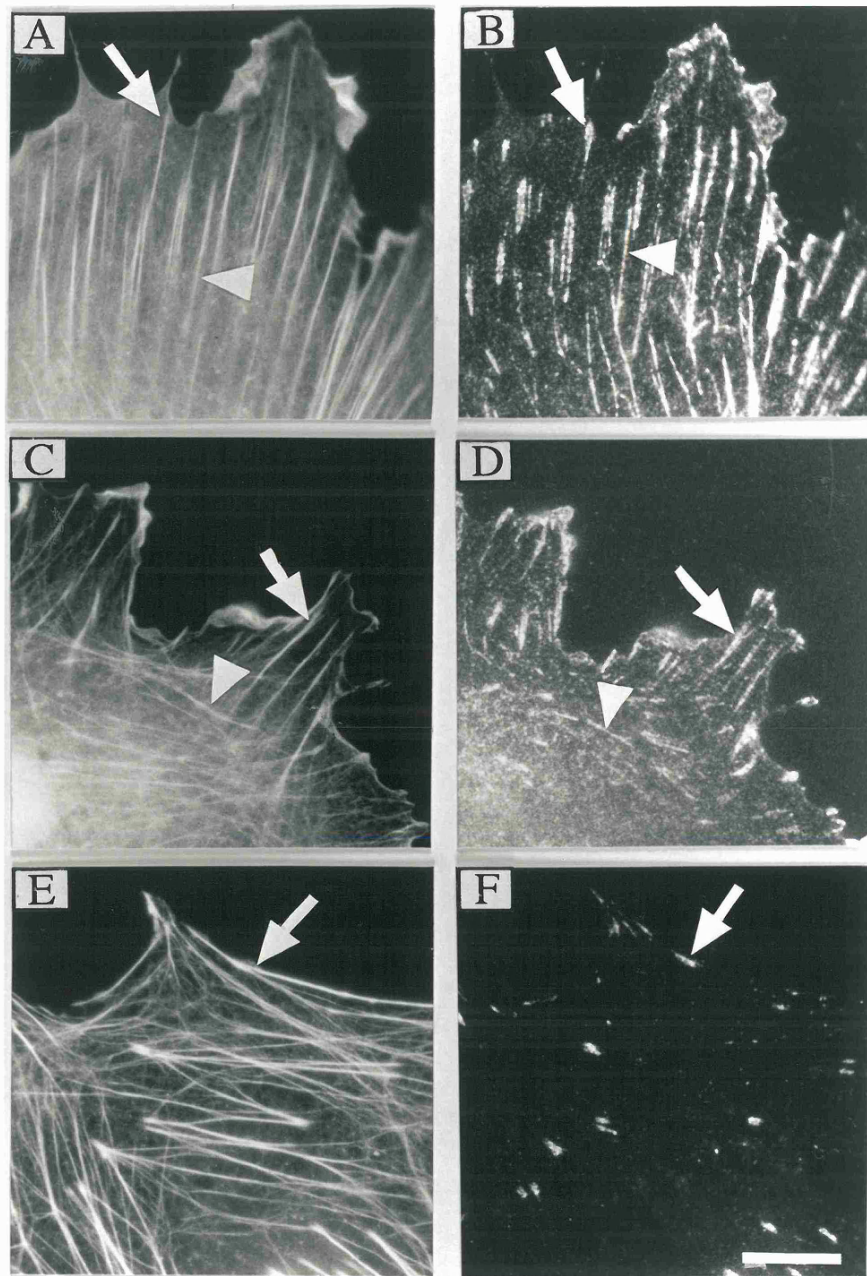
CEF (A-D) cells were fixed in formaldehyde and then permeabilised in 0.2% Triton-X-100 whilst mouse cells (E, F) were extracted in MES buffer prior to formaldehyde fixation. Talin was detected with monoclonal antibodies TA205 (B) and TD77 (D, F), and cells were co-stained for actin with FITC-phalloidin (A, C, E). Arrows represent talin staining in focal adhesions and arrowheads represent talin decoration of actin stress fibres. CEF cells - TA205 (A, B); TD77 (C, D). 3T3 cells - TD77 only (E, F). Bar 5μm.

Table 4.1. Summary of anti-human platelet talin monoclonal antibody characterisation.

	MONOCLONAL ANTIBODY					
	TA205	**TD77**	**TD74**	**TA9**	**TA44**	**TA269**
ISOTYPE	IgG1	IgG2a	IgG2a	IgG2b	IgG1	IgG1
EPITOPE (CHICK TALIN)	102-497	2269-2541	2269-2541	2269-2541	2269-2541	?
WESTERN BLOTTING	H, C	H, M, C	H	H	H, M	H, M
IMMUNO FLUORESCENCE	H, C	H, M, C	H	-	-	-
IMMUNE PRECIPITATION	H, C	H, M, C	H	H	H, M	H, M

Epitope figure represents the amino acid residues recognised by each antibody in Western blotting of chick talin fusion proteins (Fig.4.4).

Western blotting (Fig.4.1), immunofluorescence (Fig.4.5, 4.6) and immunoprecipitation (data not shown) carried out on human MRC5 fibroblasts (H), 3T3 mouse fibroblasts (M) and chick embryo fibroblasts (C). No epitope was determined for monoclonal antibody TA269. Immune precipitation of talin was performed by Simon Barry in this lab., and the antibodies were generated and isotyped in the lab. of Dr. J. M. Wilkinson, Wellcome Trust, London, U.K.

recognised chick talin fusion proteins containing residues 2269-2541. TA9, TA44 and TA269 were all able to detect human talin in Western blotting and immune precipitation but not when used for immunofluorescence. As for TD77 and TD74 the epitopes of TA9 and TA44 were mapped to chick residues 2269-2541 and TA269 was not able to recognise any of the chick talin fusion proteins. The observation that antibodies TD74, TA9 and TA44 could detect portions of chick talin when expressed as a bacterial GST-fusion protein but not intact chick talin in CEF cell lysates is slightly confusing, and it is most likely that the epitope(s) recognised by these three antibodies is lost during preparation of the cell lysates due to the denaturing conditions of the lysis buffer used.

TA269 did not recognise any of the chick talin fusion proteins used for the epitope mapping, but it was capable of recognising whole talin when used for immunoprecipitation or Western blotting of whole cell lysates made from human or mouse cells. There are several possible explanations for the inability to define the epitope of this antibody. It is conceivable that TA269 is a mammalian-specific antibody and therefore does not cross-react with chick talin, or that the epitope lies within the first 101 residues of talin that were not covered by the chick talin fusion proteins. It is also possible that the epitope of TA269 lies across the boundaries of two of the fusion proteins. It is unlikely that the epitope recognised by TA269 is lost due to denaturation of the fusion protein during the Western blotting procedure as it does recognise whole talin in Western blots.

The results obtained following Western blotting of whole cell lysates prepared from the human, chick and mouse fibroblast cell lines indicated that the six antibodies display some cross-reactivity between these three species although they all recognised talin in human cell lysates. The TA205 antibody, which mapped to the N-terminal portion of talin, recognisied only human and chick talin but not mouse talin, whereas TD77, which mapped to the C-terminus, recognised human, chick and mouse talin. This suggests a

possible region of diversity between human and chick talin compared to mouse talin within this N-terminal region of the talin molecule.

The immunofluorescence data obtained for antibodies TD77 and TA205 in CEF that were formaldehyde fixed followed by permeabilisation in Triton-X-100, revealed that talin is found, not only in focal adhesions located at the tips of actin stress fibres, but is also able to decorate the actin stress fibres. The human and mouse cells were extracted in MES buffer prior to fixation, and therefore have lost the detergent-soluble cytosolic pool of talin, only showed talin present in focal adhesions, suggesting that the association of talin with the actin cytoskeleton is only weak. As all six antibodies can detect human talin in Western blotting, the differences between the ability of the six antibodies to detect human talin in the focal adhesions of cultured MRC5 human cells by immunofluorescence is possibly a reflection of the relative affinities of each antibody for talin, although this is assuming that there is only a single epitope at the C-terminus of the protein. TA205 and TD77 both resulted in strong staining of talin in MRC5 cells and are therefore regarded as having the greatest affinity for talin, followed by TD74 which only weakly stained talin, followed by TA9, TA44 and TA269, all of which failed to stain talin in human MRC5 cells. The lack of staining of mouse talin by antibody TA205 is consistent with the Western blotting data and is presumably due to species divergence in this region of talin as discussed previously. Neither TD74, TA9, TA44 nor TA269 detected chick or mouse talin when used for immunofluorescence and this most likely a reflection of either their weak affinity for talin or they do not cross-react with either chick or mouse talin as discussed previously. However, TD74, TA9 and TA44 are all able to recognise chick talin, albeit when expressed as a GST-fusion protein, indicating that it is unlikely that the lack of immunofluorescent staining was simply due to the fact that these antibodies cannot recognise chick talin. The slight inconsistencies observed between the Western blotting data and the immunofluorescence data obtained with antibodies TD74, TA9 and TD44

may be due the presence of a cryptic epitope(s) which is being masked by a protein-protein interaction in the intact adhesion in the cultured cell and the epitope is therefore only exposed following preparation of the cell lysates used for the Western blotting. This would then raise the distinct possibility that there may be more than one epitope being recognised at the C-terminus by the TD77, TD74, TA9 and TA44 antibodies as TD77 can recognise talin in CEF lysates.

4.6 Conclusions.

The characterisation data obtained for antibodies TA205 and TD77 gave consistent data in all three cell lines and in each assay used, providing information about the species cross-reactivity of the N-terminus of the talin molecule recognised by the TA205 antibody. The inconsistencies observed between the Western blotting data and the immunofluorescence data obtained with antibodies TD74, TA9 and TD44 may be due the presence of a cryptic epitope(s) in this region which perhaps suggests that there may be more than one epitope being recognised at the C-terminus. Similarly, differences between the relative affinities of each antibody for talin in each cell line may have also contributed to the discrepancies observed between the data. Without further epitope mapping using smaller chick talin fusion proteins it is impossible to say for sure how many epitopes exist within this C-terminal region. However, this characterisation study has shown that two of the six monoclonal antibodies, TA205 and TD77, were able to detect talin in human and chick cells using Western blotting, immunofluorescence and imune precipitation. The epitopes of these two antibodies are found at either extreme of the talin molecule, which highlight them as potential reagents for use in further experiments to study the function of talin, and this is described in the following chapter.

94

CHAPTER 5

IDENTIFICATION OF FUNCTIONAL DOMAINS
IN THE TALIN MOLECULE

5.1 Introduction.

Microinjection of antibodies raised against intracellular proteins into cultured cells often results in some change of phenotype, indicating that the antibody is possibly blocking a functional site lying within its antigen. The epitopes recognised by the antibodies are often restricted to a small discreet portions of the protein, allowing the position of a functional site to be determined. This, coupled with *in vitro* experiments, makes it a powerful tool to probe the structure-function relationship of proteins involved in cell:matrix adhesions. This approach has been used successfully to identify functional domains in both vinculin (Westmeyer *et al.*, 1990) and talin (Nuckolls *et al.*, 1992). Microinjection experiments are usually carried out using monoclonal antibodies rather than polyclonal antibodies, but experiments carried by Nuckolls *et al.*, (1992), provided information about the function of the talin molecule within living cells using a polyclonal antibody. However, because they had used a polyclonal antibody, they were not able to assign functions to any particular region of the molecule. Westmeyer *et al.*, (1990) observed that microinjection of two monoclonal antibodies raised against chicken gizzard vinculin into CEF resulted in the dissociation of the actin cytoskeleton. The size and distribution of focal adhesions was also affected in the injected cells. Subsequent epitope mapping indicated that the two antibodies recognised separate regions of the vinculin protein and combined with *in vitro* experiments, it was proposed that one antibody was perturbing the vinculin-talin interaction, whilst the other appeared to be interfering with the internal architecture of the cell.

Another way to probe the function of proteins is to microinject the intact proteins or their constituent domains themselves, thus setting up a competition between the endogenous protein and the injected counterpart. This has been successful in determining the localisation patterns and possible functions of the two proteolytic fragments of talin. Nuckolls *et al.*, (1990) fluorescently-tagged and microinjected the 47kDa and 190kDa

fragments as well as intact talin into fibroblasts and epithelial cells. Both fragments were seen to disturb actin stress fibres, and both intact talin and the 47kDa fragment was seen to localise only to cell-matrix junctions compared to the 190kDa fragment which could also localise to cell-cell junctions in the epithelial cells. Proteins can now be expressed as fusion proteins with, for example, glutathione-S-transferase (GST) using the pGEX expression system available from Pharmacia. Using antibodies raised againsed the GST portion of the protein, this provides a quick method for analysing the distribution of the injected protein by immunofluorescence techniques, eliminating the laborious process of raising antibodies against separate regions of the same protein.

Using microinjection of both antibodies and fusion proteins, we have attempted to assign functions to separate domains of talin. In the previous chapter, a detailed characterisation of a panel of anti-talin monoclonal antibodies was presented. Two of these antibodies, TA205 and TD77, were observed to stain talin in human and chick fibroblasts, and more importantly, their epitopes mapped to separate regions at the N- or C-terminus of talin. The antibodies and fusion proteins containing the epitopes recognised by these antibodies were injected into fibroblasts, and the effect on the cyoskeletal architechture monitored by immunofluorescence. Motility assays were carried out with two anti-functional antibodies to assess whether they might also affect the ability of cells to migrate. Using a blot overlay-type assay, we have attempted to identify binding partners for both N- and C-terminal regions of talin and actin co-sedimentation assays were carried out on the C-terminal fusion proteins.

RESULTS.

Before describing the results obtained in this chapter, it is necessary to outline the difference between the two methods used to extract cells prior to immunostaining. To remove the soluble pool of cytosolic proteins, the cells are extracted in a Triton-X-100-

containing MES buffer and then fixed in formaldehyde allowing visualisation of only the detergent-insoluble cytoskeleton and associated proteins. Fixation in formaldehyde followed by permeabilisation in only Triton-X-100 preserves cytoplasmic integrity allowing visualisation of soluble proteins.

5.2 Microinjection of anti-talin monoclonal antibodies into human fibroblasts for identification of anti-functional antibodies.

To determine whether any of the anti-talin antibodies characterised in the previous chapter were anti-functional, they were microinjected into MRC5 human embryo lung fibroblast cells. Approximately 50 cells were injected/coverslip with 2mg/ml of each antibody, and the coverslips were returned to the incubator for 10, 30, or 60 minutes. Cells were then fixed and microinjected antibody was detected with a Texas Red-labelled anti-mouse IgG, and actin stress fibres were visualised using FITC-labelled phalloidin. Monoclonal antibodies TA205 (Figure 5.1B), TD77 (Figure 5.2B), and TD74 (data not shown) were all seen to localise to focal adhesions within 10 minutes of microinjection. The corresponding actin staining pattern was unaffected by injection of the antibody within 10 minutes (TA205 Fig.5.1A; TD77 Fig.5.2A). The remaining antibodies TA9, TA44 and TA269 did not stain talin present in the focal adhesions or in the cytoplasm (data not shown).

When the injected cells were incubated for 30 or 60 minutes and immunostained as before, only TA205 and TD77 were seen to adversely affect stress fibre integrity. The remaining 4 antibodies showed little or no disruption of the cytoskeleton following microinjection (data not shown). Not all microinjected cells were seen to have disrupted actin stress fibres, and three separate phenotypes were observed. The actin cytoskeleton in some injected cells remained intact (Fig.5.1C; Fig.5.2C) despite the presence of either TA205 (Fig.5.1D) or TD77 (Fig.5.2D) within the cytoplasm. A partially disrupted

Figure 5.1. Microinjection of anti-talin monoclonal antibody TA205 into MRC5 human fibroblast cells (see opposite).

MRC5 cells were microinjected with 2mg/ml TA205 and stained for actin with FITC-phalloidin (A, C, E, G), or for injected antibody with a Texas Red anti-mouse antibody (B, D, F, H). Injected cells were incubated for 5 minutes (A, B) or 30 minutes (C-H). After 5 minutes, cells were extracted in MES buffer prior to fixation to remove the cytoplasmic pool of injected antibody. Talin is present in focal adhesions located at the tips of the actin stress fibres (B, arrow). After 30 minutes, the cells are fixed and then permeabilised in 0.2% Triton-X-100 to indicate injected cells only. Bar 5μm
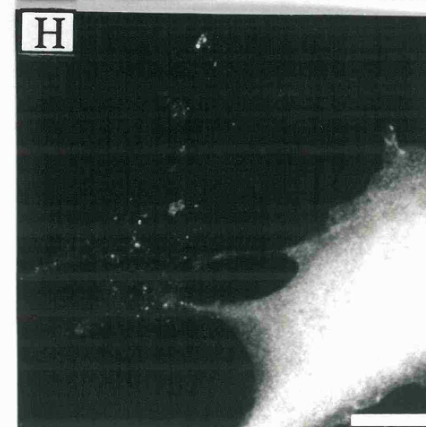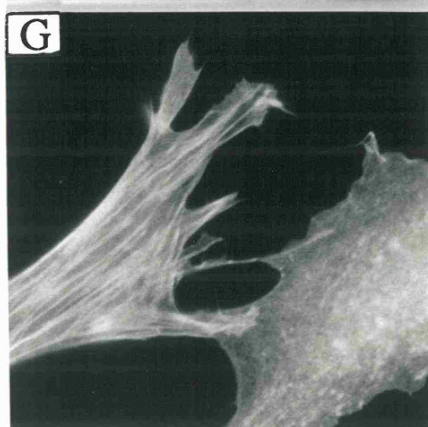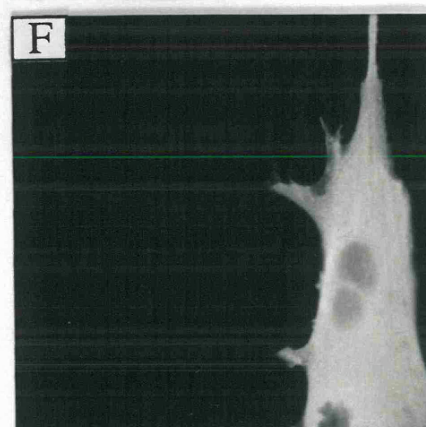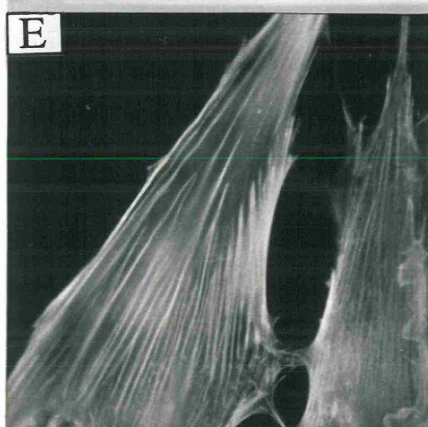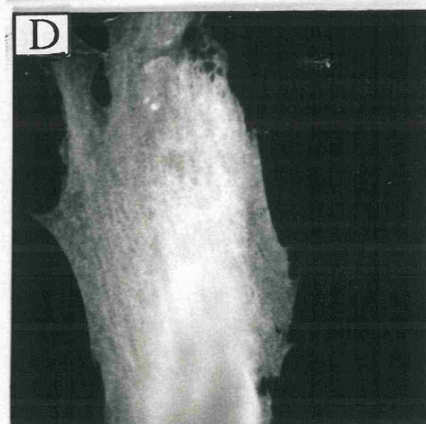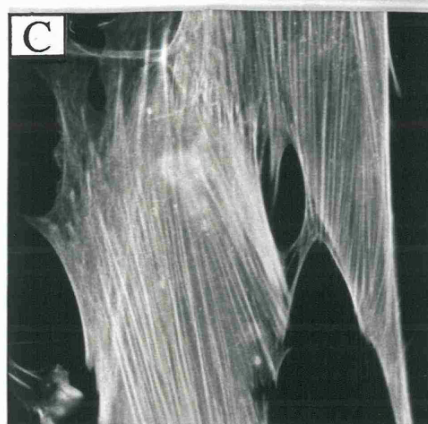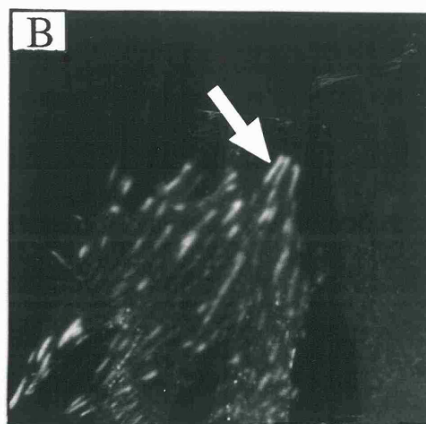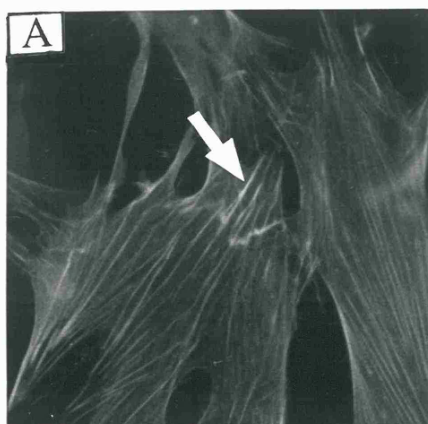
Figure 5.2. Microinjection of anti-talin monoclonal antibody TD77 into MRC5 human fibroblast cells (see opposite).

MRC5 cells were microinjected with 2mg/ml TD77 and stained for actin with FITC-phalloidin (A, C, E, G), or for injected antibody with a Texas Red anti-mouse antibody (B, D, F, H). Injected cells were incubated for 5 minutes (A, B) or 30 minutes (C-H). After 5 minutes, cells were extracted in MES buffer prior to fixation to remove the cytoplasmic pool of injected antibody. Talin is present in focal adhesions located at the tips of the actin stress fibres (B, arrow). After 30 minutes, the cells are fixed and permeabilised in 0.2% Triton-X-100 to indicate injected cells only. Bar 5μm
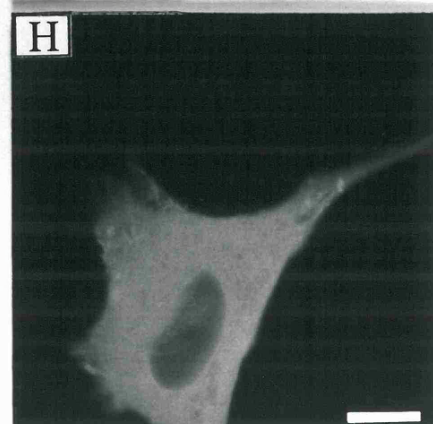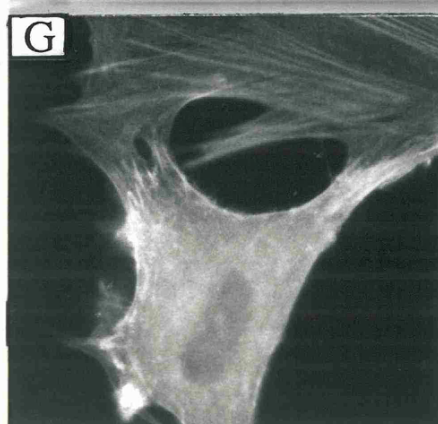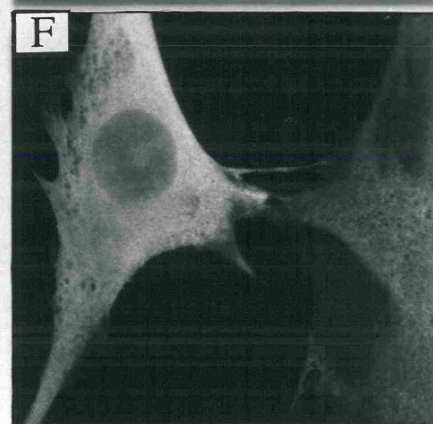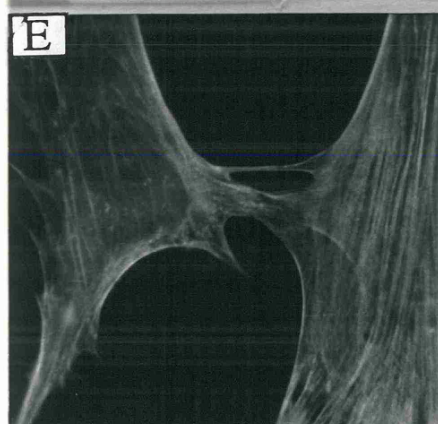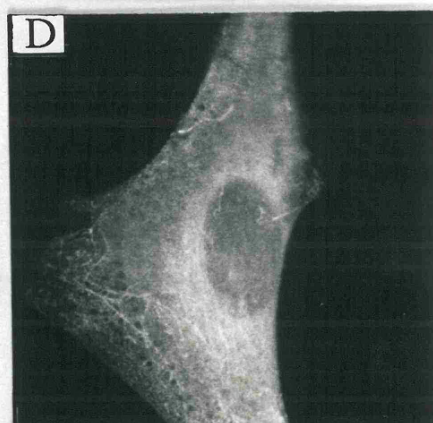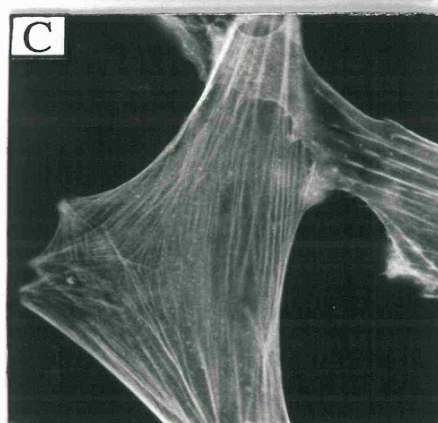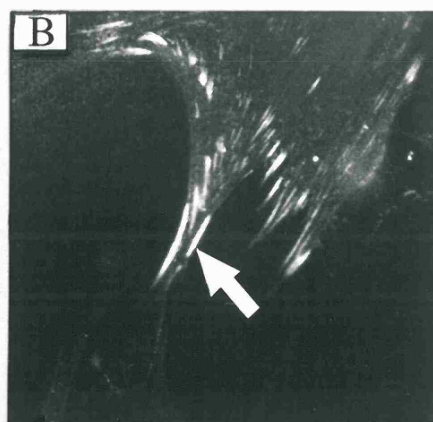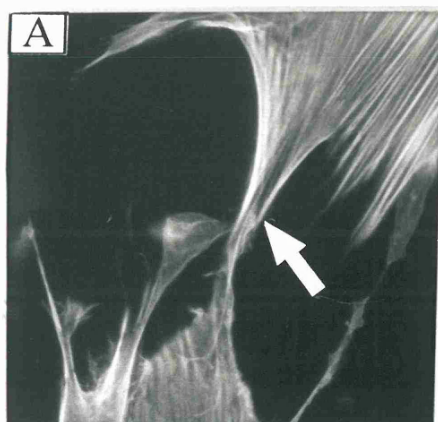
phenotype was also observed where the microinjected cell (TA205, Fig.5.1F; TD77, Fig.5.2F) displayed a reduced number of stress fibres (TA205, Fig.5.1E; TD77, Fig.5.2E), often much smaller and thinner in size when compared to neighbouring non-injected cells. The remaining cells were classified as totally disrupted as actin stress fibres were seen to be absent in these cells. The injected cells were brightly stained with the anti-mouse IgG antibody following injection with either TA205 (Fig.5.1H) or TD77 (Fig.5.2H), and the actin staining in these cells was diffuse and appeared throughout the cell cytoplasm (TA205, Fig.5.1G; TD77, Fig.5.2G).

5.3 TA205 is more efficient at disrupting stress fibre integrity compared to TD77.

All cells that had been microinjected with anti-talin antibody were classified according to the effect the injected antibody had on the integrity of the actin cytoskeleton i.e. not disrupted, partially disrupted or totally disrupted as described above. The data obtained for each category was expressed as a percentage of the total number of cells injected/experiment and the data for injections of all 6 antibodies, (60 minute incubation period), compared to non-injected cells is represented in Figure 5.3A. Data for non-injected cells was obtained by examining a portion of the coverslips that had not been injected and classifying similar numbers of cells accordingly. Only TA205 and TD77 had any dramatic effect on the stress fibres of an injected cell, and the cytoskeleton of cells injected with the remaining 4 antibodies remained largely unaffected. Comparison of TA205 and TD77 over a 30 minute time course (Fig.5.3B) revealed little difference in their ability to perturb the actin stress fibres. However, after 60 minutes (Fig.5.3C) TA205 was found to totally disrupt stress fibres in a greater percentage of cells compared to TD77.

Figure 5.3. Statistical analysis of anti-talin antibody injections into human MRC5 fibroblast cells (see opposite).

MRC5 cells were injected with anti-talin monoclonal antibodies, incubated for either 30 or 60 minutes and the affect on the integrity of the actin cytoskeleton was determined. The number of cells falling into each category - not affected, partially disrupted or totally disrupted, was determined and the results represented as a percentage of total cells injected in each experiment. The mean of 3 experiments/antibody +/- S.D is shown (B, C only). Typically, 30-50 cells were injected during each experiment.
(A) Data obtained for all 6 antibodies after a 60 minute post-injection incubation period.
(B) Data obtained for only TA205 and TD77 after a 30 minute post-injection incubation period.
(C) Data obtained for only TA205 and TD77 after a 60 minute post-injection incubation period.

A.

% of total cells injected

Level of stress fibre disruption

Legend: NON-INJECTED, TA269, TA9, TA44, TD74, TD77, TA205

B.

% total cells injected

Level of stress fibre disruption

Legend: TD77, TA205

C.

% total cells injected

Level of stress fibre disruption

Legend: TD77, TA205
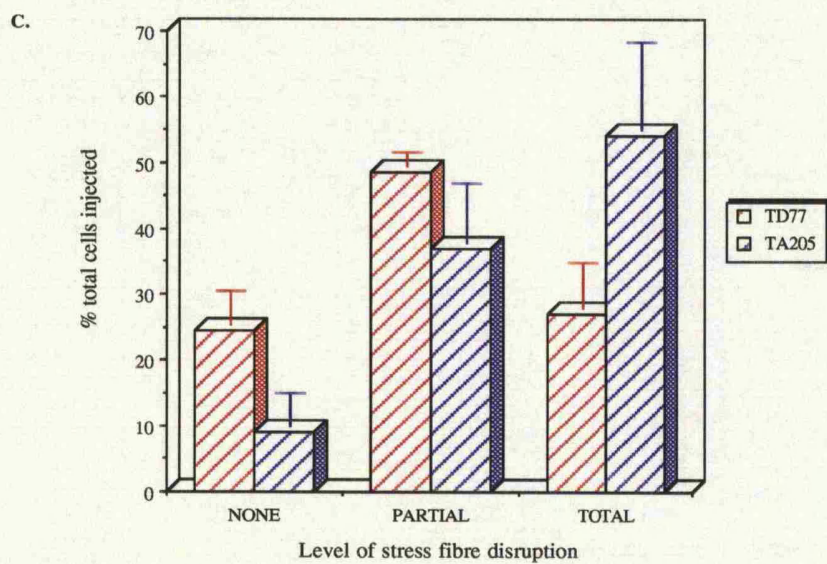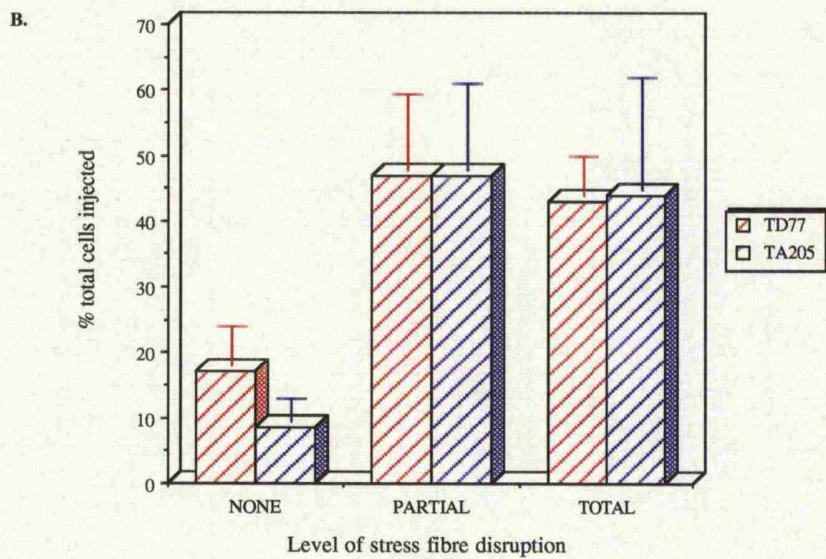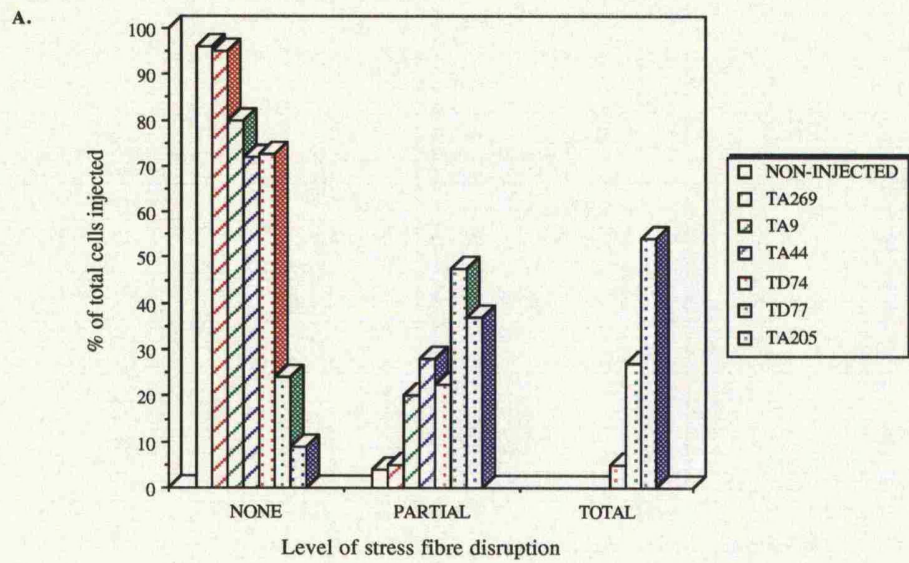
5.4 Reduction in the migratory properties of cells microinjected with anti-functional antibodies.

A wound was introduced into a confluent monolayer of CEF cells and either monoclonal antibody TA205 or TD77, or control mouse IgG was microinjected into cells along the margin of the wound. Following a 12 hour incubation period, the cells were fixed and permeabilised, and the injected antibody was visualised with a Texas Red-labelled anti-mouse antibody. The majority of cells injected with either TA205 (Figure 5.4D) or TD77 (Fig.5.4F) were seen to remain at the margin of the wound (dotted line between arrowheads) as visualised by actin staining (Fig.5.4C and E respectively). Non-injected cells were seen to have migrated into the space created in the monolayer. Cells injected with control IgG (Fig.5.4B) were seen to be as motile as the non-injected cells (Fig.5.4A).

The ability of the antibodies to inhibit the migratory properties of the cell was compared by classifing cells as either motile i.e. cells which have moved away from the margin of the wound along with other non-injected cells, or non-motile i.e. cells that remain at the margin of the wound despite significant migration of non-injected cells. The number of cells falling into either category was determined and the results are shown in Figure 5.5. As expected, injection of a control IgG did not affect the ability of the cell to migrate, with over 75% of cells injected having migrated away from the wound margin. Both TA205 and TD77 resulted in a marked reduction in the ability of the injected cell to migrate into the wound, with only 27% and 21% of cells respectively being able to move away from the wound margin.

Figure 5.4. Microinjection of anti-talin antibodies TA205 and TD77 into motile CEF cells (see opposite).

Confluent monolayers of CEF cells were partially de-nuded of cells and anti-talin antibody (2mg/ml), or control mouse antibody (2mg/ml) was microinjected into the cells lying along the margin of the wound. Following a 12 hour incubation period the cells were stained with actin (A, C, E) to visualise the monolayer, or with a Texas Red anti-mouse antibody (B, D, F) to visualise the injected cells. Injected cells are indicated by the arrows and the margin of the wound is indicated by the dotted line betwen the arrow heads. Bar 15μm.
A, B - Control IgG; C, D - TA205; E, F - TD77.
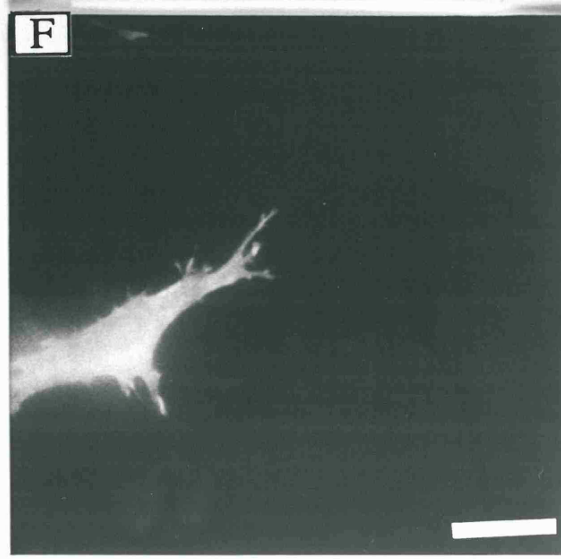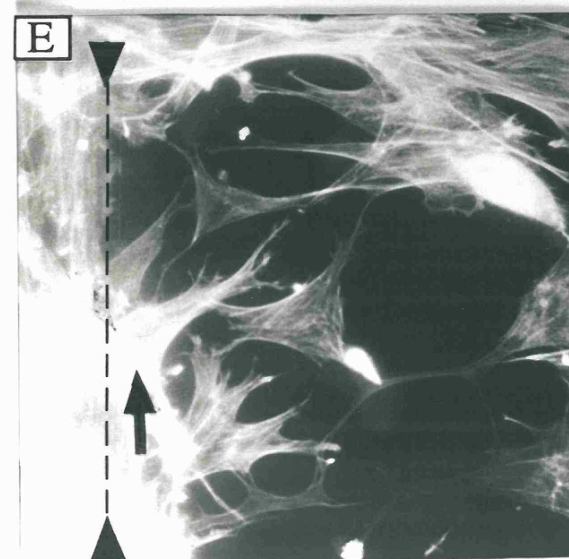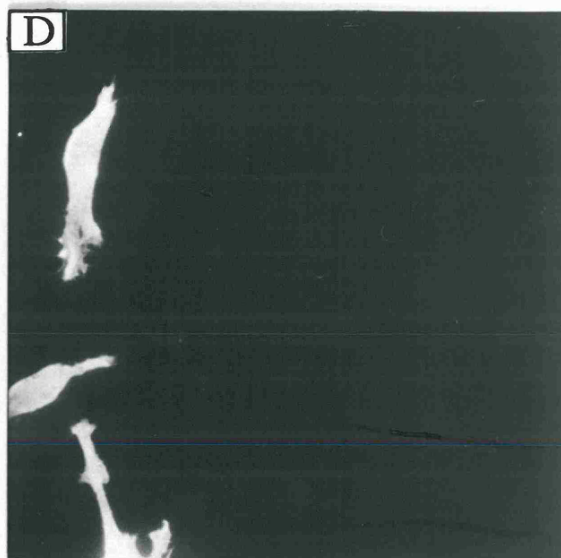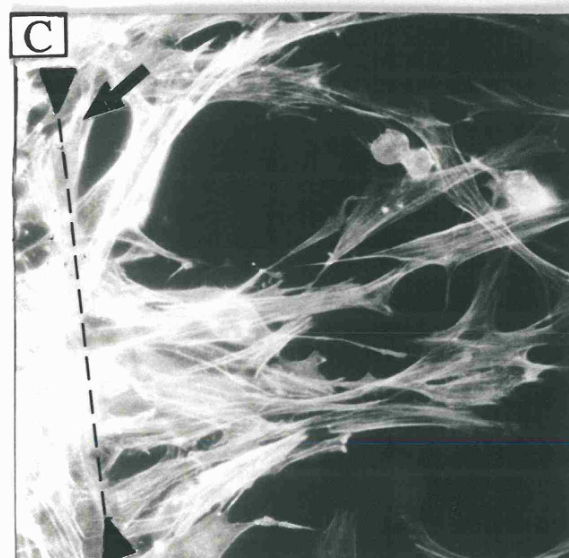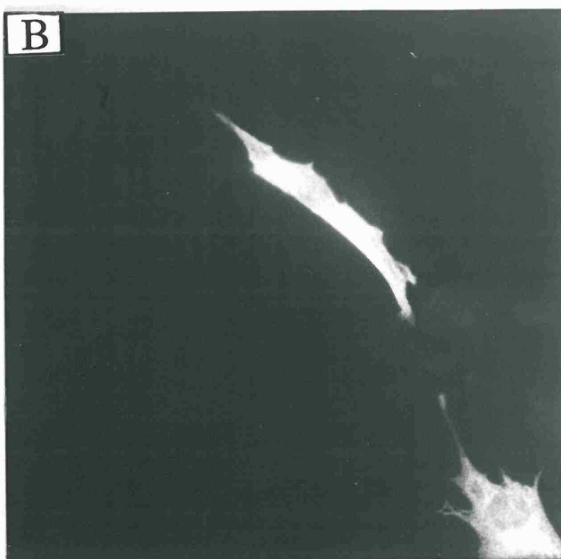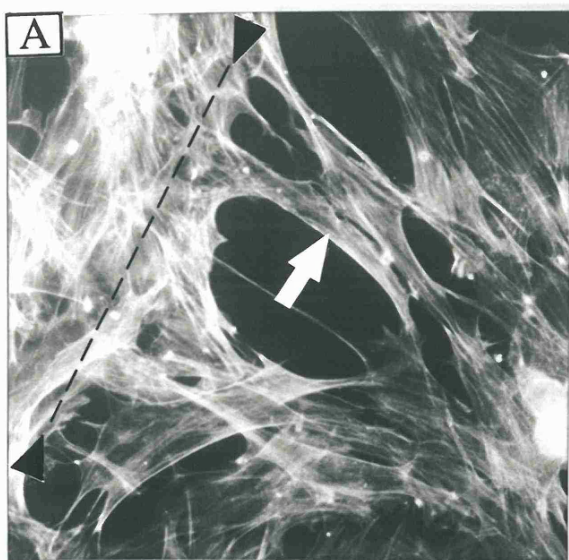
Figure 5.5. Statistical analysis of effect on motility of CEF microinjected with anti-talin monoclonal antibodies TA205 and TD77.
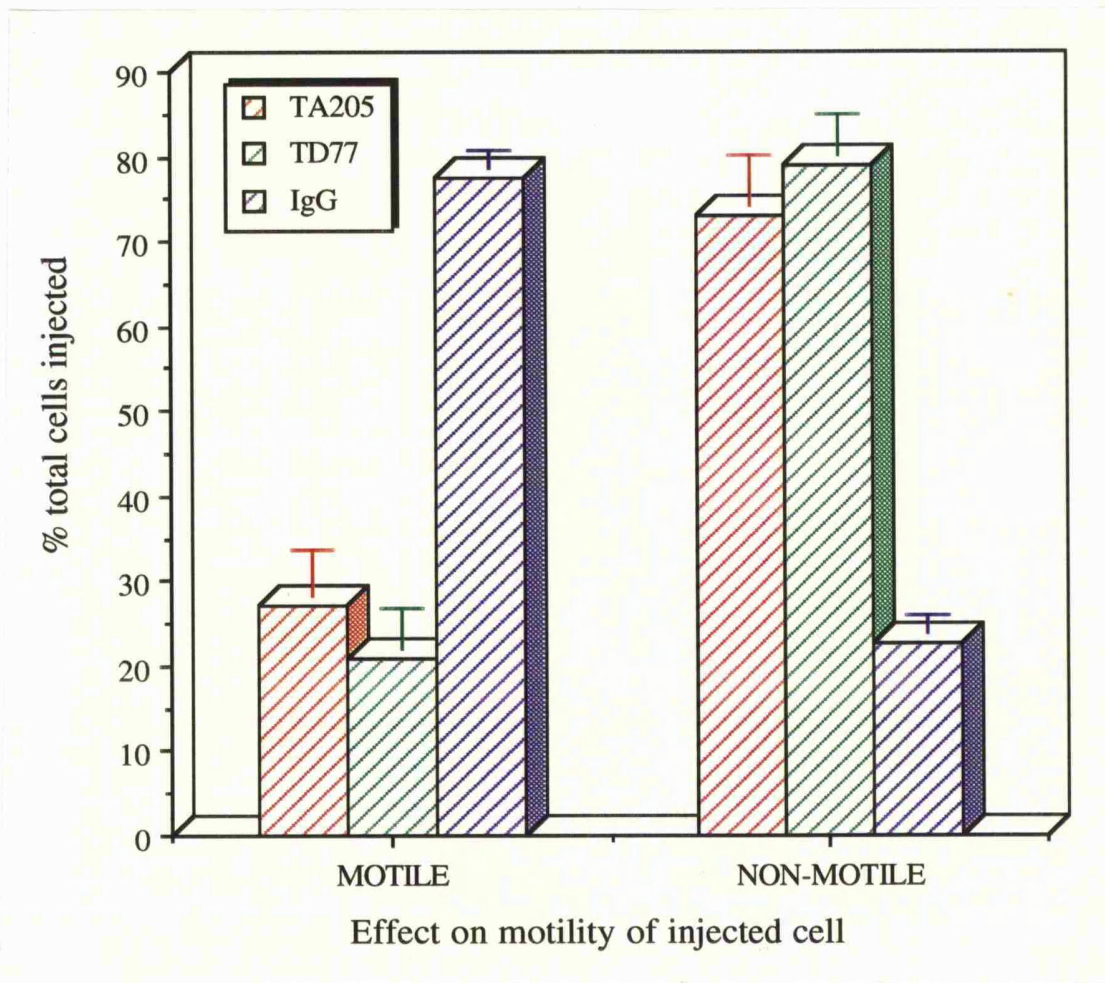
Following injection of motile CEF cells with the anti-talin antibodies or control mouse IgG, cells were classified as either motile or non-motile as described in the main text. The numbers of cells falling into either category was determined and is represented as a percent of the total number of cells/experiment. The mean of 3 experiments/antibody +/- S.D. is shown here.

5.5 Microinjection of N-terminal talin fusion proteins recognised by the anti-functional anti-talin antibody TA205.

Chick talin fusion proteins GST/102-497 and GST/102-656 were expressed in *E.coli* and purified using glutathione-agarose beads (Figure 5.6). Eluted fusion proteins were then diluted to 2mg/ml and injected into CEF cells. Following a 10 minute post-injection incubation period, the cells were either extracted in Triton-X-100-containing MES buffer and then fixed (data not shown), or fixed and then extracted in 0.2% Triton-X-100/PBS (GST/102-497, Figure 5.7; GST/102-656, Figure 5.8). The injected fusion protein was visualised using a polyclonal anti-GST antibody. Cells that had been MES extracted and fixed showed no evidence of either fusion protein, but following fixation and then extraction in 0.2% Triton-X-100, both GST/102-497 (Fig.5.7B) and GST/102-656 (Fig.5.8B) were seen to localise, albeit weakly, along stress fibres (Figs.5.7A and 5.8A respectively). The majority of either protein was associated with the detergent-soluble fraction of the cell and was seen to be distributed throughout the cytoplasm. When the injected cells were returned to the incubator for 30 minutes, fixed and Triton-X-100-extracted, and immunostained as before, the cells injected with either GST/102-497 (Fig.5.7D) and GST/102-656 (Fig.5.8D) were seen to have a disrupted actin cytoskeleton (Figs.5.7C and 5.8C respectively). In order to determine whether the fusion proteins also affected the integrity of the focal adhesions, the injections were repeated and the cells stained for both injected fusion protein and vinculin using the monoclonal antibody V284. Cells that had been injected with either GST/102-497 (Fig.5.7F) or GST/102-656 (Fig.5.8F) revealed a lack of focal adhesions as visualised by staining with the anti-vinculin antibody (Fig.5.7E and 5.8E respectively) when compared to surrounding non-injected cells (arrows, Figs.5.7 and 5.8). This loss of vinculin in focal adhesions, was not seen in all cells as expected, as previous experiments revealed that not all injections were seen to result in a total loss of actin stress fibre organisation.

100

Figure 5.6. Purified chick talin/GST fusion proteins.
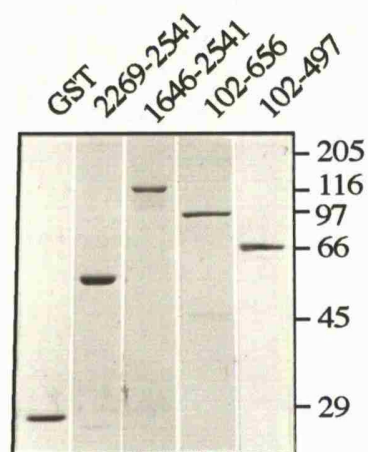
Chick talin GST-fusion proteins GST/102-656, GST/102-497, GST/1646-2541, GST/2269-2541 and GST alone were expressed in *E.coli* and purified using glutathione-agarose as an affinity matrix as described in Materials and Methods. The amino acid co-ordinates of each fusion protein is shown across the top of the figure and the molecular weight markers (kDa) are shown to the right of the figure.

Figure 5.7. Microinjection of chick talin fusion protein GST/102-497 into CEF cells.
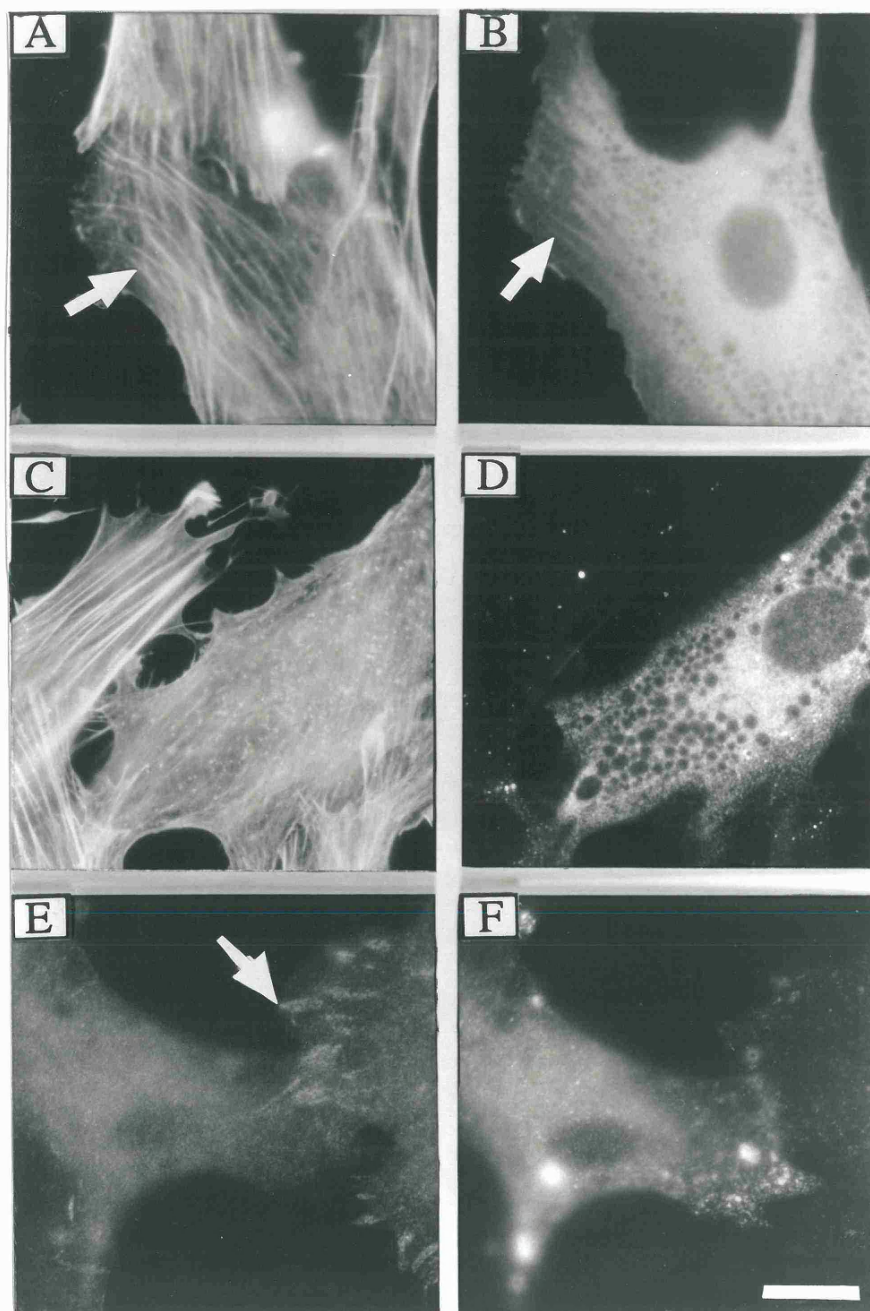
Chick talin amino-acid residues 102-497 were expressed as a GST fusion protein and microinjected into CEF cells at a concentration of 2mg/ml. After a 5 minute (A, B) or a 30 minute (C-F) incubation period, the cells were stained for either actin, using FITC-phalloidin (A, C) or vinculin, using monoclonal antibody V284 (E), and the GST-fusion protein using a polyclonal anti-GST antibody (B, D, F). The fusion protein can be seen to localise weakly to focal adhesions within 5 minutes (B, arrow). After 30 minutes, the injected fusion protein (D, F) is seen to disrupt both the actin cytoskeleton (C) and focal adhesions as visualised by vinculin staining (E). The focal adhesions in non-injected cells are unaffected (E, arrow).Bar 5μm.

Figure 5.8. Microinjection of chick talin fusion protein GST/102-656 into CEF cells.
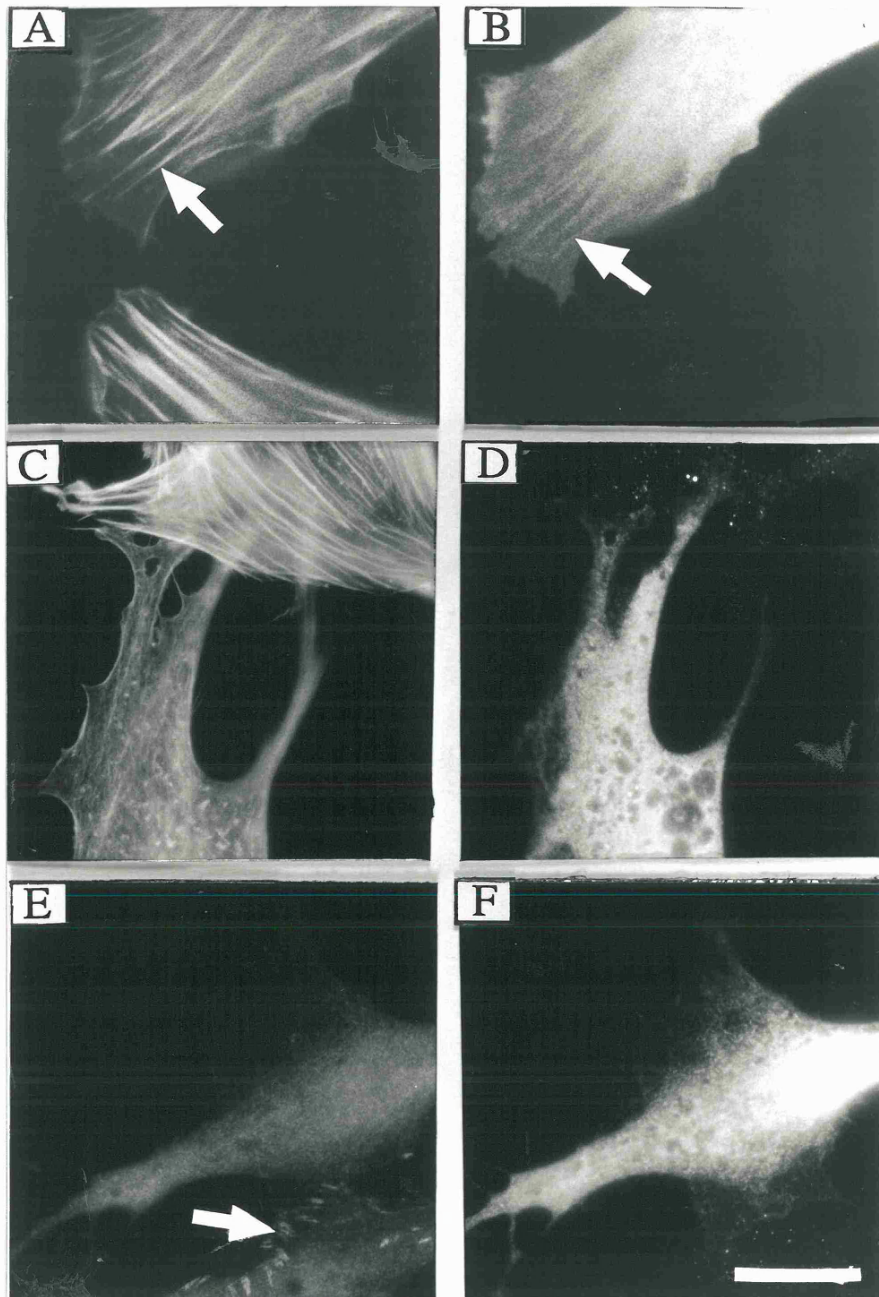
Chick talin amino-acid residues 102-656 were expressed as a GST fusion protein and microinjected into CEF cells at a concentration of 2mg/ml. After a 5 minute (A, B) or a 30 minute (C-F) incubation period, the cells were stained for either actin using FITC-phalloidin (A, C) or vinculin using monoconal antibody V284 (E), and the GST-fusion protein using a polyclonal anti-GST antibody (B, D, F). The fusion protein can be seen to localise weakly to focal adhesions (B, arrow) within 5 minutes. After 30 minutes, the injected fusion protein (D, F) is seen to disrupt both the actin cytoskeleton (C) and focal adhesions as visualised by vinculin staining (E). The focal adhesions in non-injected cells are unaffected (E, arrow). Bar 5μm.

Figure 5.9. Statistical analysis of the effect on the integrity of the actin cytoskeleton following microinjection of chick talin fusion proteins GST/102-497 and GST/102-656 into CEF cells.
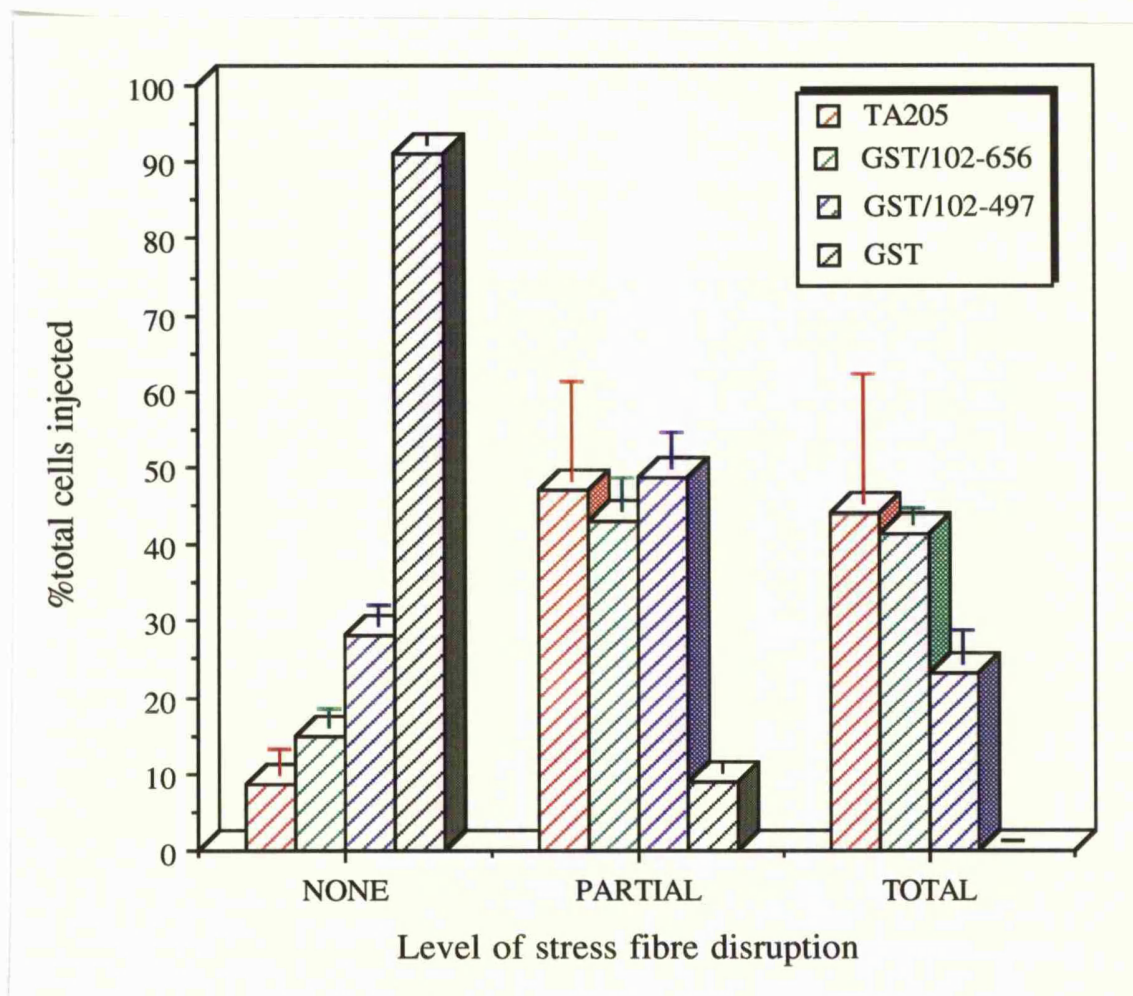
Following microinjection of CEF cells with either GST/102-497, GST/102-656 or GST alone, the amount of disruption of the actin cytoskeleton in the injected cell was assessed. The number of cells falling into each category - not affected, partially disrupted or totally disrupted, was determined and the results represented as a percentage of total cells injected in each experiment. The mean of 3 experiments/fusion protein +/- S.D is shown. Typically, 30-50 cells were injected during each experiment. The data obtained with both chick talin fusion proteins are compared to the GST protein alone and monoclonal antibody TA205.

As was observed with the antibody injections, not all the cells were equally affected by the injected fusion protein and a similar analysis was carried out. Each injected cell was classified according to the level of disruption of the actin cytoskeleton, and these figures were then expressed as a percentage of the total number of cells injected. This is shown graphically in Figure 5.9, where the fusion protein injections are compared to injection with either GST alone or the TA205 antibody. GST/102-656 was found to affect stress fibre integrity in a comparable manner to the antibody TA205 - both result in total disruption of stress fibres in over 41% of injected cells. The shorter fusion protein GST/102-497 appeared less efficient at causing a total disruption of the actin stress fibres compared to fusion protein GST/102-656 or antibody TA205.

5.6 Microinjection of C-terminal talin fusion proteins recognised by the anti-functional anti-talin antibody TD77.

Chick talin fusion proteins GST/1646-2541 and GST/2269-2541 were expressed as GST-fusion proteins in *E.coli* and purified using glutathione-agarose beads (Fig.5.6). Eluted fusion proteins were diluted to 2mg/ml and injected into CEF cells. Following a 10 minute post-injection incubation period, the cells were extracted in MES buffer and fixed prior to immunostaining for injected fusion protein and actin stress fibres. GST/1646-2541 (Figure 5.10B) and GST/2269-2541 (Figure 5.11B) were both seen to localise to focal adhesions at the ends of the actin stress fibres (Figs.5.10/5.11A, arrows). The shorter of the two fusion proteins GST/2269-2541 (Fig.5.11D) was also seen to decorate actin stress fibres (Fig.5.11D, F) as indicated by the arrowheads. After a 30 minute incubation the cells were fixed and then extracted in 0.2% Triton-X-100/PBS, and the effect each of the two fusion proteins had on the actin stress fibres was examined. Injection of GST/1646-2541 (Fig.5.10D) was able to totally disrupt actin stress fibres (Fig.5.10C), whereas GST/2269-2541 (Fig.5.11D) did not appear to affect actin stress fibres which remained intact (Fig.5.11C). The effect the injected fusion proteins had on focal adhesion

Figure 5.10. Microinjection of chick talin fusion protein GST/1646-2541 into CEF cells.
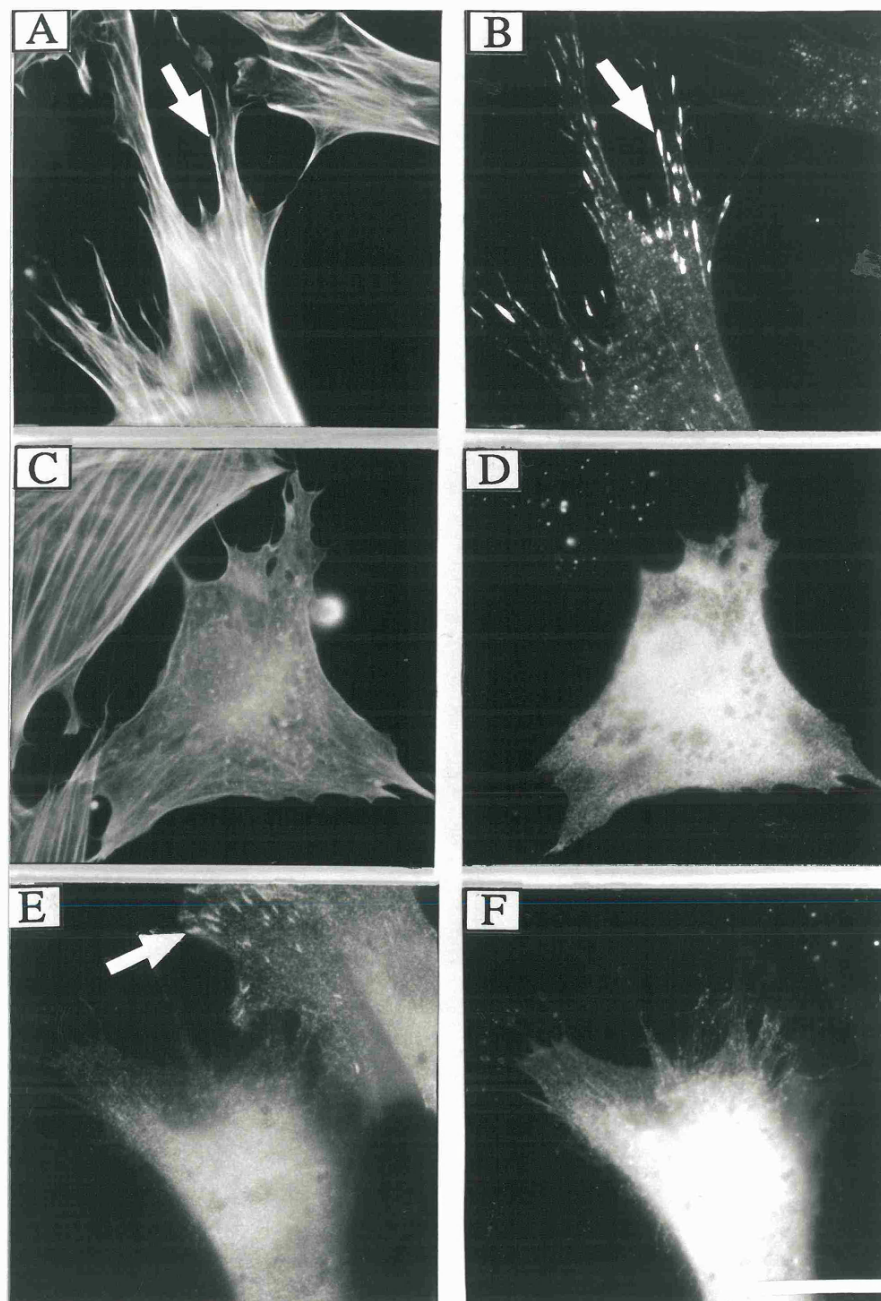
Chick talin amino-acid residues 1646-2541 were expressed as a GST fusion protein and microinjected into CEF cells at a concentration of 2mg/ml. After a 5 minute (A, B) or a 30 minute (C-F) incubation period, the cells were stained for either actin, using FITC-phalloidin (A, C), or vinculin, using monoclonal antibody V284 (E), and the GST-fusion protein using a polyclonal anti-GST antibody (B, D, F). The fusion protein can be seen to localise strongly to focal adhesions (B, arrow) within 5 minutes. After 30 minutes, presence of the injected fusion protein (D, F) is seen to disrupt both the actin cytoskeleton (C) and focal adhesions as visualised by vinculin staining (E). The focal adhesions in non-injected cells are unaffected (E, arrow). Bar 5μm.

Figure 5.11. Microinjection of chick talin fusion protein GST/2269-2541 into CEF cells.
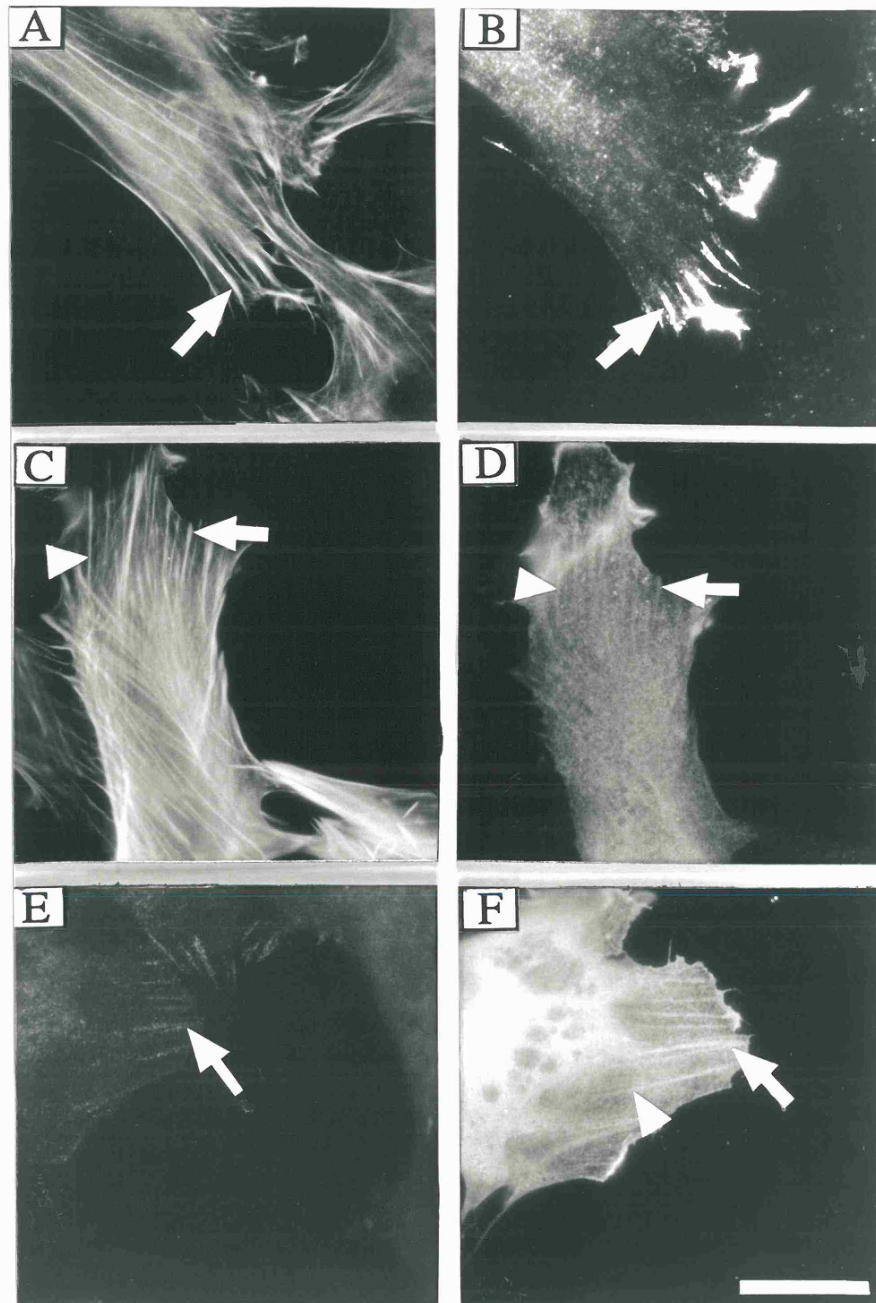
Chick talin amino-acid residues 2269-2541 were expressed as a GST fusion protein and microinjected into CEF cells at a concentration of 2mg/ml. After a 5 minute (A, B) or a 30 minute (C-F) incubation period, the cells were stained for either actin, using FITC-phalloidin (A, C), or vinculin, using monoclonal antibody V284 (E), and the GST-fusion protein using a polyclonal anti-GST antibody (B, D, F). The fusion protein can be seen to localise strongly to focal adhesions (B, arrow) within 5 minutes. After 30 minutes, presence of the injected fusion protein (D, F) does not affect either the actin cytoskeleton (C) or focal adhesions as visualised by vinculin staining (E). The focal adhesions in non-injected cells are also unaffected (E, arrow). Bar 5μm.

Figure 5.12. Statistical analysis of the effect on the integrity of the actin cytoskeleton following microinjection of the chick talin fusion proteins GST/1646-2541 and GST/2269-2541 into CEF cells.
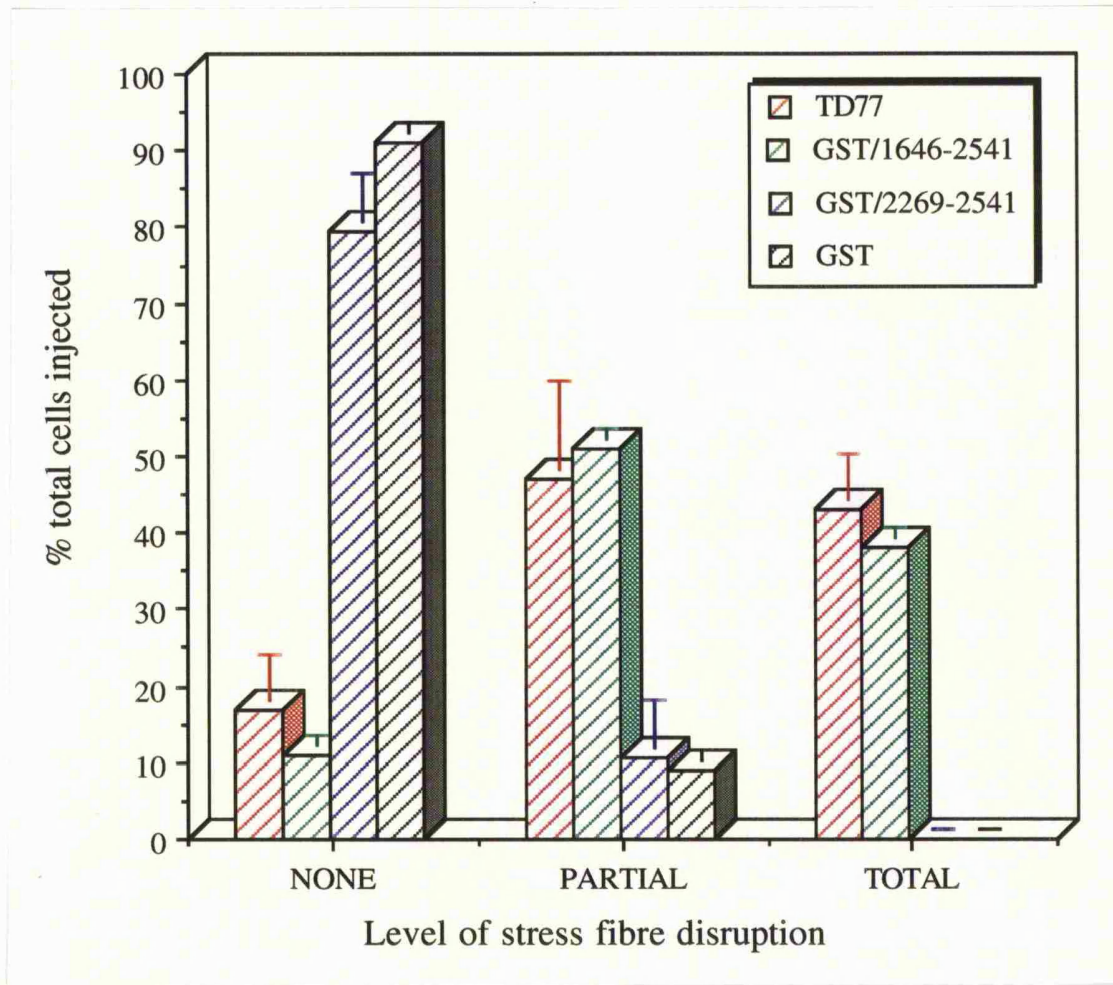
Following microinjection of CEF cells with either GST/1646-2541, GST/2269-2541 or GST alone, the level of disruption of the actin cytoskeleton in the injected cell was assessed. The number of cells falling into each category - not affected, partially disrupted or totally disrupted, was determined and the results represented as a percentage of total cells injected in each experiment. The mean of 3 experiments/fusion protein +/- S.D is shown. Typically, 30-50 cells were injected during each experiment. The data obtained with both chick talin fusion proteins are compared to the GST protein alone and monoclonal antibody TD77.

integrity was also assessed following immunostaining of injected cells with the vinculin monoclonl antibody V284. In some of the cells injected with GST/1646-2541 (Fig.5.10F), there was a loss of vinculin staining (Fig.5.10E) whereas intact focal adhesions could be clearly seen in neighbouring cells (arrow Fig.5.10E). Focal adhesions in cells injected with GST/2269-2541 (Fig.5.11F) were unaffected by the fusion protein, and the vinculin staining was essentially identical to the surrounding non-injected cells (arrow Fig.5.11E).

Once again, injected cells were classified according to the effect the fusion protein had on the actin stress fibres as described earlier. Comparison of the effect of the C-terminal fusion proteins to antibody TD77 revealed that only GST/1646-2541 gave similar results to those obtained with TD77 (Figure 5.12B). GST/2269-2541, however was comparatively poor at disrupting the actin stress fibres, with over 75% of the cells exhibiting an intact actin cytoskeleton (Fig.5.12A).

5.7 Microinjection of GST into CEF does not affect actin stress fibre integrity.

GST was expressed in *E.coli* and purified using glutathione-agarose beads as an affinity matrix (Fig.5.6). Purified GST was diluted to 2mg/ml and injected into CEF and the cells returned to the incubator for 10 or 30 minutes. Following fixation and permeabilisation in Triton-X-100 injected cells were immunostained for GST (Figure 5.13B, D) and actin stress fibres (Fig.5.13A, C). Injected cells were seen to exhibit a normal actin cytoskeleton, with no disruption to the fibres after either the 10 minute (Fig.5.13A, B) or 30 minute (Fig.5.13C, D) post-injection incubation period. Injected fusion protein was seen to have a diffuse distribution throughout the cytoplasm of the cell, indicating no specific localisation of the GST protein.

Figure 5.13. Microinjection of GST protein into CEF cells.
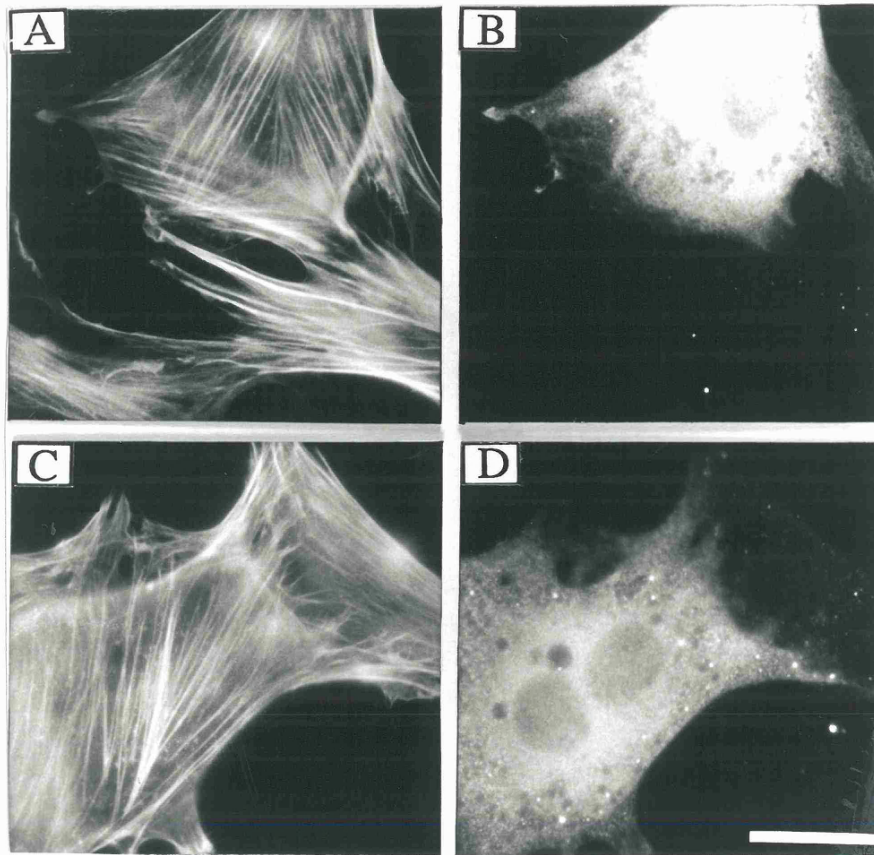
The 26kDa GST protein was injected into CEF cells at a concentration of 2mg/ml. After either a 5 minute (A, B), or a 30 minute (C, D), incubation period, the injected cells were stained for actin using FITC-phalloidin (A, C) or GST protein using a polyclonal anti-GST antibody (B, D). Bar 5μm.

5.8 Attempts to identify binding partners for GST-fusion proteins spanning the N- and C-terminal regions of talin using a blot overlay-type assay.

Total cell protein prepared from CEF cells was resolved by SDS-PAGE and electroblotted to nitrocellulose. Fusion proteins GST/102-497, GST/102-656, GST/1646-2541 and GST/2269-2541 and GST alone were incubated with the blots overnight. The bound fusion protein was detected with an anti-GST antibody, and fusion proteins spanning residues 102-656, 1646-2541 and 2269-2541 were all seen to bind to a single protein of approximately 110kDa (Figure 5.14A). No bands were identified in the filters probed with either GST/102-497 or the GST control. The blots were subsequently re-probed for vinculin using V284, an anti-vinculin monoclonal antibody, and vinculin was identified in all blots at the same mobility as the protein identified by the fusion proteins (Fig.5.14B). No other bands could be identified using this assay.

5.9 Identification of an actin-binding site within residues 2269-2541 of talin.

The C-terminal fusion proteins GST/1646-2541 and GST/2269-2541 were purified as described earlier and spun at 100,000g in the presence (+) and absence (-) of freshly polymerised F-actin. The supernatant (S) and the pellet (P) were separated and equal amounts of each were analysed by SDS-PAGE, and the proteins visualised by Coomassie blue staining (Figure 5.15). Neither GST/1646-2541, GST/2269-2541 nor GST alone were seen in the pellet fraction in the absence of actin. When actin was included in the assay, both GST/1646-2541 and GST/2269-2541 were clearly seen in the pellet fraction along with the actin. A small trace amount of GST was also seen in the pellet fraction when actin was included in the assay, but this can be regarded as non-specific pelleting as previous experiments (for example see relevant tracks in Figure 5.16) did not show this.

103

Figure 5.14. Identification of binding partners for the chick talin fusion proteins using a blot overlay-type assay.
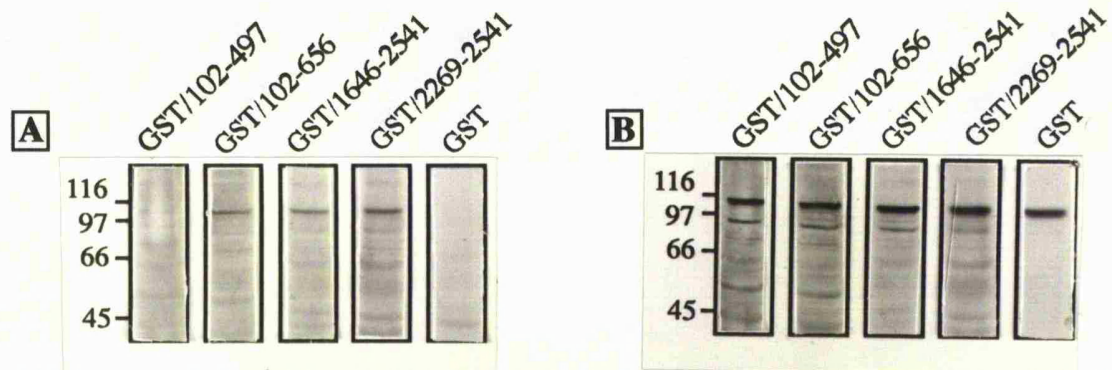
(A) Equal amounts of total cell protein from CEF were resolved by SDS-PAGE and electroblotted to nitrocellulose. Chick talin fusion proteins GST/102-497, GST/102-656, GST/1646-2541, GST/2269-2541 or GST alone were incubated with the nitrocellulose strips overnight and bound fusion protein detected with a polyclonal anti-GST antibody. (B) The filters were stripped and re-probed for vinculin using monoclonal antibody V284.

The amino acid co-ordinates of the talin/GST fusion proteins are shown above each lane and the molecular weight markers (kDa) are shown to the left of each lane.

Figure 5.15. Actin co-sedimentation of chick talin fusion proteins GST/1646-2541 and GST/2269-2541.
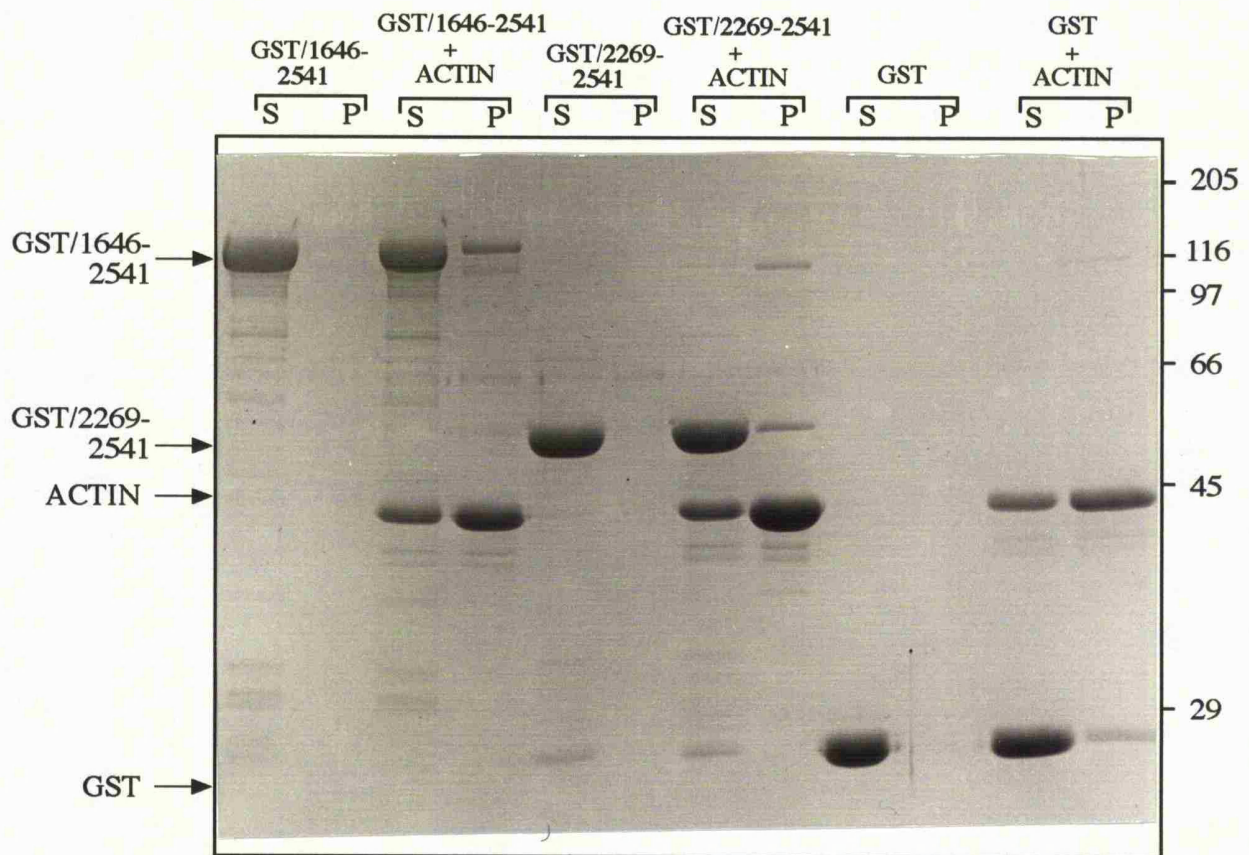
The two most C-terminal talin fusion proteins, GST/1646-2541 and GST/ 2269-2541, were centrifuged at 100,000g without or with an equal amount of freshly polymerised F-actin. Equal samples of the supernatant (S) and the pellet (P) were resolved by SDS-PAGE, and the proteins stained with Coomassie Blue. The positions of the fusion proteins and actin are shown to the left of the figure and the molecular weight markers (kDa) are indicated to the right of the figure.

Figure 5.16. Actin co-sedimentation of chick talin fusion proteins GST/1646-2541 and GST/2269-2541 with anti-talin monoclonal antibody TD77.
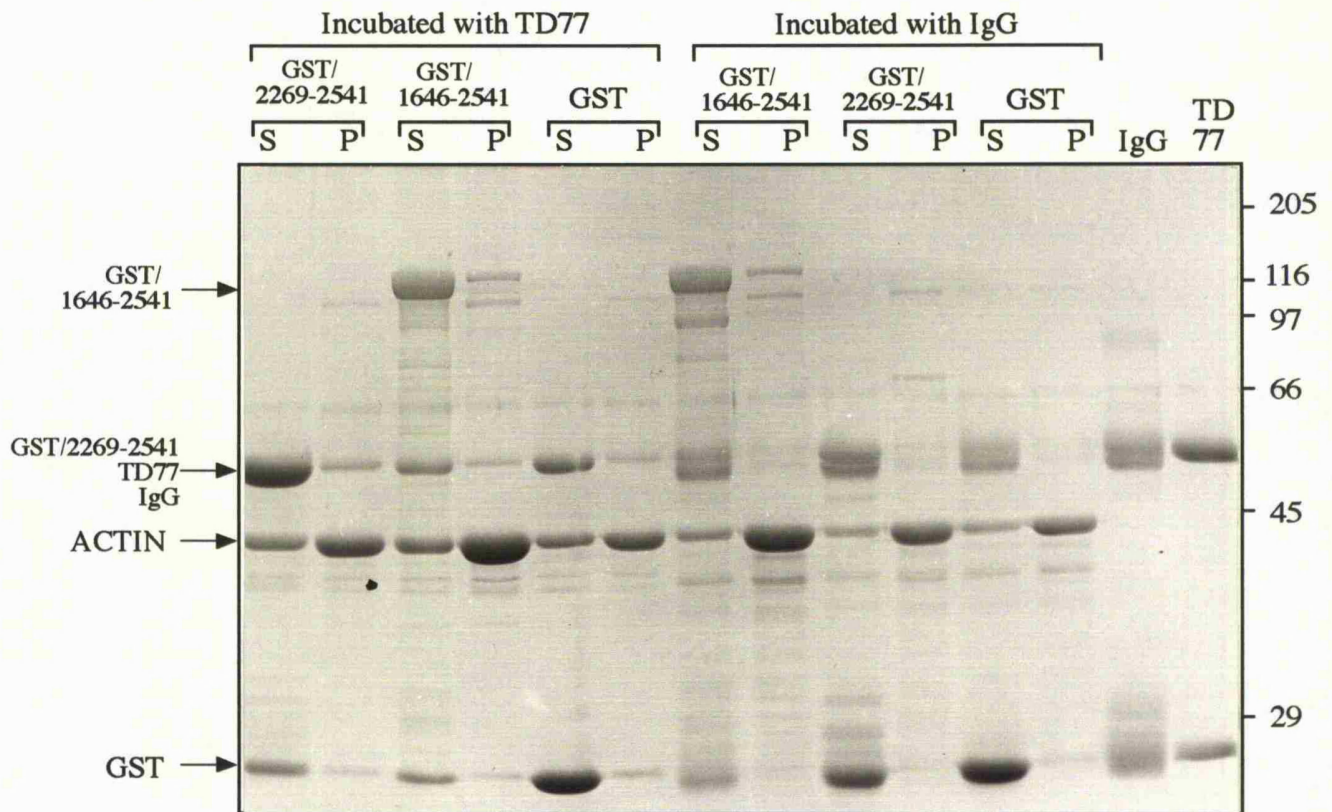
The talin fusion proteins GST/1656-2541 and GST/2269-2541 were mixed with an excess molar amount of either TD77, the anti-talin monoclinal antibody, or mouse IgG prior to centrifugation at 100,000g with an equal amount of freshly polymerised F-actin. Equal amounts of both supernatant (S) and pellet (P) were analysed by SDS-PAGE and the protein stained with Coomassie Blue. The positions of the fusion proteins, actin and antibodies involved are indicated to the left of the figure and the molecular weight markers (kDa) are shown to the right.

In order to determine whether the epitope recognised by the monoclonal antibody TD77 included, or was close to, the actin-binding site, the co-sedimentation assays were repeated in the presence of a molar excess of either monoclonal TD77 or a control mouse IgG (Figure 5.16). Unfortunately, both the IgG and TD77 antibodies run with approximately the same mobility as the GST/2269-2541 fusion protein on the SDS-polyacrylamide gels, and both antibodies can be seen in the pellet fraction (see GST lanes for best example), making interpretation of this particular result impossible. When GST/1646-2541 was incubated with TD77, in the presence of actin, there did not appear to be a significant reduction in the amount of fusion protein found in the pellet. Incubation with control IgG does not appear to affect the ability of GST/1646-2541 to pellet along with actin. GST remains unaffected by incubation with either antibody, with both TD77 and IgG being found in the pellet fraction along with the actin, whilst the GST is seen only in the supernatant fraction.

5.10 Discussion.

Anti-talin monoclonal antibodies TA205 and TD77 affect stress fibre integrity and cell motility.

From a panel of six anti-talin monoclonal antibodies, two were identified (TA205 and TD77) which were able to disrupt actin cytoskeleton integrity in human MRC5 fibroblasts, and inhibit the motility of CEF cells. Previous epitope mapping of these antibodies showed that TA205 recognised an epitope within the N-terminal region of talin spanning amino acids 102-497, whilst TD77 recognised an epitope within the C-terminal residues 2269-2541 (see Chapter 4 of this thesis). TA205 was seen to stain focal adhesions more strongly than TD77 when used for routine immunofluorescent staining of human fibroblasts, but following microinjection of the two antibodies, both were seen to localise to focal adhesions with equal intensity. This observation may reflect a difference

in affinities for talin between the two antibodies which is overcome by introducing high concentrations of antibody into the cell via microinjection. When the incubation period was increased to 30-60 minutes, cells injected with TA205 or TD77 displayed a loss of organised actin stress fibres. Closer examination of the actin stress fibres in the injected cells revealed three different phenotypes and the observation that all cells were not equally affected may be attributable to variable amounts of antibody injected into the cells, or it may be a reflection of the motility of the cell, as a more motile cell would exhibit less stable adhesions and therefore be more susceptible to the presence of the antibody.

Analysis of the numbers of cells falling into each of the three phenotypic categories over a 30 minute time period, revealed that both monoclonal antibodies TA205 or TD77 performed approximately equally with regard to the disruption of the actin cytoskeleton. However, after 60 minutes, TA205 was seen to result in the total disruption of actin stress fibres in a greater percentage of cells compared to TD77. This may be due to differences in relative affinities of the antibodies for talin, as it was observed earlier that TA205 was superior to TD77 when used for immunofluorescence studies. This correlation between immunofluorescent staining and ability to disrupt the actin cytoskeleton following microinjection is also shown for monoclonal antibody TD74. This antibody only weakly stained talin when used for immunofluorescence, and was seen to result in total disruption of actin stress fibres in only 5% of injected cells. It was not possible to examine the effect that microinjection of the mouse monoclonal antibodies had on the focal adhesions of injected cells as virtually all antibodies against focal adhesion components are also mouse monoclonal antibodies.

The effect the two anti-functional antibodies on cell migration was assessed and CEF injected with control mouse IgG were not affected and mostly seen to be included in the migrating pack of cells. Over 75% of the cells injected with either anti-functional antibody

were seen to be retained in the wound margin, and not present in the pack of cells that had migrated away from the site of the wound. The remaining 25% of cells injected with the talin antibodies that were able to migrate from the baseline probably represent a variability in the amount of antibody injected into the cell, as the cells present in a confluent monolayer are small and densly packed and therefore more difficult to inject.

The data indicate that talin is indeed a key component of cell-matrix junctions which is consistent with observations made previously by Nuckolls et al., (1992) who microinjected a polyclonal anti-talin antibody into either newly-spreading or well-spread CEF. The antibody inhibited the further spreading of newly-plated cells and frequently induced the injected cells to round up, whilst the spread cells were unaffected by the antibody. Similarly, the migration of CEF was inhibited by the presence of the antibody leading the authors to propose that precipitation of the cytosolic soluble pool of talin has little effect on the talin already incorporated into the mature adhesions but was closely involved in the formation of new focal contacts.

The epitopes recognised by anti-functional antibodies TA205 and TD77 span functional domains of talin.

Talin residues 165-373 within the N-terminus show limited sequence homology to the N-terminal region of the band 4.1/ERM family of proteins that is thought to be involved in mediating an interaction between the cytoskeleton and integral membrane protein and/or membrane components themselves (Rees et al., 1990). Indeed, this domain within the band 4.1 protein has been recently identified as containing a binding site for the cytoplasmic domain of the transmembrane protein glycophorin C as well as the peripheral membrane protein p55 (Marfatia et al., 1994), and expression of ezrin N-terminal amino acids 1-309 demonstrated that they only localised to cell surface protrusions and were not associated with actin stress fibres i.e. were found in the detergent-soluble fraction

106

(Algrain *etal.*, 1993b).The N-terminal talin fusion protein GST/102-497 was also found

to be detergent-soluble following microinjection into CEF cells i.e. displayed a diffuse

cytosolic staining pattern and only weakly localised to the actin stress fibres following

fixation and Triton-X-100 permeabilisation. This observation is consistent with the results

obtained by both Gilmore *etal.*, (1993), who stably expressed talin residues 102-497 in

NIH3T3 cells and also found that this polypeptide was extracted from the cell following

treatment with detergents, and Nuckolls *etal.*, (1990) who demonstrated that the 47kDa

portion of talin only weakly localises to focal adhesions following microinjection into

fibroblasts and the majority of the protein was diffusely distributed throughout the

cytoplasm. Also the N-terminal region of talin has been shown to interact with charged

lipids *in vitro* (Dietrich *etal.*, 1993; Niggli *etal.*, 1994) i.e. it can interact directly with the

membrane components, and talin has also been shown to redistribute to the membrane in

activated platelets in an integrin-independent fashion (Bertagnolli *et al.*, 1993).   As the

data suggests there is considerable evidence that the N-terminal region of talin and the

band 4.1/ERM family of homologous proteins is directly involved in cytoskeleton-plasma

membrane linkages.

The very weak localisation to focal adhesions and actin-containing structures by these talin

N-terminal fusion proteins was somewhat surprising as the same talin residues 102-656,

when stably expressed in NIH3T3 cells are seen to localise to focal adhesions and were

resistant to detergent extraction (Gilmore *etal.*, 1993). This failure of residues 102-656 to

localise to focal adhesions following microinjection may be explained by the possibility

that the fusion protein was unable to establish interactions with other focal adhesion

components during the 30 minute incubation period. Also, the 47kDa fragment is known

to contain a region responsible for targeting the full length molecule to focal contacts

(Nuckolls *etal.*, 1990), but unfortunately the chick talin cDNA available to us that was

used to construct the fusion proteins did not span residues 1-101, and the focal adhesion

targeting sequence may well lie in the region of the protein coded for by this particular stretch of the cDNA.

Both GST/102-656 and GST/102-497 were able to totally disrupt actin stress fibres following a 30 minute post-injection incubation period i.e they were competing with endogenous talin for talin binding proteins that are essential for cytoskeletal integrity. The observation that GST/102-656 was more effective at disrupting stress fibres compared to GST/102-497 may be explained by the fact that GST/102-656 spans at least one of three vinculin-binding sites in the talin molecule (Gilmore *et al.*, 1993), whereas GST/102-497 does not contain any vinculin-binding sites. The ability of GST/102-497 to disrupt actin stress fibres is perhaps a little more difficult to explain as no specific interactions have been attributed to this region of talin, although it is very possible that the fusion protein competes for the interaction between endogenous talin and the cell membrane resulting in release of the focal adhesion and associated stress fibres.

GST/1646-2541 and GST/2269-2541 were both seen to localise to focal adhesions following extraction in MES buffer prior to fixation, demonstrating that these two C-terminal fusion proteins have a strong association with the detergent-insoluble actin cytoskeleton. However, the two fusion proteins demonstrated differing abilities to disrupt the actin cytoskeleton. GST/1646-2541 is known to span at least two vinculin-binding sites between residues 1646-2268 (Gilmore *et al.*, 1993) and residues 1929-2029 (A. P. Gilmore and D. R. Critchley; unpublished observations). This would suggest that the GST/1646-2541 fusion protein is able to compete with endogenous talin for the interaction with vinculin leading to the replacement of intact talin with the fusion protein in focal contacts. The fusion proteins may also contain binding sites for other focal adhesion proteins e.g. integrins, that may also contribute to this disruptive influence.

Although the GST/2269-2541 fusion protein has also been shown to interact with vinculin, albeit weakly and only in blot overlay-type assays (Gilmore *et al.*, 1993; this thesis), it was unable to disrupt actin stress fibres and focal adhesions. As the GST/2269-2541 fusion protein was shown to also decorate actin stress fibres following microinjection into cultured cells, it would indicate that this region of talin has a greater affinity for actin stress fibres compared to vinculin and that the talin-F-actin interaction does not perturb stress fibre integrity thus preserving cytoskeletal organisation. This lack of disruption by the shorter C-terminal fusion protein may also be explained by the great abundance of actin in the cell suggesting that that even though excess quantities of fusion protein are injected into the cell they are still insufficient to overcome the endogenous talin-F-actin interaction. It is interesting to note that GST/1646-2541, which also contains this C-terminal actin-binding site, did not decorate actin stress fibres following microinjection into CEF, and was seen to disrupt stress fibre and focal adhesion integrity, suggesting that GST/1646-2541 has a greater affinity for vinculin than actin and disruption of this vinculin-talin interaction does affect focal adhesion integrity.

The experiments described above demonstrate that two anti-talin monoclonal antibodies, TA205 and TD77, recognise epitopes that span functional domains within the N- and C-terminus of talin respectively. The data suggests that a possible membrane-association site lies within the within the N-terminus of talin and an actin-binding site is present at the C-terminus of the molecule. By comparison to experiments performed on several members of the band 4.1/ERM family of proteins, it would appear that a membrane-interaction site is a common feature of the N-terminus of the proteins, and an actin-binding site is a common feature of the C-terminus. As described in the next section, an actin-binding site is confirmed within the C-terminal 272 residues of talin.

Identification of binding partners for the N- and C-terminal talin fusion proteins.

The above results demonstrate that talin amino acids 102-497 and 2269-2541 contain functional domains, it was important to determine whether these regions represent binding sites for another cytoskeletal protein. Using a blot overlay type-assay, the C-terminal fusion proteins (GST/1646-2541, GST/2269-2541), and the longer of the two N-terminal proteins, (GST/102-656) all recognised a protein that co-migrated with vinculin. Incubations with GST/102-497 or GST alone did not appear to bind vinculin even though vinculin was subsequently detected on these filters with the V284 anti-vinculin antibody. The result of this blot overlay-type assay are consistent with similar experiments carried out by Gilmore *et al.*, (1993). Unfortunately, no other bands were identifiable in this assay as there was quite a high background due to several lower molecular weight degradation fragments of vinculin. With hindsight, it is perhaps surprising that a band corresponding to actin at approximately 45kDa, was not seen on the filters probed with either of the C-terminal fusion proteins, as experiments confirming an interaction between these fusion proteins and actin is described later in the chapter. It is possible that the binding site for talin within actin is destroyed by the denaturing conditions used in the assay, or that the actin was not present in an appropriate conformation.

It is disappointing that no binding partners were identified for the N-terminal fusion protein GST/102-497 recognised by the TA205 monoclonal antibody, as this region does contain a site important to talin function. The results obtained here, and from other groups indicate that this region is involved in a membrane interaction. It is possible that any binding site recognised by the fusion protein was destroyed by the denaturing conditions under which the blot overlay assay was carried out. The method used to prepare the cell lysates may also have affected the assay. Following solubilization of the cell monolayer in RIPA buffer, the lysates were spun to pellet any insoluble debris and it is possible that the

discarded debris may have also contained possible binding partners for this region. Experiments carried out by Dr. R. Hynes using the yeast 2-hybrid system have also failed to identify any binding partner for the GST/102-656 fusion protein (personal communication, R. Hynes). However, immune precipitation experiments carried out using a GST fusion protein spanning the N-terminal region of the merlin/schwannomin protein, which shares homology to the N-terminal regions of other members of the band 4.1/ERM family, revealed at least two proteins that were capable of interacting with this domain (Takeshima *et al.*, 1994). Unfortunately, the authors have not yet investigated the nature or identy of either of these two proteins.

An actin-binding site is contained within residues 2269-2541 at the C-terminus of talin.

The actin-talin interaction was initially demonstrated by (Muguruma *et al.*, 1990). Further experiments by Kaufmann *et al.*, (1991) and Muguruma *et al.*, (1992) confirmed that talin also played a role in promoting actin nucleation, and can increase the rate of actin polymerisation. This C-terminal region of talin displays limited sequence identity to the recently identified yeast actin-binding protein Sla2p (Holtzman *et al.*, 1994), and has a similar cellular distribution to the C-terminal actin-binding site of ezrin (Algrain *et al.*, 1993b; Turunen *et al.*, 1994). With these results in mind, and from our own observations following microinjection of the talin fusion proteins, the two C-terminal fusion proteins GST/1646-2541 and GST/2269-2541 were used in an actin cosedimentation assay. Both C-terminal fusion proteins were able to pellet in the presence of actin compared to GST alone confirming that the GST moiety of the talin fusion protein was not responsible for the actin-binding capacity of either fusion protein.

It was important to ascertain whether the anti-talin monoclonal antibody TD77 was able to block the ability of the fusion protein to pellet with the F-actin and the cosedimentation

experiments were repeated in the presence of actin only, following a prior incubation of each of the fusion proteins with an excess of antibody TD77. Unfortunately TD77 did not appear to completely inhibit the binding of GST/1646-2541 to actin, as some of the fusion protein was still seen in the pellet. This could be explained by the possibility that the fusion protein has a greater affinity for the actin rather than the TD77 antibody, or that the antibody recognises a different epitope. It was more difficult to determine the effect the TD77 antibody had on the GST/2269-2541/actin interaction as the antibody runs with same mobility as GST/2269-2541 on the SDS-polyacrylamide gels, and it can also found in the pellet fraction. Therefore any reduction in the amount of GST/2269-2541 in the pellet was masked by the presence of TD77 antibody, making it difficult to draw any definitive conclusions from the competition experiments carried out with the TD77 antibody.

Preliminary experiments by Dr. S. McIver (MRC Molecular Biology Laboratory, Hills Road, Cambridge) have demonstrated that the N-terminal fusion protein GST/102-656 is also able to pellet with actin in a cosedimentation assay, indicating that there is possibly another actin-binding site at the N-terminal of the molecule. This is somewhat surprising as the actin cosedimentation data of Muguruma *et al.*, (1990) quite clearly demonstrates that the 47kDa fragment of talin does not interact with F-actin. However, the localisation of these N-terminal talin fusion proteins as demonstrated in this study indicated that although they were mainly associated with the detergent-soluble fraction of the cell they were seen to decorate actin stress fibres but only weakly.

5.11 Conclusions.

This study attempted to investigate the structure-function relationship of talin using a panel of previously characterised anti-talin monoclonal antibodies. Identification of two anti-functional antibodies by microinjection techniques, and from previously known epitope

112

mapping data enabled us to conclude that talin contains two functional domains, located in separate regions of the N- and C-terminal portions of the protein. Both domains were essential for the formation of focal adhesions in migrating CEF cells and could also disrupt previously-formed adhesions in non-motile MRC5 fibroblast cells. A functional site has been assigned to residues 102-497 in this study, and although no interaction with membrane components or integral membrane components was proven in this study, it seems most likely that it does indeed perform such a function.

An actin binding site, located in the C-terminal 272 residues of talin was demonstrated in this report. This observation, coupled with the fact that the N-terminus is proposed to interact with membrane proteins, suggests a role for talin as a key linker protein in the focal adhesion, although it is unlikely to mediate a direct link from the membrane to the actin stress fibres as there is little evidence for redundancy among the other focal adhesion proteins. Talin has also been identified as an actin-nucleating protein (Muguruma *et al.*, 1990), and it is possible that recruitment of talin to the focal adhesion, presumably through association with integrins, is a trigger for polymerisation of the actin stress fibres. The subsequent insertion of the actin stress fibres into the focal adhesion in this manner could the stabilise the focal adhesion complex and allow for recruitment of other proteins. It also seems possible that talin contains another actin-binding site at the C-terminus but this observation needs further clarification.

APPENDIX 1

CELLULAR LOCALISATION OF THE UTROPHIN
ACTIN-BINDING DOMAIN

APPENDIX 1

A collaboration between Dr. Lance Hemmings (Professor Critchley's lab). and Dr. Steve Winder (Dr. John Kendrick Jones' lab.) was directed towards identification of the actin-binding site in utrophin, a homologue of the dystrophin protein. Utrophin amino acid residues 1-261 were expressed as a GST-fusion protein by Dr. Hemmings and I subsequently microinjected this protein into CEF. The localisation pattern of the GST-fusion protein was examined by immunofluorescence in an identical manner described in Materials and Methods. The utrophin actin-binding domain was shown to localise to focal adhesions and was able to distribute along the length of actin stress fibres. Further *in vitro* experiments fully characterised the biochemical properties of the actin binding activity of the molecule. This demonstrated that the actin-binding domains from dystrophin and utrophin are functionally identical raising the possibility that the utrophin may be able to subsetitute for the defective dystrophin in DMD or BMD patients.

This work was published in January 1995 in the Journal of Cell Science and a copy of the paper follows this summary of the work. The work was also presented in poster form at the Biochemical Society Meeting, Leicester University, April 1995 and the Abstract was included in the Meeting report as detailed below.

Winder, S. J., L. Hemmings, S. K. Maciver, S. J. Bolton, J. M. Tinsley, K. E. Davies, D. R. Critchley and J. Kendrick-Jones. 1995. Utrophin actin binding domain: Analysis of F-actin and G-actin binding and cellular targeting. *J. Cell Sci.*, 108:63-71

Winder, S. J., L. Hemmings, S. J. Bolton, S. K. Maciver, J. M. Tinsley, K. E. Davies, D. R. Critchley and J. Kendrick-Jones. 1995. Calmodulin regulation of utrophin actin binding. *Biochem. Soc. Trans.*, 23:397S

Utrophin actin binding domain: analysis of actin binding and cellular targeting

S. J. Winder[1,*], L. Hemmings[2], S. K. Maciver[1], S. J. Bolton[2], J. M. Tinsley[3], K. E. Davies[3], D. R. Critchley[2] and J. Kendrick-Jones[1]

[1]Medical Research Council Laboratory of Molecular Biology, Hills Road, Cambridge CB2 2QH, UK
[2]Department of Biochemistry, University of Leicester, University Road, Leicester LE1 7RH, UK
[3]Institute of Molecular Medicine, John Radcliffe Hospital, Headington, Oxford OX3 9DU, UK

*Author for correspondence

SUMMARY

Utrophin, or dystrophin-related protein, is an autosomal homologue of dystrophin. The protein is apparently ubiquitously expressed and in muscle tissues the expression is developmentally regulated. Since utrophin has a similar domain structure to dystrophin it has been suggested that it could substitute for dystrophin in dystrophic muscle. Like dystrophin, utrophin has been shown to be associated with a membrane-bound glycoprotein complex. Here we demonstrate that expressed regions of the predicted actin binding domain in the NH2 terminus of utrophin are able to bind to F-actin in vitro, but do not interact with G-actin. The utrophin actin binding domain was also able to associate with actin-containing structures, stress fibres and focal contacts, when microinjected into chick embryo fibroblasts. The expressed NH2-terminal 261 amino acid domain of utrophin has an affinity for skeletal F-actin (K_d 19±2.8 μM), midway between that of the corresponding domains of α-actinin (K_d 4 μM) and dystrophin (K_d 44 μM). Moreover, this utrophin domain binds to non-muscle actin with a ~4-fold higher affinity than to skeletal muscle actin. These data (together with those of Matsumura et al. (1992) *Nature*, 360, 588-591) demonstrate for the first time that utrophin is capable of performing a functionally equivalent role to that of dystrophin. The NH2 terminus of utrophin binds to actin and the COOH terminus binds to the membrane associated glycoprotein complex, thus in non-muscle and developing muscle utrophin performs the same predicted 'spacer' or 'shock absorber' role as dystrophin in mature muscle tissues. These data suggest that utrophin could replace dystrophin functionally in dystrophic muscle.

Key words: actin binding, dystrophin, utrophin

INTRODUCTION

Dystrophin is a 427 kDa membrane cytoskeletal protein with sequence homologies to the spectrin family of proteins. On the basis of these sequence homologies the protein can be divided into four distinct domains: The NH2-terminal actin binding domain is separated from the COOH-terminal Ca^{2+}-binding, cysteine-rich and membrane-binding domains by a long series of spectrin-like triple-helical coiled coil repeats (Koenig et al., 1988). The protein is believed to form a flexible link between the actin cytoskeleton and the membrane and extracellular matrix via a membrane-associated glycoprotein complex. Lesions in the dystrophin gene, located on the X-chromosome, lead to the Duchenne or Becker muscular dystrophies, characterised by elevated serum creatine kinase levels and progressive muscular weakness leading to death in the case of Duchenne patients, usually by the third decade. The absence of sufficient functional dystrophin in muscle fibres results in disruptions to the cell membranes and consequent necrosis and loss of function (Emery, 1987).

Utrophin is a 395 kDa protein with considerable sequence homology to dystrophin (Tinsley et al., 1992). On the basis of this sequence homology, it has been predicted that utrophin, like dystrophin, is able to interact with the actin-based cytoskeleton via its NH2 terminus and is anchored at the inner membrane leaflet by a dystrophin-associated glycoprotein complex (DAG). Unlike dystrophin, the utrophin gene is located on chromosome 6 (Love et al., 1989) and may be able to replace dystrophin functionally, thus presenting a unique opportunity for potential treatment of sufferers of muscular dystrophy. Utrophin is present in normal muscle, in brain, at the neuromuscular junctions of normal and dystrophic muscle, in the muscles and other tissues of the *mdx* and *dy* mice and in several cultured cell lines (Nguyen thi Man et al., 1991, 1992; Khurana et al., 1992; Ohlendieck et al., 1991; Pons et al., 1991; Love et al., 1991). Furthermore, like dystrophin, immunohistochemical studies reveal that utrophin is localised to the membrane (Khurana et al., 1992; Nguyen thi Man et al., 1991, 1992) and is associated with a glycoprotein complex, comprising subunits that are antigenically indistinguishable from those of the

dystrophin-associated glycoprotein complex (Matsumura et al., 1992). Utrophin, therefore, is ideally suited to act as a functional replacement for dystrophin in dystrophic tissues. In developing or regenerating muscle tissues, utrophin can be detected at the plasma membrane before dystrophin, with utrophin localisation becoming gradually less distinct as dystrophin levels increase (Clerk et al., 1993; Helliwell et al., 1992; Khurana et al., 1992; Takèmitsa et al., 1991). In order for utrophin to replace dystrophin functionally, it must also form a connection to the underlying actin cytoskeleton. The expressed NH$_2$-terminal domains of dystrophin have been shown to bind to F-actin in vitro (Hemmings et al., 1992; Way et al., 1992b). Despite considerable sequence homology (80%) between the NH$_2$ termini of dystrophin and utrophin (Tinsley et al., 1992), it has not been demonstrated that utrophin binds to actin. Since dystrophin and utrophin represent only a small fraction of total cellular protein, purification protocols for both proteins (Ervasti et al., 1991; Matsumura et al., 1993; Pons et al., 1990) have not yielded sufficient material for thorough biochemical analyses. We have, therefore, chosen to produce the NH$_2$-terminal domain of utrophin by bacterial expression. We report here the actin binding characteristics and intracellular targeting of the NH$_2$-terminal actin binding domain of utrophin.

MATERIALS AND METHODS

Expression vector constructs

The cloning, expression and purification of dystrophin residues 1-246 (DMD246) have been described previously (Way et al., 1992b). Utrophin residues 1-112 and 113-371 (designated UTR112 and UTR113-371 respectively) were expressed as non-fusion proteins using the pET vector pMW172 (Way et al., 1990). Using the 5′ utrophin clone (116 92.2; Tinsley et al., 1992) as template, a DNA fragment encoding NH$_2$-terminal residues 1-112 was produced using PCR, with a 5′ primer containing an *Nde*I site and a 3′ primer that extended the sequence by 5 nucleotides and included a TGA stop and *Hind*III site. This fragment was subcloned into the *Nde*I/*Hind*III sites of pMW172 to give pMW172/UTR112. UTR113-371 was constructed using PCR from the adjacent 5′ utrophin clone, 89.2. A 5′ primer extending the nucleotide sequence by 2 bases and an *Nde*I site, was used together with a 3′ primer to generate a construct equivalent to utrophin residues 113-484. UTR113-371 was generated by subcloning the PCR product after cleavage at *Nde*I/*Hind*III, using an endogenous *Hind*III site at residue 371, into the *Nde*I/*Hind*III sites of pMW172 to give pMW172/UTR113-371. Residues 1-261 of utrophin (UTR261), the homologous construct to DMD246 (utrophin contains a 15 amino acid insertion at the NH$_2$ terminus) was expressed as a glutathione S-transferase (GST) fusion protein in a pGEX-2 vector (Smith and Johnson, 1988). Using the 5′ human utrophin clone (89.2) as template, a DNA fragment encoding residues 114-261 was produced using PCR with a 5′ primer containing a *Bam*HI site and a 3′ primer containing an *Eco*RI site. This fragment was subcloned into the *Bam*HI/*Eco*RI sites of the pGEX-2 expression vector (pGEX-2/114-261). The 5′ human utrophin clone (116 92.2) was then used as a PCR template to produce a DNA fragment encoding NH$_2$-terminal residues 1-112. The 5′ and 3′ primers used in this case produced *Bam*HI sites on both ends of this fragment (the 3′ primer also extended the sequence by 2 nucleotides), which was then inserted into the *Bam*HI site of the pGEX-2/114-261 vector, thereby fusing the utrophin coding sequence in frame. The authenticity of the construct was determined by restriction mapping and PCR analysis across the entire utrophin coding sequence using the specific 116 92.2 5′ and 89.2 3′ primers. The junction of the two fragments produced a *Bam*HI

site and resulted in the conservative substitution of threonine residue 113 for serine. A schematic representation of the extent of the various constructs is shown beneath the alignment in Fig. 6. The fidelity of all PCR-generated constructs was verified by sequencing.

Expression and purification of dystrophin and utrophin constructs

Dystrophin residues 1-246 (DMD246) was expressed in *Escherichia coli* strain BL21(DE3) and purified as described previously (Way et al., 1992b). UTR112 and UTR113-371 were expressed in *E. coli* strain BL21(DE3) pLysS following a 2 hour induction with 0.5 mM IPTG. Both constructs expressed in low yield and were recovered from the inclusion body fraction using the procedure of Nagai et al. (1985) as described by Way et al. (1990) with the following modifications; 0.25% deoxycholate was included in all but the final washing steps and the resuspended pellets were sonicated each time in order to break up the cell debris. Final cleaned inclusion body preparations were taken up in 30 ml 20 mM Tris-HCl, pH 8.0, 1 mM EGTA, 1 mM DTT (Buffer A) plus 8 M urea. After diluting the urea concentration to 6 M with Buffer A and centrifugation at 35,000 g for 30 minutes, the supernatant fractions were applied to a column of DEAE-Sephacel, previously equilibrated in Buffer A. UTR113-371 bound to DEAE-Sephacel and was eluted with a linear gradient of NaCl from 0 to 500 mM in Buffer A. UTR112 did not bind to DEAE, the pooled flow-through fractions were applied to a column of CM-Sephadex and eluted with a linear gradient of NaCl from 0 to 500 mM in Buffer A. Suitable column fractions (as determined by SDS-PAGE) were pooled and dialysed against Buffer A containing 4 M, 2 M, 1 M and 0.5 M urea, and then into Buffer A containing 200 mM NaCl, for at least 3 hours in each buffer. UTR113-371 was finally dialysed into Buffer A at pH 9.0.

E. coli BL21(DE3) containing the pGEX/UTR261-GST plasmid were grown overnight and expression was induced by the addition of 0.5 mM IPTG for 2 hours, cells were recovered by centrifugation and lysed by lysozyme treatment. The UTR261-GST fusion protein was recovered from the supernatant fraction of cellular extracts and purified on DEAE-Sephacel in Buffer A, as described above. The GST portion was removed from UTR261-GST by thrombin digestion (1:2000, 21 hours at 37°C) in Buffer A containing 2.5 mM CaCl$_2$. The digest was dialysed against Buffer A and centrifuged at 25,000 g for 10 minutes before being applied to DEAE-Sephacel in Buffer A as described above. All purified expressed proteins were subjected to gel filtration chromatography on Sephacryl S-200 to obtain a monomeric fraction, concentrated on Amicon Diaflo PM10 membranes or Centricon 10 micro-concentrators (where necessary) and clarified by centrifugation at 424,000 g for 15 minutes. Protein concentrations were calculated from A_{280} values using extinction coefficients for cysteine, tryptophan and tyrosine (Mach et al., 1992). ε_{280} M^{-1} cm^{-1} values for expressed constructs are: DMD246, 51,988; UTR112, 7,020; UTR113-371, 40,774; UTR261, 39,160. UTR261-GST and GST alone, for use in microinjection studies, were expressed and purified essentially as described by Smith and Johnson (1988): overnight cultures of pGEX-2/UTR261 in *E. coli* strain MC1061 were diluted 1:10 and following a further incubation (1 hour at 37°C), expression was induced by the addition of IPTG (0.1 mM). After a further 3 hours at 37°C, cells were harvested, lysed, and the protein was isolated by binding to glutathione agarose beads. Purified protein was eluted in 10 mM Tris-HCl, pH 7.0, 10 mM NaCl, 5 mM reduced glutathione, suitable for direct microinjection. Protein concentrations were determined by A_{280} as described above. Protein purity was checked on SDS-PAGE and determined to be >98% in all cases.

Actin purification

Rabbit skeletal muscle actin was prepared from acetone powder (MacLean-Fletcher and Pollard, 1980) as described by Maciver et al. (1991), with some further modifications. Acetone powder was extracted only once before centrifugation and filtration. Once filtered

the solution was adjusted to 2 mM $MgCl_2$ and 0.8 M KCl and stirred slowly for 30 minutes at 4°C. Resulting F-actin was recovered by centrifugation (96,000 g, 4°C for 2 hours) before dialysis against 3 changes of G buffer (2 mM Tris-HCl, pH 8.0, 0.2 mM ATP, 0.5 mM DTT, 0.2 mM $CaCl_2$, 1 mM NaN_3) over three days. G-actin was clarified by centrifugation, as described above, and applied to a column of Sephacryl S-200 in the same buffer. The peak and trailing fractions were pooled and concentration was determined by ε_{290} = 0.0264 μM^{-1} cm^{-1}. Pyrene-labelled skeletal G-actin was prepared as described by Pollard (1984). Non-muscle actin was prepared from expired human platelets (East Anglia Blood Transfusion Service, Cambridge, UK). Approximately 20 g of packed platelets were stirred on ice for 15 minutes in acetone containing 1 mM PMSF. Platelets were filtered through Whatman no. 41 filter paper and washed 3 times with 30 ml of ice-cold acetone each time. After the final wash, the platelets were dried overnight, weighed, and processed as for skeletal actin, described above. Minor contaminants in the final platelet actin preparation contributed significantly to A_{290} measurements, platelet actin concentration therefore, was determined by densitometric scanning (Molecular Dynamics Computing Densitometer 300A) of platelet actin and known concentrations of skeletal muscle actin on SDS-polyacrylamide gels.

F-actin binding assays

F-actin binding was assessed by sedimentation in a Beckman TL100 benchtop ultracentrifuge (15 minutes, 386,000 g, 4°C), using ~12 μM F-actin in 20 mM Tris-HCl, pH 8.0, 100 mM NaCl, 2 mM $MgCl_2$, 1 mM ATP, 1 mM DTT and either 0.1 mM $CaCl_2$ or 1 mM EGTA (Winder and Walsh 1990). For actin binding experiments with UTR113-371, NaCl was omitted and the pH increased to 9.0 to prevent precipitation of UTR113-371. Data were quantified by volume integration of SDS-polyacrylamide gels on a Molecular Dynamics 300A scanning densitometer. The amount of protein bound to actin was calculated from the known concentrations of proteins in the assay and the ratios of each protein in the supernatant and pellet, with corrections for trapping, as described previously (Way et al., 1992a,b). Statistical analysis was by Student's t-test. Falling-ball viscometry was performed as described by MacLean-Fletcher and Pollard (1980). Final F-actin concentrations of 5 μM and 10 μM were used to examine the effects of increasing concentrations of UTR261 on severing and crosslinking of actin filaments respectively.

Actin polymerisation assays

The effect of UTR261 on actin polymerisation kinetics was measured by observing the change in pyrene-labelled actin fluorescence during polymerisation of 7.5 μM G-actin in the presence or absence of 15 μM UTR261. Polymerisation was initiated by the addition of KCl, $MgCl_2$ and EGTA to 50 mM, 0.1 mM and 0.1 mM, respectively. Fluorescence was monitored in a Perkin Elmer LS 50B Luminescence Spectrometer.

G-actin binding assays

The interaction of UTR261 with G-actin was assessed by gel filtration of 1:1 stoichiometric mixtures of UTR261 with either G-actin with ATP bound (ATP-actin) or G-actin with ADP bound (ADP-actin; Pollard, 1986) as compared to either UTR261 or G-actin alone. Gel filtration was carried out at room temperature on a Sephacryl S-200 column equilibrated with G-buffer (2 mM Tris-HCl, pH 8.0, 0.2 mM ATP, 0.5 mM DTT, 0.2 mM $CaCl_2$, 1 mM NaN_3). In a separate experiment, 0.5 mg UTR261 was first chromatographed on a Sephacryl S-200 column equilibrated with G-buffer and a second sample of UTR261 was chromatographed on a Sephacryl S-200 column equilibrated with F-buffer (G-buffer containing 50 mM KCl, 0.1 mM $MgCl_2$, 0.1 mM EGTA). Protein elution profiles were monitored at A_{280}.

Cell culture and microinjection

Chick embryo fibroblasts (CEF) were cultured in Dulbecco's Minimal Essential Medium, supplemented with 10% tryptose phosphate broth, 5% newborn calf serum and 1% chick serum. Cells were seeded on glass coverslips at least 3 days prior to injection. All coverslips were etched with a cross, to aid relocation of the injected cells. Living CEF cells were microinjected with UTR261-GST or GST essentially as described by Graessman et al. (1980). Approximately 50 cells were each injected with 10^{-10} ml (1-10% of cell volume; Kreis and Birchmeier 1982) of each protein (2 mg/ml). Following injection, cells were returned to a 37°C incubator for 40 minutes prior to fixing and immunostaining.

Immunostaining and microscopy

Cells were fixed in 3.7% formaldehyde in phosphate buffered saline (PBS: pH 7.0) and permeabilised in 0.2% Triton X-100/PBS. Cells injected with UTR261-GST or GST alone were stained with a rabbit polyclonal anti-GST antibody (a generous gift from Dr E. Moiseyeva, University of Leicester, Leicester, UK) diluted 1 in 10, and a Texas Red-labelled goat anti-rabbit secondary antibody (Amersham, UK). F-actin containing structures were visualised by staining with FITC-phalloidin (Sigma). Where cells were double stained for vinculin and UTR261-GST, a mouse monoclonal anti-vinculin antibody (V284, a generous gift from Dr J. M. Wilkinson, Wellcome Trust, London, UK), diluted 1 in 200, was used with a Texas Red-labelled sheep anti-mouse Ig secondary antibody for vinculin detection, and an FITC-labelled goat anti-rabbit Ig secondary antibody for detection of the anti-GST antibody. Endogenous α-actinin was visualised by staining with a rabbit anti-chicken smooth muscle α-actinin polyclonal antibody (Jackson et al., 1988) diluted 1 in 50, and a Texas Red-labelled goat anti-rabbit secondary antibody. All antibodies were diluted in PBS containing 0.1% bovine serum albumin and 0.02% azide and all secondary antibodies were used at a 1 in 50 dilution. Fixed and stained cells were viewed on a Bio-Rad MRC 600 confocal imaging system using a ×63 lens. Photographs were taken on Kodak Technical Pan film (50 ASA) and exposed for the same length of time for each double-labelled pair.

RESULTS

Interaction of utrophin with F-actin

The UTR261-GST fusion protein expressed in very high yield and was shown to bind F-actin. UTR261 was easily separated from the GST-fusion protein by thrombin cleavage and recovered in soluble form at high concentration. Typical yields were ~200 mg/litre of culture. The partial utrophin actin binding domain proteins (UTR112 and UTR113-371) were both recovered in soluble form from the inclusion body fraction of *E. coli* lysates. Whilst both these proteins bound to F-actin, it was only possible to partially purify UTR112 and yields were insufficient to achieve saturable binding in F-actin binding assays.

Partially purified UTR112 remained soluble following sedimentation (Fig. 1A, lane 1). UTR112 (lowest of the three bands, UTR112 was identified as the prominent 13 kDa band that appeared in the total cell lysate following IPTG induction) bound quite tightly to actin and was recovered almost entirely in the pellet fraction (Fig. 1A, lane 4) whilst co-purifying proteins remained in the supernatant. UTR113-371 was highly soluble (Fig. 1B, lane 3) and bound weakly to actin (Fig. 1B, lane 2). Densitometric analysis of SDS-polyacrylamide gels of UTR113-371 binding to actin (Fig. 1C) showed a maximum
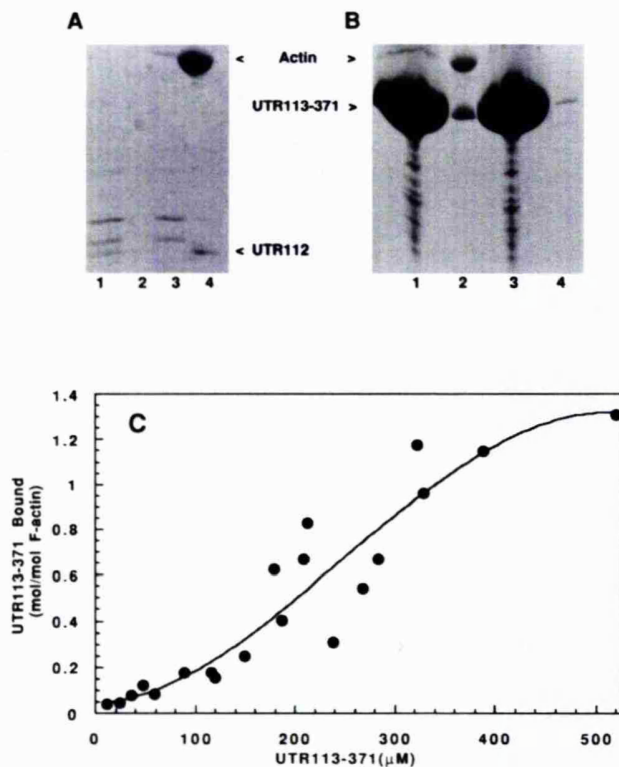
Fig. 1. Binding of UTR112 and UTR113-371 to actin. (A) 15% SDS-polyacrylamide gel of partially purified UTR112 (~20 µg/ml) subjected to sedimentation in the absence (lanes 1 and 2) and presence (lanes 3 and 4) of F-actin (13.7 µM). UTR112 is the lowest of the three prominent bands. (B) 15% SDS-polyacrylamide gel of UTR113-371 (520 µM) subjected to sedimentation in the presence (lanes 1 and 2) and absence (lanes 3 and 4) of F-actin (13.7 µM). Samples were separated by an empty lane for clarity. (C) Actin binding curves for UTR113-371 binding to F-actin in the presence of calcium. Increasing concentrations of UTR113-371 (5-520 µM) were mixed with F-actin (13.7 µM). Following a 10 minute incubation at room temperature samples were sedimented in an ultracentrifuge. Supernatant and pellet fractions were analysed by 15% SDS-PAGE and densitometry as described in Materials and Methods. Bound UTR113-371 is expressed as a molar ratio per F-actin monomer. Saturation of UTR113-371 binding to skeletal F-actin was achieved at a ratio of 1.3 UTR113-371:1 actin monomer. The affinity interpolated from 50% binding was determined to be 275 µM.

Fig. 2. Actin binding curves (main graph) and derived Scatchard plots (inset) for UTR261 binding to skeletal muscle actin (○) and to platelet actin (●). Skeletal actin (12 µM) was mixed with increasing concentrations of UTR261 from 0.1-425 µM. Platelet actin (10 µM) was mixed with UTR261 (0.1-125 µM). Following a 10 minute incubation at room temperature samples were sedimented in an ultracentrifuge. Supernatant and pellet fractions were analysed by 15% SDS-PAGE and densitometry as described previously by Way et al. (1992a). Bound UTR261 is expressed as a molar ratio per F-actin monomer. Saturation of UTR261 binding to both skeletal and platelet F-actin was achieved at a ratio of 2 UTR261:1 actin monomer (main graph). Scatchard analysis of the binding data (inset) revealed that UTR261 bound to skeletal and non muscle actins with affinities of 19±2.8 µM (R=0.79) and 5±1 µM (R=0.76), respectively.

binding of UTR113-371 to actin at ~1 mol UTR113-371/mol F-actin with an affinity (interpolated from 50% maximum binding) of 275 µM. Similar results were obtained in the presence or absence of calcium.

As determined by sedimentation assay, UTR261 bound to skeletal muscle actin in the presence of Ca^{2+}. Identical results were achieved in the absence of Ca^{2+} (presence of EGTA) as has been shown for the homologous dystrophin protein DMD246 (Way et al., 1992b). pH (range 6.0-9.0) and salt concentration (0-100 mM) had little effect on the binding of UTR261 to actin. Similarly, the binding of UTR261 and DMD246 to platelet actin were calcium-independent (data not shown). Densitometric analysis of pellet and supernatant fractions from the sedimentation assay on SDS-polyacrylamide

gels, showed maximum binding of UTR261 to both platelet and skeletal muscle actin at ~2 moles of UTR261 per mole of actin (Fig. 2). Scatchard analysis of these data (Fig. 2 inset), revealed that UTR261 bound to platelet actin with significantly ($P<0.001$) ~4-fold higher affinity (5±1 µM) than to skeletal muscle actin (19±2.8 µM). DMD246 also bound to platelet actin with ~4-fold higher affinity (13±2.3 µM) than to skeletal muscle actin (44 µM; Way et al., 1992). Whilst UTR261 bound to skeletal actin with 2.3-fold higher affinity than DMD246, it also bound to platelet actin with a 2.6-fold higher affinity than DMD246. These results suggest that utrophin has an overall greater affinity for F-actin than dystrophin.

Falling-ball viscometry of actin at either 5 µM or 10 µM in the presence of increasing concentrations of UTR261 (Fig. 3A) indicated that UTR261 did not crosslink, cap or sever actin filaments. These data are also consistent with UTR261 being unable to sequester actin monomers and as such having no effect on the critical concentration of actin.

Interaction of utrophin with G-actin

With a 2-fold molar excess of UTR261 to actin there was no significant effect of UTR261 on the polymerisation kinetics of pyrene-labelled actin (Fig. 3B). A slight increase in initial polymerisation was observed, probably a result of dimer stabilisation, as UTR261 does not bind G-actin with high affinity (see Fig. 4) or sever actin filaments (Fig. 5A). A similar effect has been reported for myosin S1 (Tawada and Oosawa, 1969).
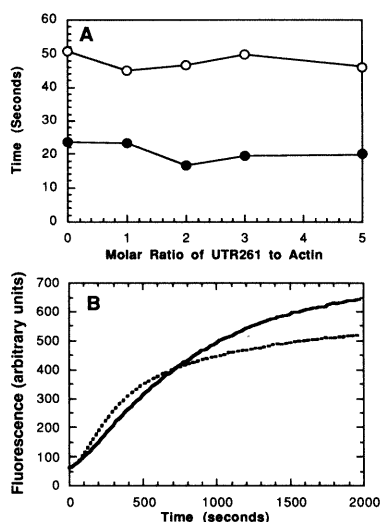
Fig. 3. Effect of UTR261 on the viscosity of F-actin (A) and on the spontaneous polymerisation of actin (B). (A) Falling-ball viscometry in 5 µM (●) or 10 µM (○) actin, polymerised in the presence of increasing molar ratios of UTR261 to actin, from 0 to 5 moles of UTR261/mole of actin. Balls were timed over 2 cm at 5 µM actin and over 1 cm at 10 µM actin. (B) The spontaneous polymerisation of actin was followed fluorimetrically by monitoring the increase in fluorescence, over time, of pyrene-labelled actin (7.5 µM) in the absence (continuous line) or presence (broken line) of a 2-fold molar excess of UTR261.

Fig. 4. Does UTR261 bind to monomeric ATP- or ADP-actin? (A) Gel filtration of G-actin (○), UTR261 (△) and mixtures of UTR261/ADP-actin (▽) and UTR261/ATP-actin (□) on Sephacryl S-200 as described in Materials and Methods. (B) UTR261 (0.5 mg) was subjected to gel filtration on a column of Sephacryl S-200 equilibrated with either G-buffer (△) or F-buffer (◊). Elution profiles were measured by absorbance at 280 nm.

Furthermore, the number of filament ends, determined by the rate of polymerisation of G-actin added at steady state, was equal in the presence or absence of UTR261 (data not shown). The decrease in polymerisation rate seen after ~700 seconds is probably due to a slight decrease in the actin monomer on rate in the presence of UTR261 (data not shown).

Although the data from falling-ball experiments (Fig. 5A) suggested indirectly that UTR261 was incapable of binding monomeric actin, we explored the possibility of a high affinity interaction between UTR261 and G-actin by gel filtration. UTR261 and G-actin ran at their true monomeric molecular masses on a calibrated column of Sephacryl S-200. If UTR261 interacted with either ATP-actin or ADP-actin, one would expect a reduction in the absorbance around fraction 23 (Fig. 4A), the UTR261 elution point, and/or a shift in the apparent actin elution point (fractions 19 and 20) to a lower fraction number. As can be seen from Fig. 4A, this was not the case for either ATP-actin or ADP-actin. The UTR261/ATP-actin elution profile showed a sharp peak at fraction 20 (actin) and a prominent shoulder at fraction 23 (UTR261) characteristic of the individual proteins. The UTR261/ADP-actin elution profile similarly showed two peaks, at fractions 20 and 23, of actin and UTR261, respectively. Furthermore, UTR261 also ran as a monomer under F-actin binding conditions (F-buffer) with only a slight shift

(1 fraction later) in elution time compared to G-buffer (Fig. 4B). Under these conditions it is clear that UTR261 does not bind to G-actin with high affinity in either its ATP-bound or ADP-bound forms and is a monomer under both G- and F-buffer conditions.

Intracellular localisation of microinjected UTR261-GST

Endogenous α-actinin was detected in CEF cells with an antibody to chicken smooth muscle α-actinin, and as expected, localised to actin-containing stress fibres and focal contacts (Fig. 5A,B; Jackson et al., 1988). CEF cells microinjected with GST alone showed no distinct targeting of GST (Fig. 5D) when compared to localisation of actin-containing structures (Fig. 5C). Cells microinjected with the UTR261-GST fusion protein and visualised with an antibody against the GST part of the molecule, showed a clear localisation of UTR261-GST to actin-containing structures. UTR261-GST was localised to actin stress fibres (Fig. 5E,F) and was also associated with focal contacts as shown by the co-localisation with vinculin (Fig. 5G,H). Vinculin staining was limited to the tips of stress fibres (Fig. 5G) in the region of the focal contacts, and UTR261-GST staining was evident down the length of the stress fibres extending to the very tip of the stress fibre in the vinculin-containing region (Fig. 5H).
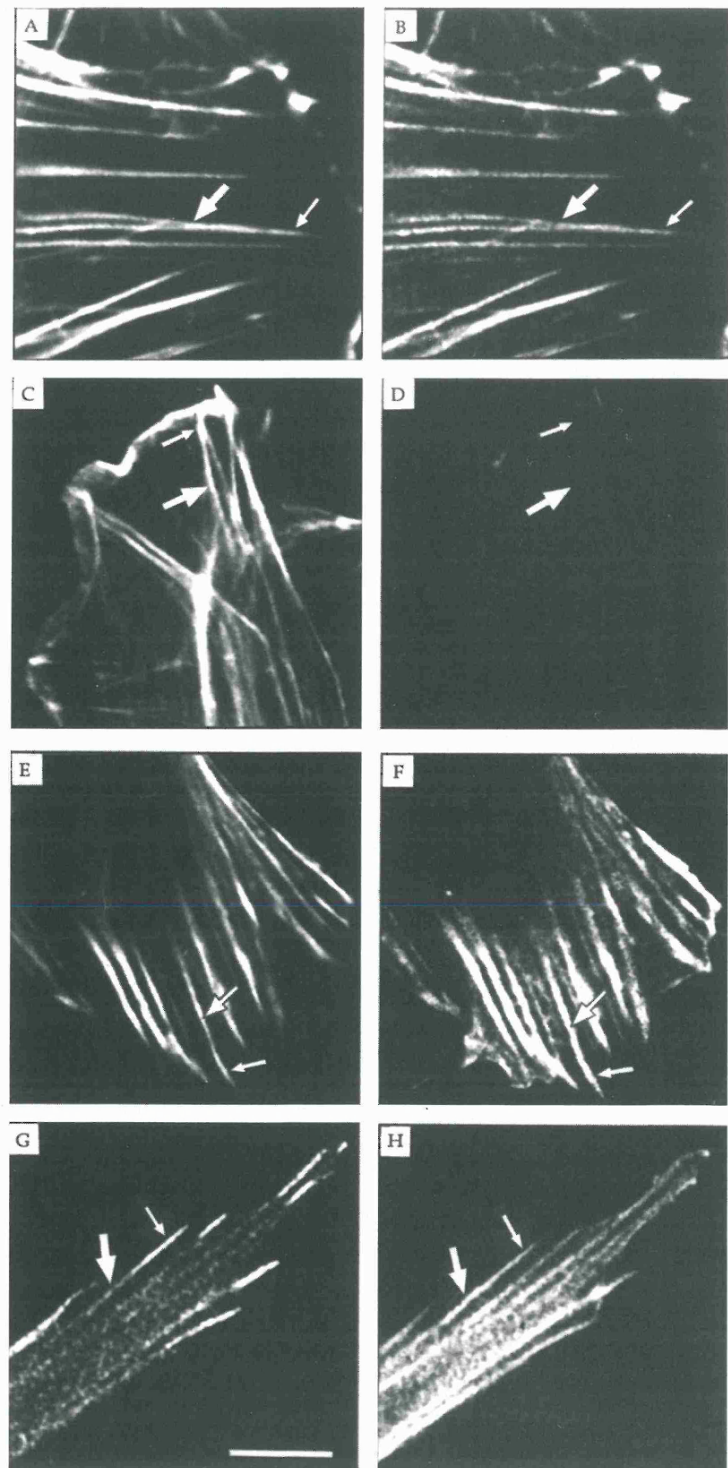
Fig. 5. Immunolocalisation of UTR261-GST fusion-protein and GST microinjected into chick embryo fibroblasts (CEF) cells. Uninjected cells were stained for actin (A) and α-actinin (B). Proteins microinjected were GST (C,D) and UTR261-GST (E-H). Injected cells were stained for GST (D) and UTR261-GST (F,H) using a rabbit anti-GST antibody. Double-staining for actin (A,C,E) and vinculin (G) was achieved using FITC-phalloidin and a monoclonal anti-vinculin antibody, respectively. Large arrows indicate the location of actin stress fibres and small arrows the location of focal contacts. Bar, 10 μm.

DISCUSSION

Binding studies using whole purified dystrophin confirmed that the native molecule does bind to actin (Ervasti and Campbell, 1993; Fabbrizio et al., 1993; Senter et al., 1993). Using molecular approaches to express regions of the NH$_2$-terminal actin binding domains of dystrophin, utrophin and α-actinin, it has been possible to localise the actin binding sites to certain regions of these domains. Fig. 6 shows a Clustal V alignment of the proposed actin binding regions of β-spectrin, α-actinin,

```
              ABS1
aac  28  AWEKQQRKTFTAWCNSHLRKAGTQ-IENIEEDFRDGLKLMLLLEVISGERLAKPERGKMR
dmd  11  EREDVQKKTFTKWVNAQFSKFGKQHIENLFSDLQDGRRLLDLLEGLTGQKLPK-EKGSTR
spc  27  EREVVQKKTFTKWVNSHLARVSCR-ITDLYKDLRDGRMLIKLLEVLSGEMLPKPTKGKMR
utr  50  EHNDVQKKTFTKWINARFSKSGKPPINDMFTDLKDGRKLLDLLEGLTGTSLPK-ERGSTR
         .*.****.**...    ..   *..*.**.*..***..*.*.*..*.*
       1 ◀.......................................................
       1 ◀━━━━━━━━━━━━━━━━━━━━━━━━━━━━━━━━━━━━━━━━━━━━━━━━━━━━━━━━━


              ABS2
aac  VHKISNVNKALDFIASKGVKLVSIGAEEIVDGNVKMTLGMIWTIILRFAIQDISV-----
dmd  VHALNNVNKALRVLQNNNVDLVNIGSTDIVDGNHKLTLGLIWNIILHWQVKNVMKNIMAG
spc  IHCLENVDKALQFLKEQRVHLENMGSHDIVDGNHRLVLGLIWTIILRFQIQDIVVQTQEG
utr  VHALNVNNRVLQVLHQNNVELVNIGGTDIVDGNHKLTLGLLWSIILHWQVKDVMKDVMSD
     .*..**..*...*  .....  .. . ***** . ..**.* .**.    ....
     ...................................◀━ ━ ━ ━ ━ ━ ━ ━ ━ ━ ━


      ABS3
aac  -EETSAKEGLLLWYQRHTAPYKNVNIQNFHISWKDXLGFCALIHRHRPELIDYGKLR-KD  201
dmd  LQQTNSEKILLSWVRQSTRNYPQVNVINFTTSWSDGLALNALIHSHRPDLFDWNSVVCQQ  191
spc  RETRSAKDALLLWCQMHTAGYPHVNVTNFTSSWKDGLAFNALIHKHRPDLIDFDKLK-DS  206
utr  LQQTNSEKILLSWVRQTTRPYSQVNVLNFTTSWTDGLAFNAVLHRHKPDLFSWDKVV-KM  229
     ...  .  ** .  .*  *..**..** .** ***.. *.. * *.*.*.
     ━ ━ ━ ━ ━ ━ ━ ━ ━ ━ ━ ━ ━ ━ ━ ━ ━ ━ ━ ━ ━ ━ ━ ━ ━ ━ ━▶371
                                                          ▶261
```

Fig. 6. Clustal V alignment (Higgins et al., 1992) of the N-terminal actin binding domains of α-actinin (aac), dystrophin (dmd), β-spectrin (spc), and utrophin (utr). Sequences were translated from DNA sequences in the EMBL database. Chicken smooth muscle α-actinin, residues 29-200 (Baron et al., 1987); human dystrophin, residues 12-190 (Koenig et al., 1988); human utrophin, residues 28-205 (Tinsley et al., 1992); human β-spectrin, residues 51-228 (Karinch et al., 1990). * Indicates identity between all four sequences and . similarity between all four sequences. The boxed regions (ABS 1-3) correspond to predicted actin binding sites referred to in the Discussion. The double-headed arrows beneath the alignment indicate the position and lengths of the utrophin constructs described in Materials and Methods. Dotted arrow, UTR112; broken arrow, UTR113-371; filled arrow, UTR261.

dystrophin and utrophin. As nomenclature of these subdomains is not consistent, we have renamed them actin binding sites (ABS) 1, 2 and 3 from NH2- to COOH-terminal, respectively. ABS1 (Levine et al., 1990, 1992; Fabbrizio et al., 1993) or the NH2 terminus of A domain (de Arruda et al., 1990) is the shortest (10 residues) but most highly conserved ABS, sharing 80% similarity between the four proteins. α-Actinin (Hemmings et al., 1992; Kuhlman et al., 1992; Way et al., 1992a), dystrophin (Fabbrizio et al., 1993) and utrophin (herein) constructs lacking this ABS are still able to bind to actin, some without any apparent reduction in affinity. ABS2 is the largest of these sites (28 residues long, 78% similarity between the four proteins) and is found in a diverse group of actin binding proteins (de Arruda et al., 1990). In *Dictyostelium* ABP-120, this site has been shown to be sufficient and necessary for actin binding (Bresnick et al., 1990, 1991). Similarly with α-actinin, both in vitro assays (Kuhlman et al., 1992; Way et al., 1992a) and transfection studies (Hemmings et al., 1992) indicate that ABS2 is essential for actin binding. Furthermore, NH2-terminal dystrophin constructs lacking this domain and ABS1 (but containing ABS3) were not able to bind to actin (Winder and Kendrick-Jones, unpublished observations). Conversely, a dystrophin-fusion protein lacking ABS2 but containing ABS1 was able to bind actin with *higher* affinity than proteins containing ABS1+ABS2 or ABS1+2+3 (Fabbrizio et al., 1993). Utrophin residues 1-112 containing ABS1 and the first eight residues of ABS2 bound to actin quite

tightly. The adjacent region (residues 113-371) comprising the COOH-terminal 20 residues of ABS2 and all of ABS3 also bound to actin but with low affinity. ABS3 (B domain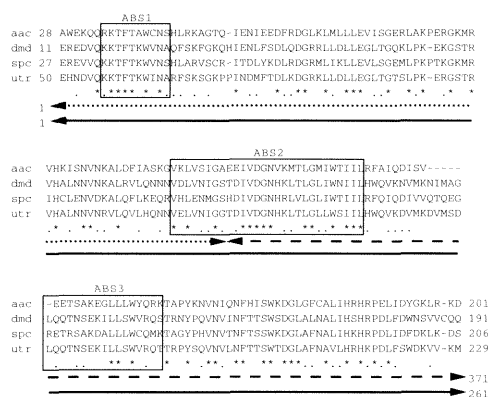; de Arruda et al., 1990; ABS2; Levine et al., 1992) is the least conserved and least studied of these domains. Peptides corresponding to this site were shown to interact with actin by proton NMR (Levine et al., 1992). A dystrophin fragment containing only ABS3 did not interact with actin (results not shown) nor did a similar region from α-actinin (Way et al., 1992a). ABS1, 2 and 3 contain a majority of basic and hydrophobic amino acids, and whilst the removal of one or other of these sites may not have a great effect on the ability of the whole domain to bind actin, each site taken in isolation appears to be able to interact with actin to some extent. It is most likely that in the folded conformation of this domain, all three sites are involved in binding to actin (Fabbrizio et al., 1993), although only elucidation of the three-dimensional structure of this or a related domain will answer these questions unequivocally. It must be remembered, however, that all the studies mentioned above, have addressed the ability of discrete domains, peptides or fusion and non-fusion proteins, to bind to actin. The affinity of the whole molecule or a higher-order multimer for actin may be much higher (or lower) than the domain in isolation.

Fabbrizio et al. (1993) have demonstrated that dystrophin ABS1 and ABS3 can be crosslinked to distinct regions on actin, whereas ABS2 was not crosslinked, suggesting a difference between the binding of α-actinin and dystrophin to actin. Utrophin binding to actin, 2 mol utrophin/mol actin, represents another difference between this closely related group of proteins. This observed stoichiometry may reflect the simultaneous binding of two distinct subdomains (only two subdomains of dystrophin are crosslinked to actin; Fabbrizio et al., 1993) from two UTR261 molecules to their respective subdomains on one F-actin monomer. The equivalent and highly similar domains of α-actinin and dystrophin bound to actin with a stoichiometry of 1:1 (Way et al., 1992a,b). UTR261 is a monomer under G-actin and F-actin salt conditions (Fig. 4B), and it is not able to crosslink actin filaments (Fig. 5A). This raises several possibilities regarding the binding and orientation of the utrophin NH2 terminus on actin. Whilst it is clear that dystrophin dimers can be seen in the EM (Pons et al., 1990; Sato et al., 1992) there is no direct evidence to suggest that these are parallel or antiparallel dimers. With two utrophin NH2 termini bound per actin, the two utrophin domains could either come from one dimer (parallel) or from two dimers (antiparallel) whose NH2 termini are in close proximity. Given, however, that the stoichiometry of two utrophins per actin was obtained under saturating binding conditions and that the binding was non-cooperative it is arguable that in vivo there may be insufficient utrophin to achieve this stoichiometry.

The demonstrated ability of the NH2 terminus of utrophin to bind to actin in vitro and in vivo is a clear indication that utrophin may be able to replace dystrophin functionally in dystrophic muscle. Utrophin is capable, via its COOH-terminal domain, of binding to an apparently identical DAG to that which dystrophin is anchored (Matsumura et al., 1992) and, via its NH2 terminus, of binding to actin. Thus, utrophin is capable of forming a direct functional link between the actin cytoskeleton and via the DAG and laminin, the extracellular matrix (Ervasti and Campbell, 1993). Several isoforms of the 59 kDa

DAG have recently been described (Adams et al., 1993; Yamamoto et al., 1993; Yang et al., 1994) with different tissue distributions, suggesting some functional diversity. Furthermore, we have now shown that homologous NH_2-terminal domains of both dystrophin and utrophin (DMD246 and UTR261, respectively) bind to platelet actin (the cytoplasmic β-isoform of actin) with an apparent ~4-fold higher affinity than to skeletal (α-isoform) actin. These data suggest that in muscle cells, dystrophin and utrophin do not form a functional link to the contractile apparatus as has been suggested (Brown and Lucy, 1993) but that the associations of dystrophin and utrophin are wholly within the submembrane cytoskeletal domain. The levels of β-actin mRNA in skeletal muscle are low and peripherally located (Kislauskis et al., 1993), i.e. in the submembrane region. Whilst β-actin protein levels may also be low, as are dystrophin and utrophin, given their respective locations in the same cellular compartment, they are likely to interact functionally. The inability of utrophin to bind to G-actin with high affinity confirms the lack of effect of utrophin in the regulation of actin polymerisation kinetics and further points to the utrophin- (and dystrophin-) actin interaction being solely structural. Utrophin and dystrophin bind to filamentous actin in the submembrane cytoskeleton as an anchor, with important regulatory events probably taking place at the utrophin/dystrophin DAG/membrane interfaces. Clearly, in non-muscle cells that contain dystrophin (neurons) and utrophin (neurons and many other cell types), there is no α-(skeletal muscle) actin isoform present and dystrophin or utrophin could only bind to the β- (cytoplasmic) isoform of actin. The higher affinity of the actin binding domains in these two proteins for the β-isoform of actin probably reflects the importance of this interaction in non-muscle cells *and* muscle cells. Mutations in the dystrophin gene leading to dysfunction of the protein result in a perturbation of this membrane cytoskeleton linkage, causing membrane damage, with consequent changes in Ca^{2+} homeostasis (McArdle et al., 1992; Turner et al., 1991) and osmotic stability (Menke and Jockusch, 1991), as well as the well documented leakage of creatine kinase from damaged muscle cells with associated necrosis and loss of function. Despite the large size of the utrophin gene (~1 Mb; Pearce et al., 1993) no lesion in this gene has yet been identified, leading to the suggestion that utrophin is essential and any mutations may be lethal (Tinsley and Davies, 1993). If a suitable muscle-specific promoter were found that could be used to up-regulate utrophin expression specifically there would be a greater chance of therapeutic intervention. To that end, these and ongoing studies will help define the precise functional roles for dystrophin and utrophin in muscle and non-muscle cells.

REFERENCES

Adams, M. E., Butler, M. H., Dwyer, T. M., Peters, M. F., Murnane, A. A. and Froehner, S. C. (1993). Two forms of mouse syntrophin, a 58 kd dystrophin-associated protein, differ in primary structure and tissue distribution. *Neuron* **11**, 531-540.

Baron, M. D., Davison, M. D., Jones, P. and Critchley, D. R. (1987). The sequence of chick α-actinin reveals homologies to spectrin and calmodulin. *J. Biol. Chem.* **262**, 17623-17629.

Bresnick, A. R., Warren, V. and Condeelis, J. (1990). Identification of a short sequence essential for actin binding by *Dictyostelium* ABP-120. *J. Biol. Chem.* **265**, 9236-9240.

Bresnick, A. R., Janmey, P. A. and Condeelis, J. (1991). Evidence that a 27-residue sequence is the actin-binding site of ABP-120. *J. Biol. Chem.* **266**, 12989-12993.

Brown, S. C. and Lucy, J. A. (1993). Dystrophin as a mechano-chemical transducer in skeletal muscle. *BioEssays* **15**, 413-419.

Clerk, A., Morris, G. E., Dubowitz, V., Davies, K. E. and Sewry, C. A. (1993). Dystrophin-related protein, utrophin in normal and dystrophic human fetal skeletal muscle. *Histochem. J.* **25**, 554-561.

de Arruda, M. V., Watson, S., Lin, C.-S., Levitt, J. and Matsudaira, P. (1990). Fimbrin is a homologue of the cytoplasmic phosphoprotein plastin and has domains homologous with calmodulin and actin gelation proteins. *J. Cell Biol.* **111**, 1069-1079.

Emery, A. E. H. (1987). *Duchenne Muscular Dystrophy*, pp. 315. Oxford University Press, Oxford.

Ervasti, J. M., Kahl, S. D. and Campbell, K. P. (1991). Purification of dystrophin from skeletal muscle. *J. Biol. Chem.* **266**, 9161-9165.

Ervasti, J. M. and Campbell, K. P. (1993). A role for the dystrophin glycoprotein complex as a transmembrane linker between laminin and actin. *J. Cell Biol.* **122**, 809-823.

Fabbrizio, E., Bonet-Kerrache, A., Leger, J. J. and Mornet, D. (1993). Actin-dystrophin interface. *Biochemistry* **32**, 10457-10463.

Graessman, A., Graessman, M. and Mueller, C. (1980). Microinjection of early SV40 DNA fragments and T antigen. *Meth. Enzymol.* **65**, 816-825.

Helliwell, T. R., Nguyen thi Man, Morris, G. E. and Davies, K. E. (1992). The dystrophin-related protein, utrophin, is expressed on the sarcolemna of regenerating human skeletal muscle fibres in dystrophies and inflammatory myopathies. *Neuromusc. Disord.* **2**, 177-184.

Hemmings, L., Kuhlman, P. A. and Critchley, D. R. (1992). Analysis of the actin-binding domain of α-actinin by mutagenesis and demonstration that dystrophin contains a functionally homologous domain. *J. Cell Biol.* **116**, 1369-1380.

Higgins, D. G., Bleasby, A. J. and Fuchs, R. (1992). Clustal-V-improved software for multiple sequence alignment. *Comput. Appl. Biosci.* **8**, 189-191.

Jackson, P., Smith, G. and Critchley, D. R. (1988). Expression of a muscle-type α-actinin cDNA clone in non-muscle cells. *Eur. J. Cell Biol.* **50**, 162-169.

Karinch, A. M., Zimmer, W. E. and Goodman, S. R. (1990). The identification and sequence of the actin-binding domain of human red blood cell β-spectrin. *J. Biol. Chem.* **265**, 11833-11840.

Khurana, T. S., Walkins, S. C., Chaffey, P., Chelly, J., Tome, F. M. S., Fardeau, M., Kaplan, J. C. and Kunkel, L. M. (1991). Immunolocalisation and developmental expression of dystrophin related protein in skeletal muscle. *Neuromusc. Disord.* **1**, 185-194.

Khurana, T. S., Watkins, S. C. and Kunkel, L. M. (1992). The subcellular distribution of chromosome 6-encoded dystrophin-related protein in the brain. *J. Cell Biol.* **119**, 357-366.

Kislauskis, E. H., Li, Z., Singer, R. H. and Taneja, K. L. (1993). Isoform-specific 3'-untranslated sequences sort α-cardiac and β-cytoplasmic actin messenger RNAs to different cytoplasmic compartments. *J. Cell Biol.* **123**, 165-172.

Koenig, M., Monaco, A. P. and Kunkel, L. M. (1988). The complete sequence of dystrophin predicts a rod-shaped cytoskeletal protein. *Cell* **53**, 219-228.

Kreis, T. E. and Birchmeier, W. (1982). Microinjection of fluorescently labeled proteins into living cells with the emphasis on cytoskeletal proteins. *Int. Rev. Cytol.* **75**, 209-227.

Kuhlman, P. A., Hemmings, L. and Critchley, D. R. (1992). The identification and characterisation of an actin-binding site in α-actinin by mutagenesis. *FEBS Lett.* **304**, 201-206.

Levine, B. A., Moir, A. J. G., Patchell, V. B. and Perry, S. V. (1990). The interaction of actin with dystrophin. *FEBS Lett.* **263**, 159-162.

Levine, B. A., Moir, A. J. G., Patchell, V. B. and Perry, S. V. (1992). Binding sites involved in the interaction of actin with the N-terminal region of dystrophin. *FEBS Lett.* **298**, 44-48.

Love, D. R., Hill, D. F., Dickson, G., Spurr, N. K., Byth, B. C., Marsden, R. F., Walsh, F. S., Edwards, Y. H. and Davies, K. E. (1989). An autosomal transcript in skeletal muscle with homology to dystrophin. *Nature* **339**, 55-58.

Love, D. R., Morris, G. E., Ellis, J. M., Fairbrother, U., Marsden, R. F., Bloomfield, J. F., Edwards, Y. H., Slater, C. P., Parry, D. J. and Davies, K. E. (1991). Tissue distribution of the dystrophin-related gene product and expression in the *mdx* and *dy* mouse. *Proc. Nat. Acad. Sci. USA* **88**, 3243-3247.

Mach, H., Middaugh, C. R. and Lewis, R. V. (1992). Statistical determination of the average values of the extinction coefficients of tryptophan and tyrosine in native proteins. *Anal. Biochem.* **200**, 74-80.

Maciver, S. K., Zot, H. G. and Pollard, T. D. (1991). Characterization of actin filament severing by actophorin from *Acanthamoeba castellanii*. *J. Cell Biol.* **115**, 1611-1620.

MacLean-Fletcher, S. D. and Pollard, T. D. (1980). Viscometric analysis of the gelation of *Acanthamoeba* extracts and purification of two gelation factors. *J. Cell Biol.* **85**, 414-428.

Matsumura, K., Ervasti, J. M., Ohlendieck, K., Kahl, S. D. and Campbell, K. P. (1992). Association of dystrophin-related protein with dystrophin-associated proteins in *mdx* mouse muscle. *Nature* **360**, 588-591.

Matsumura, K., Shasby, D. M. and Campbell, K. P. (1993). Purification of dystrophin related protein (utrophin) from lung and its identification in pulmonary artery endothelial cells. *FEBS Lett.* **326**, 289-293.

McArdle, A., Edwards, R. H. T. and Jackson, M. J. (1992). Accumulation of calcium by normal and dystrophin-deficient mouse muscle during contractile activity *in vitro*. *Clin. Sci.* **82**, 455-459.

Menke, A. and Jockusch, H. (1991). Decreased osmotic stability of dystrophin-less muscle cells from the *mdx* mouse. *Nature* **349**, 69-71.

Nagai, K., Peratz, M. and Poyart, C. (1985). Oxygen binding properties of human mutant hemoglobin synthesised in *Escherichia coli*. *Proc. Nat. Acad. Sci. USA* **82**, 7252-7255.

Nguyen thi Man, Ellis, J. M., Love, D. R., Davies, K. E., Gatter, K. C., Dickson, G. and Morris, G. E. (1991). Localization of the DMDL gene-encoded dystrophin-related protein using a panel of nineteen monoclonal antibodies: Presence at neuromuscular junctions, in the sarcolemma of dystrophic skeletal muscle in vascular and other smooth muscles, and in proliferating brain cell lines. *J. Cell Biol.* **115**, 1695-1700.

Nguyen thi Man, Le Thiet Thank, Blake, D. J., Davies, K. E. and Morris, G. E. (1992). Utrophin, the autosomal homologue of dystrophin, is widely-expressed and membrane-associated in cultured cell lines. *FEBS Lett* **313**, 19-22.

Ohlendieck, K., Ervasti, J. M., Matsumura, K., Kahl, S. D., Leveille, C. J. and Campbell, K. P. (1991). Dystrophin-related protein is localized to neuromuscular junctions of adult skeletal muscle. *Neuron* **7**, 499-508.

Pearce, M., Blake, D. J., Tinsley, J. M., Byth, B. C., Campbell, L., Monaco, A. and Davies, K. E. (1993). The utrophin and dystrophin genes share similarities in genomic structure. *Hum. Mol. Genet.* **2**, 1765-1772.

Pollard, T. D. (1984). Polymerization of ADP-actin. *J. Cell Biol.* **99**, 769-777.

Pollard, T. D. (1986). Rate constants for the reactions of ATP- and ADP-actin with the ends of actin filaments. *J. Cell Biol.* **103**, 2747-2754.

Pons, F., Augier, N., Heilig, R. and Leger, J. J. (1990). Isolated dystrophin molecules as seen by electron microscopy. *Proc. Nat. Acad. Sci. USA* **87**, 7851-7855.

Pons, F., Augier, N., Leger, J. O. C., Robert, A., Tome, F. M. S., Fardeau, M., Voit, T., Nicholson, L. V. B., Mornet, D. and Leger, J. J. (1991). A homologue of dystrophin is expressed at the neuromuscular junctions of normal individuals and DMD patients, and of normal and *mdx* mice. *FEBS Lett.* **282**, 161-165.

Sato, O., Nonomura, Y., Kimura, S. and Maruyama, K. (1992). Molecular shape of dystrophin. *J. Biochem.* **112**, 631-636.

Senter, L., Luise, M., Presotto, C., Betto, R., Teresi, A., Ceoldo, S. and Salviati, G. (1993). Interaction of dystrophin with cytoskeletal proteins: Binding to talin and actin. *Biochem. Biophys. Res. Commun.* **192**, 899-904.

Smith, D. B. and Johnson, K. S. (1988). Single-step purification of polypeptides expressed in *Escherichia coli* as fusions with glutathione S-transferase. *Gene* **67**, 31-40.

Takemitsu, M., Ishiura, S., Koga, R., Kamakura, K., Arahata, K., Nonaka, I. and Sugita, H. (1991). Dystrophin-related protein in the fetal and denervated skeletal muscles of normal and *mdx* mice. *Biochem. Biophys. Res. Commun.* **180**, 1179-1186.

Tawada, K. and Oosawa, F. (1969). Effect of the H-meromyosin plus ATP system on F-actin. *Biochim. Biophys. Acta* **180**, 199-201.

Tinsley, J. M., Blake, D. J., Roche, A., Fairbrother, U., Riss, J., Byth, B. C., Knight, A. E., Kendrick-Jones, J., Suthers, G. K., Love, D. R., Edwards, Y. H. and Davies, K. E. (1992). Primary structure of dystrophin-related protein. *Nature* **360**, 591-593.

Tinsley, J. M. and Davies, K. E. (1993). Utrophin: A potential replacement for dystrophin? *Neuromusc. Disord.* **3**, 537-539.

Turner, P. R., Fong, P., Denetclaw, W. F. and Steinhardt, R. A. (1991). Increased calcium influx in dystrophic muscle. *J. Cell Biol.* **115**, 1701-1712.

Way, M., Pope, B., Gooch, J., Hawkins, M. and Weeds, A. G. (1990). Identification of a region of segment 1 of gelsolin critical for actin binding. *EMBO J.* **9**, 4103-4109.

Way, M., Pope, B. and Weeds, A. G. (1992a). Evidence for functional homology in the F-actin binding domains of gelsolin and α-actinin: Implications for the requirements of severing and capping. *J Cell Biol.* **119**, 835-842.

Way, M., Pope, B., Cross, R. A., Kendrick-Jones, J. and Weeds, A. G. (1992b). Expression of the N-terminal domain of dystrophin in *E. coli* and demonstration of binding to F-actin. *FEBS Lett.* **301**, 243-245.

Winder, S. J. and Walsh, M. P. (1990). Smooth muscle calponin: Inhibition of the actomyosin MgATPase and regulation by phosphorylation. *J. Biol. Chem.* **265**, 10148-10155.

Yamamoto, H., Hagiwara, Y., Mizuno, Y., Yoshida, M. and Ozawa, E. (1993). Heterogeneity of dystrophin-associated proteins. *J. Biochem.* **114**, 132-139.

Yang, B., Ibraghimov-Beskrovnaya, O., Moomaw, C. R., Slaughter, C. A. and Campbell, K. P. (1994). Heterogeneity of the 59-kDa dystrophin-associated protein revealed by cDNA cloning and expression. *J. Biol. Chem.* **269**, 6040-6044.

REFERENCES

REFERENCES.

Abercrombie, M., J. E. M. Heaysman and S. M. Pegrum. 1970a. The locomotion of fibroblasts in culture. I. Movements of the leading edge. *Exptl. Cell Res.* 5 9:393-398

Abercrombie, M., J. E. M. Heaysman and S. M. Pegrum. 1970b. The locomotion of fibroblasts in culture. II. Ruffling. *Exptl. Cell Res.* 6 0:437-444

Abercrombie, M., J. E. M. Heaysman and S. M. Pegrum. 1971. The locomotion of fibroblasts in culture. IV. Electron microscopy of the leading edge. *Exptl. Cell Res.* 6 7:359-367

Abercrombie, M., and G. A. Dunn. 1975. Adhesion of fibroblasts to substratum during contact inhibition observed by interference reflection microscopy. *Exptl. Cell Res.* 9 2:57-62

Akhtar, S., S. Basu, E. Wickstrom and R. L. Juliano. 1991. Interactions of antisense DNA oligonucleotide analogs with phospholipid membranes (liposomes). *Nucl. Acids Res.* 1 9:5551-5559

Akhtar, S., and R. L. Juliano. 1992. Cellular uptake and intracellular fate of antisense oligonucleotides. *Trends Cell Biol.* 2:139-144

Algrain, M., M. Arpin and D. Louvard. 1993a. Wizardry at the cell cortex. *Curr. Biol.* 3:451-454

Algrain, M., O. Turunen, A. Vaheri, D. Louvard and M. Arpin. 1993b. Ezrin contains cytoskeleton and membrane domains accounting for its proposed role as a membrane-cytoskeletal linker. *J. Cell Biol.* 1 2 0:129-139

Anderson, R. A. and R. E. Lovrien. 1984. Glycophorin C is linked by band 4.1 protein to the human erythrocyte membrane skeleton. *Nature.* 3 0 7:655-658

Andre, E., and M. Becker-Andre. 1993. Expresion of an N-terminally truncated form of human focal adhesion kinase in brain. *Biochem. Biophys. Res. Comm.* 1 9 0:140-147.

Aoti, S., T. Nagai and K. M. Yamada. 1991. Characterisation of regions of fibronectin besides argenine-glycine-aspartic acid sequence required for adhesive function of the cell-binding domain using site-directed mutagenesis. *J. Biol. Chem.* 2 6 6:15938-15943

Arimura, C., T. Suzuki, M. Yanagisawa, M. Imamura, Y. Hamada and T. Masaki. 1988. Primary structure of chicken skeletal muscle and fibroblast α-actinins deduced from cDNA sequences. *J. Biochem.* 1 7 7:649-655

Arpin, M., M. Algrain and D. Louvard. 1994. Membrane-actin microfilament connections: an increasing diversity of players related to band 4.1. *Curr. Opin. Cell Biol.* 6:136-141

Baker, L. P., D. F. Daggett and H. B. Peng. 1994. Concentration of pp125 focal adhesion kinase (FAK) at the myotendinous junction. *J. Cell Sci.* 1 0 7:1485-1497

Baron, M. D., M. D. Davidson, P. Jones, B. Patel and D. R. Critchley. 1987. Isolation and characterisation of a cDNA encoding a chick α-actinin. *J. Biol. Chem.* 2 6 2:2558-2561

115

Barry, S. T., and D. R. Critchley. 1994. The Rho-associated assembly of focal adhesions in Swiss 3T3 cells is associated with increase tyrosine phosphorylation and the recruitment of both pp125FAK and Protein Kinase C-δ to focal adhesions. *J. Cell Sci.* 107:2033-2045

Barstead, R. J., and R. H. Waterston. 1989. The basal component of the nematode dense-body is vinculin. *J. Biol. Chem.* 264:10177-10185

Barstead, R. J., and R. H. Waterston. 1991. Vinculin is essential for muscle function in the nematode. *J. Cell Biol.* 114:715-724

Beckerle, M. C., K. Burridge, G. N. DeMartino and D. E. Croall. 1987. Colocalization of calcium-dependent protease II and one of its substrates at sites of cell adhesion.*Cell* 51:569-577

Beckerle, M. C., D. E. Miller, M. E. Bertagnolli and S. J. Locke. 1989. Activation-dependent redistribution of the adhesion plaque protein, talin, in intact human platelets. *J. Cell Biol.* 109:3333-3346

Belkin, A. M., and V. E. Koteliansky. 1987. Interaction of iodinated vinculin, metavinculin and α-actinin with cytoskeletal proteins. *Fed.Eur.Biochem.Soc.Letts.* 220:291-294

Bellas, R. E., R. Bendori and S. R. Farmer. 1991. Epidermal growth factor activation of vinculin and β1 integrin gene transcription in quiescent Swiss 3T3 cells. *J. Biol. Chem.* 266:12008-12014

Bendori, R., D. Salomon and B. Geiger. 1989. Identification of two distinct functional domains on vinculin involved in its association with focal contacts. *J. Cell Biol.* 108:2382-2393

Ben-Ze'ev, A., R. Reiss, R. Bendori and B. Gorodecki. 1990. Transient induction of vinculin gene expression in 3T3 fibroblasts stimulated by serum growth factors. *Cell Regul.* 1:621-636

Bertagnolli, M. E., S. J. Locke, M. E. Hensler, P. F. Bray and M. C. Beckerle. 1993. Talin distribution and phoshorylation in thrombin-activated platelets. *J. Cell Sci.* 106:1189-1199

Berton, G., L. Fumagalli, C. Laudanna and C. Sorio. 1994. β2 integrin-dependent protein tyrosine phosphorylation and activation of the FGR protein tyrosine kinase in human neutrophils. *J. Cell Biol.* 126:1111-1121

Blanchard, A., V. Ohanion and D. R. Critchley. 1989. The structure and function of α-actinin. *J. Muscle Res. Cell Motil.* 10:280-289

Bockholt, S. M., C. A. Otey, J. R. Glenney and K. Burridge. 1992. Localization of a 215-kDa tyrosine-phosphorylated protein that cross-reacts with tensin antibodies. *Exptl. Cell Res.* 203:39-46

Bockholt, S. M., and K. Burridge. 1993. Cell spreading on extracellular matrix proteins induces tyrosine phosphorylation of tensin. *J. Biol. Chem.* 268:14565-14567

116

Bodary, S. C., T. Lipari, C. Muir, M. Napier, R. Pitti and J. W. McLean. 1991. Deletion of cytoplasmic and transmembrane domains of GPIIIb-IIa results in a functional receptor. *J. Cell Biol.* 115:289a (abstract)

Boiziau,C., N. T. Thuong and J.-J. Toulme. 1992. Mechanisms of the inhibition of reverse transcription by antisense oligonucleotides. *Proc. Natl. Acad. Sci. USA.* 89:768-772

Brands, R., A. De Boer, C. A. Feltkamp and E. Roos. 1990. Disintegration of adhesion plaques in chicken embryo fibroblasts upon Rous Sarcoma Virus-induced transformation: different dissociation rates for vinculin and talin. *Exptl. Cell Res.* 186:138-148

Burridge, K., and J. R. Feramsico. 1980. Microinjection and localization of a 130k protein in living fibroblasts: A relation ship to actin and fibronectin. *Cell.* 19:587-595

Burridge, K., and J. R. Feramisco. 1981. Non-muscle α-actinins are calcium-sensitive actin-binding proteins. *Nature.* 294:565-567

Burridge, K., and L. Connell. 1983a. A new protein of adhesion plaques and ruffling membranes. *J. Cell Biol.* 97:359-367

Burridge, K., and L. Connell. 1983b. Talin: A cytoskeletal component concentrated in adhesion plaques and other sites of actin-membrane interaction. *Cell Motility.* 3:405-417

Burridge, K., and P. Mangeat. 1984. An interaction between vinculin and talin. *Nature.* 308:744-745

Burridge, K., K. Fath, T. Kelly, G. Nuckolls and C. Turner. 1988. Focal adhesions: Transmembrane junctions between the extracellular matrix and the cytoskeleton. *Ann. Rev. Cell Biol.* 4:487-525

Burridge, K., C. E. Turner and L. H. Romer. 1992. Tyrosine phosphorylation of paxillin and pp125FAK accompanies cell adhesion to extracellular matrix: A role in cytoskeletal assembly. *J. Cell Biol.* 119:893-903

Chang, L-J., and C. M. Stoltzfus. 1985. Gene expression from both intronless and intron-containing rous sarcoma virus clones is specifically inhibited by anti-sense RNA. *Mol. Cell Biol.* 5:2341-2348

Chang, L-J., and C. M. Stoltzfus. 1987. Inhibition of rous sarcoma virus replication by antisense RNA. *J.Virol.* 61:921-924

Chen, H-C., and J-L Guan. 1994. Association of focal adhesion kinase with its potential substrate phosphatidylinositol 3-kinase. *Proc. Natl. Acad. Sci. USA.* 91:10148-10152

Chen, Q., M. S. Kinch, T. H. Lin, K. Burridge and R. L. Juliano. 1994. Integrin-mediated cell adhesion activates mitogen-activated protein kinases. *J. Biol. Chem.* 269:26602-26605

Chrzanowska-Wodnicka, M., and K. Burridge. 1994. Tyrosine phosphorylation is involved in reorganisation of the actin cytoskeleton in response to serum or LPA stimulation. *J, cell Sci.* 107: 3643-3654

117

Chiang, M.-Y., H. Chan, M. A. Zounes, S. M. Freier, W. F. Lima and C. F. Bennett. 1991. Antisense oligonucleotides inhibit intercellular adhesion molecule 1 expression by two distinct mechanisms. *J. Biol. Chem.* 266:18162-18171

Chomczynski, P., and N. Sacchi. 1987. Single-step method for isolation by acid guanidium thiocyanate-phenol-chloroform extraction. *Analyt. Biochem.* 162:156-159

Collier, N. C., and K. Wang. 1982. Purification and properties of human platelet P235. *J. Biol. Chem.* 257:6937-6943

Colman, A. 1990. Antisense strategies in cell and developmental biology. *J. Cell Sci.* 97:399-409

Couchman, J. R., and D. A. Rees. 1979. The behaviour of fibroblasts migrating from chick heart explants: changes in adhesion, locomotion and growth, and in the distribution of actomyosin and fibronectin. *J. Cell Sci.* 39:149-165

Couchman, J. R., D. A. Rees, M. R. Green and C. G. Smith. 1982. Fibronectin has duel role in locomation and anchorage of primary chick fibroblasts and can promote entry into the division cycle. *J. Cell Biol.* 93:402-410

Coutu, M. D., and S. W. Craig. 1988. cDNA-derived sequence of chicken embryo vinculin. *Proc. Natl. Acad. Sci. USA.* 85:8535-8539

D'Souza, S. E., M. H. Ginsberg, T. A. Burke and E. F. Plow. 1990. The ligand binding site of the platelet integrin receptor GPIIb-IIIa is proximal to the second calcium binding domain of its α subunit. *J. Biol. Chem.* 265:3440-3446

Damsky, C. H., and Z. Werb. 1992. Signal transduction by integrin receptors for extracellular matrix: cooperative processing of extracellular information. *Curr. Opin. Cell Biol.* 4:772-781

Danilov, Y. N., and R. L. Juliano. 1989. Phorbol ester modulation of integrin-mediated cell adhesion: A postreceptor event. *J. Cell Biol.* 108:1925-1933

DeClue, J. E., and G. S. Martin. 1987. Phosphorylation of talin at tyrosine in Rous Sarcoma virus-transformed cells. *Mol. Cell. Biol.* 7:371-378

DePasquale, J. A., and C. S. Izzard. 1991. Accumulation of talin in nodes at the edge of the lamellipodium and separate incorporation into adhesion plaques at focal contacts in fibroblasts. *J. Cell Biol.* 113:1351-1359

Dietrich, C., W. H. Goldmann, E. Sackmann and G. Isenberg. 1993. Interaction of NBD-talin with lipid monolayers. *Fed. Eur. Biochem. Soc. Letts.* 324: 37-40

Dike, L. E., and S. R. Farmer. 1988. Cell adhesion induces expression of growth-associated genes in suspension-arrested fibroblasts. *Proc. Natl. Acad. Sci. U.S.A.* 85:6792-6796

Discher, D., M. Parra, J. G. Conboy and N. Mohandas. 1993. Mechanochemistry of the alternatively spliced spectrin-actin binding domain in membrane skeletal protein 4.1. *J. Biol. Chem.* 268:7186-7195

Elices, M. J., and M. E. Hemler. 1989. The human integrin VLA-2 is a collagen receptor on some cells and a collagen/laminin receptor on others. *Proc. Natl. Acad. Sci. USA.* 86:9906-9910

Elices, M. J., L. A. Urry and M. E. Hemler. 1991. Receptor functions for the integrin VLA-3: fibronectin, collagen and laminin binding are differentially regulated by Arg-Gly-Asp peptide and divalent cations. *J. Cell Biol.* 112:169-181

Evans, R. R., R. M. Robson and M. H. Stromer. 1984. Properties of smooth muscle vinculin. *J. Biol. Chem.* 259:3916-3924

Feinberg, A. P., and B. Vogelstein. 1983. A technique for radio-labeling DNA restriction endonuclease fragments to high specific activity. *Anal. Biochem.* 132:6-13

Felgner, P. L., T. R. Gadek, M. Holm, R. Roman, H. W. Chan, M. Wenz, J. P. Northrop, G. M. Ringold and M. Danielsen. 1987. Lipofectin: A highly efficient, lipid-mediated DNA-transfection procedure. *Proc. Natl. Acad. Sci. USA.* 84:7413-7417

Francis, G. R., and R. H. Waterston. 1985. Muscle organisation in *Caenorhabditis elegans*: localisation of proteins implicated in thin filament attachment and I-band organisation. *J. Cell Biol.* 101:1532-1549

Freyd, G., S. K. Kim and H. R. Horvitz. 1990. Novel cysteine-rich motif and homeodomain in the product of the *Ceanorhabitis elegans* cell lineage gene lin-11. *Nature.* 344:876-879

Fukami, K., T. Endo, M. Imamura and T. Takenawa. 1994. Alpha-actinin and vinculin are PIP2-binding proteins involved in signalling by tyrosine kinase. *J. Biol. Chem.* 299:1519-1522

Funayama, N., A. Nagafuchi, N. Sato, S. Tsukita and S. Tsukita. 1991. Radixin is a novel member of the band 4.1 family. *J. Cell Biol.* 115:1039-1048

Geiger, B. 1979. A 130k protein from chicken gizzard: its localization at the termini of microfilament bundles in cultured chicken cells. *Cell.* 18:193-205

Geiger, B. 1981. Microheterogeneity of avian and mammalian vinculin. *J. Mol. Biol.* 159:685-701.

Geiger, B., and S. J. Singer. 1979. The participation of a-actinin in the capping of the cell membrane components. *Cell.* 16:213-222

Geiger, B., T. Volk and T. Volberg. 1985. Molecular hetergeneity of adherens junctions. *J. Cell Biol.* 101:1523-1531

Giancotti, F. G., and E. Ruoslahti. 1990. Elevated levels of the a5b1 fibronectin receptor suppress the transformed phenotype of chinese hamster ovary cells. *Cell.* 60:849-859

119

Gilmore, A. P., P. Jackson, G. T. Waites and D. R. Critchley. 1992. Further characterisation of the talin-binding site in the cytoskeletal protein vinculin. *J. Cell Sci.* 103:719-731

Gilmore, A. P., C. Wood, V. Ohanion, P. Jackson, B. Patel, D. J. G. Rees, R. O. Hynes and D. R. Critchley. 1993. The cytoskeletal protein talin contains at least two distinct vinculin binding domains. *J. Cell Biol.* 122:337-347

Gilmore, A. P., V. Ohanion, N. K. Spurr and D. R. Critchley. 1995. Localisation of the human gene encoding the cytoskeletal protein talin to chromosome 9p. *Hum. Genetics.* in press

Girard, F., U. Strausfeld, A. Fernandez and N. J. C. Lamb. 1991. Cyclin A is required for the onset of DNA replication in mammalian fibroblasts. *Cell,* 67:1169-1179

Glenney, J. R., and L. Zokas. 1989. Novel tyrosine kinase substrates from Rous Sarcome Virus-transformed cells are present in the membrane skeleton. *J. Cell Biol.* 108:2401-2408

Goldmann, W. H., V. Niggli, S. Kaufmann and G. Isenberg. 1992. Probing actin and liposome interaction of talin and talin-vinculin complexes: A kinetic, thermodynamic and lipid labeling study. *Biochem.* 31: 7665-7671

Goldmann, W. H., A. Bremer, M. Haner, U. Aebi and G. Isenberg. 1994. Native talin is a dumbbell-shaped homodimer when it interacts with actin. *J. Struct. Biol.* 112:3-10

Gould, K. L., A. Bretscher, F. S. Esch and T. Hunter. 1989. cDNA cloning and sequencing of the protein tyrosine linase substrate, ezrin, reveals homology to band 4.1. *EMBO J.* 8:4133-4142

Graessmann, A., M. Graessmann and C. Mueller. 1980. Microinjection of Early SV40 DNA fragemtns and T antigen. *Methods Enzymol.* 65:816-825

Green, A. R., E. DeLuca and C. G. Begley. 1991. Antisense SCL suppresses self-renewal and enhances spontaneous erythroid differentiation of the human leukaemic cell line K562. *Eur. Mol. Bio. Org. J.* 10:4153-4158

Gu, M., J. D. York, I. Warshawsky and P. W. Majerus. 1991. Identification, cloning and expression of a cytosolic megakaryocyte protein-tyrosine-phosphatase with sequence homolgy to cytoskeletal protein 4.1. *Proc. Natl. Acad. Sci. USA.* 88:5867-5871

Guan, J.-L., and D. Shalloway. 1992. Regulation of focal adhesion-associated protein tyrosine kinase by both cellular adhesion and oncogenic transformation. *Nature.* 358:690-692

Guinebault, C., B. Payrastre, C. Sultan, G. Mauco, M. Breton, S. Levy-Toledano, M. Plantavid and H. Chap. 1993. Tyrosine kinases and phosphoinositide metabolism in thrombin-stimulated human platelets. *Biochem. J.* 292:851-856

Hanks, S. K., M. B. Calab, M. C. Harper and S. K. Patel. 1992. Focal adhesion protein-tyrosine kinase phosphorylation in response to cell attachment to fibronectin. *Proc. Natl. Acad. Sci. USA.* 89:8487-8491

120

Hayashi, Y., B. Haimovich, A. Reszka, D. Boettiger and A. Horwitz. 1990. Expression and function of chicken integrin β1 subunit and its cytoplasmic domain mutants in mouse NIH 3T3 cells. *J. Cell Biol.* **110**:175-184

Hayashi, Y., T. Iguchi, T. Kawashima, Z. Bao Z, C. Yacky, D. Boettiger and A. F. Horwitz. 1991. Repression of integrin β1 subunit expression by antisense RNA. *Cell Struc. Funct.* **16**:241-249

Heise, H., T. Bayerl, G. Isenberg and E. Sackmann, 1991. Human platelet P235, a talin-like actin binding protein binds selectively to mixed lipid layers. *Biochem. et Biophysica Acta.* **1061**:121-131

Helene, C. 1991. Rational design of sequence-specific oncogene inhibitors based on antisense and antigene oligonucleotides. *Eur. J. Cancer.* **27**:1466-1471

Hemmings, L., P. A. Kuhlman and D. R. Critchley. 1992. Analysis of the actin-binding domain of α-actinin by mutagenesis and demonstration that dystrophin contains a functionally homologous domain. *J. Cell Biol.* **116**:1369-1380

Herman, B., and W. J. Pledger. 1985. Platelet-derived growth factor-induced alterations in vinculin and actin distribution in Balb/c 3T3 cells. *J. Cell Biol.* **100**:1031-1040

Herman, B., M. A. Harrington, N. E. Olashaw and W. J. Pledger. 1986. Identification of the cellular mechanisms responsible for platelet-derived growth factor induced alterations in cytoplasmic vinculin distribution. *J. Cell Physiol.* **126**:115-125

Hildebrand, J. D., M. D. Schaller and J. T. Parsons. 1993. Identification of sequences required for efficient localization of the focal adhesion kinase, pp125FAK, to cellular focal adhesions. *J. Cell Biol.* **123**:993-1005

Hirst, R., A. Horwitz, C. Buck and L. Rohrschneider. 1986. Phosphorylation of the fibronectin receptor complex in cells transformed by oncogenes that encode tyrosine kinases. *Proc. Natl. Acad. Sci.USA.* **83**:6470-6474

Hitt, A. L., and E. J. Luna. 1994. Membrane interactions with the actin cytoskeleton. *Curr. Opin. Cell Biol.* **6**:120-130

Hock, R. S., J. M. Sanger and J. W. Sanger. 1989. Talin dynamics in living microinjected non-muscle cells. *Cell Motil. Cytoskel.* **14**:271-287

Holt, J. T., T. V. Gopal, A. D. Moulton and A. W. Nienhuis. 1986. Inducible production of c-fos antisense RNA inhibits 3T3 cell proliferation. *Proc. Natl. Acad. Sci. USA.* **83**:4794-4798

Holtzman, D. A., S. Yang and D. G. Drubin. 1993. Synthetic-lethal interactions identify two novel genes SLA1 and SLA2, that control membrane cytoskeletal assembly in Saccharomyces cerevisiae. *J. Cell Biol.* **112**:635-644

Horvath, A. R., M. A. Elmore and S. Kellie. 1990. Differential tyrosine-specific phosphorylation of integrin in Rous sarcoma virus transformed cells with a differing transformed phenotype. *Oncogene.* **5**:1349-1357

121

Horwitz, A., K. Duggan, C. Buck, M. C. Beckerle and K. Burridge. 1986. Interaction of plasma membrane fibronectin receptor with talin - a transmembrane linkage. *Nature.* 320:531-533

Housey, G. M, M. D. Johnson, W. L. W. Hsiao, C. A. O'Brian, J. P. Murphy, P. Kirschmeier and I. B. Weinstein. 1988. Overproduction of protein kinase C causes disordered growth control in rat fibroblasts. *Cell.* 52:343-354.

Huang, M.-H., L. Lipfert, M. Cunningham, J. S. Brugge, M. H. Ginsberg and S. J. Shattil. 1993. Adhesive ligand binding to integrin αIIbβ3 stimulates tyrosine phosphorylation of novel protein substrates before phosphorylation of pp125FAK. *J. Cell Biol.* 122:473-483

Humphries, M. J., S. K. Akiyama, A. Komoriya, K. Olden and K. M. Yamada. 1986. Identification of an alternately spliced adhesion site in human plasma fibronectin that possessess cell-type specificity. *J. Cell Biol.* 103:2637-2647

Humphries, M. J., A. Komoriya, S. K. Akiyama, K. Olden and K. M. Yamada. 1987. Identification of two distinct regions of the type III connecting segment of human plasma fibrinogen that promote cell type-specific adhesion. *J. Biol. Chem.* 262:6886-6892.

Humphries, M. J. 1990. The molecular basis and specificity of integrin-ligand interactions. *J. Cell Sci.* 97:585-592

Hynes, R. O. 1973. Alteration of cell-surface proteins by viral transformation and by proteolysis. *Proc. Natl. Acad.Sci. USA.* 70:3170-3174

Hynes, R. O. 1987. Integrins: A family of cell surface receptors. *Cell.* 48:549-554
Hynes, R. O., and A. D. Lander. 1992. Contact and adhesive specificities in the associations, migrations and targeting of cells and axons. *Cell.* 68:303-322

Hynes, R. O. 1992. Integrins: Versatility, modulation and signalling in cell adhesion. *Cell.* 69:11-25

Isenberg, G., K. Leonard and B. M. Jockusch. 1982. Structural aspects of vinculin-actin interaction. *J. Mol. Biol.* 158:231-249

Izant, J. G., and H. Weintraub. 1984. Inhibition of thymidine kinase gene expression by anti-sense RNA: A molecular appraoch to genetic analysis. *Cell,* 36:1007-1015

Jackson, C. W., N. K. Hutson, S. A. Steward and P. E. Stenberg. 1992. A unique talin antigenic determinant and anomolous megakaryocyte talin distribution associated with abnormal platelet formation in the Wistar Furth rat. *Blood.* 79:1729-1737

Jackson, C. W., N. K. Hutson, S. A. Steward and D. J. G. Rees. 1993. Detection of a mutation in the cytoskeletal protein, talin, in the Wistar-Furth (WF) rat - a rat strain with defective platelet formation and a high tumour incidence. *Blood.* 82 supplement:340a (abstract)

Jaken, S., K. Leach and T. Klauck. 1989. Association of type 3 Protein Kinase C with focal contacts in rat embryo fibroblasts. *J. Cell Biol.* 109:697-704

Jockusch, B. M, and G. Isenberg. 1981. Interaction of α-actinin and vinculin with actin: Opposite effects on filament network formation. *Proc. Natl. Acad. Sci. USA.* 1981:3005-3009

Johansson, M. W., E. Larsson, B. Luning, E. B. Pasquale and E. Ruoslahti. 1994. Altered localisation and cytoplasmic domain-binding properties of tyrosine-phosphorylated β1 integrin. *J. Cell Biol.* 126:1299-1309

Johnson, R. P., and S. W. Craig. 1994. An intramolecular association between the head and tail domains of vinculin modulates talin binding. *J. Biol. Chem.* 269:12611-12619

Johnson, R. P., and S. W. Craig. 1995. F-actin binding site masked by the intramolecular association of vinculin head and tail domains. *Nature.* 373:261-265

Jones, P., G. J. Price, V. Ohanion, A. L. Lear and D. R. Critchley. 1989. Identification of a talin binding site in the cytoskeleton protein vinculin. *J. Cell Biol.* 109:2917-1927

Joshi, S., A. Van Brunschot, S. Asad, I. Van Der Lest, S. E. Read and A. Bernstein. 1991. Inhibition of human immunodeficiency virus type 1 multiplication by antisense and sense RNA expression. *J.Virol.* 65:5524-5530

Juliano, R. L., and S. Haskill. 1993. Signal transduction from the extracellular matrix. *J. Cell Biol..* 120:577-585

Juliano, R. 1994. Signal transduction by integrins and its role in the regulation of tumour growth. *Cancer and Metastasis Reviews.* 13:25-30.

Kaufmann, S., T. Piekenbrock, W. H. Goldmann, M. Barmann and G. Isenberg. 1991. Talin binds to actin and promotes filament nucleation. *Fed. Eur. Biochem. Soc.* 284:187-191

Kellie, S., B. Patel, A. Mitchell, D. R. Critchley, N. M. Wigglesworth and J. A. Wyke. 1986a. Comparison of the relative importance of tyrosine-specific vinculin phosphorylation and the loss of surface-associated fibronectin in the morphology of cells transformed by rous sarcoma virus. *J. Cell Sci.* 82:129-142

Kellie, S., B. Patel, N. M. Wigglesworth, D. R. Critchley and J. A. Wyke. 1986b. The use of Rous sarcoma virus transformation mutants with differing tyrosine kinase activities to study the relationship between vinculin phosphorylation, pp60[v-src] location and adhesion plaque integrity. *Expt. Cell Res.* 165:216-228

Kiley, S. C., and S. Jaken. 1994. Protein kinase C: interactions and consequences. *Trends Cell Biol.* 4:223-227

Kim, S. K., and B. J. Wold. 1985. Stable reduction of thymidine kinase activity in cells expressing high levels of anti-sense RNA. *Cell.* 42:129-138

Kirchhofer, D., J. Grzesiak and M. D. Piersbacher. 1991. Calcium as a potential physiological regulator of integrin-mediated cell adhesion. *J. Biol. Chem.* 266:4471-4477

Kornberg, L. J., H. S. Earp, C. E. Turner, C. Prockop and R. L. Juliano. 1991. Signal transduction by integrins: Increased protein tyrosine phosphorylation caused by clustering of β1 integrins. *Proc. Natl. Acad. Sci.USA.* 88:8392-8396

Kornberg, L., H. Earp S, J. T. Parsons, M. Schaller and R. L. Juliano. 1992. Cell adhesion or integrin clustering increases phosphorylation of a focal adhesion-associated tyrosine kinase. *J. Biol. Chem.* 267:23439-23442

Kreis, T. E., and Birchmeier. 1982. Microinjection of fluorescently labeled proteins into living cells with emphasis on cytoskeletal proteins. *Int. Rev. Cytolo.* 75:209-227

Kroemker, M., A-H. Rudiger, B. M. Jockusch and M. Rudiger. 1994. Intramolecular interactions in vinculin control α-actinin binding to the vinculin head. *Fed. Eur. Biochem. Soc. Letts.* 355:259-262

Kuhlman, P. A., L. Hemmings and D. R. Critchley. 1992. The identification and characterization of an actin-binding site in α-actinin by mutagenesis. *Fed. Eur. Biochem. Soc Letts.* 304:201-206

Kulkarni, G. V., and C. A. G. McCulloch. 1994. Serum deprivation induces apoptotic cell death in a subset of Balb/c 3T3 fibroblasts. *J. Cell Sci.* 107:1169-1170

Kumagai, N., N. Morii, K. Fujisawa, Y. Nemoto and S. Narumiya. 1993. ADP-ribosylation of rho p21 inhibits lysophosphatidic acid-induced protein tyrosine phosphorylation and phosphotidylinositol 3-kinase activation in cultured Swiss 3T3 cells. *J. Biol. Chem.* 268:24535-24538

LaFlamme, S. E., L. A. Thomas, S. S. Yamada and K. M. Yamada. 1994. Single subunit chimeric integrins as mimics and inhibitors of endogenous integrin functions in receptor localisation, cell spreading and migration, and matrix assembly. *J. Cell Biol.* 126:1287-1298

Lallier, T., and M. Bronner-Fraser. 1993. Inhibition of neural crest cell attachment by integrin antisense oligonucleotides. *Science.* 259:692-695

Landis, R. C., A. McDowell, C. L. Holness, A. J. Littler, D. L. Simmons and N. Hogg. 1994. Involvement of the "I" domain of LFA-1 in selective binding to ligands ICAM-1 and ICAM-3. *J. Cell Biol.* 126:529-537

Lankes, W. T., and H. Furthmayr. 1991. Moesin: A member of the protein 4.1-talin-ezrin family of proteins. *Proc. Natl. Acad. Sci. USA.* 88:8297-8301

Lazarides, E., and K. Burridge. 1975. α-actinin: Immunofluorescence localisation of a muscle structural protein in nonmuscle cells. *Cell.* 6:269-298

Leavsley, D. I., M. A. Schwartz, M. Rosenfield and D. A. Cheresh. 1993. Integrin β1 and β3 mediated endothelial cell migration is triggered through distinct signalling mechanisms. *J. Cell Biol.* 121:163-170

Lehtonen, E., V-P. Lehto, R. A. Badley and I. Virtanen. 1983. Formation of vinculin plaques precedes other cytoskeletal changes during retinoic acid-induced teratcarcinoma cell differentiation. *Exptl. Cell Res.* 144:191-197.

Li, M. L., J. Aggeler, D. A. Farson, C. Hatier, J. Hassell and M. J. Bissell. 1987. Influence of a reconstituted basement membrane and its components on casein gene expression and secretion in mouse mammary epithelial cells. *Proc. Natl. Acad. Sci. USA.* 84:136-140.

Li. W., H. Mischak, J-C. Yu, L-M. Wang, J. F. Mushinski, M. A. Heidaran and J. H. Pierce. 1994. Tyrosine phosphorylation of protein kinase C∂ in response to its activation. *J. Biol. Chem.* 269:2349-2352

Liotta, L. A., C. N. Rao and U. M. Wewer. 1986. Biochemical interactions of tumor cells with the basement membrane. *Ann. Rev. Biochem.* 55:1037-1057

Lipfert, L., B. Haimovich, M. D. Schaller, B. S. Cobb, J. T. Parsons and J. S. Brugge. 1992. Integrin-dependent phosphorylation and activation of the protein tyrosine kinase pp125FAK in platelets. *J. Cell Biol.* 119:905-912

Lo,S. H., and L. B. Chen. 1994. Focal adhesion as a signal transduction organelle. *Cancer and Metastasis Reviews.* 13:9-24

Loftus, J. C., T. E. O'Toole, E. F. Plow, A. Glass, A. L. Frelinger and M. H. Ginsberg. 1990. A β3 integrin mutation abolishes ligand binding and alters divalent cation-dependent conformation. *Science.* 249:915-918

Luna, E. J., and A. L. Hitt. 1992. Cytoskeleton-plasma membrane interactions. *Science.* 258:955-964

Maher, P. A., E. B. Pasquale, J. Y. J. Wang and S. J. Singer. 1985. Phosphotyrosine-containing proteins are concentrated in focal adhesions and intercellular junctions in normal cells. *Proc. Natl. Acad. Sci. USA.* 82:6576-6580

Marfatia, S. M., R. A. Branton and A. H. Christi. 1994. *In vitro* binding studies suggest a membrane-associated complex between erythroid p55, band 4.1 and glycophorin C. *J. Biol. Chem.* 1994:8631-8634

McGregor, A., A. D. Blanchard, A. J. Rowe and D. R. Critchley. 1994. Identification of the vinculin-binding site in the cytoskeletal protein α-actinin. *Biochem. J.* 301:225-233.

McClay, D. R., and C. A. Ettensohn. 1987. Cell adhesion in morphogenesis.*Ann. Rev. Cell Biol.* 3:319-345

McLachlan, A. D., M. Stewart, R. O. Hynes and D. J. G. Rees. 1994. Analysis of repeated motifs in the talin rod. *J. Mol. Biol.* 235:1278-1290

Melani, C., L. Rivoltini, G. Parmiani, B. Calabretta and M. P. Colombo. 1991. Inhibition of proliferation by c-myb antisense oligonucleotides in colon adenocarcinoma cell lines that express c-myb. *Cancer Res.* 51:2897-2901

Melton, D. A., P. A. Kreig, M. R. Rebagliati, T. Maniatis and M. R. Green. 1984. Efficient *in vitro* synthesis of biologically active RNA and RNA hybridisation probes from plasmids containing a bacteriophage SP6 promoter. *Nuc. Acids Res.* 12:7035-7056

Melton, D. A. 1985. Injected anti-sense RNAs specifically block messanger RNA translation in vivo. *Proc. Natl. Acad. Sci. USA.* 82:144-148

Menkel, A. R., M. Kroemer, P. Bubeck, M. Ronsiek, G. Nikolai and B. M. Jockusch. 1994. Characterisation of an F-actin-binding domain in the cytoskeltal protein vinculin. *J. Cell Biol.* 126:1231-1240

Moiseyeva, E. P., P. A. Weller, N. I. Zhidkoza, E. B. Corben, B. Patel, I. J. Jasinska, V. E. Koteliansky and D. R. Critchley. 1993. Organization of the human gene encoding the cytoskeletal protein vinculin and the sequence of the vinculin promoter. *J. Biol. Chem.* 268:4318-4325

Molony, L., D. McCaslin, J. Abernethy, B. Paschal and K. Burridge. 1987. Properties of talin from chicken gizzard smooth muscle. *J. Biol.Chem.* 262:7790-7795

Monia, B. P., J. F. Johnston, D. J. Ecker, M. A. Zounes, W. F. Lima and S. M. Freier. 1992. Selective inhibition of mutant Ha-ras mRNA expression by antisense oligonucleotides. *J. Biol. Chem.* 267:19954-19962

Moolenaar,W. H. 1994. LPA:a novel lipid mediator with diverse biological actions. *Trends Cell Biol.* 4:213-219

Moroni, M. C., M. C. Willingham and L. Beguinot. 1992. EGF-R antisense RNA blocks expression of the epidermal growth factor receptor and suppresses the transforming phenotype of a human carcinama cell line. *J. Biol. Chem.* 267:2714-2722

Muguruma, M., S. Matsumura and T. Fukazawa. 1990. Direct interactions between talin and actin. *Biochem. Biophys. Res. Comm.* 171:1217-1223

Muguruma, M., S. Matsumura and T. Fukazawa. 1992. Augmentation of a-actinin-induced gelation of actin by talin. *J. Biol. Chem.* 267:5621-5624

Murray, J. A. H. 1992. Antisense RNA and DNA. Modern cell Biology Series. Ed. J. B. Harford. Wiley-Liss Inc.

Nagai, T., N. Yamakawa, S. Aota, S. S. Yamada, S. K. Akiyama, K. Olden and K. M. Yamada. 1991. Monoclonal antibody characterisation of two distant sites required for function of the central cell-binding domain of fibronectin in cell adhesion, cell migration and matrix assembly. *J. Cell Biol.* 114:1295-1305

Niggli,V., S.Kaufmann, W.H.Goldmann, T.Weber and G.Isenberg. 1994. Identification of functional domains in the cytoskeletal protein talin.*Eur.J.Biochem.* 224:951-957

Nishikura, K., and J. M. Murray. 1987. Antisense RNA of proto-oncogene c-fos blocks renewed growth of quiescent 3T3 cells. *Mol. Cell Biol.* 7:639-649

Nobes, C. D., P. Hawkins, L. Stephens and A. Hall. 1995. Activation of the small GTP-binding proteins rho and rac by growth factor receptors. *J. Cell Sci.* 108:225-233

Nuckolls, G. H., C. E. Turner and K. Burridge. 1990. Functional studies of the domains of talin. *J. Cell Biol.* 110:1635-1644

Nuckolls, G. H., L. H. Romer and K. Burridge. 1992. Microinjection of antibodies against talin inhibits spreading and migration of fibroblasts. *J. Cell Sci.* 102:753-762

O'Halloran, T., M. C. Beckerle and K. Burridge. 1985. Identification of talin as a major cytoplasmic protein implicated in platelet activation. *Nature.* 317:449-451

Osen-Sand, A., M. Catsicas, J. K. Staple, K. A. Jones, G. Ayala, J. Knowles, G. Greeningloh and S. Catsicas. 1993. Inhibition of axonal growth by SNAP-25 antisense oligonucleotides *in vitro* and *in vivo. Nature.* 364:445-448

Otey, C. A., F. M. Pavalko and K. Burridge. 1990a. An interaction between α-actinin and the β1 integrin subunit in vitro. *J. Cell Biol.* 111:721-729

Otey, C., W. Griffiths and K. Burridge. 1990b. Characterization of monoclonal antibodies to chicken gizzard talin. *Hybridoma.* 9:57-62

Otey, C. A, G. B. Vasquez, K. Burridge and B. W. Erickson. 1993. Mapping of the α-actinin binding site within the β1 integrin cytoplasmic domain. *J. Biol. Chem.* 268:21193-21197

Panaretto, B. A. 1994. Aspects of growth factor signal transduction in the cell cytoplasm. *J. Cell Sci.* 107:747-752

Parise, L. V. 1989. The structure and function of platelet integrins. *Curr. Opin. Cell Biol.* 1:947-952.

Parr, T., G. T. Waites, B. Patel, D. B. Millake and D. R. Critchley. 1992. A chick skeletal-muscle α-actinin gene gives rise to two alternatively spliced isoforms which differ in the EF hand Ca2+-binding domain. *Eur. J. Biochem.* 210:801-809

Pasquale, E. B., P. A. Maher and S. J. Singer. 1986. Talin is phosphorylated on tyrosine in chicken embryo fibroblasts transformed by Rous sarcoma virus. *Proc. Natl. Acad. Sci. USA.* 83:5507-5511

Pasternack, G. R., R. A. Anderson, T. L. Leto and V. T. Marchesi. 1985. Interactions between protein 4.1 and band 3. *J. Biol. Chem.* 260: 3676-3683

Pavalko, F. M., and K. Burridge. 1991. Disruption of the actin cytoskeleton after microinjection of the proteolytic fragments of α-actinin. *J. Cell Biol.* 114:481-491

Pawson, T., and J. Schlessinger. 1993. SH2 and SH3 domains. *Curr. Biol.* 3:434-442

Perlaky, L., B. C. Valdez, R. K. Busch, R. G. Larson, S. M. Jhiang, W. W. Zhang, M. Brattain and H. Busch. 1992. Increased growth of NIH/3T3 cells by transfection with human p120 complementary DNA and inhibition by a p120 antisense construct. *Cancer Res.* 52:428-436

Piersbacher, M. D., and E. Ruoslahti. 1984. Cell attachement activity of fibronectin can be duplicated by small synthetic fragments of the molecule. *Nature.* 309:30-33

Plantefaber, L. C., and R. O. Hynes. 1989. Changes in integrin receptors on oncogenicaly transformed cells. *Cell.* 56:281-290

Potts, J. R., and I. D. Campbell. 1994. Fibronectin structure and assembly. *Curr. Opin. Cell Biol.* 6:648-655

Price, G. J.,P. Jones, M. D. Davidson, B. Patel, I. C. Eperon and D. R. Critchley. 1987. Isolation and characterisation of a vinculin cDNA from chick embryo fibroblasts. *Biochem. J.* 245:595-603

Price, G. J., P. Jones, M. D. Davidson, B. Patel, R. Bendori, B. Geiger and D. R. Critchley. 1989. Primary sequence and domain structure of chicken vinculin. *Biochem.J.* 259:453-461

Rankin, S., and E. Rozengurt. 1994. Platelet-derived growth factor modulation of focal adhesion kinase (p125FAK) and paxillin tyrosine phosphorylation in Swiss 3T3 cells. *J. Biol. Chem.* 269:704-710

Rees, D. J. G., S. E. Ades, S. J. Singer and R. O. Hynes. 1990. Sequence and domain structure of talin. *Nature.* 347:685-689

Regen, C. M., and A. F. Horwitz. 1992. Dynamics of β1 integrin-mediated adhesive contacts in motile fibroblasts. *J. Cell Biol.* 119:1347-1359

Rhodes, A., and W. James. 1990. Inhibition of heterologous strains of HIV by antisense RNA. *AIDS.* 5:145-151

Ridley, A. J., and A. Hall. 1992. The small GTP-binding protein rho regulates the assembly of focal adhesions and actin stress fibres in response to growth factors. *Cell.* 70:389-399

Ridley, A. J., and A. Hall. 1994. Signal transduction pathways regulating Rho-mediated stress fibre formation: requirement for a tyrosine kinase. *Euro. Mol. Biol. Org. J.* 13:2600-2610

Rifkin, D. B., R. M. Crowe and R. Pollack. 1979. Tumour promoters induces changes in the chick embryo fibroblast cytoskeleton. *Cell.* 18:361-368

Ringold, G. M., K. R. Yamamoto, G. M. Tomkins, J. M. Bishop and H. E. Varmus. 1975. Dexamethasone-mediated induction of mouse mammary tumor virus RNA: A system for studying glucocorticoid action. *Cell.* 6:299-305

Rodriguez Fernandez, J. L., B. Geiger, D. Salomon and A. Ben-Ze'ev. 1992a. Overexpression of vinculin suppresses cell motility in BALB/c 3T3 cells. *Cell Motil. Cytoskel.* 22:127-134

Rodriguez Fernandez, J. L., B. Geiger, D. Salomon, I. Sabanay, M. Zoller and A. Ben-Ze'ev. 1992b. Suppression of tumorigenicity in transformed cells after transfection with vinculin cDNA. *J. Cell Biol.* 119:427-438

Rodriguez Fernandez, J. L., B. Geiger, D. Salomon and A. Ben-Ze'ev. 1993. Suppression of vinculin expression by antisense transfection confers changes in cell morphology, motility and anchorage-dependent growth of 3T3 cells. *J. Cell Biol.* 122:1285-1294

Rouslahti, E. 1988. Fibronectin and its receptors. *Ann. Rev. Biochem.* 57:375-413

Rouleau, G. A., P. Merel, M. Lutchman, M. Sanson, J. Zucman, C. Marineau, K. Hoang-Xuan, S. Demczuk, C. Desmaze, B. Plougastel, S. Pulst, G. Lenoir, E. Bijlsma, R. Fashold, J. Dumanski, P. De Jong, D. Parry, R. Eldrige, A. Aurias, O. Delattre and G. Thomas. 1993. Alteration in a new gene encoding a putative membrane-organising protein causes neuro-fibromatosis type 2. *Nature.* 363:515-521

Sadler, I., A. W. Crawford, J. W. Michelson and M. C. Beckerle. 1992. Zyxin and cCRP: Two interactive LIM domain proteins associated with the cytoskeleton. *J. Cell Biol.* 119:1573-1587

128

Salmons, B., B. Groner, R. Friis, D. Muellener and R. Jaggi. 1986. Expression of antisense mRNA in H-ras transfected NIH/3T3 cells does not suppress the transformed phenotype. *Gene.* 45:215-226

Sambrook, J., E. F. Fritsch and T. Maniatis. 1989. Molecular cloning: A laboratory manual. Cold Spring Harbor Laboratories, Cold Spring Harbor, N. Y.

Samuels, M., R. M. Ezzell, T. J. Cardozo, D. R. Critchley, J.-L. Coll and E. D. Adamson. 1993. Expression of chicken vinculin complements the adhesion-defective phenotype of a mutant mouse F9 embryonal carcinoma cell. *J. Cell Biol.* 121:909-921

Sanchez-Mateos, P., M. R. Campanero, M. A. Balboa and F. Sanchez-Madrid. 1993. Co-clustering of β1 integrins, cytoskeletal proteins, and tyrosine-phosphorylated substrates during integrin-mediated leukocyte aggregation. *J. Immunol.* 151:3817-3828

Sanger, F., S. Nickel and A. R. Coulsen. 1977. DNA sequencing with chain terminating inhibitors. *Proc. Natl. Acad. Sci.USA.* 74:5463-5433

Schaller, M. D., C. A. Borgman, B. S. Cobb, R. R. Vines, A. B. Reynolds and J. T. Parsons. 1992. pp125FAK, a structurally distinctive protein-tyrosine kinase associated with focal adhesions. *Proc. Natl. Acad. Sci. USA.* 89:5192-5196

Schaller, M. D., C. A. Borgman and J. T. Parsons. 1993. Autonomous expression of a noncatalytic domain of the focal adhesion-associated protein tyrosine kinase pp125FAK. *Mol. Cell Biol.* 13:785-791

Schaller, M. D., and J. T. Parsons. 1993. Focal adhesion kinase: an integrin-linked protein tyrosine kinase. *Trends Cell Biol.* 3:258-262

Schaller, M. D., J. D. Hildebrand, J. D. Shannon, J. W. Fox, R. R. Vines and J. T. Parsons. 1994. Autophosphorylation of the focal adhesion kinase, pp125FAK, directs SH2-dependent binding of pp60src. *Mol. Cell Biol.* 14:1680-1688

Schaller, M. D., and J. T. Parsons. 1994. Focal adhesion kinase and associated proteins. *Curr. Opin. Cell Biol.* 6:705-710

Schmidhauser, C., G. F. Casperson, C. A. Myers, K. T. Sanzo, S. Bolten and M. J. Bissell. 1992. A novel transcription enhancer is involved in the prolactin- and extracellular matrix-dependent regulation of β-casein gene expression. *Mol. Biol. Cell.* 3:699-709

Schmidt, C. E., A. F. Horwitz, D. A. Lauffenberger and M. P. Sheetz. 1993. Integrin-cytoskeletal interactions in migrating fibroblasts are dynamic, asmmetric and regulated. *J. Cell Biol.* 123:977-991

Schulze, H., A. Huckriede, A. A. Noegel, M. Schleicher and B. M. Jockusch. 1989. α-Actinin synthesis can be modulated by antisense probes and is autoregulated in non-muscle cells. *Eur. Mol. Biol. Org. J.* 8:3587-3593

Schwartz, M. A. 1992. Transmembrane signalling by integrins. *Trends Cell Biol.* 2:304-308.

Sefton, B. M., T. Hunter, B. E.H and S. J. Singer. 1981. Vinculin: A cytoskeletal target of the transforming protein of Rous Sarcoma Virus. *Cell.* 24:165-174

Selinfreund, R. H., S. W. Barger, M. J. Welsh and L. J. Van Eldik. 1990. Antisense inhibition of glial S100β production results in alterations in cell morphology, cytoskeletal organization and cell proliferation. *J. Cell Biol.* 111:2021-2028

Seufferlein, T., and E. Rozengurt. 1994. Lysophosphatidic acid stimulates tyrosine phosphorylation of focal adhesion kinase, paxillin and p130. *J. Biol. Chem.* 269:9345-9351

Shear, C. R., and R. J. Bloch. 1985. Vinculin in subsarcolemmal densities in chicken skeletal muscle: localisation and relationship to intracellular and extracellular structures. *J. Cell Biol.* 101:240-256

Shibaski, F., K. Fukami, Y. Fukui and T. Takenawa. 1994. Phosphatidylinositol 3-kinase binds to α-actinin through the p85 subunit. *Biochem. J.* 302: 551-557

Shiffer, K. A., and S. R. Goodman. 1984. Protein 4.1: Its association with the human erythrocyte membrane. *Proc. Natl. Acad. Sci. USA.* 81:4404-4408

Simon, K. and K. Burridge, 1991. Characterization of the interaction between talin and the cytoplasimc domain of β1 integrin. *J. Cell Biol.* 115: 351a (abstract)

Simons, M., E. R. Edelman, J.-L. DeKeyser, R. Langer and R. D. Rosenberg. 1992. Antisense c-myb oligonucleotides inhibit intimal arterial smooth muscle cell accumulation in vivo. *Nature.* 359:67-70

Simons, P. C. and L. Elias. 1993. The 47kDa fragment of talin is a substrate for protein kinase P. *Blood.* 82: 3343-3349

Sklar, M. D., E. Thompson, M. J. Welsh, M. Liebert, J. Harney, H. B. Grossman, M. Smith and E. V. Prochownik. 1991. Depletion of c-myc with specific antisense sequences reverses the transformed phenotype in ras oncogene-transformed NIH 3T3 cells. *Mol. Cell Biol.* 11:3699-3710

Small, J. V. 1985. Geometry of actin-membrane attachement in smooth muscle cell: the localisation of vinculin and α-actinin. *EMBO J.* 4:45-49

Smith, D. B., and K. S. Johnson. 1988. Single-step purification of polypeptides expressed in *Escherichia coli* as fusions with glutathione S-transferase. *Gene.* 67:31-40

Smith, J. W., and D. A. Cheresh. 1988. The Arg-Gly-Asp binding domain of the vitronectin receptor. *J. Biol. Chem.* 263:18726-18731

Smith, J. W., and D. A. Cheresh. 1990. Integrin (αvβ3)-ligand interaction. *J. Biol. Chem.* 265:2168-2172

Solowska, J., J-L. Guan, E. E. Marcantonio, J. E. Trevithick, C. A. Buck and R. O. Hynes. 1989. Expression of normal and avian integrin subunits in rodent cells. *J. Cell Biol.* 109:853-861

Springer, T. A. 1990. Adhesion receptors of the immune system. *Nature.* 346:425-434.

Steel, D. M., and H. Harris. 1989. The effect of antisense RNA to fibronectin on the maliginancy of hybrids between melanoma cells and normal fibroblasts. *J. Cell Sci.* 93:515-524

Streuli, C. H., and M. J. Bissell. 1990. Expression of extracellular matrix components is regulated by substratum. *J. Cell Biol.* 110:1405-1415

Strickland, S., and V. Mahdarvi. 1978. The induction of differentiation in teratocarcinoma stem cells by retinoic acid. *Cell.* 15:393-403.

Takeshima, H., I. Izawa, P. S. Y. Lee, N. Safdar, V. A. Levin and H. Saya. 1994. Detection of cellular proteins that interact with the NF2 tumour suppresor gene product. *Oncogene.* 9:2135-2144

Takeuchi, K., N. Sato, H. Kasahara, N. Funayama, A. Nagafuchi, S. Yonemura, S. Tsukita and S. Tsukita. 1994. Perturbation of cell adhesion and microvilli formation by antisense oligonucleotides to ERM family members. *J. Cell Biol.* 125:1371-1384

Tamkun, J. W., D. W. DeSimone, D. Fonda, R. S. Patel, C. Buck, A. F. Horwitz and R. O. Hynes. 1986. Structure of integrin, a glycoprotein involved in the transmembrane linkage between fibronectin and actin. *Cell.* 46:271-282

Tamm, I., T. Kikuchi, J. Krueger and J. S. Murphy. 1992. Dissociation between early loss of actin fibres and subsequent cell death in serum-deprived quiescent Balb/c 3T3 cells. *Cell. Signalling.* 4:675-686

Tapley, P. , A. F. Horwitz, C. A. Buck, K. Burridge, K. Duggan, R. Hirst and L. Rohrschneider. 1989. Integrins isolated from Rous Sarcoma virus-transformed chicken embryo fibroblasts.*Oncogene.* 4:325-333

Tarone, G., D. Cirillo, F. G. Giancotti, P. M. Comoglio and P. C. Marchisio. 1985. Rous sarcoma virus-transformed fibroblasts adhere primarily at discrete protrusions of the ventral membrane called podosomes. *Exptl. Cell Res.* 159:141-157

Tawil, N., P. Wilson and S. Carbonetto. 1993. Integrins in point contacts mediate cell spreading factors that regulate integrin accumulation in point contacts vs focal contacts. *J. Cell Biol.* 120:261-271

Thinakaran, G., and J. Bag. 1991. Alterations in the expression of muscle-specific genes mediated by troponin-C antisense oligonucleotide. *Expt. Cell Res.* 192:227-235

Tidball, J. G., T. O'Halloran and K. Burridge. 1986. Talin at myotendinous junctions. *J. Cell Biol.* 103:1465-1472

Tidball, J. G., and M. J. Spencer. 1993. PDGF stimulation induces phosphorylation of talin and cytoskeletal reorganisation in skeletal muscle. *J. Cell Biol.* 123:627-635

Towbin, H., T. Staehlin and J. Gordon. 1979. Electrophoretic transfer of proteins from polyacrylamide gels to nitrocellulose sheets: Proceedures and some applications. *Proc. Natl. Acad. Sci. USA.* 76:4350-4354

Trofatter, J. A., M. M. MacCollin, J. L. Rutter, J. R. Murrell, M. P. Duyao, D. M. Parry, R. Eldridge, N. Kley, A. G. Menon, K. Pulaski, V. H. Haase, C. M. Ambrose, D. Munroe, C. Bove, J. L. Haines, R. L. Martuza, M. E. MacDonald, B. R. Seizinger, M. P. Short, A. J. Buckler and J. F. Gusella. 1993. A novel moesin-, ezrin-, radixin-like gene is a candidate for the neurofibromatosis 2 tumour suppressor. *Cell.* 72:791-800

Turner, C. E., F. M. Pavalko and K. Burridge. 1989. The role of phosphorylation and limited proteolytic cleavage of talin and vinculin in the disruption of focal adhesion integrity. *J. Biol. Chem.* 264:11938-11944

Turner, C. E., J. R. Glenney and K. Burridge. 1990. Paxillin: A new vinculin-binding protein present in focal adhesions. *J. Cell Biol.* 111:1059-1068

Turner, C. E. 1991. Paxillin is a major phosphotyrosine-containing protein during embryonic development. *J. Cell Biol.* 115:201-207

Turner, C. E., N. Kramarcy, R. Sealock and K. Burridge. 1991. Localization of paxillin, a focal adhesion protein, to smooth muscle dense plaques, and the myotendinous and neuromuscular junctions of skeletal junctions. *Expt. Cell Res.* 192:651-655

Turner, C. E., M. D. Schaller and J. T. Parsons. 1993. Tyrosine phosphorylation of the focal adhesion kinase pp125FAK during development: relation to paxillin. *J. Cell Sci.* 105:637-645

Turner, C. E. and J. T. Miller. 1994. Primary sequence of paxillin contains putative SH2 andSH3 domain binding motifs and multiple LIM domains: identification of a vinculin and pp125FAK binding region. *J. Cell Sci.* 107:1583-1591.

Turunen, O., T. Wahlstrom and A. Vaheri. 1994. Ezrin has a COOH-terminal actin-binding site that is conserved in the ezrin protein family. *J. Cell Biol.* 126:1445-1453

Volk, T. and B. Geiger. 1984. A 135kD membrane protein of intracellular adherens junctions. *Eur. Mol.Biol.Org. J.* 3:2249-2260

Vostal, J. G. and N. R. Shulman. 1993. Vinculin is a major platelet protein that undergoes calcium-dependent tyrosine phosphorylation. *Biochem. J.* 294:675-680

Vuori, K., and E. Ruoslahti. 1993. Activation of protein kinase C precedes α5β1 integrin-mediated cell spreading on fibronectin. *J. Biol. Chem.* 268:21459-21462

Wachsstock, D. H., J. A. Wilkins and S. Lin. 1987. Specific interaction of vinculin with α-actinin. *Biochem. Biophys. Res. Comm.* 146:554-560.

Waites, G. T., I. R. Graham, P. Jackson, D. B. Millake, B. Patel, A. D. Blanchard, P. A. Weller, I. C. Eperon and D. R. Critchley. 1992. Mutually exclusive splicing of calcium-binding domain exons in chick α-actinin. *J. Biol. Chem.* 267:6263-6271

Weller, P. A., E. P. Ogryzko, E. B. Corben, N. I. Zhidkova, B. Patel, G. J. Price, N. K. Spurr, V. E. Koteliansky and D. R. Critchley. 1990. Complete sequence of human vinculin and assignment of the gene to chromosome 10. *Proc. Natl. Acad. Sci. USA.* 87:5667-5671

Werb, Z., P. M. Tremble, O. Behrendtsen, E. Crowley and C. H. Damsky. 1989. Signal transduction through the fibronectin receptor induces collagenase and stromelysin gene expression. *J. Cell Biol.* 109:877-889

Werth, D. K., and I. Pastan. 1984. Vinculin phosphorylation in response to calcium and phorbol esters in intact cells. *J. Biol. Chem.* 259:5264-5270

Westmeyer, A., K. Ruhnau, A. Wegner and B. M. Jockusch. 1990. Antibody mapping of functional domains of vinculin. *Eur. Mol. Biol. Org. J.* 9:2071-2078

Wilkins, J. A., and S. Lin. 1982. High affinity interaction of vinculin with actin filaments *in vitro. Cell.* 28:83-90

Wilkins, J. A., and S. Lin. 1986a. A re-examination of the interaction of vinculin and actin. *J. Cell Biol.* 102:1085-1092

Wilkins, J. A., M. A. Risinger and S. Lin. 1986b. Studies on proteins that co-purify with smooth muscle vinculin: Identification of immunologically related species in focal adhesions of nonmuscle and Z lines of muscle cells. *J. Cell Biol.* 103:1483-1494

Williams, M. J., P. E. Hughes, T. E. O'Toole and M. H. Ginsberg. 1994. The inner world of cell adhesion: integrin cytoplasmic domains. *Trends Cell Biol.* 4:109-112

Wood, C. K., C. E. Turner, P. Jackson and D. R. Critchley. 1994. Characterisation of the paxillin-binding site and the C-terminal focal adhesion targeting sequence in vinculin. *J. Cell Sci.* 107:709-717

Woods, A., J. R. Couchman, S. Johansson and M. Hook. 1986. Adhesion and cytoskeletal organisation of fibroblasts in response to fibronectin fragments. *Eur. Mol. Biol. Org. J.* 5:665-670

Woods, A., and J. R. Couchman. 1992. Protein kinase C involvement in focal adhesion formation. *J. Cell Sci.* 101:277-290

Yamada, K. M., S. S. Yamada and I. Pastan. 1976. Cell surface protein partially restores morphology, adhesiveness and contact inhibitio of movement to transformed fibroblasts. *Proc. Natl. Acad. Sci. USA.* 73:1217-1221.

Yamada, K. 1991. Adhesive recognition sequences. *J. Biol. Chem..* 266:12809-12812

Yang, Q., and N. K. Tonks. 1991. Isolation of a cDNA clone encoding a human protein-tyrosine phosphatase with homology to the cytoskeletal-associated proteins band 4.1, ezrin and talin. *Proc.Natl.Acad.Sci. USA.* 88:5949-5953

Ylanne, J., Y. Chen, T. E. O'Toole, J. C. Loftus, Y. Takada and M. H. Ginsberg. 1993. Distinct functions of integrin α and β subunit cytoplasmic domains in cell spreading and formation of focal adhesions. *J. Cell Biol.* 122:223-233

Yuruker, B., and V. Niggli. 1992. α-Actinin and vinculin in human neutrophils: reorganization during adhesion and relation to the actin network. *J. Cell Sci.* 101:403-414

Zachary, I., J. Sinnett-Smith, C. E. Turner and E. Rozengurt. 1993. Bombesin, vasopressin and endothelin rapidly stimulate tyrosine phosphorylation of the focal adhesion-associated protein paxillin in Swiss 3T3 cells. *J. Biol. Chem.* 268:22060-22065